Doctoral thesis

Characterization of iron transporters in arbuscular mycorrhiza and their impact on symbiotic functioning

Víctor Manuel López Lorca

Directora de la Tesis Doctoral

Nuria Ferrol González

Doctoral Program in Fundamental and Systems Biology

University of Granada, 2023

Editor: Universidad de Granada. Tesis Doctorales
Autor: Víctor Manuel López Lorca
ISBN: 978-84-1117-749-8
URI: https://hdl.handle.net/10481/80704

Universidad de Granada

Consejo Superior de Investigaciones Científicas

Programa de Doctorado en Biología Fundamental y de Sistemas

Characterization of iron transporters in arbuscular mycorrhiza and their impact on symbiotic functioning

Víctor Manuel López Lorca

Tesis Doctoral

Granada, 2023

Financiación y publicaciones

Este trabajo de Tesis Doctoral ha sido realizado en el Departamento de Microbiología del Suelo y la Planta (Grupo de investigación "Micorrizas") de la Estación Experimental del Zaidín (EEZ-CSIC).

Para la realización del siguiente trabajo, el graduado Víctor Manuel López Lorca fue financiado por las siguientes fuentes:

- Ayuda para Contratos Predoctorales para la Formación de Doctores (Ref. Ayuda BES-2016-078463) del Ministerio de Ciencia, Innovación y Universidades disfrutada desde el 16 de abril de 2017 hasta el 15 de septiembre de 2021
- Proyectos de Investigación del Plan Nacional AGL2015-67098 y RTI2018-098756-B-I00

Parte de los resultados presentados en esta Memoria de Tesis Doctoral se han publicado en revistas internacionales o están en vías de publicación:

- López-Lorca, V. M., Molina-Luzón, M. J., Ferrol, N. (2022). Characterization of the NRAMP Gene Family in the Arbuscular Mycorrhizal Fungus *Rhizophagus irregularis*. *Journal of Fungi*, 8(6), 592. doi: 10.3390/JOF8060592
- López-Lorca V.M., Molina-Luzón M.J., Ferrol N. Characterization of the CCC1 gene family in the arbuscular mycorrhizal fungus *Rhizophagus irregularis*. In preparation.
- López-Lorca, V. M., Molina-Luzón, M. J., Ferrol, N. Impact of arbuscular mycorrhiza on the iron deficiency response of *Solanum lycopersicum*. Submitted to *Plant Physiology and Biochemistry*
- López-Lorca V.M., Ferrol N. Physiological and transcriptomic responses of the tomato mutant *chloronerva* affected in the regulation of iron metabolism to arbuscular mycorrhiza. To be submitted to *Frontiers in Plant Science*.

A Marta

A mis padres y hermana

ÍNDICE

ACRÓNIMOS

AM	Arbuscular mycorrhizal
ANOVA	Analysis of variance
BLAST	Basic local alignment search tool
CCC	Ca2+-sensitive Cross-Complementer
EDTA	Ethylenediaminetetraacetic acid
ERM	Extraradical mycelium
FRE	Ferric reductase
FTR	Fe transporter
GFP	Green fluorescent protein
HIGO	Host-induced gene overexpression
HIGS	Host-induced gene silencing
IRT	Iron regulated transporter
IRM	Intraradical mycelium
JGI	Joint Genome Institute
MEGA	Molecular evolutionary genetics analysis
NCBI	National Center for Biotechnology Information
NRAMP	Natural resistance-associated macrophage proteins
OD	Optical density
OPT	Oligopeptide transporter
PPA	Pre-penetration apparatus
PS	Phytosiderophore
ROS	Reactive oxygen species
RT	Retro transcriptase
SD	Synthetic dextrose
SIT	Siderophore-iron transporter
VIT	Vacuolar iron transporter
ZIP	Zinc-iron permease
YPD	Yeast extract-peptone-dextrose
PAM	Periarbuscular membrane
PAS	Periarbuscular space
VIGS	Virus induced gene silencing

SUMMARY

Iron (Fe) is a critical micronutrient for the growth and survival of most organisms, playing an important structural role in proteins and as an enzyme cofactor. Despite its abundance in nature, Fe is often not available to plants, particularly in alkaline soils, since it exists mostly in its oxidized state, Fe (III). To prevent chlorosis and poor development, plants have evolved strategies to acquire Fe from the rhizosphere. Non-grasses plants use a Strategy I, which involves a plasma membrane H^+-ATPase to acidify the rhizosphere and solubilize Fe, a ferric reductase (FRO1) to reduce Fe (III) to Fe (II), and the Fe (II) transporter (IRT) for uptake across the plasma membrane. Grasses, on the other hand, employ a Strategy II, which includes the production of phytosiderophores (PS) to chelate Fe (III) and oligopeptide transporters YS1 or YS1-like to transport the PS-Fe chelates into root cells.

The establishment of beneficial associations with soil microorganisms is another strategy evolved by plants to cope with Fe deficiency. Arbuscular mycorrhizal (AM) fungi, belonging to the subphylum Glomeromycotina, are among the most prominent microorganisms that contribute to plant nutrition. These fungi form a mutualistic symbiosis with most terrestrial plant species. They colonize biotrophically the root cortex and develop an extensive network of extraradical hyphae in the soil that overgrows the soil surrounding the roots. In return for the carbon compounds provided by the plants, AM fungi deliver to the plant the nutrients they take up beyond the nutrient depletion zones developed around the roots. It is well established that AM fungi can help plants to acquire low mobility nutrients, such as phosphorus, nitrogen, zinc, copper and Fe. Besides enhancing nutrient uptake to their host plants, AM fungi provide increased tolerance against biotic and abiotic stresses. AM fungi play a crucial role in modulating plant metal acquisition over a wide range of soil metal concentrations, as they increase plant metal acquisition in soils deficient in these elements but reduce metal uptake in contaminated soils. The importance of the AM symbiosis for plant development in both Fe-deficient and Fe-contaminated soils has been established. However, little is known about the mechanisms of Fe transport and homeostasis in AM.

Within this PhD thesis to get further insights into the mechanisms of Fe homeostasis in AM, we employed a multidisciplinary approach combining *in silico*, physiological and molecular tools. We used the model AM fungus *Rhizophagus irregularis* DAOM197198 v2.0 and A1, A4, A5, B3 and C2 v1.0, which can be easily grown in *in vitro* monoxenic cultures and *in vivo* whole plant bidimensional experimental systems. For the studies on the plant side we used *Solanum lycopersicum,* an economically important crop that has been used as a model plant for studying Fe homeostasis in Strategy I plants.

As a first approach to further understand the mechanism of Fe homeostasis in AM, functional characterization of the *R. irregularis* NRAMP transporters was performed. These results are presented in **Chapter 1**. Transporters of the NRAMP family are ubiquitous metal-transition transporters, playing a key role in metal homeostasis, especially in manganese (Mn) and Fe homeostasis. The *R. irregularis* NRAMP family is composed of four members: RiSMF1, RiSMF2, RiSMF3.1 and RiSMF3.2. Phylogenetic analysis of the NRAMP sequences of different AM fungi showed that they are classified in two groups, which probably diverged early in their evolution. Since AM fungi cannot be genetically manipulated, functionality of the *RiSMF* genes was tested through heterologous complementation in yeast. Unfortunately, only *RiSMF3.2* function could be determined in the heterologous system. Complementation assays of the yeast mutant strain *smf1*Δ, unable to take up Mn, and of the *fet3*Δ*fet4*Δ, lacking the Fe uptake systems, revealed that *RiSMF3.2* encodes a plasma membrane protein mediating Mn and Fe transport from the environment. Gene-expression analyses by RT-qPCR showed that the *RiSMF* genes are differentially expressed in the extraradical (ERM) and intraradical (IRM) mycelium and differentially regulated by Mn and Fe availability. Mn starvation decreased *RiSMF1* transcript levels in the ERM but increased *RiSMF3.1* expression in the IRM. In the ERM, *RiSMF1* expression was up-regulated by Fe deficiency, suggesting a role for its encoded protein in Fe-deficiency alleviation. Expression of *RiSMF3.2* in the ERM was up-regulated at the early stages of Fe toxicity but down-regulated at later stages. These data suggest a role for RiSMF3.2 not only in Fe transport but also as a sensor of high external-Fe concentrations or that it might function as a low-affinity Fe transporter. These data altogether indicate that *R. irregularis* uses various strategies to increase Fe uptake from the environment: the previously identified plasma-membrane Fe permease RiFTR1 and the RiSMF3.2 NRAMP transporter. Moreover, in this chapter we describe, for the first time, a Mn transporter in an AM fungus.

The morphogenetic response of *R. irregularis* ERM to Fe and Mn deficiency were also assessed. Mn deficiency increased hyphal length, indicating that, under these conditions, the fungus explores a higher volume of soil, which will increase the nutrient-uptake effectiveness of the mycorrhizal root. However, Fe deficiency reduced sporulation, probably as a consequence of the inhibition of the activity of the Fe requiring enzymes involved in spore formation. Fe detection in spores developed under Fe toxicity supports the view that a survival strategy of AM fungi in metal-contaminated environments is to accumulate the excess metal in some spores of the fungal colony.

Fungi tightly regulate the cytosolic concentration through regulation of Fe uptake and storage in the vacuoles. **Fe** transport into vacuoles is mediated by transporters of the Ccc1/VIT family.

Therefore, once we identified the *R. irregularis* transporters involved in Fe transport into the cytosol in *R. irregularis*, we decided to characterize the vacuolar Fe transporters of the Ccc1/VIT family, RiCCC1.1, RiCCC1.2 and RiCCC1.3. Bioinformatic analyses of the RiCCC1 protein sequences revealed they have all the essential domains and residues required for Fe transport, including the metal binding domain (MBD) is formed by H1 and H3 helices and the C-terminal end of the second transmembrane domain. Functional analyses in yeast revealed that RiCCC1.1 and RiCCC1.2, but not RiCCC1.3, were able to rescue the growth of a *Saccharomyces cerevisiae* mutant defective in vacuolar Fe transport. RiCC1.1 and RiCCC1.2 also complemented Mn sensitivity of the *pmr1*Δ mutant yeast. The *RiCCC1* genes were differentially expressed in the ERM, IRM and arbuscules. In the ERM, *RiCCC1.2* expression was down-regulated by Fe deficiency but transiently up-regulated by Fe toxicity. These data suggest a role for RiCCC1.2 in vacuolar Fe mobilization under Fe limitation and in Fe detoxification under Fe toxic conditions. *RiCCC1.3* expression was also transiently up-regulated by Fe toxicity, while *RiCCC1.2* transcript levels decreased under Mn toxicity. Collectively, these data indicate that RiCCC1.1, RiCCC1.2 and RiCCC1.3 play a role in Fe and Mn homeostasis in *R. irregularis*.

On the host plant side, we evaluated the impact of the AM symbiosis on the Fe-deficiency response of tomato plants. Shoot Fe concentration decreased by Fe deficiency and AM colonization, whereas root Fe concentration increased in AM plants both under Fe-limiting and –sufficient conditions. Fe deficiency decreased AM colonization. We first assessed expression patterns of the previously reported tomato genes playing a role in Fe uptake and distribution in roots of non-mycorrhizal and mycorrhizal plants grown under Fe-sufficient and -deficient conditions. It was shown that *SlNRAMP1* expression increased in mycorrhizal roots under Fe-sufficient conditions, while *SlNRAMP3* and *SlCHLN* expression was down-regulated. Under Fe-deficient conditions, AM up-regulates expression the *SlFRO1*, *SlIRT1* and *SlNRAMP3* genes, encoding proteins involved in transport Fe into the cytosol. The high accumulation of Fe observed in mycorrhizal roots prompted us to assess expression patterns of genes involved in vacuolar Fe compartmentalization. To that end, the tomato genome databases were searched for VIT transporters. Functional characterization in yeast of the four members of the *SlVIT/VTL* gene family revealed that while *SlVIT1*, *SlVTL1* and *SlVTL2* encode proteins mediating Fe and Mn transport, *SlVTL2* only transports Mn. Gene expression analyses revealed that under Fe-sufficient conditions *SlVIT1* and *SlVIT2* expression was down-regulated in AM roots and that expression of the Mn vacuolar transporter SlVTL2 was up-regulated by AM under both Fe-deficient and –sufficient conditions. All these data show that expression of the tomato Fe-deficiency response

genes is differentially regulated by AM under Fe-sufficient and -deficient conditions and suggest that AM colonization is regulated by Fe. These data are described in **Chapter 3**.

To further understand the importance of the Fe in AM symbiosis we used the Fe-inefficient mutant *chloronerva* (*chln*) of tomato (**Chapter 4**). AM development was impaired in the *chln* mutant, but partially reverted its growth defect. RNA sequencing revealed a low number of differentially expressed genes in the "*chln* vs wild-type" comparison in mycorrhizal than in non-inoculated roots. Gene Ontology and Kyoto Encyclopedia of Genes and Genomes pathways enrichment analysis revealed differential metabolic responses to AM colonization between roots of wild-type and *chln* mutant plants. Expression of a subset of genes that have been previously shown to be required for AM was lower in mycorrhizal roots of *chln* mutants compared to the wild-type. The lower expression levels of the Pi starvation-induced genes in non-mycorrhizal *chln* roots compared to wild-type and the higher P concentration of the *chln* plants suggests that reduced AM colonization of *chln* may involve Pi signalling pathways. Over-expression of Fe-deficiency response genes in *chln* roots was mitigated by AM colonization, which suggests that root AM colonization contributes to increase Fe availability and distribution in the *chln* mutants. All these data together indicate that there exists a connection between AM and Fe homeostasis.

In **Chapters 3** and **4**, we have shown that Fe impacts AM fungal colonization of tomato roots. With the aim of getting further insights into the relevance of Fe on AM development and function, Chapter 5 was aimed at studying by reverse genetics the impact of the *Rhizophagus irregularis* high-affinity Fe transporter RiFTR1 that is highly expressed in arbuscules in AM development. To that end, *RiFTR1* was both silenced and overexpressed in *Medicago truncatula* roots through Host-Induced Gene Silencing (HIGS) and Host-Induced Gene Overexpressing (HIGO), respectively. RiFTR1 was partially silenced in the RNAi1 lines; however, moderate down-regulation of *RiFTR1* did not significantly influence mycorrhizal colonization by *R. irregularis*. *RiFTR1* overexpression increased mycorrhizal intensity, the number of arbuscules and expression of the AM symbiotic marker *MtPT4*. These data indicate that RiFTR1 plays a positive role in AM colonization.

RESUMEN

El hierro (Fe) es un micronutriente esencial para el crecimiento y supervivencia de la mayoría de los organismos, ya que desempeñado un papel estructural clave en muchas proteínas y actúa como cofactor de múltiples enzimas. A pesar de que el Fe es uno de los elementos más abundantes en la naturaleza, a menudo no está disponible para las plantas debido a que se encuentra principalmente en su estado oxidado, Fe (III), lo que se agrava en los suelos alcalinos. Para evitar la clorosis férrica y las deficiencias de desarrollo asociadas a la limitación de Fe, las plantas han evolucionado una serie de estrategias que les permitan obtener eficientemente el Fe presente en la rizosfera. Las plantas no gramíneas utilizan la llamada "Estrategia I", que consta de una H^+-ATPasa de membrana plasmática que acidifica la rizósfera y solubiliza el Fe, de una reductasa férrica (FRO1) que reduce el Fe (III) a Fe (II) y de un transportador específico de Fe (II) (IRT) que para su absorción a través de la membrana plasmática. Por otro lado, las gramíneas utilizan la "Estrategia II", que incluye la producción y exudación de fitosideróforos (PS) que quelan el Fe (III) y transportadores de oligopéptidos YS1 o similares que transportan los quelatos PS-Fe a las células de la raíz.

Otra estrategia utilizada por las plantas para incrementar la absorción de hierro lo es el establecimiento de asociaciones beneficiosas con microorganismos del suelo. Los hongos micorrícicos arbusculares (MA), pertenecientes al subfilo Glomeromycotina, son unos de los principales microorganismos que contribuyen a la nutrición de las plantas. Estos hongos forman una simbiosis mutualista con la mayoría de las especies de plantas terrestres. Los hongos MA colonizan biotróficamente el córtex de la raíz, al tiempo que desarrollan una red extensa de hifas en el exterior de la raíz que alcanza y explora zonas del suelo no accesibles a la raíz. A cambio de los compuestos de carbono proporcionados por las plantas, los hongos suministran a la planta los nutrientes minerales que absorben más allá de las zonas de agotamiento de nutrientes desarrolladas alrededor de las raíces. Es ampliamente reconocido que los hongos MA ayudan a las plantas a obtener nutrientes de baja movilidad, como fósforo, nitrógeno, zinc, cobre y Fe. Además de mejorar la captación de nutrientes, los hongos MA incrementan la tolerancia de la planta hospedadora a estreses bióticos y abióticos. Los hongos MA desempeñan un papel crucial en la modulación de la adquisición de metales por parte de las plantas en un amplio rango de concentraciones de metales del suelo, ya que aumentan la adquisición de metales en suelos deficitarios en estos elementos, pero la reducen en suelos contaminados. Varios estudios han puesto de manifiesto que la simbiosis MA mejora el desarrollo de las plantas tanto en suelos deficientes como contaminados con Fe. Sin embargo, los conocimientos actuales sobre los mecanismos de transporte y homeostasis de Fe en MA son muy limitados.

En esta tesis doctoral, para profundizar en el entendimiento de e los mecanismos de homeostasis de Fe en MA, hemos utilizado un enfoque multidisciplinar que implicó el uso de metodologías *in silico*, fisiológicas y moleculares. El hongo MA seleccionado para la realización de la tesis fue el hongo modelo *Rhizophagus irregularis* DAOM197198 v2.0 and A1, A4, A5, B3 and C2 v1.0 que se cultivar fácilmente en cultivos monoxénicos in vitro y en sistemas bidimensionales in vivo de plantas completas. Para los estudios a nivel de la planta, usamos *Solanum lycopersicum*, un cultivo de gran importancia económica que se ha utilizado como planta modelo para el estudio de la homeostasis de Fe en plantas que utilizan la Estrategia I de captación de Fe.

Para profundizar en el estudio de la homeostasis de Fe en MA, en primer lugar, decidimos caracterizar funcionalmente los transportadores NRAMP de *R. irregularis*. Estos resultados se presentan en el **Capítulo 1**. Los transportadores NRAMP son transportadores ubicuos de metales, que desempeñan un papel clave en la homeostasis de metales, especialmente de manganeso (Mn) y de Fe. La familia NRAMP de *R. irregularis* está compuesta por cuatro miembros: RiSMF1, RiSMF2, RiSMF3.1 y RiSMF3.2. El análisis filogenético de las secuencias NRAMP de diferentes hongos MA mostró que se clasifican en dos grupos, que probablemente divergieron al principio de su evolución. Debido a que los hongos MA no pueden ser manipulados genéticamente, la funcionalidad de los genes *RiSMF* se analizó en un sistema heterólogo, concretamente en *Saccharomyces cerevisiae*. Desafortunadamente, solo se pudo determinar la función de RiSMF3.2 en el sistema heterólogo. Los ensayos de complementación de la cepa mutante de levadura *smf1*Δ, incapaz de absorber Mn, y de *fet3*Δ*fet4*Δ, que carece de los sistemas de absorción de Fe, revelaron que *RiSMF3.2* codifica una proteína de membrana plasmática que media la absorción de Mn y Fe. Los análisis de expresión génica mediante RT-qPCR mostraron que los genes *RiSMF* se expresan de manera diferencial en el micelio extraradical (ERM) e intraradical (IRM) y que se regulan diferencialmente por la disponibilidad de Mn y Fe en el medio de cultivo. En condiciones de deficicencia de Mn disminuyeron los niveles de transcripción de *RiSMF1* en el ERM, pero aumentó la expresión de *RiSMF3.1* en el IRM. La expresión de *RiSMF1* en el ERM incrementó por la deficiencia de Fe, lo que sugiere que la proteína RiSMF1 podría estar implicada en la mitigación de la deficiencia de Fe. La expresión del gen *RiSMF3.2* en el ERM incrementó en las etapas tempranas de toxicidad de Fe, pero disminuyó en etapas posteriores. Estos resultados sugieren que RiSMF3.2 no solo actúa como un transportador de Fe, sino también podría actuar como un sensor de altas concentraciones elevadas de Fe en el medio o que puede funcionar como un transportador de Fe de baja afinidad. Todos esto datos indican que *R. irregularis* utiliza varias estrategias para aumentar la captación de Fe: la permeasa de Fe de la membrana plasmática

RiFTR1 previamente identificada y el transportador RiSMF3.2. Además, en este capítulo describimos, por primera vez, un transportador de Mn en un hongo MA.

También se evaluó la respuesta morfogénica del ERM de *R. irregularis* a la deficiencia de Fe y Mn. La deficiencia de Mn aumentó la longitud de las hifas, lo que indica que, en estas condiciones, el hongo explora un volumen mayor de suelo, por lo que aumentará la efectividad de la absorción de nutrientes por la raíz micorrizada. Sin embargo, la deficiencia de Fe redujo la esporulación, probablemente como consecuencia de la inhibición de la actividad de las enzimas que requieren Fe que están involucradas en la formación de las esporas. La acumulación de Fe detectada en las esporas desarrolladas bajo toxicidad de Fe respalda la idea de que una estrategia de supervivencia de los hongos MA en ambientes contaminados con metales es acumular parte del exceso de metal en algunas esporas de la colonia fúngica.

Los hongos controlan estrictamente la concentración en el citosol mediante la regulación de los sistemas de captación de Fe y almacenamiento en las vacuolas. El transporte de Fe hacia las vacuolas ocurre mediante la actuación de transportadores de la familia Ccc1/VIT. Por lo tanto, una vez que identificamos los transportadores de *R. irregularis* involucrados en el transporte de Fe hacia el citosol en *R. irregularis*, decidimos caracterizar los transportadores de Fe vacuolares de la familia Ccc1/VIT, RiCCC1.1, RiCCC1.2 y RiCCC1.3. Los análisis bioinformáticos de las secuencias deducidas de aminoácidos de los genes CCC1 de *R. irregularis* revelaron que tienen todos los dominios y residuos esenciales requeridos para el transporte de Fe, incluyendo el dominio de unión a metales (MBD) que está formado por las hélices H1 y H3 y el extremo C-terminal del segundo dominio transmembrana. Los análisis funcionales en levadura revelaron que RiCCC1.1 y RiCCC1.2, pero no RiCCC1.3, complementaron el fenotipo mutante de una cepa de *S. cerevisiae* defectiva en el transporte vacuolar de Fe. RiCCC1.1 y RiCCC1.2 también complementaron la sensibilidad a Mn de la cepa pmr1Δ a concentraciones tóxicas de Mn. Los genes *RiCCC1* se expresaron de manera diferencial en el ERM, IRM y arbúsculos. En el ERM, la expresión de *RiCCC1.2* disminuyó en condiciones de deficiencia de Fe, pero incrementó transitoriamente en condiciones de toxicidad. Estos resultados sugieren un papel para RiCCC1.2 en la movilización del Fe vacuolar en condiciones limitantes de Fe y en la detoxificación de Fe en condiciones de toxicidad. La expresión de *RiCCC1.3* incrementó transitoriamente por la toxicidad de Fe, mientras que los niveles de transcripción de *RiCCC1.2* disminuyeron bajo toxicidad de Mn. En conjunto, estos datos indican que RiCCC1.1, RiCCC1.2 y RiCCC1.3 juegan un papel en la homeostasis de Fe y Mn en *R. irregularis*.

A nivel de la planta hospedadora, evaluamos el impacto de la simbiosis MA en la respuesta de las plantas de tomate a la deficiencia de Fe. La concentración de Fe en la parte aérea disminuyó

por la deficiencia de Fe y la colonización MA, mientras que la concentración de Fe en la raíz aumentó en las plantas MA tanto en condiciones óptimas como deficientes de Fe. La deficiencia de Fe disminuyó la colonización MA. En primer lugar, evaluamos los patrones de expresión de genes de tomate que codifican proteínas implicadas la absorción y distribución de Fe en las raíces de las plantas no micorrizadas y micorrizadas cultivadas en condiciones óptimas y deficientes de Fe. En condiciones óptimas de Fe, la expresión de *SlNRAMP1* aumentó en las raíces micorrizadas, mientras que la de *SlNRAMP3* y *SlCHLN* disminuyó. En condiciones de deficiencia de Fe, las MAs incrementaron la expresión de los genes *SlFRO1*, *SlIRT1* y *SlNRAMP3*, que codifican proteínas involucradas en el transporte de Fe hacia el citosol. La alta acumulación de Fe observada en las raíces micorrizadas nos llevó a evaluar los patrones de expresión de los genes involucrados en la compartimentación vacuolar de Fe. Para ello, se buscaron en las bases de datos del genoma de tomate transportadores VIT. La caracterización funcional en levadura de los cuatro miembros de la familia génica *SlVIT/VTL* reveló que *SlVIT1*, *SlVTL1* y *SlVTL2* codifican proteínas que median el transporte de Fe y Mn, mientras que SlVTL2 solo transporta Mn. Los análisis de expresión génica revelaron que, en condiciones óptimas de Fe, la expresión de *SlVIT1* y *SlVIT2* disminuyó en las raíces MA y que la expresión del transportador vacuolar de Mn SlVTL2 aumentó en raíces micorrizadas, tanto en condiciones de deficiencia como de suficiencia de Fe. Todos estos datos muestran que la expresión de los genes de respuesta a deficiencia de Fe en tomate se regulan de manera diferencial por MA en condiciones de suficiencia y deficiencia de Fe, y que la colonización MA está regulada por el Fe. Estos datos se describen en el **Capítulo 3**.

Para comprender mejor la importancia del Fe en la simbiosis MA, utilizamos el mutante de Fe *chloronerva* (*chln*) deficiente en la regulación del metabolismo del Fe (**Capítulo 4**). La colonización micorrícica y la expresión de los marcadores de micorrización disminuyeron en las plantas mutantes chln. El desarrollo de las MAs revertió parcialmente el fenotipo del mutante. El análisis transcriptómico mediante RNAseq mostró que el número de genes expresados diferencialmente en la comparación "*chln* vs wild-type" fue menor en raíces micorrizadas que en las no inoculadas. Los análisis *"Gene Ontology"* y "*Kyoto Encyclopedia of Genes and Genomes pathways*" de los genes expresados diferencialmente mostraron que las respuestas metabólicas de las raíces de las plantas silvestres y mutantes la colonización MA fueron diferentes. La expresión de una serie de genes necesarios para la formación de las MAs fue menor en las raíces micorrizadas de los mutantes *chln* que en las de las plantas silvestres. La observación de que la expresión de los genes de respuesta a deficiencia de fósforo fue inferior en las raíces no micorrizadas del mutante que en las del silvestre y que la concentración de P fue superior en las plantas *chln* sugieren que la reducción de la colonización MA de los mutantes *chln* puede implicar

vías de señalización de Pi. La sobreexpresión de los genes de respuesta a la deficiencia de Fe en las raíces *chln* se mitigó por la colonización MA, lo que sugiere que las MAs contribuyen a aumentar la disponibilidad y distribución de Fe en los mutantes *chln*. Todos estos datos en su conjunto indican que existe una conexión entre las MAs y la homeostasis de Fe.

En los **Capítulos 3** y **4**, hemos demostrado que el Fe afecta la colonización micorrícica de las raíces de tomate. Con el objetivo de obtener más información sobre la relevancia del Fe en el desarrollo y función de las MAs, decidimos estudiar, utilizando técnicas de genética reversa, el impacto del transportador de alta afinidad de Fe RiFTR1 de *Rhizophagus irregularis* que se expresa en arbúsculos en el desarrollo de las MAs (**Capítulo 5**). Para ello, *RiFTR1* se silenció y sobreexpresó en raíces de *Medicago truncatula* mediante silenciamiento génico inducido por el hospedador (HIGS del inglés "host induced gene silencing") y sobreexpresión génica inducida por el hospedador (HIGO del inglés "*host induced gene overexpression*"), respectivamente. En las líneas RNAi-1 se consiguió un silenciamento parcial de *RiFTR1*, que no tuvo ningún efecto significativo sobre el desarrollo de la simbiosis. La sobreexpresión de *RiFTR1* aumentó la intensidad micorrícica, el número de arbúsculos y la expresión del marcador simbiótico MA *MtPT4*. Estos datos indican que RiFTR1 ejerce un papel positivo en la colonización MA.

INTRODUCCIÓN

1. La simbiosis micorrícica arbuscular (MA)

1.1. Tipos de micorrizas

La palabra micorriza tiene su origen en el griego "*mycos*" hongo y "*riza*" raíz y tal como su etimología indica describe la asociación simbiótica mutualista entre determinados hongos del suelo y las raíces de las plantas terrestres. Este término fue utilizado por primera vez por Bernhardt Frank en 1885, pero no es hasta mediados del siglo XX cuando empezó a comprenderse el significado y la importancia de esta asociación. Básicamente, la planta hospedadora obtiene del hongo agua y nutrientes minerales mientras que el hongo recibe compuestos carbonados procedentes de la fotosíntesis del hospedador necesarios para que el hongo complete su ciclo vital (Barea & Azcón-Aguilar, 2013) Los hongos micorrícicos colonizan la raíz y desarrollan un micelio extraradical (ERM) que crece más allá de la zona del suelo colonizada por las raíces. La estructura formada por la red de hifas está especializada en la adquisición de nutrientes minerales del suelo. Los beneficios de las micorrizas son tales que se estima que entre el 90 y 95% de las plantas terrestres son capaces de establecer algún tipo de micorriza y que la mayoría de las plantas se encuentran micorrizadas de forma natural en los ecosistemas (Brundrett & Tedersoo, 2018).

Mediante patrones morfológicos y criterios funcionales se han descrito tres tipos de micorrizas, en las que participan distintos grupos de hongos y plantas hospedadoras: las ectomicorrizas, las endomicorrizas y las ectendomicorrizas, un grupo intermedio entre las dos anteriores. Los tipos más representativos y estudiados son las ectomicorrizas y las endomicorrizas debido a su importancia forestal y agrícola, respectivamente.

Las ectomicorrizas se presentan en especies de interés forestal pertenecientes a las familias *Fagaceae*, *Pinaceae*, *Betulaceae*, *Nothofagaceae*, *Dipterocarpaceae* y *Caesalpinaceae* (Tedersoo et al., 2010). Los hongos responsables pertenecen mayoritariamente a la división Basidiomycota y algunos Ascomycetes y Zigomycotes. Se caracterizan por desarrollar "manto", un entramado compacto de hifas que rodea la superficie de la raíz (Smith & Read, 2008). Las hifas penetran en la raíz, pero no en el interior de las células. El hongo ocupa los espacios intercelulares de las células epidérmicas y corticales formando la denominada "red de Hartig", en la cual se produce el intercambio de nutrientes entre los simbiontes (Brundrett & Tedersoo, 2018).

Las endomicorrizas se caracterizan porque las hifas son capaces de penetrar en el interior de las células de la epidermis y/o córtex de la raíz, pero sin atravesar la membrana plasmática. Existen tres subgrupos fundamentales, las Ericoides, Orquidoides y micorrizas arbusculares (MA). Las dos primeras son características de las plantas pertenecientes al orden Ericales y la familia Orquidaceae, respectivamente. Las MA, objeto de esta tesis doctoral, constituyen el grupo más ampliamente distribuido por el reino vegetal (Brundrett & Tedersoo, 2018). Esta asociación

la establecen entre el 70 y el 80% de las plantas terrestres con hongos del suelo pertenecientes al subfilo Glomeromycotina, los hongos formadores de micorrizas arbusculares (hongos MA). Estos hongos son microscópicos, su distribución es universal y son simbiontes estrictos, es decir, son incapaces de completar su ciclo de vida en ausencia de una planta hospedadora, lo que dificulta su uso y estudio. Esta asociación se caracteriza por la formación de arbúsculos, unas estructuras intracelulares ramificadas en forma de árbol, dentro de las células del córtex de la raíz. Los arbúsculos se encuentran rodeados de la membrana plasmática de la célula que los alberga sin llegar a atravesarla (Figura 1). Esta membrana de las células corticales, denominada membrana periarbuscular, junto a la membrana plasmática del hongo poseen proteínas transportadoras que permiten el intercambio de nutrientes entre los organismos que forman la simbiosis. El espacio generado entre la membrana fúngica y vegetal se denomina espacio periarbuscular.

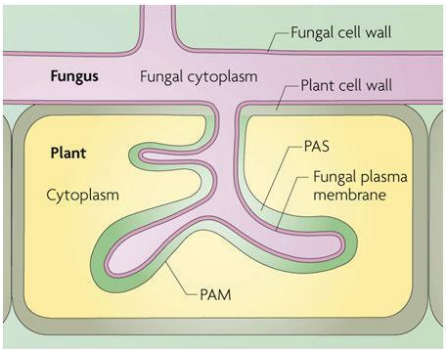

Figura 1. Esquema de una célula cortical colonizada por un arbúsculo. Se indican los componentes de la interfase simbiótica: Membrana periarbuscular (PAM, del inglés "periarbuscular membrane"), espacio periarbuscular (PAS, del inglés "periarbuscular space") y membrana plasmática del hongo (Parniske, 2008).

1.2. Filogenia de los hongos MA

El primer registro fósil, consistente en esporas e hifas sin asociación con restos vegetales, sugieren que el origen de los hongos MA se remonta al Ordovícico, momento en el que tuvo lugar la colonización del medio terrestre por las plantas, hace unos 460 millones de años. Pirozynski & Malloch (1975) sugirieron que los hongos MA habían desempeñado un papel clave en esta transición, ayudando a los antecesores de las plantas actuales en la absorción de agua y nutrientes. Sin embargo, los primeros fósiles bien preservados de la simbiosis MA son rizomas micorrícicos de hace 407 millones de años, por lo que se ha cuestionado si los hongos micorrícicos se originaron en el Ordovícico o posteriormente con el aumento en la complejidad vegetal que tuvo lugar en el Silúrico (Brundrett & Tedersoo, 2018). Las evidencias filogenómicas emplazan el origen de los hongos MA en el período Silúrico medio a tardío, hace unos 420 millones de años (Bonfante & Venice, 2020; Hoysted et al., 2018).

Antes de la aplicación de las técnicas moleculares al estudio de los hongos MA, su identificación se basaba en el análisis de características con valor taxonómico de las esporas, como por ejemplo forma, color, tamaño, presencia de septos o conexión con la hifa que la sustenta. Los primeros intentos para clasificar los hongos MA se remontan a finales del siglo XIX y principios del XX cuando se incluyeron en la familia *Endogonazeae*, perteneciente al filo polifilético Zigomycota. Sin embargo, estas similitudes morfológicas no siempre reflejan fielmente relaciones filogenéticas. Mediante el análisis de la secuencia del gen que codifica la subunidad pequeña del ARN ribosómico, Schüβler y colaboradores (2001), separaron los hongos MA en un nuevo filo monofilético Glomeromycota. No obstante, en 2016 Spatafora y colaboradores determinaron el carácter parafilético de los Zigomycetes y los dividieron en dos filos Zoopagomicota y Mucoromycota, en este último fueron incluidos los hongos MA dentro del subfilo Glomeromycotina. Posteriormente, Wijayawardene y colaboradores (2018) volvieron a separar el filo Glomeromycota, por lo que aún no hay consenso en su clasificación taxonómica (Figura 2).

Dentro del subfilo Glomeromycotina, la clasificación también ha sufrido variaciones con la incorporación de técnicas moleculares. Actualmente el filo está representado por 1 clase, 4 órdenes, 12 familias, 44 géneros y 341 especies (lista actualizada en noviembre de 2021 de la web http://www.amf-phylogeny.com/).

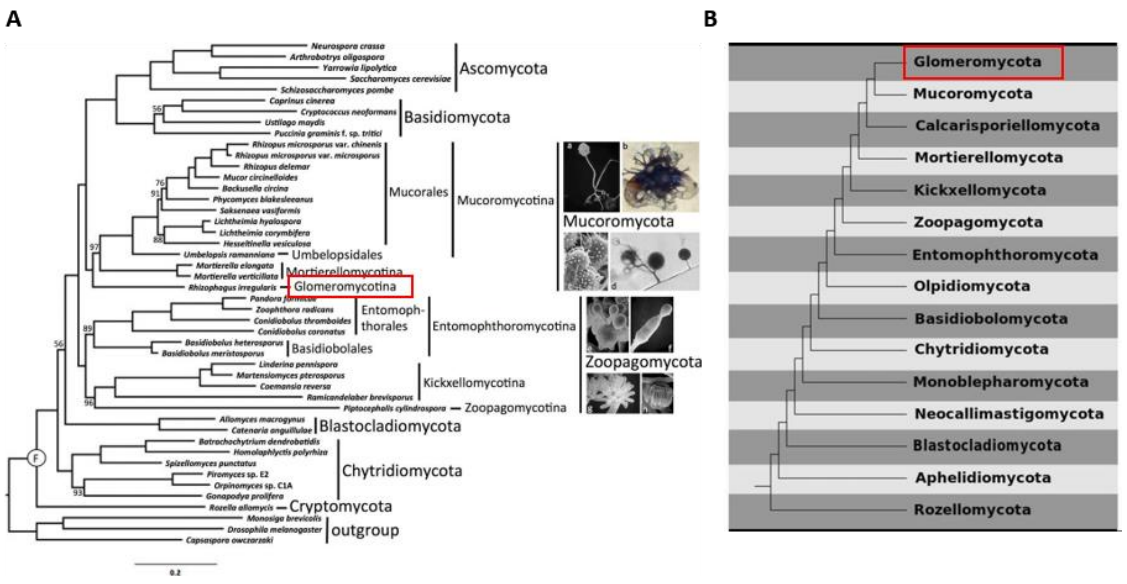

Figura 2. Filogenias propuestas para los hongos MA. **A**, Filogenia propuesta por Spatafora y colaboradores (2016) en la que se considera a los hongos MA pertenecientes al subfilo Glomeromycotina. **B**, filogenia propuesta por Wijayawardene y colaboradores (2018) en la que los hongos MA son incluidos en el filo Glomeromycota. La ubicación de los hongos MA en las filogenias está indicada con un cuadro rojo.

1.3. Características generales de los hongos MA

La principal característica que los define es su biotrofía obligada, es decir, todos los hongos MA requieren de una planta hospedadora para completar su ciclo de vida, quizá debido a su evolución conjunta durante millones de años. Actualmente se considera que la incapacidad de los hongos MA para sintetizar ácidos grasos *de novo* es responsable de la biotrofía obligada del hongo (Wewer et al., 2014a). Por ello, en estudios destinados a la obtención de biomasa fúngica en cultivos axénicos los medios de cultivo están siendo suplementados con los ácidos grasos (S)-12-methyltetradecanoico (Kameoka et al., 2019) y miristato (Sugiura et al., 2020), habiéndose obtenido resultados prometedores. No obstante, es posible obtener material fúngico libre de material vegetal y de otros microorganismos, ya que es posible cultivarlos *in vitro* en cultivos monoxénicos con raíces transformadas con *Agrobacterium rhizogenes*. Este tipo de cultivo no está adaptado para todos los hongos MA, por lo que la mayoría de estudios moleculares se centran en la especie *Rhizophagus irregularis* debido a su capacidad para crecer en cultivos monoxénicos (St-Arnaud et al., 1996) y porque fue el primer genoma que se secuenció de un hongo MA (Chen et al., 2018; Tisserant et al., 2013).

Los hongos MA poseen hifas cenocíticas y esporas multinucleadas. El número de núcleos varía entre especies, desde los 720 de *Scutellospora castanea* (Hosny et al., 1998) a los 2600 en especies del género *Gigaspora* (Bécard & Pfeffer, 1993; Cooke et al., 1987). Jany y Pawlowska (2010) propusieron que el principal mecanismo para la formación de estas esporas multinucleadas podría ser el flujo masivo de núcleos desde la hifa de sustentación hacia la espora en formación. Aunque no se hayan detectado experimentalmente células meióticas, el descubrimiento de la presencia de genes implicados en la meiosis (Halary et al., 2011; Tisserant et al., 2012, 2013) y de genes tipo MAT (mating-type) relacionados con el apareamiento fúngico en Dikarya (Corradi & Brachmann, 2017; Ropars et al., 2016) en el genoma de *R. irregularis* cuestionan la visión de que los hongos MA no tengan capacidad para reproducirse también sexualmente. Para aumentar el patrimonio genético, los núcleos son capaces de viajar por las hifas y ser transferidos a de un micelio a otro genéticamente diferente mediante procesos de anastomosis (Figura 3). También existen evidencias de recombinación entre núcleos de un mismo individuo (Chen et al., 2018). Para que esto ocurra los núcleos deben tener una similaridad de al menos el 99.8% mediante un proceso similar a la meiosis, aunque no se observa apareamiento.

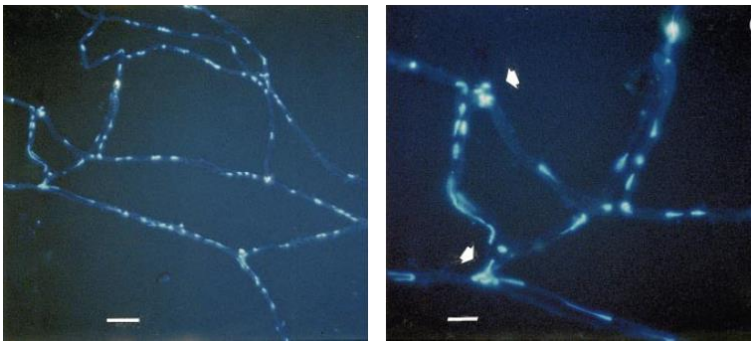

Figura 3. Anastomosis de hifas de ERM del hongo *Funeliformis mosseae* teñidas con DAPI y visualizadas mediante un microscopio de fluorescencia. Las flechas indican acumulación núcleos en las zonas de fusión de hifas (Giovannetti et al., 2001).

La biotrofía obligada y los múltiples núcleos presentes tanto en esporas como en micelio, limitan la aplicación de técnicas de biología molecular destinadas a estudios de funcionalidad génica. Se ha conseguido expresar de forma transitoria el gen reportero β-glucuronidase (GUS) en *Gigaspora rosea* (Forbes et al., 1998) y los marcadores fluorescentes proteína verde fluorescente (*green fluorescence protein*, GFP) y proteína fluorescente roja (*red fluorescent protein*, DsRED) en *R. intraradices* (Helber & Requena, 2008) mediante bombardeo de partículas, pero no se han definido aún protocolos de transformación genética estable para los hongos MA, por lo que los estudios de caracterización funcional tradicionalmente se llevan a cabo en sistemas heterólogos en levadura (Sanders, 1999). La aproximación más novedosa es el uso de estrategias de silenciamiento génico inducido por la planta ("*host induced gene silencing*", HIGS) o por virus ("*virus induced gene silencing*",VIGS), aunque su aplicación es compleja y no siempre exitosa, sobre todo para genes con niveles de transcripción bajos en el micelio intrarradical (IRM) (Helber et al., 2011; Kikuchi et al., 2016; Voß et al., 2018).

Finalmente, se han identificado bacterias endosimbióticas en el citoplasma de algunos hongos MA, cuyos origen y función no están claros (Bianciotto et al., 2000, 2003; Desirò et al., 2014; Naumann et al., 2010). Dentro de la familia Gigasporaceae existe un tipo de endosimbionte con forma de bacilo que, al igual que los propios hongos, son incapaces de desarrollar su ciclo de vida de forma independiente. Estudios moleculares revelan una relación de estas bacterias (identificadas como *Candidatus Glomeribacter gigasporarum*) con *Burkholderia*. Existen evidencias de que estas bacterias pueden afectar la morfología de las esporas y modificar el crecimiento presimbiótico de *Gigaspora margarita* (Lumini et al., 2007). Otro tipo de endosimbionte con forma de coco denominado BLOs (del inglés *bacterium-like organisms*), detectado tanto en esporas como hifas de hongos MA (MacDonald et al., 1982), están relacionadas con Mollicutes, un grupo de bacterias carentes de pared que son parásitos celulares de algunas plantas y animales (Naumann

et al., 2010). La presencia de estas bacterias endosimbiontes añade otro nivel de complejidad al estudio de las micorrizas.

1.4. Establecimiento de la simbiosis

Usualmente el establecimiento de la simbiosis está descrito en tres etapas, aunque en realidad es un proceso asincrónico, por lo que en la misma raíz colonizada podemos encontrar al hongo en sus distintos estadios de desarrollo, lo cual dificulta su estudio.

La primera etapa es la fase de crecimiento asimbiótico en la que la espora es capaz de germinar y crecer de forma autónoma durante un breve periodo de tiempo. De hecho, las esporas pueden experimentar varias rondas de germinación y retracción de las hifas hasta encontrar una raíz que pueda ser colonizada (Azcón-Aguilar et al., 1999). Las esporas son estructuras inactivas que germinarán cuando las condiciones del entorno sean favorables para colonizar un hospedador. El establecimiento de la simbiosis MA se lleva a cabo mediante una serie de pasos controlados genéticamente y comienza con la segunda fase, la fase presimbiótica, donde se establece una comunicación molecular previa al contacto físico entre simbiontes (Nadal & Paszkowski, 2013) (Figura 4). Las plantas exudan estrigolactonas que estimulan la germinación de las esporas cercanas a la raíz. Las estrigolactonas son moléculas pertenecientes al grupo de las lactonas terpenoides derivadas del metabolismo de los carotenoides y que son liberadas a la rizosfera por la mayoría de las plantas a través de las raíces, especialmente en condiciones de deficiencia de fósforo (Ruyter-Spira et al., 2013). Estas moléculas incrementan la ramificación y elongación de las hifas y estimulan la germinación y actividad metabólica de los hongos MA (Akiyama et al., 2005). La secreción de estrigolactonas por parte de la raíz y su rápida degradación genera un gradiente de concentración que proporciona información posicional acerca de la proximidad de la raíz (Kretzschmar et al., 2012). Los flavonoides también están implicados en la etapa presimbiótica, ya que al incrementar la concentración del flavonoide quercetina en los exudados radiculares se incrementa la colonización de los hongos MA (Tian et al., 2021).

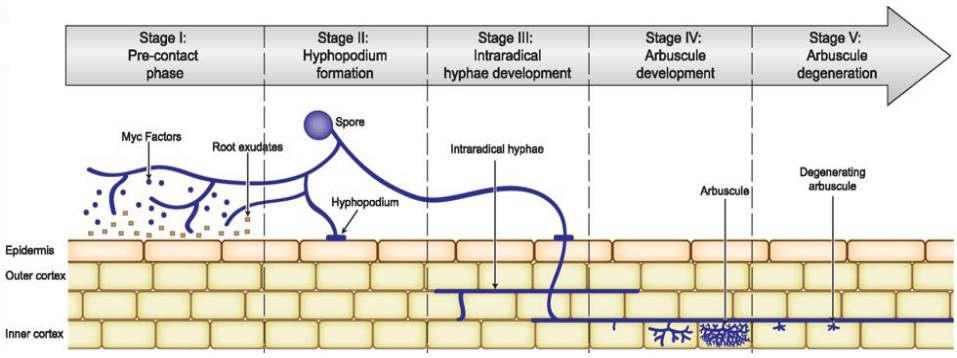

Figura 4. Etapas del desarrollo de la simbiosis MA (Pimprikar & Gutjahr, 2018).

Simultáneamente, los hongos MA también producen factores difusibles, llamados factores Myc ("Myc factors") (Genre et al., 2013; Kosuta et al., 2003; Maillet et al., 2011), que incluyen lipo-quito-oligosacáridos (Myc-LCOs) muy similares a los factores Nod secretados por *Rhizobium*, tetra o penta-quito-oligosacáridos (Myc-COs) y oligómeros de quitina. Los picos de Ca^{2+} que desencadenan los factores Myc en la planta son muy similares a los producidos en la señalización simbiótica *Rhizobium*-leguminosa, habiéndose comprobado que ambas simbiosis comparten parte de una ruta de señalización denominada "common symbiosis pathway"(Genre & Russo, 2016; Oldroyd, 2013).

La fase simbiótica comienza cuando una hifa del hongo MA entra en contacto con la superficie de una raíz y forma una estructura de adhesión denominada hifopodio o apresorio. Antes de que el hongo comience a penetrar, en la raíz comienza una reorganización celular que da lugar a la formación de una especie de túnel transcelular, llamado aparato de pre-penetración, a través del cual la hifa penetra en la raíz y es guiada hasta las células del córtex donde forman los arbúsculos (Genre et al., 2008). Los arbúsculos no son estructuras permanentes, su vida media es de entre 8 y 9 días (Alexander et al., 1989; Javot et al., 2007), trascurrido ese tiempo colapsan, se degradan y se forman nuevos arbúsculos. Todas las estructuras intracelulares del hongo están aisladas del citoplasma de la célula hospedadora mediante la membrana plasmática de las células del hospedador, generándose entre ambas la llamada interfase simbiótica. En esta interfase se produce el intercambio bidireccional de nutrientes, principalmente, en las células colonizadas por arbúsculos.

Simultáneamente a la colonización radical, el hongo desarrolla una red de ERM en el suelo. Las hifas exploradoras, relativamente más gruesas, exploran y extienden el micelio hasta distintos microhábitats. Eventualmente estas hifas sufrirán ramificaciones, hifas secundarias, que seguirán ramificándose sucesivamente (Bago et al., 1998). Sobre las hifas se desarrollan unas estructuras ramificadas de absorción, llamadas BAS, del inglés "branching absorbing structures", citológicamente similares a los arbúsculos, cuya función es la absorción de agua y nutrientes del suelo ((Bago, 2000; Bago et al., 1998; Kameoka et al., 2019). Los BAS son estructuras con una vida media de unos 21 días, tras los cuales retraen su contenido citoplasmático, a menos que desarrollen esporas, cerrándose de este modo el ciclo vital del hongo.

1.5. Beneficios de la simbiosis MA

Como se ha mencionado anteriormente la simbiosis MA es una relación mutualista basada en el intercambio bidireccional de nutrientes entre el hongo y la planta.

1.5.1. Beneficios obtenidos por el hongo

Como biotrofo obligado, el hongo depende del suministro de compuestos carbonados, en forma de carbohidratos o de lípidos, por parte de la planta hospedadora para su desarrollo. Se han descrito transportadores de azúcares de la planta pertenecientes a las familias SUT (transportadores de sacarosa), MST (transportadores de monosáridos) y SWEET (Manck-Götzenberger & Requena, 2016; Tamayo et al., 2022) cuya expresión se induce en raíces micorrizadas. Por otro lado, el transportador de alta afinidad de monosacáridos MST2 del hongo MA *R. irregularis* es el principal responsable de la captación de monosacáridos de la interfase simbiótica y su silenciamiento génico provoca una drástica disminución de la colonización intrarradical del hongo y la aparición de arbúsculos truncados (Helber et al., 2011).

Estudios más recientes muestran que los hongos MA son auxótrofos en ácidos grasos y, por tanto, altamente dependientes de los ácidos grasos procedentes de la planta. El análisis del genoma de los hongos MA no ha revelado la presencia de ningún gen que codifique miembros del complejo FAS (del inglés *fatty acid synthase*) (Kamel et al., 2017; Lin et al., 2014; Tisserant et al., 2012, 2013), esencial para la síntesis de ácidos grasos *de novo* (Tang et al., 2016; Wewer et al., 2014b). Experimentalmente se ha observado que, en leguminosas mutantes carentes de genes implicados en la biosíntesis de lípidos, los arbúsculos que se formaban estaban poco desarrollados y que se reducía la colonización (Bravo et al., 2017; Keymer & Gutjahr, 2018; Pimprikar et al., 2016; Wang et al., 2012). La alta dependencia de ácidos grasos y la elevada cantidad de lípidos que se acumulan en las esporas podrían explicar cómo el hongo se sustenta durante la fase presimbiótica hasta la formación de los primeros arbúsculos, en donde podría obtener ácidos grasos de la planta (Lanfranco et al., 2018). Dado que se ha demostrado que los hongos MA son capaces de absorber monosacáridos del suelo (Helber et al., 2011), actualmente se considera que la dependencia de la transferencia de ácidos grasos procedentes de la planta hospedadora es el principal motivo de su biotrofía obligada (Lanfranco et al., 2018).

Se estima que la planta destina hasta el 20% del carbono fijado en la fotosíntesis al simbionte fúngico (Roth & Paszkowski, 2017), una alta inversión que generalmente es compensada por los beneficios que la simbiosis proporciona a la planta.

1.5.2. Beneficios obtenidos por la planta hospedadora

La mejora del estado nutricional e hídrico es el principal beneficio que obtienen las plantas micorrizadas. El incremento del volumen de suelo que puede ser explorado gracias al desarrollo del ERM, más allá de la zona de depleción de nutrientes, explica en gran medida la mejora en la adquisición de agua, macro y micronutrientes como el fósforo, el cobre, el zinc o el hierro (Javot

et al., 2007; Smith et al., 2011). En las plantas micorrizadas coexisten dos sistemas de captación de nutrientes, la vía directa a través de las células epidérmicas de la raíz, en la que están implicados transportadores de nutrientes expresados en las células epidérmicas de la raíz, y la vía indirecta o micorrícica mediante las hifas del hongo, en la que intervienen transportadores expresados en el ERM y transportadores del hongo y de la planta expresados en las membranas plasmáticas de ambos organismos que componen la interfase simbiótica (Wipf et al., 2019) (Figura 5).

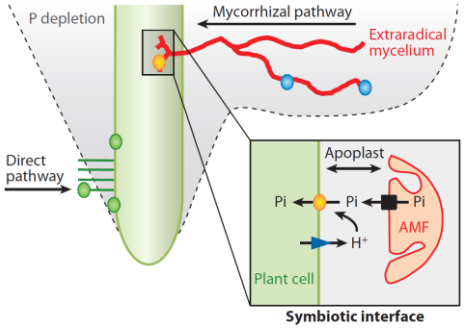

Figura 5. Esquema de las vías de adquisición de nutrientes en raíces micorrizadas. Modificada de Smith & Smith, 2011.

La planta hospedadora no solo recibe beneficios nutricionales. La simbiosis MA también incrementa la resistencia de las plantas a estreses tanto bióticos como abióticos que no puede ser explicada únicamente por la mejora de su estado nutricional. Paradójicamente, las micorrizas no solo mejoran la absorción de micronutrientes de baja movilidad en el suelo, sino que incrementan la resistencia de las plantas al estrés causado por concentraciones elevadas metales pesados (Ferrol et al., 2016; Riaz et al., 2021; Schutzendubel & Polle, 2002). Las micorrizas también protegen del ataque de microorganismos patógenos e insectos, tanto en el sistema radicular como aéreo, gracias al "*priming*" inducido durante la colonización del hongo MA que genera una activación más eficiente de los sistemas de defensa de la planta (Jung et al., 2012; Pozo et al., 2010; Rivero et al., 2021). En condiciones de estrés hídrico y salino, los hongos MA, además de proporcionar agua procedente de reservorios inaccesibles para las raíces (Ruth et al., 2011), pueden modificar el ajuste osmótico de la planta (Ruíz-Lozano et al., 2011; Sheng et al., 2011), regular la expresión de acuaporinas (Aroca et al., 2007; Calvo-Polanco et al., 2014, 2016; Quiroga et al., 2017) y proteger de las especies reactivas de oxígeno (ROS) generadas por las condiciones de estrés osmótico (Quiroga et al., 2017; Zou et al., 2021).

La simbiosis MA también tiene impacto en la calidad del suelo (Rillig et al., 2015), en la composición microbiana de la rizosfera (Artursson et al., 2006; Barea et al., 2005; Wang et al., 2021) y en la estructura y composición de las comunidades vegetales (Cipollini et al., 2012; Klironomos et al., 2000; van der Heijden et al., 2008; Wagg et al., 2011). Gracias a la capacidad de

anastomosis entre hifas de ERM, distintas especies vegetales se conectan a través de sus raíces e intercambiar información y recursos (Simard, 2018).

1.6. Mecanismos de transporte de nutrientes en MA

El estudio del transporte de nutrientes en MA ha estado centrado principalmente en el fósforo, nitrógeno, azufre, potasio y algunos micronutrientes.

1.6.1. Transporte de fósforo

La mejora de la nutrición fosforada ha sido considerada tradicionalmente el principal proceso por el cual la simbiosis mejora el crecimiento vegetal (Barea et al., 2008; Ferrol et al., 2019). El fósforo es un macronutriente de baja movilidad que se encuentra en el suelo principalmente en forma de dihidrógeno fosfato $H_2PO_4^-$ (Pi). La absorción por la planta rápidamente consume el Pi presente en la solución del suelo que rodea la raíz, generándose una zona de depleción alrededor de las mismas. En respuesta, las plantas han desarrollado una serie de mecanismos para paliar la escasez, tales como secreción de fosfatasas, exudación de ácidos grasos, alteraciones en la arquitectura del sistema radica y establecimiento de simbiosis con los hongos MA.

La absorción del fósforo por la vía micorrícica comienza con la absorción del Pi del suelo a través del ERM. Se han caracterizado en varios hongos MA cotransportadores $Pi:H^+$ (PT) homólogos al transportador de alta afinidad PHO84 de levadura *Saccharomyces cerevisiae* (Ferrol et al., 2019). Al transportador caracterizado en *Gigaspora margarita* (GigmPT; Xie et al., 2016) se le atribuye función de transceptor, es decir, no actúa únicamente como transportador sino también como receptor de Pi (Kriel et al., 2011). Parte del Pi captado por el ERM es rápidamente almacenado en la vacuola, donde se forman cadenas de polifosfatos (poliP), siendo estas vacuolas cargadas del poliP las responsables de translocar el fósforo al IRM (Ezawa et al., 2004; Hijikata et al., 2010). Una vez llegan a los arbúsculos, las cadenas de poliP son hidrolizadas de nuevo a Pi mediante la acción de fosfatasas y es transportado desde la vacuola al citosol. Recientemente se identificado y caracterizado un transportador de Pi de *R. irregularis* (RiPT7) que estaría implicado en la exportación de Pi desde el arbúsculo al espacio periarbuscular (Xie et al., 2022). La célula hospedadora absorbe el Pi a través de transportadores presentes en la membrana periarbuscular inducidos específicamente por la simbiosis y que han sido caracterizados en numerosas especies vegetales, como *Medicago truncatula* (MtPT4), *Oryza sativa* (OsPT11) y *Zea mays* (ZmPth1;6) entre otras (Harrison et al., 2002; Javot et al., 2007; Yang et al., 2012). La captación de Pi por la vía micorrícica es tan importante que el desarrollo de la simbiosis provoca la represión de los transportadores de Pi de la planta presentes en las células epidérmicas (Liu et al., 1998).

1.6.2. Transporte de nitrógeno

Hasta un 42% del nitrógeno de la planta puede proceder de la vía micorrícica (Mäder et al., 2000). Los hongos pueden absorber el nitrógeno del suelo tanto en forma inorgánica (NO_3^- y NH_4^+) como orgánica (péptidos pequeños y aminoácidos) (Govindarajulu et al., 2005; Jin et al., 2005). Se han identificado y caracterizado varios transportadores de nitrógeno en varios hongos MA. Concretamente en *R. irregularis* se han descrito tres transportadores de amonio (Calabrese et al., 2016; López-Pedrosa et al., 2006; Pérez-Tienda et al., 2011) y un transportador de nitrato (Tian et al., 2010), además se ha descrito una permeasa de aminoácidos en *Funneliformis mosseae* (Cappellazzo et al., 2008). Una vez tomado del suelo, la mayoría del nitrógeno inorgánico es incorporado a arginina y translocado en el interior de vacuolas hasta el IRM (Cruz et al., 2007; Govindarajulu et al., 2005). Ya en los arbúsculos se metaboliza la arginina y el NH_4^+ es liberado y exportado al espacio periarbuscular donde será captado por los transportadores de la planta presentes en la membrana periarbuscular (Govindarajulu et al., 2005; Tian et al., 2010). Se han descritos transportadores de amonio inducidos por micorrizas en *M. truncatula*, *Lotus japonicus*, *Glycine max*, *Sorgum bicolor* y *O. sativa* (Gomez et al., 2009; Guether et al., 2009; Kobae et al., 2010; Pérez-Tienda et al., 2014), de entre los cuales, los de *L. japonica*, *G. max* y *M. truncatula* han sido localizados en células colonizadas por arbúsculos (Breuillin-Sessoms et al., 2015; Guether et al., 2009; Kobae et al., 2010). En plantas de arroz se ha identificado recientemente un transportador de nitrato que media el transporte simbiótico de nitrógeno junto con un transportador de amonio (Wang et al., 2020).

1.6.3. Transporte de micronutrientes

La simbiosis MA también incrementa la absorción de micronutrientes cuando las plantas crecen en suelos deficientes (Liu et al., 2000; Ryan & Angus, 2003). El zinc, cobre, hierro, y manganeso son micronutrientes poco móviles en el suelo, por lo que el incremento del área explorada y explotada por el ERM puede mejorar el estado nutricional de la planta hospedadora. Por otro lado, cuando las concentraciones de estos metales alcanzan niveles supraóptimos en el suelo, los hongos MA también son capaces de aliviar la toxicidad e incrementar la tolerancia de la planta (Ferrol et al., 2016). La homeostasis de metales en la simbiosis MA se consigue gracias a la actuación coordinada de una serie de procesos que controlan no sólo la adquisición del metal del suelo, sino también su distribución a través de la planta y del hongo, utilización y almacenamiento en los diferentes compartimentos subcelulares. Todos estos procesos requieren de la actuación de proteínas transportadoras de metales codificadas por familias multigénicas y que están localizadas en diferentes membranas subcelulares (Atkinson & Guerinot, 2011).

El conocimiento actual sobre cerca de los transportadores de los hongos MA implicados en la absorción de metales del suelo es limitado. Tamayo y colaboradores (2014) definieron el metalotransportoma del hongo modelo *R. irregularis,* en el que identificaron un total de 30 genes que codifican posibles trasportadores de micronutrientes pertenecientes a las a las familias CTR (transportadores de Cu), P_{1B}-ATPasas (ATPasas transportadoras de metales), OFet (transportadores de Fe dependientes de oxidasas), VIT (transportadores de Fe vacuolares), NRAMP ("natural resistance-associated marcrophage protein"), CDF (facilitadores de difusión de cationes), SIT (transportadores de complejos sideróforo-Fe) y y ZIP (permeasas de Fe y zinc) (Figura 6).

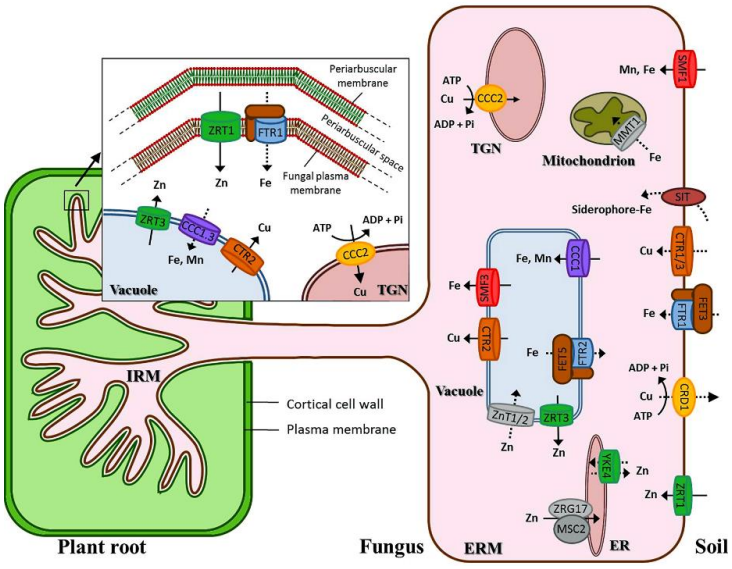

Figura 6. Representación esquemática de los potenciales sistemas de transporte de Cu, Zn y Fe de *R. irregularis* (Tamayo et al., 2014).

1.6.3.1. Transporte de Cu

Se ha comprobado que entre el 60 y 75% del Cu de la planta es captado a través de la vía micorrícica (Lee & George, 2005; X.-L. Li et al., 1991). Poco se conoce acerca de los mecanismos de transporte del Cu. En *M. truncatula* se ha identificado y caracterizado un transportador de Cu de la familia COPT (MtCOPT2) inducido por micorrización y localizado en células colonizadas por arbúsculos que podría intervenir en la absorción de Cu del espacio periarbuscular (Senovilla et al., 2020). En cuanto a los sistemas de transporte del hongo, se han caracterizado dos transportadores de la familia CTR en *R. irregularis*, *RiCTR1* que codifica un transportador de membrana plasmática que se expresa mayoritariamente en ERM e implicado en la captación de Cu del suelo, y *RiCTR2* que codifica un transportador de membrana vacuolar que se expresa mayoritariamente en IRM, responsable de la movilización de las reservas de Cu. Además, se ha

identificado un tercer miembro de esta familia génica, *RiCTR3*A que actuaría como un receptor de Cu en condiciones de toxicidad (Gómez-Gallego et al., 2019).

1.6.3.2. Transporte de Zn

El aporte de Zn por parte de los hongos MA a la planta hospedadora ha sido ampliamente estudiado y revisado (Cavagnaro, 2014; Coccina et al., 2019). La primera evidencia directa de la capacidad de los hongos MA para transferir Zn del suelo a la planta proceden de estudios en los que se utilizó ^{65}Zn como marcador solo accesible al ERM (Cooper & Tinker, 1978). El transporte de Zn está estrechamente ligado al transporte de P en la mayoría de las plantas, lo que supone una dificultad añadida a la hora de analizar la contribución de Zn por vía micorrícica. En sustratos fertilizados con baja concentración de P se incrementa a absorción de P, Zn y otros micronutrientes, sin embargo, el transporte y la colonización son menores cuando la concentración de P es alta (Watts-Williams et al., 2015; Watts-Williams & Cavagnaro, 2014). En *M. truncatula* se ha identificado un transportador de la familia ZIP, MtZIP14, que se expresa en células colonizadas por arbúsculos y que está implicado en la captación del Zn a través de la vía simbiótica por la membrana periarbuscular (Watts-Williams et al., 2020).

1.6.3.3. Transporte de Mn

Los estudios realizados sobre el efecto de las MA en la captación de son escasos y muestran resultados contradictorios. Así, en algunos casos se observa una menor absorción de Mn en plantas micorrizadas (Corrêa et al., 2014; A. Liu et al., 2000), mientras que en otros la absorción de Mn fue mayor (Eivazi & Weir, 1989; Lehmann & Rillig, 2015). Los transportadores implicados en la absorción de Mn por el ERM aún no se han caracterizado. Como el transporte de Mn comparte la ruta de entrada con el Fe, miembros de las familias NRAMP, VIT y ZIP mencionados anteriormente podrían mediar el transporte de Mn.

1.6.3.4. Transporte de Fe

Los sistemas de transporte de Fe, objeto de estudio en esta tesis doctoral, se describen en el Apartado 3 junto con los conocimientos actuales sobre el papel de las micorrizas en la nutrición férrica.

2. Homeostasis de Fe en eucariotas

2.1. Esencialidad del Fe

El Fe es un micronutriente esencial para todos los seres vivos. Las funciones que desempeña en las células están relacionadas con su capacidad de transferir electrones de forma reversible

mediante cambios en su estado de oxidación-reducción. En plantas participa en procesos tan importantes como la fotosíntesis, la síntesis de clorofila, la respiración y la nutrición nitrogenada. Sin embargo, a pesar de su esencialidad, el Fe reacciona en las células con el oxígeno, generando especies de oxígeno reactivo, que inhiben el crecimiento y desarrollo de los organismos. De ahí, que los organismos hayan desarrollado estrategias altamente eficientes que les permitan controlar la homeostasis de Fe (Connorton et al., 2017). Uno de los principales mecanismos de regulación de la homeostasis de Fe es la adaptación de los sistemas de captación del metal a las condiciones externas.

2.2. Sistemas de transporte de Fe

2.2.1. Hongos

Para absorber Fe en ambientes limitantes del metal algunos hongos emplean un sistema de captación reductiva de alta afinidad (Kosman, 2010), mientras que otros utilizan un sistema mediado por sideróforos (Haas et al., 2008). Otros hongos pueden utilizar ambos sistemas. El sistema de captación reductivo requiere de la actuación de tres proteínas que catalizan la reducción y captación de Fe en dos pasos. En primer lugar, el Fe férrico es reducido a Fe ferroso mediante la actuación de una reductasa férrica. El Fe(II) generado es absorbido por un complejo protéico compuesto por una multicobre oxidasa de hierro o ferroxidasa (Fet3) que oxida el Fe(II) a Fe(III) y una permeasa de Fe que transporta el Fe (III) al citosol (de Silva et al., 1995; Stearman et al., 1996). El Fe(II) también puede ser captado directamente por transportadores pertenecientes a la familia NRAMP localizados en la membrana plasmática (Cellier & Gros, 2004).

El sistema de captación de Fe mediado por sideróforos consiste en la síntesis y secreción de sideróforos al medio y posterior captación del complejo sideróforo-Fe mediante transportadores de alta afinidad de sideróforos pertenecientes a la familia SIT (“Siderophore Iron Transporter) (Haas et al., 2008; Saha et al., 2013).

En caso de exceso de Fe en el cytosol, éste puede ser almacenado en las vacuolas a través de proteínas transportadoras pertenecientes a la familia CCC1, homóloga a la familia VIT (“Vacuolar Iron Transporter”) descrita en plantas (Li et al., 2001).

2.2.2. Plantas

Aunque el Fe es el cuarto elemento más abundante en la litosfera, generalmente es poco accesible para las plantas. De hecho, en los suelos alcalinos y calcáreos, frecuentes en España y regiones semiáridas, el Fe se encuentra en forma de óxidos e hidróxidos de muy baja solubilidad,

siendo deficitario para las plantas. A lo largo de la evolución, las plantas han adoptado multitud de estrategias adaptativas para solucionar este estrés nutricional (Grotz & Guerinot, 2006).

Concretamente, en condiciones de deficiencia de Fe, las gramíneas utilizan la Estrategia II de captación de Fe, que consiste en la síntesis y secreción a la rizosfera de sideróforos, que quelan el Fe(III) presente en el suelo, y posterior absorción de los quelatos sideróforo-Fe(III) a través de un transportador específico. Las plantas dicotiledóneas y monocotiledóneas no gramíneas utilizan la Estrategia I, que implica la activación de una H^+-ATPasa que acidifica la rizosfera y solubiliza los quelatos de Fe, la reducción del Fe(III) a Fe(II) mediante la actividad de una reductasa férrica (FRO) y posterior absorción del Fe(II) mediante el transportador de hierro de alta afinidad IRT1. o de baja afinidad NRAMP1(Figura 7). Sin embargo, las plantas que desarrollan la Estrategia I, son también capaces de secretar a la rizosfera cumarinas o compuestos funcionalmente equivalentes capaces de quelar Fe(III) que luego será reducido mediante la actuación de la reductase férrica FRO para ser finalmente transportado al citoplasma a través de transportadores tipo IRT (Sisó-Terraza et al., 2016; Tsai & Schmidt, 2017) . Sin embargo, recientemente se ha comprobado en *Arabidopsis* que el complejo Fe(III)-cumarina puede ser absorbido directamente por las raíces en condiciones alcalinas (Robe et al., 2021). Por otro lado, el arroz y la cebada poseen un homologo funcional de IRT capaz de transportar Fe(II) bajo condiciones de bajo oxígeno (Cheng et al., 2007; Ishimaru et al., 2006), por lo que la distinción entre plantas que aplican las Estrategias I y II es a veces difusa.

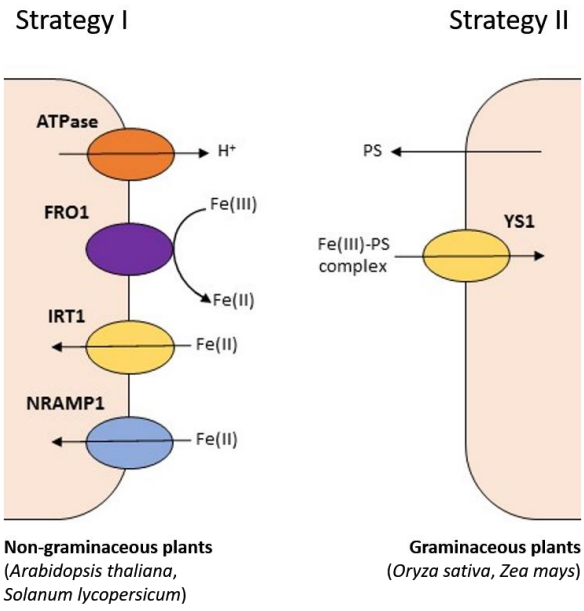

Figura 7. Representación esquemática de las estrategias de captación de Fe del suelo de plantas gramíneas y no gramíneas.

La mayoría del Fe tomado por las raíces necesita ser transportado a otros tejidos. Debido a su toxicidad y baja solubilidad, el transporte a larga distancia del Fe requiere de quelantes de bajo

peso molecular que eviten la producción de especies de oxígeno reactivo y su precipitación. En el citosol el Fe se encuentra principalmente formando complejos con la nicotianamina (NA). La NA es un aminoácido no proteico sintetizado a partir de la S-adenosil-metionina por la nicotianamina sintasa. Los complejos Fe(II)- NA se transportan a través de los plasmodesmos hacia la endodermis para ser cargado en el xilema, posiblemente, a través de transportadores tipo YSL y ferroportinas (DiDonato et al., 2004; Morrissey et al., 2009). El Fe también puede trasladarse por vía apoplástica hasta la endodermis, pero, al alcanzar la banda de Caspary todo el Fe pasa al simplasto. Una vez el xilema el Fe es oxidado a Fe(III) y quelado con citrato y malato (Flis et al., 2016; Rellán-Álvarez et al., 2010). Una vez alcanzado el tejido de destino, principalmente las hojas maduras, el Fe vuelve a entrar en el simplasto, donde es reducido a Fe(II) mediante la acción de proteínas FRO y quelado con la NA. El transporte de Fe desde las hojas maduras hacia los órganos sumidero (semillas, flores y hojas jóvenes) ocurre a través del floema, donde el Fe se encuentra en forma de quelatos con NA. La carga del Fe en el floema ocurre mediante transportadores tipo OPT (Mendoza-Cózatl et al., 2014; Zhai et al., 2014).

En la célula, el Fe puede ser almacenado bien en las vacuolas o ligado a ferritinas. El transporte del Fe hacía la vacuola ocurre mediante la actuación de transportadores de la familia VIT (Kim et al., 2006). Por otro lado, las reservas vacuolares de Fe pueden ser movilizadas mediante la acción de transportadores tipo NRAMP (Lanquar et al., 2005). La ferritina es una proteína de almacenamiento de Fe(III) presente en distintos reinos biológicos y se localiza principalmente en los plastidios (Zielińska-Dawidziak, 2015).

3. Homeostasis de Fe en MA

3.1. Contribución de las MAs a la captación de Fe

Los resultados obtenidos hasta la fecha sobre la contribución de la simbiosis MA a la nutrición férrica son variables e inconsistentes. Un meta-análisis donde se incluyeron >200 estudios mostraron que los hongos MA ejercían, en general, un efecto positivo sobre la nutrición férrica de la planta hospedadora, aunque este efecto solo era significativo en las raíces, observándose que los beneficios dependían de factores edáficos y de la duración del experimento (Lehmann & Rillig, 2015). Experimentos de marcaje isotópico con ^{59}Fe en sistemas de cultivo compartimentados en los que tan solo el hongo MA tiene acceso al compartimento al que se se le añade el ^{59}Fe han permitido determinar la contribución de las MA a la nutrición férrica de la planta. Estos estudios han puesto de manifiesto captación de Fe a través de la vía micorrícica en plantas de sorgo y de maíz (Caris et al., 1998; Kobae et al., 2014), pero no en plantas de cacahuete (Caris et al., 1998). Quizá esta diferencia se deba a las diferentes estrategias de captación de Fe que desarrollan ambas plantas (Kim & Guerinot, 2007). El cacahuete es una dicotiledónea que

utiliza la Estrategia I para absorber Fe, mientras que el sorgo y el maíz son gramíneas que usan la Estrategia II.

Otros estudios han mostrado que, en suelos contaminados con Fe, las MAs reducen la acumulación del metal en la planta y, por tanto, su toxicidad (Juwarkar & Jambhulkar, 2008). Los mecanismos subyacentes de este efecto dual de las micorrizas en relación con el Fe se desconocen en gran medida (Ferrol et al., 2016), aunque es lógico pensar que se debe a la acción de un conjunto de mecanismos destinados a mantener la homeostasis de este metal tanto en la planta como en el hongo. Actualmente se sabe muy poco sobre el efecto que el desarrollo de la simbiosis ejerce sobre la regulación de estos sistemas homeostáticos de Fe de la planta.

3.2. Transporte de Fe en MAs

El transporte de Fe en MAs comienza con la captación del Fe presente en la solución del suelo por las hifas del ERM, proceso que ocurre a través de una vía reductiva de captación de Fe. En el hongo *R. irregularis*, se han caracterizado tres componentes de esta vía: los transportadores RiFTR1 y RiFTR2 y la reductasa férrica RiFRE (Tamayo et al., 2018). RiFTR1 es una permeasa de alta afinidad de Fe localizada en la membrana plasmática que desempeña un papel principal en la adquisición del metal tanto por ERM como IRM, mientras que RiFTR2 se localiza en membranas intracelulares y participa en la regulación de la homeostasis de Fe bajo condiciones de deficiencia. Aunque el genoma de *R. irregularis* carece de genes Sid, que codifican la ornitina-N5-monoxigenasa implicada en la biosíntesis de sideróforos del tipo hidroxamato, los principales sideróforos fúngicos, (Tamayo et al., 2014), recientemente se ha comprobado que los hongos MA disponen de la maquinaria genética necesaria para la síntesis de sideróforos del tipo rizoferrina. Concretamente, en los genomas de los hongos MA *Gigaspora rosea*, *R. irregularis, Glomus cerebriformis* y *Diversispora epigea* se ha identificado un gen ortólogo al de la rizoferrina sintasa, una sintetasa de péptidos no ribosomal, de *Rhizopus delemar* (Haselwandter et al., 2020). De hecho, estos autores aislaron de raíces micorrizadas una bis-imidorhizoferrina, denominada glomuferrina.

Es previsible que los transportadores de las familias NRAMP y VIT identificados en el genoma de *R. irregularis* (Tamayo et al., 2014), aún por caracterizar, también desempeñen un papel clave en la homeostasis de Fe en los hongos MA.

Al inicio de esta tesis doctoral no existía ningún estudio sobre el efecto de las MAs en la homeostasis de Fe de la planta hospedadora. Recientemente, se ha comprobado que, en girasol y membrillero, dos plantas que utilizan la Estrategia I de captación de Fe, la simbiosis MA incrementa la actividad reductasa férrica y la expresión del gen FRO1 en condiciones limitantes de Fe (Kabir et al., 2020; Rahimi et al., 2021). Además, en raíces de girasol se induce la expresión

del gen *IRT1* (Kabir et al., 2020). En raíces de sorgo, planta que utiliza la Estrategia II, las MAs contribuyen a la mitigación de la deficiencia de Fe incrementando la movilización del Fe mediante la producción y secreción de fitosideróforos, ya que en condiciones de deficiencia las MAs incrementan la expresión de los genes que codifican la sintetasa de ácido deoximugineico SbDMAS2 y la nicotina sintasa SbNAS2, implicadas en la biosíntesis de sideróforos, y el transportador SbYS1responsable de la captación complejos Fe-sideróforo (Prity et al., 2020).

OBJECTIVES

Despite iron (Fe) is the fourth most abundant element on the Earth's crust, its availability is limited in soil since it exists mainly as insoluble ferric hydroxides and thus bio-unavailable. Fe bioavailability is further reduced in alkaline soils, which comprise about one third of the world´s arable land. Iron deficiency is an important limiting factor in crop growth, yield and nutritional value of food crops. Plants, as primary producers, are the gateway for iron to enter the food chain. Iron-deficiency anemia is a major health issue, estimated by the World Health Organization to affect over 30% of the world´s population. On the other hand, residues from anthropogenic activities, such as mining or the abusive use of fertilizers, have led to the accumulation of iron in soils, affecting negatively both natural and agronomic ecosystems. Therefore, it is crucial for plants to tightly regulate Fe uptake to maintain Fe homeostasis in order to prevent both Fe deficiency and toxicity.

The importance of the AM symbiosis for plant development in both iron-deficient and iron-contaminated soils has been established in the Introduction. However, current knowledge about the contribution of AM fungi to plant Fe uptake and on the mechanisms of Fe homeostasis in AM homeostasis is scarce.

With the aim of getting further insights into the mechanisms of Fe homeostasis in AM, the main objective of this PhD Thesis was to characterize fungal transporters involved in Fe uptake and compartmentalization and to assess the impact of the symbiosis on host plant Fe homeostasis. To attain this main objective, the following specific objectives were established:

1. Characterization of metal transporters of the NRAMP and vacuolar iron transport (VIT) families in the AM fungus *Rhizophagus irregularis* (Chapters 1 and 2)

2. Analysis of the impact of the AM symbiosis on the iron deficiency response of the host plant (Chapter 3)

3. Assessment of the importance of iron for AM development and function (Chapters 4 and 5).

RESULTS

CHAPTER 1:

Characterization of the NRAMP gene family in the arbuscular mycorrhizal fungus *Rhizophagus irregularis*

Adapted from López-Lorca, V. M., Molina-Luzón, M. J., Ferrol, N

Characterization of the NRAMP Gene Family in the Arbuscular Mycorrhizal Fungus *Rhizophagus irregularis*.

Journal of Fungi 2022, 8, 592. doi: 10.3390/JOF8060592

Abstract

Transporters of the NRAMP family are ubiquitous metal-transition transporters, playing a key role in metal homeostasis, especially in Mn and Fe homeostasis. In this work, we report the characterization of the NRAMP family members (*RiSMF1*, *RiSMF2*, *RiSMF3.1* and *RiSMF3.2*) of the arbuscular mycorrhizal (AM) fungus *Rhizophagus irregularis.* Phylogenetic analysis of the NRAMP sequences of different AM fungi showed that they are classified in two groups, which probably diverged early in their evolution. Functional analyses in yeast revealed that *RiSMF3.2* encodes a protein mediating Mn and Fe transport from the environment. Gene-expression analyses by RT-qPCR showed that the *RiSMF* genes are differentially expressed in the extraradical (ERM) and intraradical (IRM) mycelium and differentially regulated by Mn and Fe availability. Mn starvation decreased *RiSMF1* transcript levels in the ERM but increased *RiSMF3.1* expression in the IRM. In the ERM, *RiSMF1* expression was up-regulated by Fe deficiency, suggesting a role for its encoded protein in Fe-deficiency alleviation. Expression of *RiSMF3.2* in the ERM was up-regulated at the early stages of Fe toxicity but down-regulated at later stages. These data suggest a role for RiSMF3.2 not only in Fe transport but also as a sensor of high external Fe concentrations. Both Mn- and Fe-deficient conditions affected ERM development. While Mn deficiency increased hyphal length, Fe deficiency reduced sporulation.

Introduction

Transition metals, such as iron (Fe) and manganese (Mn), are essential micronutrients necessary for the correct development and survival of all organisms. These metals play important roles in multiple biochemical processes, since they have structural roles in many proteins and act as enzyme cofactors. However, at high concentrations, they generate noxious reactive oxygen species (ROS) that are deleterious for growth and development (Marschner, 1995; Schutzendubel & Polle, 2002). Therefore, metal homeostasis must be strictly balanced at the cell and whole-organism level. To maintain cellular metal homeostasis, all organisms have evolved a series of mechanisms, including metal uptake, chelation, trafficking and storage systems (Festa & Thiele, 2011). Metal transporters play a major role in keeping appropriate metal concentrations in the different cellular compartments (Hall & Williams, 2003). One of the most ubiquitous classes of metal transporters are the natural-resistance-associated macrophage proteins (NRAMPs) (Nevo & Nelson, 2006).

The NRAMP family represents an evolutionary-conserved strategy for acquiring and trafficking essential transition metals, such as Mn and Fe. All NRAMP transporters possess a highly conserved core of 10–12 transmembrane domains and two motifs that are essential for

their transport function, the DPGN metal-binding domain at the first transmembrane domain and a high-conserved metal-transport motif in the cytoplasmic loop, between transmembrane domains 8 and 9 (Cellier et al., 1995). Members of the NRAMP family have been identified and characterised in many organisms, ranging from bacteria to mammals. The model yeast *Saccharomyces cerevisiae* has three homologs of this family in its genome: SMF1, SMF2 and SMF3 (West et al., 1992). Smfp1 and Smfp2 were, initially, identified as extremely hydrophobic proteins that supress a lethal mutation in the yeast-mitochondrial-processing protein. Thereafter, they were shown to be Mn transporters that can, also, transport other divalent metal ions (Chen et al., 1999). Smf1 is located at the plasma membrane and is responsible for Mn uptake, while Smf2p is located in intracellular vesicles and imports Mn for Mn-requiring enzymes. Smf3p localises at the vacuolar membrane and regulates vacuolar Fe transport (Portnoy et al., 2002). While Smf1p and Smfp2 are induced by Mn deficiency and, to a lesser extent, by Fe deficiency (Portnoy et al., 2000), Smf3p is strongly induced under Fe starvation (Portnoy et al., 2002). Orthologues of the SMF genes have been characterised in other fungi, including *Cryptococcus neoformans* (Agranoff et al., 2005), *Schizosaccharomyces pombe* (Maeda et al., 2004; Tabuchi et al., 1999) and *Aspergillus niger* (Fejes et al., 2020), among others. Most fungal NRAMP family transporters have been involved in Mn homeostasis. For example, the SMF1 transporter of *Candida albicans* plays a role in Mn assimilation under alkaline conditions (Bensen et al., 2004), and the high-affinity PsMnt transporter of the white-rot fungus *Phanerochaete sordida* is involved in cellular Mn accumulation under Mn-deficient conditions (Mori et al., 2018). Other fungal NRAMP transporters, such as the plasma-membrane Fe-transporter EpNramp of the dark endophyte *Exophiala pisciphila* (Wei et al., 2016) and the *Cryptococcus neoformans* Mn-transporter smf1 have been, also, involved in Cd tolerance (Toh-e et al., 2022), as their expression is down-regulated by Cd toxicity. In *A. niger*, deletion of the high-affinity Mn transporter DmtA leads to defects in germination and hyphal morphology (Fejes et al., 2020). However, NRAMP transporters in arbuscular mycorrhizal (AM) fungi remain uncharacterised.

AM fungi are obligate plant mutualistic microorganisms of the subphylum Glomeromycotina, within the Mucoromycota (Spatafora et al., 2016), that form a symbiotic association with most plant species (Azcón-Aguilar & Barea, 2015). The fungus colonises the root and forms highly branched structures, called arbuscules, inside the cortical cells. Outside the root, the fungus develops an extensive network of hyphae in the soil that can absorb nutrients beyond the depletion zone that develops around the roots. This extraradical mycelium (ERM) provides a new pathway to the plant, for the uptake of low-mobility nutrients in the soil, mainly P, N and some transition metals (Zn, Fe and Cu). In return, the plant provides sugar and lipids to the

fungus (Casieri et al., 2013; Luginbuehl et al., 2017). This nutrient exchange takes place in the arbuscule-colonised cortical root cells. Besides enhancing nutrient uptake to their host plants, AM fungi provide increased tolerance against biotic and abiotic stresses, including drought, salinity or metal toxicity (Ferrol et al., 2016; Quiroga et al., 2017; Rivero et al., 2021).

AM fungi play a crucial role in modulating plant metal acquisition, over a wide range of soil metal concentrations, as they increase plant metal acquisition in soils deficient in these elements but reduce metal uptake in contaminated soils (Ferrol et al., 2016; Riaz et al., 2021). Despite the importance of AM fungi for plant metal homeostasis, very few metal transporters have been characterised in these organisms. Up to now, just three components of the reductive iron uptake pathway (RiFTR1, RiFTR2 and RiFRE) and three copper transporters of the CTR family (RiCTR1-3) have been characterised in the model fungus *Rhizophagus irregularis* (Gómez-Gallego et al., 2019; Tamayo et al., 2018). Iron uptake by the ERM starts with the reduction of Fe^{3+} to Fe^{2+} in the soil solution by the plasma-membrane ferric reductase RiFre1. Then, Fe^{2+} is taken up by the plasma-membrane Fe permease RiFTR1 (Tamayo et al., 2018). Although RiFTR2 function has not been determined, it has been proposed to play a role in Fe homeostasis under Fe-limiting conditions. Regarding the *R. irregularis* Cu transporters, RiCTR1 mediates Cu uptake by the ERM from the environment, RiCTR2 is involved in mobilization of Cu vacuolar stores and RiCTR3a has been suggested to function as a Cu transceptor involved in Cu tolerance (Gómez-Gallego et al., 2019). Previous bioinformatics analysis of the *R. irregularis* genome identified four NRAMP family members (*RiSMF1*, *RiSMF2*, *RiSMF3.1* and *RiSMF3.2*) that remain uncharacterised (Tamayo et al., 2014).

The aim of this work was to characterise the *R. irregularis* NRAMP family members, in order to get further insights into the role of the NRAMP transporters in the AM symbiosis and into the mechanisms of the metal homeostasis in AM fungi. Data presented in this manuscript describe, for the first time, a Mn transporter in an AM fungus and show that *R. irregularis* uses various strategies for Fe uptake from the environment.

Materials and Methods

RiSMFs sequence analyses

Putative *RiSMFs* sequences were, previously, identified by Tamayo et al. (2014). Additional searches were performed in the filtered-model datasets of the *R. irregularis* isolates DAOM197198 v2.0 and A1, A4, A5, B3 and C2 v1.0 (Chen et al., 2018) deposited at the JGI (Joint Genome Institute) (https://genome.jgi.doe.gov/portal/ (accessed on 10 May 2022), using as a query the previously identified RiSMF candidates. These candidate sequences were used to perform

additional Blastp searches in JGI and NCBI (National Center for Biotechnology Information) databases to find NRAMP homologs of other Glomeromycotina species. Primer3 (https://primer3.ut.ee/ (accessed on 25 May 2018) was used to design the gene-specific primers. Homology and similarity comparisons were performed with SIAS (http://imed.med.ucm.es/Tools/sias.html (accessed on 19 April 2022)). To search the protein-family domains and functional sites, InterProScan (http://www.ebi.ac.uk/Tools/InterProScan/ (accessed on 19 April 2022) was used. Potential transmembrane domains were predicted using TOPCONS (https://topcons.cbr.su.se/ (accessed on 30 March 2022)). Structural models of the proteins were generated using the MyDomains tool of Prosite (https://prosite.expasy.org/mydomains/ (accessed on 11 April 2022). The 3D models were predicted using the SWISS-MODEL software (https://swissmodel.expasy.org/_(accessed on 12 May 2022), based on the crystal structure of *Eremococcus coleocola* divalent metal cation transporter MntH (ID: 5m87.1A). The alignment of putative amino acid sequences of NRAMPs from different fungi was performed with Clustal Omega (https://www.ebi.ac.uk/Tools/msa/clustalo/ (accessed on 27 January 2022), and phylogenetic relationships were obtained applying the neighbour-joining method, implemented in MEGA-X (Kumar et al., 2018). FIMO (http://meme-suite.org/tools/fimo (accessed on 4 February 2022) was used to scan protein sequences, to find the Consensus Transport Motif (CTM).

Biological materials and growth conditions

The AM fungal isolate used in this study was *Rhizophagus irregularis* DAOM197198. The fungal inoculum used for the monoxenic cultures and for the seedlings was obtained from monoxenic cultures. AM monoxenic cultures were established in bi-compartmental Petri dishes, containing solid M medium (Chabot et al., 1992), to allow for separation of the root compartment (RC) from the hyphal compartment (HC) (St-Arnaud et al., 1996). Cultures were started by placing several segments of non-mycorrhizal *Agrobacterium rhizogenes* transformed-carrot (*Daucus carota*) roots and a piece of fungal inoculum containing ERM, fragments of mycorrhizal roots and spores in the RC. Plates were incubated in the dark at 24 °C, until the other compartment was profusely colonised by the fungus and roots (6–8 weeks). Then, the RC was removed and refilled with fresh liquid M medium, and the ERM was allowed to colonise this compartment during 20 days (control plates).

Mn-deficient conditions were applied by growing the ERM in liquid M medium without Mn in the same conditions as the control plates. Fe-deficient conditions were induced by exposing the ERM grown in liquid M medium without Fe to 0.5 mM ferrozine for 3 days, as described by Tamayo et al. (2018).

Two experiments were set up to assess the effect of Fe toxicity on *RiSMF* expression: a short- and a long-term experiment. In the short-term experiment, the ERM grown in liquid M media control was exposed for 16 h to 45 mM EDTAFe (III) sodium salt. In the long-term experiment, the ERM was grown in liquid M media, supplemented with 45 mM Fe for 20 days. ERM from the different treatments were collected using tweezers, washed with distilled water, dried on filter paper, frozen in liquid N and stored at −80 °C until used.

R. irregularis ERM was also collected from chicory mycorrhizal plants grown in the *in vivo* whole-plant bidimensional experimental system (Pepe et al., 2017). Chicory (*Cichorium intybus L.*) seeds were surface sterilised and germinated in autoclaved HCl-washed sand under sterile conditions. Sand was washed before sterilisation with 0.03 M HCl to eliminate metal traces and then rinsed with distilled water until pH 7. Seedlings were allowed to grow in a growth chamber under 16 h light at 24 °C and 8 h dark at 20 °C for two weeks. Then, seedlings were transferred to pots containing 50 mL of sterilised HCl-washed sand and inoculated with 3 mL of AM fungal inoculum, obtained in monoxenic cultures and containing 1650 spores. To prevent substrate desiccation, pots were introduced in sun-transparent bags (Sigma-Aldrich, B7026, St. Louis, MO, USA). Plants were watered with half-strength (0.5X) Hoagland nutrient solution and grown for one month at 24 °C day/20 °C night and in a 16 h light photoperiod. To induce Mn- or Fe-deficient conditions, plants were watered with Hoagland solution without $MnCl_2$ or EDTA Fe (III) sodium salt, respectively. Then, the root system of each plant was washed with distilled water, wrapped in a nylon net (41 μm mesh, Millipore NY4100010, Merk, Darmstadt, Germany) and sandwiched between two 13 cm membranes of mixed-cellulose esters (0.45 μm pore diameter size, MF-Millipore HAWP14250, Merk, Darmstadt, Germany). The sandwiched root systems were placed into 14 cm diameter petri plates, having a hole on the edge to allow shoot growth, and filled with sterile HCl-washed sand. Petri plates containing plants were sealed with parafilm, wrapped with aluminium foil, placed into sun-transparent bags and maintained in a growth chamber. Plates were incubated for another month, until ERM colonised the Millipore membrane. Finally, ERM spreading from the nylon net onto the membranes was collected with tweezers. At harvesting, plant biomass was determined by measuring shoot and root fresh weights. ERM and root systems were frozen in liquid N and stored at −80 °C until used. An aliquot of the roots was separated to estimate mycorrhizal colonization.

The *Saccharomyces cerevisiae* yeast strains used in this study were *smf1*Δ, a single mutant lacking the plasma-membrane transporter Smf1 (Cohen et al., 2000), and *fet3*Δ*fet4*Δ, a double mutant defective in both high- and low-affinity iron transport (Eide et al., 1996). Yeast cells were

grown on YPD or minimal synthetic dextrose (SD) medium supplemented with the appropriate amino acids.

RNA extraction and gene expression analyses

Total RNA was extracted from ERM developed in monoxenic and sandwich cultures using the RNeasy Plant Mini Kit (Qiagen, Hilden, Germany), in accordance with the instructions of the manufacturer. Total plant RNA was isolated from chicory roots by using the phenol/SDS method followed by LiCl precipitation (García-Rodríguez et al., 2007). RNAs were treated with DNase using the RNA-free DNAse set (PROMEGA, Madison, WI, USA), in accordance with the protocol of the manufacturer. cDNAs were synthetised from 1 μg of total DNase-treated RNA in a 20 μL reaction using Super-Script IV Reverse Transcriptase (Invitrogen, Vilnius, Lithuania), in accordance with the instructions of the manufacturer.

RiSMFs gene expression was analysed by real-time RT-PCR, using a QuantStudio 3 (Applied Biosystem, Waltham,MA, USA) in the synthetised cDNAs. Each 12 μL reaction contained 1 μL of a 1:10 dilution of cDNA, 0.25 μL each primer and 6 μL iTaq (Bio-Rad, Hercules, CA, USA). Specificity of the different primer sets (Supplementary Table 1) was analysed by PCR amplification of *R. irregularis* and chicory cDNA. The real-time RT-PCR program consisted of an initial incubation at 95 °C for 30 s, followed by 40 cycles of 95 °C for 15 s, 60 °C for 30 s and 72 °C for 30 s, where the fluorescence signal was measured, and a final step with a heat-dissociation protocol to check the specificity of the PCR-amplification procedure. The efficiency of the different primer pairs was determined through a real-time RT-PCR on several dilutions of cDNA. The results obtained for the different treatments were standardised to *RiEF1α*. Real-time RT-PCR determinations were carried out on at least three independent biological samples from three replicate experiments. Real-time RT-PCR reactions were performed at least three times for each biological sample with the threshold cycle (Ct) determined in triplicate. Relative expression level was calculated using the $2^{-\Delta Ct}$ method and the standard error was computed from the average of the ΔCt values for each biological sample.

Heterologous expression

The coding regions of the *R. irregularis* NRAMP genes were amplified from ERM cDNA by PCR using the corresponding primers pairs (Supplementary Table 1) and cloned into the yeast-expression-vector pDRf1-GW using the Gateway technology (Invitrogen, Carlsbad, CA, USA). The respective full-length cDNA sequences were flanked with the sequences attB1 and attB2, to be recognised by the BP Clonase enzyme. PCR products were, first, cloned into pDONr221 and, then, cloned into the yeast expression vector pDRf1-GW, in accordance with the instructions of

the manufacturer. All constructs were verified by sequencing. Although a PCR band of the expected size was obtained for *RiSMF2*, all attempts we did to clone it failed. *S. cerevisiae* mutant strains *smf1*Δ and *fet3*Δ*fet4*Δ were transformed with the pDRf1-RiSMF1, pDRf1-RiSMF3.1 or pDRf1-RiSMF3.2 constructs or with the empty vector (negative control) using a lithium-acetate-based method (Schiestl & Gietz, 1989). Yeast transformants were selected in SD medium by uracil autotrophy. For drop tests, yeast transformants were harvested by centrifugation from a liquid culture grown to the exponential phase in SD medium without uracil, washed three times with milli-Q H_2O and adjusted to a final OD_{600} of 1. Then, 5 µL of serial 1:10 dilutions were spotted on the corresponding selective medium. *fet3*Δ*fet4*Δ transformants were spotted onto SD without uracil pH 3.5 supplemented with 100 µM $FeCl_3$ or SD without uracil pH 5.4. The transformed *smf1*Δ strain were spotted onto SD without uracil plates supplemented with 50 mM MES pH 6, 6.25 mM EGTA and supplemented or not with 500 µM $MnSO_4$.

RiSMFs subcellular localization

Subcellular localization of RiSMFs was performed with carboxi-terminal fusions of these genes to the enhanced green fluorescent protein (eGFP) in the *S. cerevisiae* mutant *smf1*Δ. *RiSMF1*, *RiSMF3.1* and *RiSMF3.2* open-reading frames were PCR amplified without their stop codon using the corresponding primers (Supplementary Table 1), and cloned into the yeast expression vector pGWFDR196 using the Gateway technology (Invitrogen). Mutant yeasts were transformed with the pGWFDR196:RiSMF constructs or with the empty vector (negative control). Functionality of the GFP-fusion proteins was tested in complementation assays, as previously described. For the localization assays of the RiSMFs, yeast cells were grown to the exponential phase in liquid SD without uracil, washed with distilled water and visualised with a Leica DMi8 microscope. GFP-tagged proteins were observed using a 483-501 nm excitation filter and a 512–548 nm emission filter.

Histochemical staining of Fe

Spores developed in monoxenic cultures in control plates and in M medium supplemented with 45mM EDTA-Fe (III)Na were stained with the PERLS reagent for Fe detection. Briefly, spores were harvested with tweezers, transferred to a microtube, rinsed with milli-Q H_2O and placed on a slide. Spores were incubated with an equal volume of 4% (*v*/*v*) HCl and 4% (*w*/*v*) K-ferrocyanide (Perls stain solution) for 2 min at room temperature. Negative stain controls were prepared by incubating a set of spores with HCl. Spores were washed with dH_2O and bright-light visualised with a Nikon SMZ1000 binocular.

Mycorrhizal colonization and ERM development

Mycorrhizal colonization was estimated in an aliquot of the root system of each chicory plant stained with trypan blue following the Trouvelot method (Trouvelot et al., 1986). Expression of the *R. irregularis* elongation factor 1α (*RiEF1*α) in roots was also used as a molecular marker of the abundance of the AM fungus. ERM development in the *in vivo* whole-plant bidimensional experimental system was assessed by staining the ERM with trypan blue on the Millipore membranes. Hyphal length and spore density were calculated under a Nikon SMZ1000 binocular microscope a in three 1 cm^2 squares. The number of spores was counted over the three squares and the hyphal length (L) was estimated by the number of hyphal intersections with the grid (N) using the modified Newmann´s formula (Marsh, 1971), L(cm) = N × (11/14) × grid unit(cm), where 11/14 is the ideal size of the grid side, to obtain the estimation in cm and grid unit = 1 cm. Three replicate plates were considered per treatment.

Statistical analyses

Statgraphics Centurion XVI software was used for the statistical analysis of means and standard error determinations. For comparison of treatments, a one-way ANOVA followed by a Duncan test ($p < 0.05$) were performed.

Results

The NRAMP family of R. irregularis

The genome of *R. irregularis* harbours four genes putatively encoding NRAMPs that were previously named according to their *S. cerevisiae* homologues (Tamayo et al., 2014). Their full-length cDNAs contain open reading frames of 1422–1665 nucleotides. The deduced amino acid sequences of *RiSMF1*, *RiSMF2*, *RiSMF3.1* and *RiSMF3.2* comprise 554, 473, 501 and 525 amino acid residues, respectively, and have a calculated molecular mass of 52.77–61.07 kDa. The amino terminus of all RiSMFs faces the cytosol. RiSMF1 and RiSMF2 have 11 transmembrane domains, while RiSMF3.1 and RiSMF3.2 have 12 (Figures 1a, d). They all contain the NRAMP family domain DPGN, which is essential for metal binding, and the consensus transport motif GQSSTITGTYAGQY(/F)V(/I)MQGFLD(/E/N) in the cytoplasmic loop between transmembrane domains 8 and 9 (Figures 1a, b). Alignment of the full-length cDNAs with the genomic DNA sequences revealed the presence of three introns in *RiSMF1*, one in *RiSMF2*, five in *RiSMF3.1* and four in RiSMF3.2 (Figure 1c). Sequence similarity among the deduced amino acid sequences of the different RiSMFs ranges from 38 to 60%, with RiSMF3.1 and RiSMF3.2 showing the highest degree of similarity (60%). The *R. irregularis* NRAMP proteins show high amino acid sequence

conservation, with NRAMPs of *S. cerevisiae* (26 to 38%) and of other kingdoms, such as the NRAMP proteins of the bacteria *Paenibacillus* sp. (30 to 40%), *Arabidopsis thaliana* (28 to 42%) and *Caenorhabditis elegans* (30 to 40%) (Table 1).

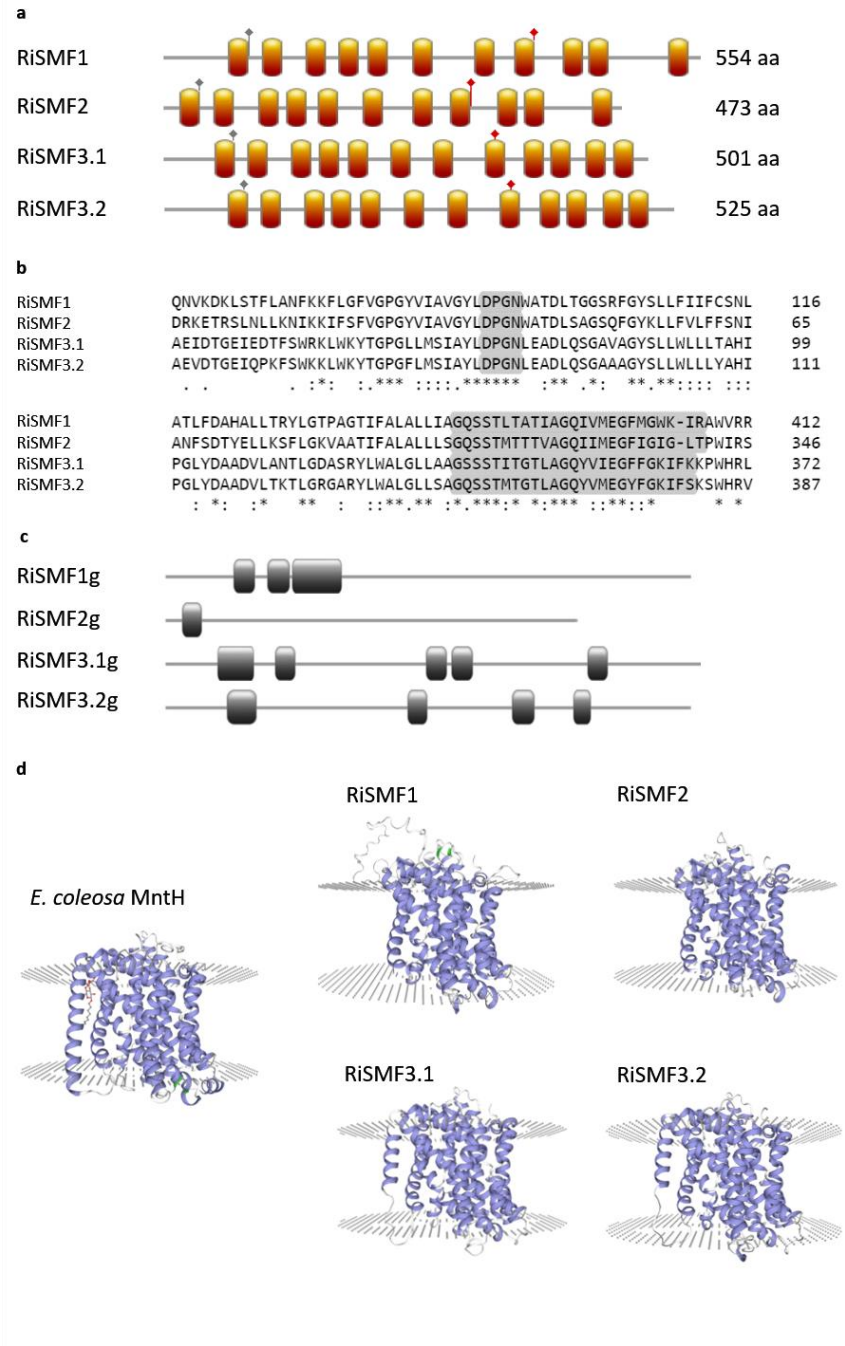

Figure 1. (**a**) Representation of the structure of *R. irregularis* NRAMP transporters. Orange boxes represent transmembrane domains, grey diamonds show the position of the DPGN motif and red diamonds show the position of consensus transport motif. (**b**) Multiple Sequence Alignment of the four protein sequences, with the DPGN and consensus transport motif highlighted. * indicates positions which have a single, fully conserved residue; : indicates conservation between groups of strongly similar properties; . indicates conservation between groups of weekly similar properties, (**c**) Exon/intron organization of *RiSMF* genes. Exons and introns are represented by grey lines and grey boxes, respectively. (d) Predicted 3D structure of RiSMF transporters. Tertiary structures were predicted by SWISS-MODEL software, based on the template of *E. coleosa* MntH (ID: 5m87.1A). α-helices and β-lamina are represented in blue and green, respectively.

Table 1. Percent similarity matrix of NRAMP proteins from *Rhizophagus irregularis* (Ri), *Saccharomyces cerevisiae* (Sc), *Paenibacillus sp.* (Ps), *Arabidopsis thaliana* (At) and *Caenorhabditis elegans* (Ce).

RiSMF1	100%	45.40%	32.70%	31.97%
RiSMF2	45.40%	100%	28.46%	30.07%
RiSMF3.1	32.70%	28.46%	100%	55.47%
RiSMF3.2	31.97%	30.07%	55.47%	100%
ScSMF1	37.95%	34.01%	28.02%	28.90%
ScSMF2	37.66%	35.62%	27.59%	28.92%
ScSMF3	36.20%	34.45%	26.86%	26.42%
AtNRAMP3	30.65	28.90%	39.12%	41.45%
AtNRAMP4	30.80%	29.19%	39.41%	42.04%
Ps WP_193723414.1	40.58%	38.97%	30.51%	32.26%
Ce WP_040990443.1	30.36%	29.34%	40.58%	40.87%
	RiSMF1	**RiSMF2**	**RiSMF3.1**	**RiSMF3.2**

A phylogenetic analysis of the NRAMP sequences of different kingdoms revealed that the *R. irregularis* NRAMPs were grouped in two different clades (Group I and Group II). Group I clusters RiSMF1, RiSMF2 and other Glomeromycotina sequences within the branch of fungal NRAMPs. RiSMF3.1, RiSMF3.2 and other Glomeromycotina sequences were clustered in a branch placed between the two groups of plant NRAMP sequences (Group II). Four NRAMP gene sequences were identified in the genome of AM fungi, belonging to the order Glomerales, whereas two were found in the genome of *Gigaspora rosea* and two in the genome of *Diversispora epigea*. All species analysed harbour NRAMP genes in Groups I and II (Figure 2).

Figure 2. Phylogenetic relationships of the *R. irregularis* NRAMP proteins with homologous sequences from selected species representative of the different kingdoms. The yellow and orange circles indicate the Glomeromycotan Group I and Group II sequences, respectively. The neighbour-joining tree was created with MEGA-X. Protein JGI or NCBI identification numbers are indicated. Fungi: An, *Aspergillus niger*; Bc, *Botrytis cinerea*; Cc, *Coprinopsis cinerea*; Cn, *Cryptococcus neoformans*; De, *Diversispora epigaea*; Gc, *Glomus cerebriforme*; Gm, *Gigaspora margarita*; Gr, *Gigaspora rosea*; Lb, *Laccaria bicolor*; Nc, *Neurospora crassa*; Pi, *Piriformospora indica*; Pg, *Puccinia graminis*; Rc, *Rhizophagus clarus*; Rd, *Rhizophagus diaphanus*; Ri, *Rhizophagus irregularis*; Sc, *Saccharomyces cerevisiae*; Slu, *Suillus luteus*; Tb, *Tuber melanosporum*; Um, *Ustilago maydis*. Plants: At, *Arabidopsis thaliana*; Gm, *Glycine max*; Mt, *Medicago truncatula*; Os, *Oryza sativa*; Sl, *Solanum lycopersicum*. Bacteria: Bj, *Bradyrhizobium japonicum*; Cs, *Chroococcus sp*; Gb, *Gemmatimonadaceae bacterium*; Mp, *Mesorhizobium plurifarium*; Ob, *Opitutaceae bacterium*; Ps, *Paenibacillus sp*; Rl, *Rhizobium leguminosarum*; Rp, *Rhizobium phaseoli*; Sb, *Spirochaetes bacterium*. Animals: Ce, *Caenorhabditis elegans*; Dr, *Danio rerio*; Hs, *Homo sapiens*; Mm, *Mus musculus*. The *R. irregularis* sequences are in bold.

Functional characterization of RiSMFs in yeast

Since AM fungi cannot be genetically manipulated, functionality of the RiSMFs was tested trough heterologous complementation in yeast. As a first step to investigate their function, the ability of RiSMF1, RiSMF3.1 and RiSMF3.2 to complement the phenotype of a yeast strain disrupted in the *SMF1* gene (*smf1*Δ) was tested. Unfortunately, functionality of RiSMF2 could not be analysed, as we were unable to clone its full-length cDNA into the yeast-expression vector. Yeast smf1, a NRAMP homologue, encodes a plasma-membrane Mn transporter with a broad metal specificity. *smf1*Δ cells fail to grow on SD medium containing high concentrations of the divalent chelator EGTA, an effect that is relieved by Mn (Supek et al., 1996). Expression of *RiSMF3.2*, under the control of the yeast PMA1 promoter, complemented the phenotype of the *smf1*Δ cells. However, a strain transformed with the empty vector pDRF1-GW or with the pDRf1:RiSMF1 or pDRf1:RiSMF3.1 plasmids could not grow on SD media supplemented with 6.25 mM EGTA (Figure 3a). These data demonstrate that *RiSMF3.2* cDNA encodes a functional protein that mediates Mn transport.

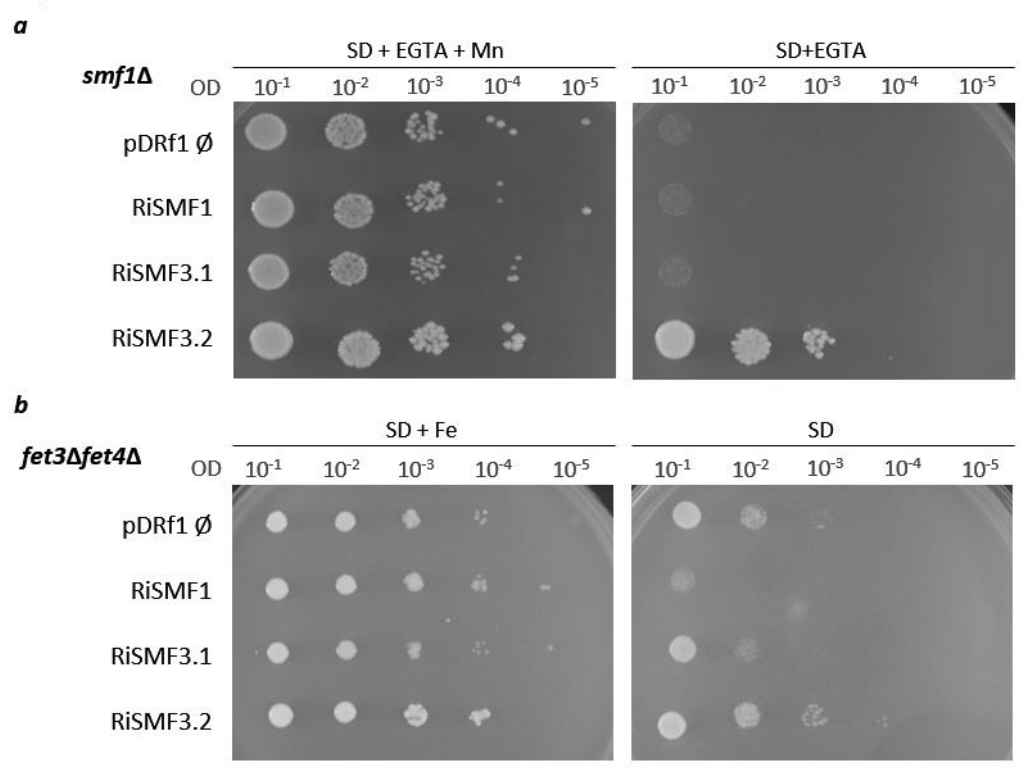

Figure 3. Analysis of RiSMFs function in yeast. (**a**) *smf1*Δ yeast cells transformed with the empty vector or expressing RiSMF1, RiSMF3.1 or RiSMF3.2 were plated on SD-URA medium with 50 mM MES buffer pH 6, 6.25 mM EGTA and supplemented or not with 500 μM $MnSO_4$. (**b**) *fet3*Δ*fet4*Δ cells transformed with the empty vector or expressing RiSMF1, RiSMF3.1 or RiSMF3.2 were plated on SD-URA medium pH 3.5, supplemented with 100 μM $FeCl_3$, or pH 5.4, non-supplemented with Fe. The cultures were diluted to ODs of 10^{-1} to 10^{-5} (as indicated) and spotted on the corresponding selective media.

Subsequently, we tested whether the RiSMFs were able to complement the yeast Fe transport mutant *fet3*Δ*fet4*Δ. This strain is defective in both low- and high-affinity Fe uptake systems and requires high Fe concentrations in its medium of growth as well as a more acidic environment to increase this micronutrient availability (Dix et al., 1994). Therefore, the positive controls were prepared by growing the *fet3*Δ*fet4*Δ cells transformed with the empty vector pDRF1-GW or with the pDRf1:RiSMF1, pDRf1:RiSMF3.1 or pDRf1:RiSMF3.2 plasmids on SD-URA medium pH 3.5, supplemented with 100 ◎M $FeCl_3$. As it was observed for the *smf1*Δ mutant, only RiSMF3.2 restored the ability of *fet3*Δ*fet4*Δ to grow on SD medium (pH 5.4) that was not supplemented with Fe (Figure 3b). These data provide additional evidence that RiSMF3.2 is a metal transporter. Therefore, RiSMF3.2 is a functional homologue of the yeast plasma-membrane smf1 transporter, which mediates transport of Mn and Fe.

To determine subcellular localization of RiSMF3.2 in the heterologous system and to assess whether the failure of RiSMF1 and RiSMF3.1 to complement the phenotypes of the *smf1*Δ and *fet3*Δ*fet4*Δ cells might be because the proteins were located in an intracellular membrane, C terminal GFP-tagged versions of these proteins were expressed in the *smf1*Δ strain under the control of the PMA1 promoter. Functionality of the RiSMF-fusion proteins was assessed before their visualization by fluorescence microscopy. None of the RiSMF-GFP fusion proteins complemented the mutant phenotype of the *smf1*Δ strain (Figure 4a). Cells expressing the RiSMF-GFP fusion proteins showed a general cytosolic fluorescent signal, similar to the one showed by control cells expressing the soluble GFP (Figure 4b). These data suggest a degradation of the misfolded fusion proteins in the proteasomes, a phenomenon, previously, observed in yeast-membrane protein-expression assays (Kauffman et al., 2002).

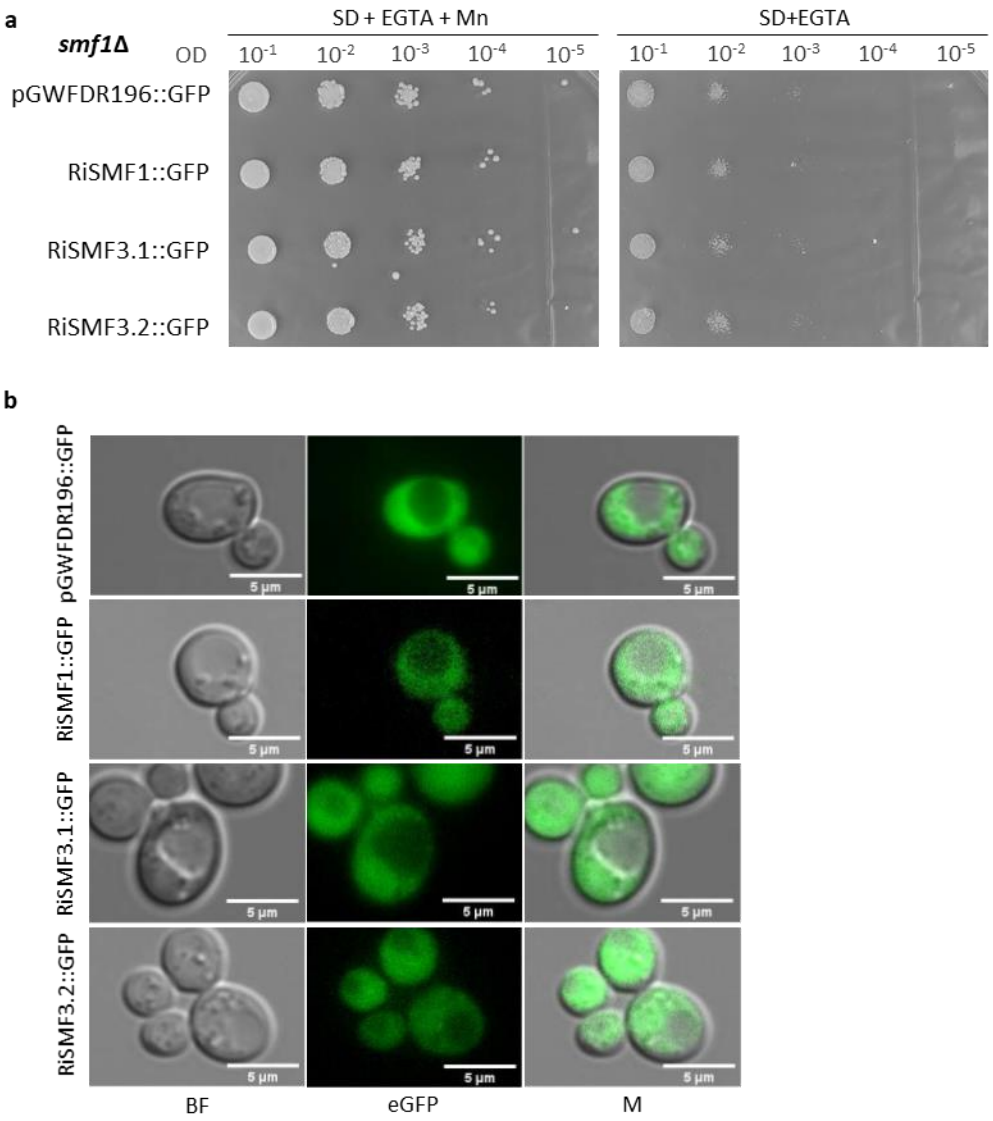

Figure 4. (**a**) *smf1*Δ yeast cells expressing GFP (empty vector pGWFDR196) or C-terminal GFP-tagged version of RiSMF1, RiSMF3.1 or RiSMF3.2 were plated on SD-URA media with 50 mM MES buffer pH 6, 6.25 mM EGTA and supplemented or not with 500 µM $MnSO_4$. The cultures were diluted to ODs of 10^{-1} to 10^{-5} (as indicated) and spotted on the corresponding selective media. (**b**) *smf1*Δ cells expressing GFP (empty vector pGWFDR196) and C-terminal GFP-tagged versions of RiSMF1, RiSMF3.1 or RiSMF3.2 were visualized in a fluorescence microscope. BF, bright field; eGFP, enhanced GFP fluorescence; M, merged images.

RiSMF genes are differentially expressed in various fungal structures

To try to understand the biological function of the *RiSMF*s, their expression levels in various fungal structures were investigated by RT-qPCR in ERM and IRM, grown in association with chicory plants in the *in vivo* whole-plant experimental sandwich system, and in ERM grown in monoxenic cultures. Transcripts of the four *R. irregularis* NRAMP family members were detected, both in the ERM and IRM (Figure 5). Interestingly, *RiSMF1* and *RiSMF2* expression levels were different in ERM grown in monoxenic cultures and in the whole-plant sandwich culture system,

which might be due to the different physiological and developmental stages of both ERM. The ERM grown in monoxenic cultures was developed in association with a root organ culture lacking the plant stem and leaves, which might affect development of the fungus. *RiSMF1* was the most highly expressed isoform both in the ERM and IRM, and no significant differences were observed between *RiSMF3.1* and *RiSMF3.2* expression in ERM and IRM. highly expressed gene in the ERM

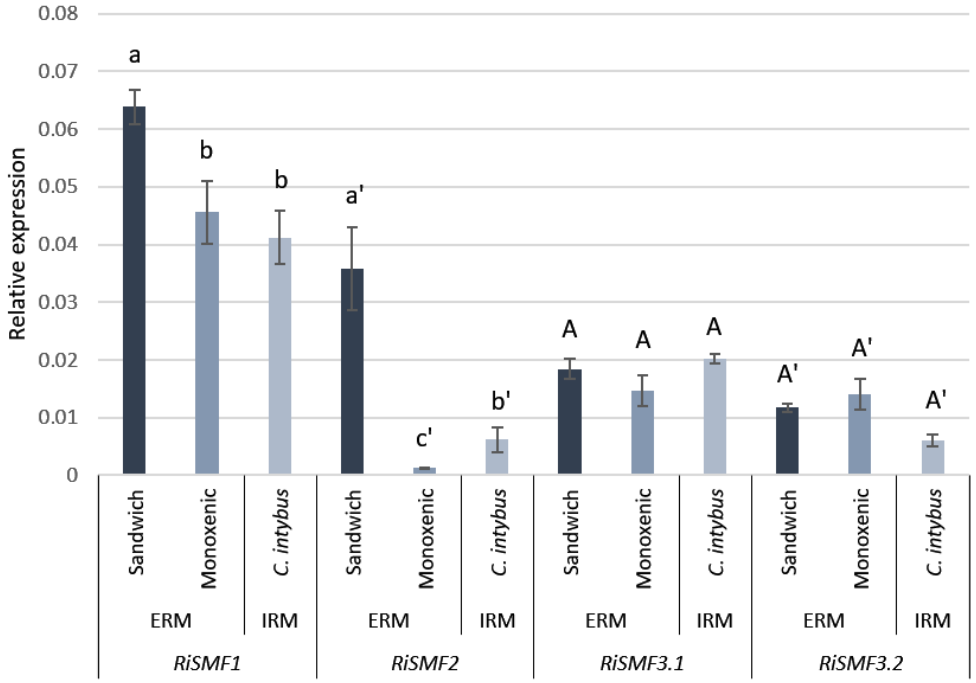

Figure 5. Expression patterns of *R. irregularis SMF* genes. Gene expression was analysed in RNAs isolated from chicory mycorrhizal roots (IRM), ERM collected in the *in vivo* whole-plant bidimensional culture system and ERM from monoxenic cultures. Relative gene-expression levels were calculated using the $2^{-\Delta CT}$ method, with *RiEF1α* as internal control. Bars represent standard error. Different letter types indicate statistical data for each gene. Different letters indicate significant differences ($P < 0.05$; $n = 3$) between treatments.

Starvation regulates RiSMF1 and RiSMF3.1 expression

To gain further information about the potential roles of the RiSMF isoforms, their expression levels were analysed by real-time RT-PCR in ERM and IRM grown in association with chicory plants in the *in vivo* sandwich system under Mn-sufficient and Mn-limiting conditions. Mn deficiency decreased *RiSMF1* transcript levels in the ERM and increased *RiSMF3.1* expression in the IRM (Figure 6a).

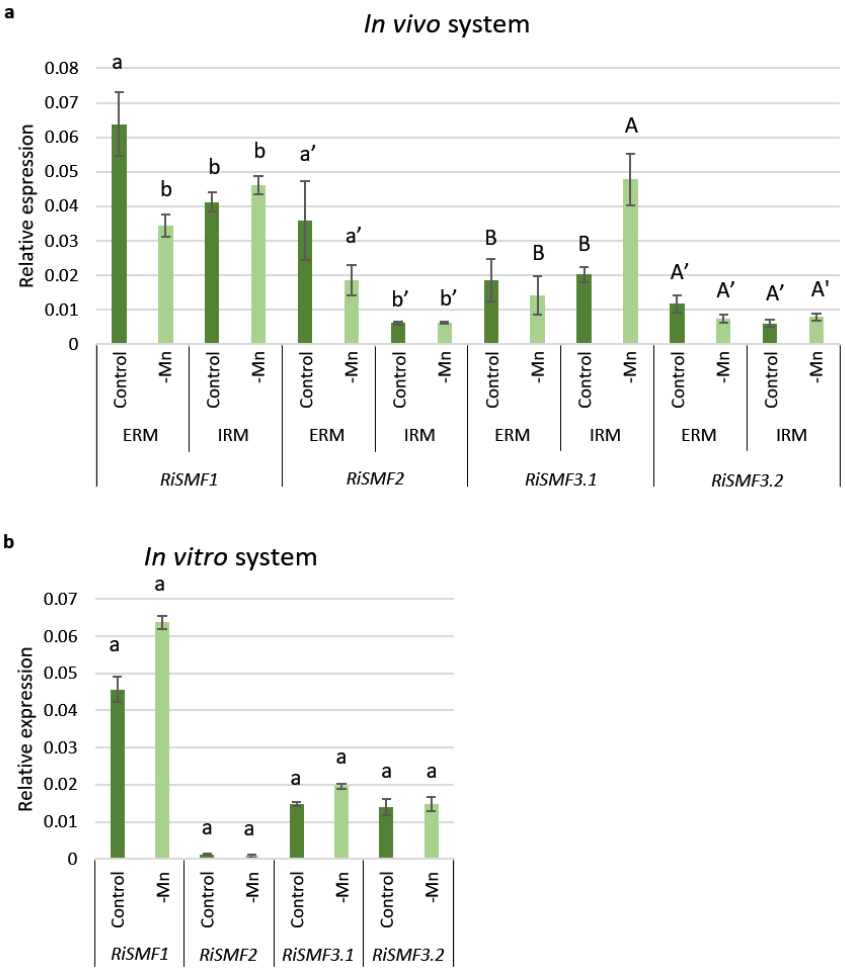

Figure 6. Effect of Mn deficiency on *RiSMF*s expression. (**a**) Gene expression was analysed in RNAs isolated from mycorrhizal roots (IRM) and ERM collected from chicory plants, developed in the whole-plant bidimensional culture system (*in vivo* system) and watered with half-strength Hoagland solution (control, 4.5 µM) or a modified nutrient solution without Mn (-Mn). (**b**) Gene expression was analysed in RNAs isolated from ERM developed in monoxenic cultures (*in vitro* system) in liquid M media without Mn (-Mn) or containing 2 µM Mn (control). Relative-gene-expression levels were calculated, using the $2^{-\Delta CT}$ method with *RiEF1α* as internal control. Bars represent standard error. Different letter types indicate statistical data for each gene. Different letters indicate significant differences ($P < 0.05$; n = 3) between treatments.

The effect of Mn availability on *RiSMF*s expression was also analysed in RNAs isolated from ERM grown in vitro in monoxenic cultures with and without Mn. Expression of none of the *RiSMF* genes was significantly affected by Mn deficiency in the ERM grown in the in vitro culture system (Figure 6b).

Impact of Fe availability on RiSMFs expression

Taking into account that fungal NRAMPs are regulated by Fe and that *RiSMF3.2* has an Fe transport function, the effect of Fe availability on *RiSMF*s expression was assessedto get further insights into their roles in *R. irregularis*. Firstly, the effect of Fe starvation was analysed in ERM and IRM grown in the *in vivo* sandwich system under control and Fe-deficient conditions. A two-fold increase in *RiSMF1* expression was observed in the ERM developed in plants watered with

a nutrient solution without Fe. However, *RiSMF2*, *RiSMF3.1* and *RiSMF3.2* transcript levels were not significantly affected neither in ERM nor IRM (Figure 7a). Up-regulation of *RiSMF1* by Fe deficiency was also observed when the ERM was grown *in vitro* in monoxenic cultures (Figure 7b).

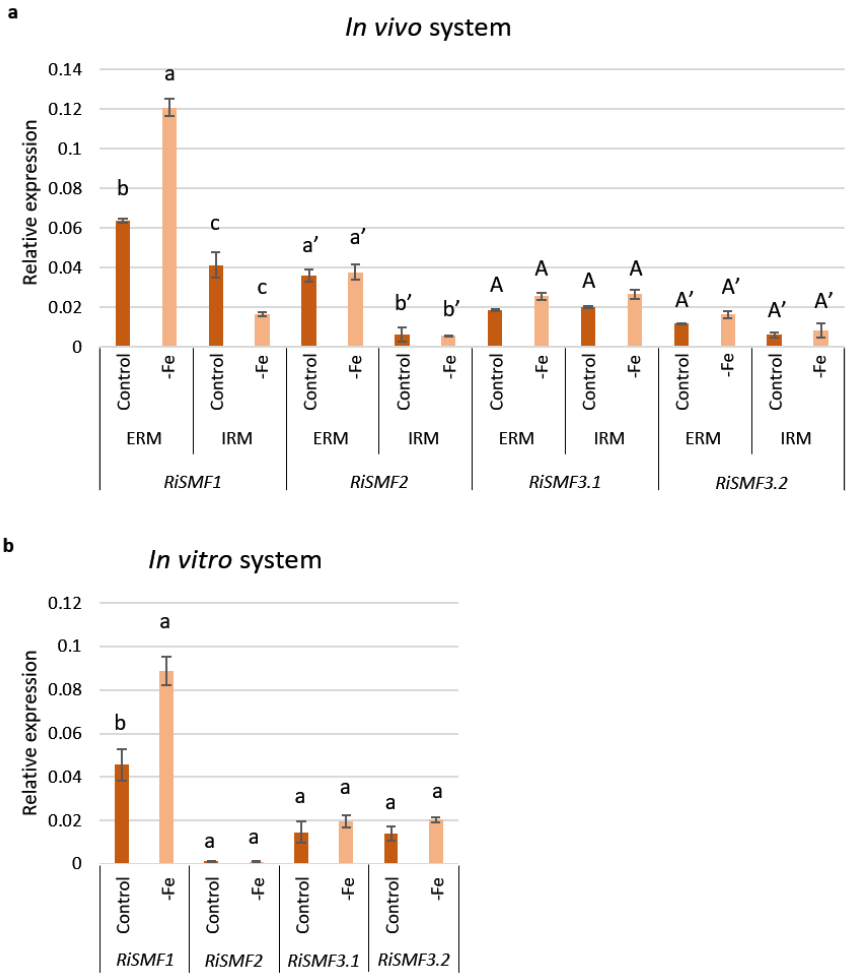

Figure 7. Effect of Fe deficiency on *RiSMF*s expression. (**a**) Gene expression was analysed in RNAs isolated from mycorrhizal roots (IRM) and ERM collected from chicory plants developed in the whole plant bidimensional culture system (*in vivo* system) watered with half-strength Hoagland solution (control, 50 µM Fe) or a modified nutrient solution without Fe (-Fe). (**b**) Gene expression was analysed in RNAs isolated from ERM developed in monoxenic cultures (*in vitro* system) in liquid M media lacking Fe and exposed 3 days to 0.5 mM ferrozine (-Fe) or in M medium containing 45 µM Fe (control). Relative gene expression levels were calculated using the $2^{-\Delta CT}$ method with *RiEF1α* as internal control. Bars represent standard error. Different type letters indicate statistical data for each gene. Different letters indicate significant differences ($P < 0.05$; n =3) between treatments.

To assess whether the *R. irregularis* NRAMPs could play a role on ERM Fe tolerance, *RiSMF*s expression was analysed in ERM grown in monoxenic cultures and exposed for 16 h to 45 mM Fe and in ERM grown for 20 days in a medium supplemented with 45 mM Fe. Transcript levels of *RiSMF1*, *RiSMF2* and *RiSMF3.1* were not significantly affected by Fe toxicity. However, expression of *RiSMF3.2* was transiently up-regulated by Fe toxicity. A 2.5-fold increase was

observed 16 h after Fe addition, while a three-fold decrease was observed when the ERM was grown for 20 days in the presence of 45 mM Fe (Figure 8a).

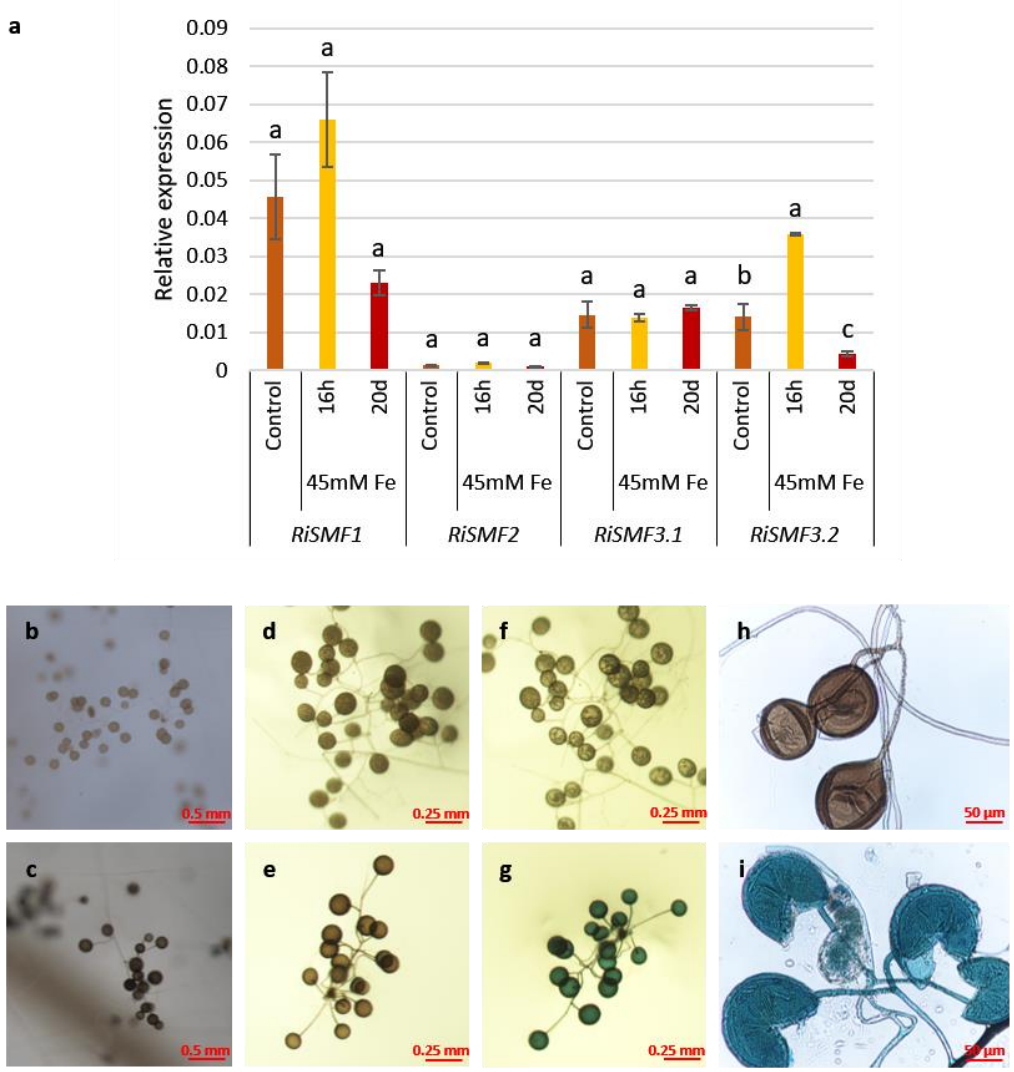

Figure 8. Effect of Fe toxicity on ERM *RiSMF*s expression and Fe accumulation. (**a**) Gene expression was analysed in RNAs isolated from ERM developed in monoxenic cultures in M medium (control), M medium and exposed 3 d for 16 h to 45 mM Fe (16 h) or grown for 20 d in media supplemented with 45 mM Fe (20 d). Relative expression levels were calculated, using the $2^{-\Delta CT}$ method with *RiEF1α* as internal control. Bars represent standard error. Different letters indicate significant differences ($P < 0.05$; $n = 3$), in comparison to the corresponding control value. (**b**–**i**) Fe detection in the ERM by Perls staining. ERM grown in M media supplemented with H_2O (b, control) or supplemented with 45 mM Fe (c, Fe toxicity). Spores from the control plates (**b**,**d**,**f**,**h**) and from the Fe-toxicity conditions (**c**,**e**,**g**,**i**), before (**d**,**e**) and after (**f**–**i**) the addition of Perls stain solution. Crushed spores developed under control, (**h**) Fe toxicity (**i**) and exposed to Perls stain solution. Blue precipitate indicates Fe accumulation.

Spores formed under Fe toxic conditions showed a dark brown colour, suggesting that they might have a high Fe content. To test this hypothesis, spores were incubated in the Perls Prussian blue staining solution (HCl and K-ferrocyanide), which specifically stains Fe labile iron in biological tissues by forming a blue precipitate of ferric ferrocyanide (Prusian blue) (Perls, 1867). After incubation in the staining solution, the spores turned blue. A blue precipitate was detected

in the internal cell wall layers of the crushed spores developed under Fe toxicity, but not in spores grown under control conditions (Figure 8b–i). Moreover, a blue precipitate was detected in the ERM and spore cytoplasm. These data are indicative of Fe accumulation in the fungal spores and ERM.

Impact of Mn and Fe deficiency on R. irregularis development

Taking into account that in fungi Mn deficiency impacts hyphal development and sporulation (Fejes et al., 2020), the effect of Mn deficiency on the development of the ERM and IRM of *R. irregularis* was evaluated in the chicory plants grown in the *in vivo* system. As revealed by Trouvelot quantification of trypan blue-stained roots and by expression analysis of the *R. irregularis EF1α* gene mycorrhizal-colonization levels were not affected by Mn deficiency (Table 2). Spore density, measured in membranes of the sandwich cultures, was not affected either, but an increase in hyphal length was observed under Mn-deficient conditions (Table 2).

Table 2. Effect of Mn deficiency on ERM development and mycorrhizal colonization

	Control	**-Mn**
Spores/cm²	98.67 ± 21.75a	96.28 ± 24.86a
Hyphal length (cm)	93.76 ± 14.07b	197.97 ± 14.22a
RiEF1α	0.20 ± 0.03a	0.15 ± 0.02a
F%	98.60 ± 0.50a	93.09 ± 1.54a
M%	61.93 ± 2.22a	64.94 ± 2.47a
m%	62.71 ± 2.21a	64.62 ± 2.91a
A%	46.61 ± 1.59a	45.77 ± 3.98a
a%	74.98 ± 0.63a	74.66 ± 2.7a

Hyphal length and number of spores were determined in the ERM grown on the nitrocellulose membranes of the whole plant bidimensional culture systems watered with half-strength Hoagland solution (control, 4.5 μM Mn) or with a modified nutrient solution without Mn (-Mn). Mycorrhizal colonization was assessed molecularly by determining the relative expression of *RiEF1α* and histochemically by using the Trouvelot method in roots of chicory roots collected from the culture systems fertilised with and without Mn. F%, frequency of mycorrhiza in the root system; M%, intensity of the mycorrhizal colonization in the root system; m%, intensity of the mycorrhizal colonization in the root fragments; A%, arbuscule abundance in the root system; a%, arbuscule abundance in mycorrhizal parts of root fragments. Values are means ± standard error. Different letters indicate statistically significant differences ($P < 0.05$) among treatments.

As observed for the Mn-deficiency experiment, IRM development in chicory roots was not affected by Fe deficiency. However, sporulation was significantly reduced, while hyphal length was not significantly affected when the ERM was developed under Fe-limiting conditions (Table 3).

Table 3. Effect of Fe deficiency on ERM development and mycorrhizal colonization

	Control	-Fe
Spores/cm²	100.21 ± 20.89a	42.50 ± 10.78b
Hyphal length (cm)	95.80 ± 6.01a	115.01 ± 6.12a
RiEF1α	0.18 ± 0.05a	0.20 ± 0.01a
F%	97.12 ± 2.00a	90.88 ± 2.69a
M%	61.93 ± 4.34a	49.55 ± 8.42a
m%	60.75 ± 3.50a	54.27 ± 8.70a
A%	39.36 ± 6.81a	32.04 ± 7.05a
a%	71.95 ± 7.31a	59.72 ± 9.36a

Hyphal length and number of spores were determined in the ERM grown on the nitrocellulose membranes of the whole-plant bidimensional culture systems watered with half-strength Hoagland solution (control, 50 μM Fe) or with a modified nutrient solution without Fe (-Fe). Mycorrhizal colonisation was assessed molecularly, by determining the relative expression of *RiEF1α*, and histochemically by using the Trouvelot method in chicory roots collected from the culture systems fertilised with and without Fe. F%, frequency of mycorrhiza in the root system; M%, intensity of the mycorrhizal colonization in the root system; m%, intensity of the mycorrhizal colonization in the root fragments; A%, arbuscule abundance in the root system; a%, arbuscule abundance in mycorrhizal parts of root fragments. Values are means ± standard error. Different letters indicate statistically significant differences ($P < 0.05$) among treatments.

Discussion

A previous genome-wide analysis of metal transporters in *R. irregularis* revealed the presence of four gene sequences, *RiSMF1*, *RiSMF2*, *RiSMF3.1* and *RiSMF3.2*, putatively encoding transporters of the NRAMP family (Tamayo et al., 2014). Mining of the more recent *R. irregularis* genome and transcriptome databases confirms that the *R. irregularis* NRAMP family is composed of four members. In this work, we functionally characterised RiSMF3.2 and analysed gene expression patterns of the *R. irregularis* NRAMP family members. Our data indicate that the *RiSMF* genes are differentially regulated by Mn and Fe availability and that *RiSMF3.2* encodes a functional Mn and Fe transporter.

The obligate biotrophic and multinucleate nature of AM fungi prevents the use of the most common strategies to investigate the functionality of a gene of interest. To bypass this technical constrain, we tried to assess the function of the *RiSMF* gene products in yeast. Unfortunately, we could only determine the transport function of RiSMF3.2 in the heterologous system.

Despite only RiSMF3.2 presented a metal transport activity in yeast, the four *R. irregularis* NRAMP sequences contain all the structural features of NRAMP proteins. In fact, they contain the conserved transmembrane motif GQSSTITGTYAGQY(/F)V(/I)MQGFLD(/E/N) and the DPGN motif characteristic of the NRAMP family (Cellier et al., 1995). Numerous mutational studies have shown that both domains are essential for the metal-transport activity of NRAMP transporters (Bozzi & Gaudet, 2021). For example, conservative substitutions of the aspartate (D) and asparagine (N) residues impaired metal binding of the ScaNramp of *Staphylococcus capitis* (Ehrnstorfer et al., 2014) and eliminated metal transport in human NRAMP2 (Bozzi et al., 2016)

and *Ecoli* Nramp (Chaloupka et al., 2005). Thus, this motif in the *R. irregularis* NRAMP proteins should also play a role in metal binding.

The phylogenetic analysis revealed that the Glomeromycotina NRAMP sequences are divided in two subfamilies, a Group I belonging to the clade grouping fungal NRAMP sequences and a Group II that is independent from the clusters formed by animal, plant, fungal and bacterial sequences. Group II is more closely related to known plant NRAMP sequences than to fungal sequences. In addition to the divergence in primary amino acid sequence between genes from Group I and II, they display some differences in gene organization. Members of Group II are more fragmented and have three–four introns, located at conserved positions at the carboxy-terminus. This sequence divergence suggests an early evolutionary separation between the two groups of Glomeromycotina NRAMPs. The observation that all AM fungal species analysed have NRAMP genes from Group I and Group II suggests that both groups are required for proper metal homeostasis in AM fungi. Further studies are required to determine if proteins of the two groups display different transport functions.

The finding that RiSMF3.2 reverts the mutant phenotype of the *smf1*Δ and *fet3*Δ*fet4*Δ strains lacking, respectively, the high-affinity Mn transporter smf1 and the iron uptake systems indicates that *RiSMF3.2* encodes a NRAMP transporter that mediates Mn and Fe uptake. Although subcellular localization of RiSMF3.2 could not be demonstrated in yeast, it is the functional orthologue of the plasma-membrane smf1 transporter. The other members of the *R. irregularis* NRAMP family could not be characterised in the heterologous system because, as revealed by the yeast localization assays, they were not expressed in the yeast membranes, most likely as a consequence of an artefact of the heterologous system. Although the principles of targeting seem to be conserved between organisms, the heterologous proteins may lack the sequences required for targeting to the correct compartment in the cell, so problems regarding the correct folding and targeting of the heterologous expressed proteins can occur (Frommer & Ninnemann, 1995).

RiSMF1 function could not be determined, but it seems to be involved in Mn and Fe homeostasis, as its expression levels in the ERM are regulated by Mn and Fe availability. The contrasting expression patterns of *RiSMF1* in the ERM grown in the *in vivo* and *in vitro* cultures systems under Mn deficient conditions may be because the ERM grown in monoxenic cultures is not Mn harvested. Since the culture medium of the root compartment contains Mn, it is possible that Mn is transferred from the IRM to the ERM in the monoxenic cultures. Down-regulation of *RiSMF1* by Mn deficiency is striking, as high-affinity metal transporters are expected to be up-regulated under metal deficient conditions. However, unexpected regulation patterns of NRAMP genes by Mn have been observed in various organisms. For example, expression of the *Aspergillus*

oryzae AoNramp1 gene increases under Mn toxicity (Fan et al., 2021) and transcript levels of the cucumber *CsNRAMP1*, *CsNRAMP4* and *CsNRAMP5* genes decrease under Mn deficiency (Zhang et al., 2021). How Mn availability affects NRAMP gene expression remains to be investigated. As it has been described for the yeast smf1p and smf2p transporters, the *RiSMFs* could also be regulated at the post-translational level by Mn (Portnoy et al., 2000).

Up-regulation of *RiSMF1* expression in the ERM under Fe-limiting conditions suggests a role for its encoded protein in Fe-deficiency alleviation. Since the RiSMF1 subcellular location could not be determined in the heterologous system, its role in Fe homeostasis could either be due to its capacity to increase Fe uptake from the environment or to mobilise the vacuolar Fe stores under Fe-limiting conditions. Although *RiSMF3.2* transcript levels were not regulated by Fe deficiency, the yeast-complementation assays revealed that it encodes a plasma-membrane Fe transporter of the NRAMP family involved in Fe uptake. The observation that *RiSMF3.2* transcript levels were not regulated by Fe deficiency might be because it encodes a low-affinity Fe transporter that operates under replete Fe concentrations. Although yeast smf1p is a high-affinity transporter, the *Arabidopsis thaliana* AtNRAMP1 has been shown to be a low-affinity transporter that contributes to Fe uptake under Fe sufficient conditions (Castaings et al., 2016). Recent work by Tamayo et al. (2018) has identified two *R. irregularis* Fe permeases (RiFTR1 and RiFTR2) involved in Fe homeostasis. RiFTR1 is involved in high-affinity Fe acquisition by the plasma membrane and RiFTR2 in Fe homeostasis under Fe-limiting conditions. These data, altogether, suggest that *R. irregularis* uses various strategies to increase Fe uptake from the environment depending on the external Fe concentration, the plasma-membrane RiFTR1 and RiSMF3.2 transporters. Similarly, multiple systems operate at the cell surface for Fe uptake in *S. cerevisiae*, the high-affinity Fe transporters Ftr1p and smfp1 and the low-affinity transporter Fet4p (Chen et al., 1999; Dix et al., 1994; Stearman et al., 1996). Additional studies at the protein level are needed to understand whether RiSMF1 mediates Fe uptake from the environment or mobilises the Fe vacuolar stores and the relative contribution of the different Fe transporters to Fe uptake by the ERM.

As expected for an uptake plasma-membrane transporter, *RiSMF3.2* expression levels decreased when the ERM was grown in a media containing 45 mM Fe for 20 d. A similar expression pattern was observed by Tamayo et al. (2018) for the Fe transporters RiFTR1 and RiFTR2 under these experimental conditions. Yeast NRAMP Smf1p, the orthologue of RiSMF3.2, is also down-regulated by metal toxicity (Liu & Culotta, 1999). Transcriptional down-regulation of the *R. irregularis* proteins mediating Fe transport into the cytosol will limit uptake of toxic levels of Fe by the ERM. However, the effect of Fe toxicity on *RiSMF3.2* expression 16 h after the addition

of 45 mM Fe resulting in enhanced transcript levels was striking. This difference implies that the contribution of RiSMF3.2 at the early stages of Fe toxicity would be to increase Fe uptake, leading to an increased Fe toxicity. Alternatively, it could be hypothesised that RiSMF3.2 could act as a sensor of high external Fe concentrations to activate the signalling cascades involved in Fe tolerance. In fact, nutrient sensing in fungi can be mediated by transceptors, proteins with both transport and receptor functions (Conrad et al., 2014; Johns et al., 2021). In the absence of a methodology to silence AM fungal genes in the ERM, it is not possible to understand the biological significance of this transient increase in *RiSMF3.2* mRNA levels.

Gene expression of the *RiSMF*s in the IRM reveals the importance of keeping both Mn and Fe homeostasis during the *in planta* phase of the fungus. Further studies are required to determine the host cues regulating *RiSMFs* expression in the IRM, and if they are involved in metal uptake from the apoplast of the symbiotic interface. Up-regulation of *RiSMF3.1* expression by Mn deficiency in the IRM suggests that, under Mn starvation, the fungus needs to increase its Mn cytosolic content, in order to provide it to the Mn-requiring enzymes, such as the mitochondrial Mn superoxide dismutase and the Golgi-located enzymes involved in the glycosylation of secretory proteins (Crowley et al., 2000). In fact, the yeast smf2p transporter has been shown to be a central player in Mn trafficking to the mitochondria and other cellular sites (Luk & Culotta, 2001). Taking into account that expression of the *RiSMF* genes is not affected by Fe deficiency in the IRM and the high expression levels reported for the high-affinity transporter RiFTR1 in the IRM (Tamayo et al., 2018), it is likely that RiFTR1 is the major player in Fe homeostasis, in the structures the fungus develops in the root.

Numerous studies have shown that AM fungi increase plant acquisition of the essential metals Zn, Cu and Fe; however, information about the role of the symbiosis in plant Mn nutrition and on the underlying mechanisms is scarce. While a few studies have shown that Mn uptake is higher in mycorrhizal plants (Eivazi & Weir, 1989; Lehmann & Rillig, 2015) it has been, repeatedly, reported that Mn acquisition decreases in mycorrhizal plants (Kothari et al., 1991). AM fungi have been shown to reduce the number of Mn-reducing bacteria (Posta et al., 1994) or increase the number of Mn-oxidizing bacteria in the rhizosphere (Arines et al., 1992), decreasing indirectly Mn availability. Nevertheless, the observed hyphal length observed under Mn-deficient conditions indicates that, under these conditions, the fungus explores a higher volume of soil, which will increase the nutrient-uptake effectiveness of the mycorrhizal root. Under field conditions, Mn uptake by mycorrhizal roots may depend on which of the two functions (Mn availability in the mycorrhizosphere or volume of soil exploited by the mycorrhizal root) prevails in the soil.

Regarding the effect of Mn on the developmental partner of the ERM, the increased hyphal length observed, when the fungus grows in the absence of Mn, agrees with previous observations for other nutrients (Bago et al., 2004; Olsson et al., 2014). As proposed by Bago et al. (2004) and Olsson et al. (2014), this growth pattern is probably designed to explore and exploit more efficiently the growth medium. An effect of Mn deficiency on hyphal development has been also reported in *Aspergillus niger* (Fejes et al., 2020). Although Fe deficiency did not affect hyphal length, it decreased sporulation. Fe is an essential micronutrient that is a cofactor of numerous enzymes thanks to its ability to easily accept and release electrons (Hänsch & Mendel, 2009; Lippard & Berg, 1994). Therefore, inhibition of sporulation might be as a consequence of the inhibition of the activity of the enzymes required for spore formation when the fungus is grown in media lacking Fe. Previous studies have shown that AM fungal-spore formation is affected by nutrient availability (Eivazi & Weir, 1989). Detection of Fe in the spores developed under Fe toxicity agrees with previous observations for other metals, such as Cu, Zn and Cd (Cornejo et al., 2013; Garcia et al., 2020; González-Guerrero et al., 2008), and supports the hypothesis that a survival strategy of AM fungi in metal-contaminated environments is to accumulate the excess metal in some spores of the fungal colony. Iron accumulation in the fungus will reduce plant Fe availability, which will explain, at least partially, the improved performance of mycorrhizal plants, in soils affected by iron mining tailing (Zago et al., 2019; Zanchi et al., 2021).

In conclusion, this chapter describes, for the first time, characterization of the NRAMP family members, the *RiSMF* genes, in an AM fungus. The *R. irregularis* SMF genes are expressed both in the ERM and IRM and are differentially regulated by environmental Fe and Mn. *RiSMF3.2* encodes a protein mediating Mn and Fe transport from the environment, being the first Mn transporter reported in an AM fungus. These data indicate *R. irregularis* uses various strategies to increase Fe uptake from the environment: the previously identified plasma-membrane Fe permease RiFTR1 and the RiSMF3.2 NRAMP transporter. Further studies are required to understand the relative contribution of these transporters to Fe uptake by the IRM and the ERM and to elucidate the role of the other members of the *R. irregularis* NRAMP family.

References

Agranoff, D., Collins, L., Kehres, D., Harrison, T., Maguire, M., & Krishna, S. (2005). The Nramp orthologue of *Cryptococcus neoformans* is a pH-dependent transporter of manganese, iron, cobalt and nickel. *Biochemical Journal*, *385*(1), 225–232. https://doi.org/10.1042/BJ20040836

Arines, J., Porto, M. E., & Vilariño, A. (1992). Effect of manganese on vesicular-arbuscular mycorrhizal development in red clover plants and on soil Mn-oxidizing bacteria. *Mycorrhiza*, *1*(3), 127–131. https://doi.org/10.1007/BF00203260

Azcón-Aguilar, C., & Barea, J. M. (2015). Nutrient cycling in the mycorrhizosphere. *Journal of Soil Science and Plant Nutrition*, *15*. https://doi.org/10.4067/S0718-95162015005000035

Bago, B., Cano, C., Azcón-Aguilar, C., Samson, J., Coughlan, A. P., & Piché, Y. (2004). Differential morphogenesis of the extraradical mycelium of an arbuscular mycorrhizal fungus grown monoxenically on spatially heterogeneous culture media. *Mycologia*, *96*(3), 452–462. https://doi.org/10.1080/15572536.2005.11832944

Bensen, E. S., Martin, S. J., Li, M., Berman, J., & Davis, D. A. (2004). Transcriptional profiling in Candida albicans reveals new adaptive responses to extracellular pH and functions for Rim101p. *Molecular Microbiology*, *54*(5), 1335–1351. https://doi.org/10.1111/j.1365-2958.2004.04350.x

Bozzi, A. T., Bane, L. B., Weihofen, W. A., McCabe, A. L., Singharoy, A., Chipot, C. J., Schulten, K., & Gaudet, R. (2016). Conserved methionine dictates substrate preference in Nramp-family divalent metal transporters. *Proceedings of the National Academy of Sciences*, *113*(37), 10310–10315. https://doi.org/10.1073/pnas.1607734113

Bozzi, A. T., & Gaudet, R. (2021). Molecular Mechanism of Nramp-Family Transition Metal Transport. *Journal of Molecular Biology*, *433*(16), 166991. https://doi.org/10.1016/j.jmb.2021.166991

Casieri, L., Ait Lahmidi, N., Doidy, J., Veneault-Fourrey, C., Migeon, A., Bonneau, L., Courty, P.-E., Garcia, K., Charbonnier, M., Delteil, A., Brun, A., Zimmermann, S., Plassard, C., & Wipf, D. (2013). Biotrophic transportome in mutualistic plant–fungal interactions. *Mycorrhiza*, *23*(8), 597–625. https://doi.org/10.1007/s00572-013-0496-9

Castaings, L., Caquot, A., Loubet, S., & Curie, C. (2016). The high-affinity metal Transporters NRAMP1 and IRT1 Team up to Take up Iron under Sufficient Metal Provision. *Scientific Reports*, *6*(1), 37222. https://doi.org/10.1038/srep37222

Cellier, M., Privé, G., Belouchi, A., Kwan, T., Rodrigues, V., Chia, W., & Gros, P. (1995). Nramp defines a family of membrane proteins. *Proceedings of the National Academy of Sciences*, *92*(22), 10089–10093. https://doi.org/10.1073/pnas.92.22.10089

Chabot, S., Bécard, G., & Piché, Y. (1992). Life Cycle of *Glomus Intraradix* in Root Organ Culture. *Mycologia*, *84*(3), 315–321. https://doi.org/10.1080/00275514.1992.12026144

Chaloupka, R., Courville, P., Veyrier, F., Knudsen, B., Tompkins, T. A., & Cellier, M. F. M. (2005). Identification of Functional Amino Acids in the Nramp Family by a Combination of Evolutionary Analysis and Biophysical Studies of Metal and Proton Cotransport *in Vivo*. *Biochemistry*, *44*(2), 726–733. https://doi.org/10.1021/bi048014v

Chen, E. C. H., Morin, E., Beaudet, D., Noel, J., Yildirir, G., Ndikumana, S., Charron, P., St-Onge, C., Giorgi, J., Krüger, M., Marton, T., Ropars, J., Grigoriev, I. v., Hainaut, M., Henrissat, B., Roux, C., Martin, F., & Corradi, N. (2018). High intraspecific genome diversity in the model arbuscular mycorrhizal symbiont *Rhizophagus irregularis*. *New Phytologist*, *220*(4), 1161–1171. https://doi.org/10.1111/nph.14989

Chen, X.-Z., Peng, J.-B., Cohen, A., Nelson, H., Nelson, N., & Hediger, M. A. (1999). Yeast SMF1 Mediates H+-coupled Iron Uptake with Concomitant Uncoupled Cation Currents. *Journal of Biological Chemistry*, *274*(49), 35089–35094. https://doi.org/10.1074/jbc.274.49.35089

Cohen, A., Nelson, H., & Nelson, N. (2000). The Family of SMF Metal Ion Transporters in Yeast Cells. *Journal of Biological Chemistry*, *275*(43), 33388–33394. https://doi.org/10.1074/jbc.M004611200

Conrad, M., Schothorst, J., Kankipati, H. N., van Zeebroeck, G., Rubio-Texeira, M., & Thevelein, J. M. (2014). Nutrient sensing and signaling in the yeast *Saccharomyces cerevisiae*. *FEMS Microbiology Reviews*, *38*(2), 254–299. https://doi.org/10.1111/1574-6976.12065

Cornejo, P., Pérez-Tienda, J., Meier, S., Valderas, A., Borie, F., Azcón-Aguilar, C., & Ferrol, N. (2013). Copper compartmentalization in spores as a survival strategy of arbuscular mycorrhizal fungi in Cu-polluted environments. *Soil Biology and Biochemistry*, *57*, 925–928. https://doi.org/10.1016/j.soilbio.2012.10.031

Crowley, J. D., Traynor, D. A., & Weatherburn, D. C. (2000). Enzymes and Protein Containing Manganese: An Overview. In *Metal Ions in Biological Systems* (Vol. 37, pp. 209–278).

Dix, D. R., Bridgham, J. T., Broderius, M. A., Byersdorfer, C. A., & Eide, D. J. (1994). The *FET4* gene encodes the low affinity Fe(II) transport protein of *Saccharomyces cerevisiae*. *Journal of Biological Chemistry*, *269*(42), 26092–26099. https://doi.org/10.1016/S0021-9258(18)47163-3

Ehrnstorfer, I. A., Geertsma, E. R., Pardon, E., Steyaert, J., & Dutzler, R. (2014). Crystal structure of a SLC11 (NRAMP) transporter reveals the basis for transition-metal ion transport. *Nature Structural & Molecular Biology*, *21*(11), 990–996. https://doi.org/10.1038/nsmb.2904

Eide, D., Broderius, M., Fett, J., & Guerinot, M. L. (1996). A novel iron-regulated metal transporter from plants identified by functional expression in yeast. *Proceedings of the National Academy of Sciences*, *93*(11), 5624–5628. https://doi.org/10.1073/pnas.93.11.5624

Eivazi, F., & Weir, C. C. (1989). Phosphorus and mycorrhizal interaction on uptake of P and trace elements by maize. *Fertilizer Research*, *21*(1), 19–22. https://doi.org/10.1007/BF01054731

Fan, J., Zhang, H., Li, Y., Chen, Z., Chen, T., Zeng, B., & Zhang, Z. (2021). Identification and characterization of Nramp transporter AoNramp1 in *Aspergillus oryzae*. *Biotech*, *11*(10), 452. https://doi.org/10.1007/s13205-021-02998-z

Fejes, B., Ouedraogo, J.-P., Fekete, E., Sándor, E., Flipphi, M., Soós, Á., Molnár, Á. P., Kovács, B., Kubicek, C. P., Tsang, A., & Karaffa, L. (2020). The effects of external Mn2+ concentration on hyphal morphology and citric acid production are mediated primarily by the NRAMP-family transporter DmtA in *Aspergillus niger*. *Microbial Cell Factories*, *19*(1), 17. https://doi.org/10.1186/s12934-020-1286-7

Ferrol, N., Tamayo, E., & Vargas, P. (2016). The heavy metal paradox in arbuscular mycorrhizas: from mechanisms to biotechnological applications. *Journal of Experimental Botany*, *67*(22), 6253–6265. https://doi.org/10.1093/jxb/erw403

Festa, R. A., & Thiele, D. J. (2011). Copper: An essential metal in biology. *Current Biology*, *21*(21), R877–R883. https://doi.org/10.1016/j.cub.2011.09.040

Frommer, W. B., & Ninnemann, O. (1995). Heterologous Expression of Genes in Bacterial, Fungal, Animal, and Plant Cells. *Annual Review of Plant Physiology and Plant Molecular Biology*, *46*(1), 419–444. https://doi.org/10.1146/annurev.pp.46.060195.002223

Garcia, K. G. V., Mendes Filho, P. F., Pinheiro, J. I., do Carmo, J. F., de Araújo Pereira, A. P., Martins, C. M., de Abreu, M. G. P., & Oliveira Filho, J. de S. (2020). Attenuation of Manganese-Induced Toxicity in *Leucaena leucocephala* Colonized by Arbuscular Mycorrhizae. *Water, Air, & Soil Pollution*, *231*(1), 22. https://doi.org/10.1007/s11270-019-4381-9

García-Rodríguez, S., Azcón-Aguilar, C., & Ferrol, N. (2007). Transcriptional regulation of host enzymes involved in the cleavage of sucrose during arbuscular mycorrhizal symbiosis. *Physiologia Plantarum*, *129*(4), 737–746. https://doi.org/10.1111/j.1399-3054.2007.00873.x

Gómez-Gallego, T., Benabdellah, K., Merlos, M. A., Jiménez-Jiménez, A. M., Alcon, C., Berthomieu, P., & Ferrol, N. (2019). The *Rhizophagus irregularis* Genome Encodes Two CTR Copper Transporters That Mediate Cu Import Into the Cytosol and a CTR-Like Protein Likely Involved in Copper Tolerance. *Frontiers in Plant Science*, *10*, 604. https://doi.org/10.3389/fpls.2019.00604

González-Guerrero, M., Melville, L. H., Ferrol, N., Lott, J. N. A., Azcón-Aguilar, C., & Peterson, R. L. (2008). Ultrastructural localization of heavy metals in the extraradical mycelium and spores of the arbuscular

mycorrhizal fungus *Glomus intraradices*. *Canadian Journal of Microbiology*, *54*(2), 103–110. https://doi.org/10.1139/W07-119

Hall, J. L., & Williams, L. E. (2003). Transition metal transporters in plants. *Journal of Experimental Botany*, *54*(393), 2601–2613. https://doi.org/10.1093/JXB/ERG303

Hänsch, R., & Mendel, R. R. (2009). Physiological functions of mineral micronutrients (Cu, Zn, Mn, Fe, Ni, Mo, B, Cl). *Current Opinion in Plant Biology*, *12*(3), 259–266. https://doi.org/10.1016/j.pbi.2009.05.006

Johns, L. E., Goldman, G. H., Ries, L. N. A., & Brown, N. A. (2021). Nutrient sensing and acquisition in fungi: mechanisms promoting pathogenesis in plant and human hosts. *Fungal Biology Reviews*, *36*, 1–14. https://doi.org/10.1016/j.fbr.2021.01.002

Kauffman, K. J., Pridgen, E. M., Doyle, F. J., Dhurjati, P. S., & Robinson, A. S. (2002). Decreased Protein Expression and Intermittent Recoveries in BiP Levels Result from Cellular Stress during Heterologous Protein Expression in *Saccharomyces cerevisiae*. *Biotechnology Progress*, *18*(5), 942–950. https://doi.org/10.1021/bp025518g

Kothari, S. K., Marschner, H., & Römheld, V. (1991). Effect of a vesicular-arbuscular mycorrhizal fungus and rhizosphere micro-organisms on manganese reduction in the rhizosphere and manganese concentrations in maize (Zea mays L.). *New Phytologist*, *117*(4), 649–655. https://doi.org/10.1111/j.1469-8137.1991.tb00969.x

Kumar, S., Stecher, G., Li, M., Knyaz, C., & Tamura, K. (2018). MEGA X: Molecular Evolutionary Genetics Analysis across Computing Platforms. *Molecular Biology and Evolution*, *35*(6), 1547–1549. https://doi.org/10.1093/molbev/msy096

Lehmann, A., & Rillig, M. C. (2015). Arbuscular mycorrhizal contribution to copper, manganese and iron nutrient concentrations in crops – A meta-analysis. *Soil Biology and Biochemistry*, *81*, 147–158. https://doi.org/10.1016/j.soilbio.2014.11.013

Lippard, S. J., & Berg, J. M. (1994). *Principles of bioinorganic chemistry*. University Science Books.

Liu, X. F., & Culotta, V. C. (1999). Post-translation Control of Nramp Metal Transport in Yeast. *Journal of Biological Chemistry*, *274*(8), 4863–4868. https://doi.org/10.1074/jbc.274.8.4863

Luginbuehl, L. H., Menard, G. N., Kurup, S., van Erp, H., Radhakrishnan, G. v., Breakspear, A., Oldroyd, G. E. D., & Eastmond, P. J. (2017). Fatty acids in arbuscular mycorrhizal fungi are synthesized by the host plant. *Science*, *356*(6343), 1175–1178. https://doi.org/10.1126/science.aan0081

Luk, E. E.-C., & Culotta, V. C. (2001). Manganese Superoxide Dismutase in *Saccharomyces cerevisiae* Acquires Its Metal Co-factor through a Pathway Involving the Nramp Metal Transporter, Smf2p. *Journal of Biological Chemistry*, *276*(50), 47556–47562. https://doi.org/10.1074/jbc.M108923200

Maeda, T., Sugiura, R., Kita, A., Saito, M., Deng, L., He, Y., Yabin, L., Fujita, Y., Takegawa, K., Shuntoh, H., & Kuno, T. (2004). Pmr1, a P-type ATPase, and Pdt1, an Nramp homologue, cooperatively regulate cell morphogenesis in fission yeast: The importance of Mn2+ homeostasis. *Genes to Cells*, *9*(1), 71–82. https://doi.org/10.1111/j.1356-9597.2004.00699.x

Marschner, H. (1995). Functions of Mineral Nutrients: Micronutrients. In *Marschner's Mineral Nutrition of Higher Plants* (pp. 313–404). Elsevier. https://doi.org/10.1016/B978-0-08-057187-4.50015-1

Marsh, B. A. (1971). Measurement of Length in Random Arrangements of Lines. *The Journal of Applied Ecology*, *8*(1), 265. https://doi.org/10.2307/2402144

Mori, T., Nagai, Y., Kawagishi, H., & Hirai, H. (2018). Functional characterization of the manganese transporter smf2 homologue gene, PsMnt, of Phanerochaete sordida YK-624 via homologous overexpression. *FEMS Microbiology Letters*, *365*(8), 50. https://doi.org/10.1093/femsle/fny050

Nevo, Y., & Nelson, N. (2006). The NRAMP family of metal-ion transporters. *Biochimica et Biophysica Acta (BBA) - Molecular Cell Research*, *1763*(7), 609–620. https://doi.org/10.1016/j.bbamcr.2006.05.007

Olsson, O., Olsson, P. A., & Hammer, E. C. (2014). Phosphorus and carbon availability regulate structural composition and complexity of AM fungal mycelium. *Mycorrhiza*, *24*(6), 443–451. https://doi.org/10.1007/s00572-014-0557-8

Pepe, A., Sbrana, C., Ferrol, N., & Giovannetti, M. (2017). An in vivo whole-plant experimental system for the analysis of gene expression in extraradical mycorrhizal mycelium. *Mycorrhiza*, *27*(7), 659–668. https://doi.org/10.1007/s00572-017-0779-7

Perls, M. (1867). Nachweis von Eisenoxyd in gewissen Pigmenten. *Archiv Für Pathologische Anatomie Und Physiologie Und Für Klinische Medicin*, *39*(1), 42–48. https://doi.org/10.1007/BF01878983

Portnoy, M. E., Jensen, L. T., & Culotta, V. C. (2002). The distinct methods by which manganese and iron regulate the Nramp transporters in yeast. *Biochemical Journal*, *362*(1), 119–124. https://doi.org/10.1042/bj3620119

Portnoy, M. E., Liu, X. F., & Culotta, V. C. (2000). *Saccharomyces cerevisiae* Expresses Three Functionally Distinct Homologues of the Nramp Family of Metal Transporters. *Molecular and Cellular Biology*, *20*(21), 7893–7902. https://doi.org/10.1128/MCB.20.21.7893-7902.2000

Posta, K., Marschner, H., & Römheld, V. (1994). Manganese reduction in the rhizosphere of mycorrhizal and nonmycorrhizal maize. *Mycorrhiza*, *5*(2), 119–124. https://doi.org/10.1007/BF00202343

Quiroga, G., Erice, G., Aroca, R., Chaumont, F., & Ruiz-Lozano, J. M. (2017). Enhanced Drought Stress Tolerance by the Arbuscular Mycorrhizal Symbiosis in a Drought-Sensitive Maize Cultivar Is Related to a Broader and Differential Regulation of Host Plant Aquaporins than in a Drought-Tolerant Cultivar. *Frontiers in Plant Science*, *8*. https://doi.org/10.3389/fpls.2017.01056

Riaz, M., Kamran, M., Fang, Y., Wang, Q., Cao, H., Yang, G., Deng, L., Wang, Y., Zhou, Y., Anastopoulos, I., & Wang, X. (2021). Arbuscular mycorrhizal fungi-induced mitigation of heavy metal phytotoxicity in metal contaminated soils: A critical review. *Journal of Hazardous Materials*, *402*, 123919. https://doi.org/10.1016/j.jhazmat.2020.123919

Rivero, J., Lidoy, J., Llopis-Giménez, Á., Herrero, S., Flors, V., & Pozo, M. J. (2021). Mycorrhizal symbiosis primes the accumulation of antiherbivore compounds and enhances herbivore mortality in tomato. *Journal of Experimental Botany*, *72*(13), 5038–5050. https://doi.org/10.1093/jxb/erab171

Schiestl, R. H., & Gietz, R. D. (1989). High efficiency transformation of intact yeast cells using single stranded nucleic acids as a carrier. *Current Genetics*, *16*(5–6), 339–346. https://doi.org/10.1007/BF00340712

Schutzendubel, A., & Polle, A. (2002). Plant responses to abiotic stresses: heavy metal-induced oxidative stress and protection by mycorrhization. *Journal of Experimental Botany*, *53*(372), 1351–1365. https://doi.org/10.1093/jexbot/53.372.1351

Spatafora, J. W., Chang, Y., Benny, G. L., Lazarus, K., Smith, M. E., Berbee, M. L., Bonito, G., Corradi, N., Grigoriev, I., Gryganskyi, A., James, T. Y., O'Donnell, K., Roberson, R. W., Taylor, T. N., Uehling, J., Vilgalys, R., White, M. M., & Stajich, J. E. (2016). A phylum-level phylogenetic classification of zygomycete fungi based on genome-scale data. *Mycologia*, *108*(5), 1028–1046. https://doi.org/10.3852/16-042

St-Arnaud, M., Hamel, C., Vimard, B., Caron, M., & Fortin, J. A. (1996). Enhanced hyphal growth and spore production of the arbuscular mycorrhizal fungus Glomus intraradices in an in vitro system in the absence of host roots. *Mycological Research*, *100*(3), 328–332. https://doi.org/10.1016/S0953-7562(96)80164-X

Stearman, R., Yuan, D. S., Yamaguchi-Iwai, Y., Klausner, R. D., & Dancis, A. (1996). A Permease-Oxidase Complex Involved in High-Affinity Iron Uptake in Yeast. *Science*, *271*(5255), 1552–1557. https://doi.org/10.1126/science.271.5255.1552

Supek, F., Supekova, L., Nelson, H., & Nelson, N. (1996). A yeast manganese transporter related to the macrophage protein involved in conferring resistance to mycobacteria. *Proceedings of the National Academy of Sciences*, *93*(10), 5105–5110. https://doi.org/10.1073/pnas.93.10.5105

Tabuchi, M., Yoshida, T., Takegawa, K., & Kishi, F. (1999). Functional analysis of the human NRAMP family expressed in fission yeast. *Biochemical Journal*, *344*(1), 211–219. https://doi.org/10.1042/bj3440211

Tamayo, E., Gómez-Gallego, T., Azcón-Aguilar, C., & Ferrol, N. (2014). Genome-wide analysis of copper, iron and zinc transporters in the arbuscular mycorrhizal fungus *Rhizophagus irregularis*. *Frontiers in Plant Science*, *5*, 547. https://doi.org/10.3389/fpls.2014.00547

Tamayo, E., Knight, S. A. B., Valderas, A., Dancis, A., & Ferrol, N. (2018). The arbuscular mycorrhizal fungus *Rhizophagus irregularis* uses a reductive iron assimilation pathway for high-affinity iron uptake. *Environmental Microbiology*, *20*(5), 1857–1872. https://doi.org/10.1111/1462-2920.14121

Toh-e, A., Ohkusu, M., Ishiwada, N., Watanabe, A., & Kamei, K. (2022). Genetic system underlying responses of Cryptococcus neoformans to cadmium. *Current Genetics*, *68*(1), 125–141. https://doi.org/10.1007/s00294-021-01222-y

Trouvelot, A., Kough, J. L., & Gianinazzi-Pearson, V. (1986). Estimation of vesicular arbuscular mycorrhizal infection levels. Research for methods having a functional significance. *Physiological and Genetical Aspects of Mycorrhizae = Aspects Physiologiques et Genetiques Des Mycorhizes: Proceedings of the 1st European Symposium on Mycorrhizae, Dijon, 1-5 July 1985*. https://agris.fao.org/agris-search/search.do?recordID=US201301430989

Wei, Y.-F., Li, T., Li, L.-F., Wang, J.-L., Cao, G.-H., & Zhao, Z.-W. (2016). Functional and transcript analysis of a novel metal transporter gene EpNramp from a dark septate endophyte (Exophiala pisciphila). *Ecotoxicology and Environmental Safety*, *124*, 363–368. https://doi.org/10.1016/j.ecoenv.2015.11.008

West, A. H., Clark, D. J., Martin, J., Neupert, W., Hartl, F. U., & Horwich, A. L. (1992). Two related genes encoding extremely hydrophobic proteins suppress a lethal mutation in the yeast mitochondrial processing enhancing protein. *Journal of Biological Chemistry*, *267*(34), 24625–24633. https://doi.org/10.1016/S0021-9258(18)35810-1

Zago, V. C. P., das Dores, N. C., & Watts, B. A. (2019). Strategy for phytomanagement in an area affected by iron ore dam rupture: A study case in Minas Gerais State, Brazil. *Environmental Pollution*, *249*, 1029–1037. https://doi.org/10.1016/j.envpol.2019.03.060

Zanchi, C. S., Batista, É. R., Silva, A. O., Barbosa, M. V., Pinto, F. A., dos Santos, J. V., & Carneiro, M. A. C. (2021). Recovering Soils Affected by Iron Mining Tailing Using Herbaceous Species with Mycorrhizal Inoculation. *Water, Air, & Soil Pollution*, *232*(3), 110. https://doi.org/10.1007/s11270-021-05061-y

Zhang, H., Li, G., Cao, N., Yang, H., & Zhu, F. (2021). Genome-wide identification and expression analysis of NRAMP transporter genes in *Cucumis sativus* and *Citrullus lanatus*. *Canadian Journal of Plant Science*, *101*(3), 377–392. https://doi.org/10.1139/cjps-2020-0062

Supplementary Table 1. Oligonucleotides used in this study. Overhangs are underlined

Primer	Sequence (5'-3')[a]	Application
qRiSMF1.F	GGGTGTCGTTACAGGAATGG	Real Time PCR
qRiSMF1.R	TGCAACTCCCCAAGGTAAAG	Real Time PCR
qRiSMF2.F	TAGCGCAAGCATGTAAAGCA	Real Time PCR
qRiSMF2.R	GCTGTCGATATTTATCCTTTTCC	Real Time PCR
qRiSMF3.1.F	AACGAAGATAGGCCTTTACCA	Real Time PCR
qRiSMF3.1.R	CCGTGATGCATCTCCCAAG	Real Time PCR
qRiSMF3.2.F	CCACTTGATGGAAAACAAGAA	Real Time PCR
qRiSMF3.2.R	CGAAGAATTTTTATCCCGAATG	Real Time PCR
qRiEF1αF	GCTATTTTGATCATTGCCGCC	Real Time PCR
qRiEF1αR	TCATTAAAACGTTCTTCCGACC	Real Time PCR
qCiEF1αF	CATGCGTCAGACGGTTGCTGT	Real Time PCR
qCiEF1αR	CTTCACTCCCTTCTTGGCTGC	Real Time PCR
RiSMF1.GW5	AAAGCAGGCTTCATGAATTATCCGACAAAAGA	Cloning RiSMF1
RiSMF1.GW3	GAAAGCTGGGTCTTACAAAGTACCTTCAATCG	Cloning RiSMF1
RiSMF1.GW3gfp	GAAAGCTGGGTCTTCCAAAGTACCTTCAATCG	Cloning RiSMF1 with STOP codon modified
RiSMF3.1.GW5	AAAGCAGGCTTCATGCAACAAGGGAAAATAGT	Cloning RiSMF3.1
RiSMF3.1.GW3	GAAAGCTGGGTCTCAATCTGAGATATTATTAA	Cloning RiSMF3.1
RiSMF3.1.GW3gfp	GAAAGCTGGGTCTTCATCTGAGATATTATTAA	Cloning RiSMF3.1 with STOP codon modified
RiSMF3.2.GW5	AAAGCAGGCTTCATGCAACAAGGGAAAATAGT	Cloning RiSMF3.2
RiSMF3.2.GW3	GAAAGCTGGGTCTTATCCCGAATGATTTGTCA	Cloning RiSMF3.2
RiSMF3.2.GW3gfp	GAAAGCTGGGTCTTCTCCCGAATGATTTGTCA	Cloning RiSMF3.2 with STOP codon modified

CHAPTER 2:

Characterization of the CCC1 gene family in the arbuscular mycorrhizal fungus *Rhizophagus irregularis*

Adapted from López-Lorca V.M., Molina-Luzón M.J., Ferrol N. (in preparation)

Abstract

Iron transport into vacuoles is mediated by transporters of the Ccc1/VIT family. Here, report characterization of the Ccc1/VIT family members (*RiCCC1.1*, *RiCCC1.2* and *RiCCC1.3*) of the arbuscular mycorrhizal (AM) fungus *Rhizophagus irregularis*. Bioinformatic analysis of the three RiCCC1 protein sequences revealed they have all the essential domains and residues required for Fe transport. RiCCC1.1 and RiCCC1.2, but not RiCCC1.3, were able to rescue the growth of a *Saccharomyces cerevisiae* mutant defective in vacuolar iron transport. RiCC1.1 and RiCCC1.2 also complemented a yeast manganese transporter mutant. The *RiCCC1* genes were differentially expressed in the extraradica mycelium (ERM), intraradical (IRM) mycelium and arbuscules. In the ERM, *RiCCC1.2* expression was down-regulated by Fe deficiency but transiently up-regulated by Fe toxicity. These data suggest a role for RiCCC1.2 in vacuolar Fe mobilization under Fe limitation and in Fe detoxification under Fe toxic conditions. *RiCCC1.3* expression was also transiently up-regulated by Fe toxicity, while *RiCCC1.2* transcript levels decreased under Mn toxicity. Collectively, these data indicate that RiCCC1.1, RiCCC1.2 and RiCCC1.3 play a role in iron and manganese homeostasis in *R. irregularis*.

Introduction

Iron is an essential micronutrient for growth and development of all organisms, as it plays an important role in various physiological and biochemical pathways. However, excess levels of Fe in the cell are toxic. Since there are no cellular mechanisms for Fe excretion into the environment, organisms protect themselves from Fe toxicity by regulating a series of mechanisms that control its acquisition, distribution and compartmentalization. Animals, plants, bacteria and archaea, but not fungi, possess a protein called ferritin capable of accumulating Fe in a bioavailable form that plays a role in Fe detoxification (Arosio et al., 2009). Fungi store excess Fe in their vacuoles through transport proteins belonging to the Ccc1/Vacuolar Iron Transporter (VIT) family, not only to protect themselves from Fe toxicity, but also as a reserve of Fe that can be mobilized and exported through specific transporters in case the cytosolic metal levels decrease (Lanquar et al., 2005; Singh et al., 2011). With the exception of animals, the Ccc1/VIT family has been reported in many organisms including bacteria, fungi and plants. The first member of this family, the *ScCCC1* (Ca^{2+}-sensitive Cross-Complementer) protein, was identified in the model fungus *Saccharomyces cerevisiae* (Li et al., 2001). Although the excess of Fe can access the vacuole of *S. cerevisiae* by endocytosis (Li et al., 2001), ScCcc1 protein is responsible for about 60% of the Fe transported to the vacuole (Cockrell et al., 2014; Li et al., 2001), where it is stored in the form of Fe^{3+} as part of low molecular mass polyphosphate chains (Nguyen et al., 2019). ScCcc1

is transcriptionally and post-transcriptionally regulated by Fe. In response to high Fe concentration, the transcription factor ScYap5 activates the expression of the *ScCCC1* gene (Li et al., 2008; Li & Ward, 2018). In response to Fe deficiency, the transcription factors ScAft1 and ScAft2 activate a large group of genes involved in Fe uptake, mobilization from the vacuole, mitochondrial Fe import and proteins involved in Fe metabolism (Ramos-Alonso et al., 2020). Genomic and biophysical studies have shown that ScCcc1 also contributes to Mn homeostasis by transporting Mn from the cytosol to the vacuole and to Golgi vesicles (Cockrell et al., 2014; Lapinskas et al., 1996; Li et al., 2008).

Thanks to the recent description of the crystal structure of the *Eucalyptus grandis* EgVIT1 protein, it has been possible to identify the essential domains and residues for Fe transport (Kato et al., 2019). The Ccc1/VIT family proteins have 5 transmembrane domains, 3 α-helices (H1, H2 and H3) facing the cytosol between transmembrane domains 2 and 3 (Sorribes-Dauden et al., 2020), a cytosolic amino-terminal end and a carboxy-terminus facing the vacuolar lumen. The metal binding domain (MBD) is formed by H1 and H3 helices and the C-terminal end of the second transmembrane domain (Kato et al., 2019). Ccc1/VIT proteins function as a dimer, being the ion-translocating channel the ten transmembrane domains of the homodimer. The mechanisms of Fe homeostasis are well understood in yeast. However, current knowledge on the mechanisms of Fe protection from excess cytosolic Fe in arbuscular mycorrhizal (AM) fungi, one of the most prominent group of microorganisms engaging a symbiotic relationship with higher plants, is still unknown. AM fungi are soil-borne microorganisms belonging to the Glomeromycotina subphylum within the Mucoromycota (Spatafora et al., 2016). The AM fungus colonises the rootand develops highly branched structures inside cortical cells, called arbuscules. The extraradical mycelium (ERM) the fungus develops in the soil provides the plant with a pathway for the absorption of low-mobility nutrients, but, paradoxically, AMs also increase the resistance of host plants to heavy metal stress (Ferrol et al., 2016; Riaz et al., 2021). AM fungi can improve metal tolerance by increasing water absorption (Ruth et al., 2011), improving the nutritional status of the host (Lehmann & Rillig, 2015; Wipf et al., 2019), increasing shoot biomass and modifying root morphology (Camenzind et al., 2016; Comas et al., 2014) and reducing oxidative stress caused by the metal (Devi et al., 2019; Riaz et al., 2021; Sharma et al., 2017). Besides, AM fungi can reduce the bioavailability of heavy metals in the soil by secreting low molecular weight organic compounds and spores (Ghasemi Siani et al., 2017), through the production and secretion of glomalin, a glycoprotein with a high metal affinity that is produced abundantly on hyphae and spores in roots and soil (Cornejo et al., 2008; Ferreira Vilela & Barbosa, 2019; Ghasemi Siani et al., 2017), and by accumulating the metal in fungal structures (Wu et al.,

2016, 2019).Up to now, little is known about the Fe homeostasis in AM fungi. In the model fungus *R. irregularis*, Fe (III) is reduced to Fe (II) in the soil solution trough the activity of the plasma-membrane ferric reductase RiFre1. Then, the plasma-membrane Fe transporters located in ERM RiFTR1 and RiSMF3.2 take Fe^{2+} from soil (López-Lorca et al., 2022; Tamayo et al., 2018). RiFTR1 and RiSMF3.2 are also involved in Fe tolerance by reducing Fe uptake, as their expression in the ERM were down-regulated in the presence of high Fe concentrations. A previous bioinformatic analysis of the genome of the AM fungus *R. irregularis* identified three members of the Ccc1/VIT family (*RiCCC1.1*, *RiCCC1.2* and *RiCCC1.3*) (Tamayo et al., 2014). The aim of this work was to characterize the members of the Ccc1/VIT family of *R. irregularis* to delve into the mechanisms of metal homeostasis in AM fungi.

Materials and Methods

Biological materials and growth conditions

The AM fungal isolate used in this study was *Rhizophagus irregularis* DAOM197198 grown in monoxenic cultures and in the *in vivo* whole plant bidimensional experimental system (Pepe et al., 2017). AM monoxenic cultures were stablished in two-compartment Petri dishes to separate the root compartment and the hyphal compartment. Ri T-DNA transformed carrot (*Daucus carota*) roots and a piece of fungal inoculum (ERM, fragments of mycorrhizal roots and spores) were placed in the root compartment, filled with M medium (Chabot et al., 1992). Plates were incubated in the dark at 24°C for 6–8 weeks, until the hyphal compartment was profusely colonised by the fungus and roots. Then, the root compartment was removed and refilled with fresh liquid M medium, where ERM was allowed to grow in the same conditions for 20 days (control plates).

For Fe deficiency treatment, ERM grown in liquid M medium without Fe was exposed to 0.5 mM ferrozine for 3 days, as described by Tamayo et al. (2018). Mn-deficient conditions were established by growing ERM in liquid M medium lacking Mn. Treated cultures were grown in the same conditions as the control plates.

To assess the effects of Fe tocicty on *RiCCC1s* expression, short- and a long-term experiments were set up. In the short-term experiment, ERM grown in control liquid M media was exposed for 16 h to 45 mM EDTAFe (III) sodium salt. In the long-term experiment, liquid M medium was supplemented with 45 mM EDTAFe (III) sodium salt and ERM was allowed to grow for 20 days. For Mn toxicity conditions, ERM control was exposed for 16 h to 1 mM $MnCl_2$. ERM from the different treatments were collected using tweezers, washed with distilled water, dried on filter paper, frozen in liquid N and stored at -80°C until used.

R. irregularis ERM was also collected from mycorrhized chicory (*Cichorium intybus* L.) plants grown in the *in vivo* whole plant bidimensional experimental system described by Pepe et al. (2017). Chicory seeds were surface-sterilized and germinated for 2 weeks in autoclaved sand. To removed metal traces, sand was HCl-washed before sterilization with 0.03 M HCl and rinsed with distilled water until pH 7. Then, seedlings were transplanted into 50 ml pots filled with HCl-washed sand and inoculated with 3 ml of AM fungus inoculum obtained in monoxenic cultures and containing 1650 spores. Pots were introduced in sun-transparent bags to prevent substrate desiccation and maintained for a month at 24°C day / 20°C night in a 16 h light photoperiod. Plants were watered with a 0.5X Hoagland nutrient solution once a week which lacked EDTA Fe (III) sodium salt or $MnCl_2$ to induce Fe or Mn deficiency respectively. Then, the root system of each plant was washed with distilled water, wrapped in a nylon net (41 μm mesh, Millipore NY4100010), sandwiched between two 13 cm membranes of mixed-cellulose esters (0.45 μm pore diameter size, MF-Millipore HAWP14250) and placed in 14 cm diameter Petri dishes having a hole on the edge to allow shoot growth. Petri plates were filled with HCl-washed sand, sealed with parafilm, wrapper with aluminium foil and introduced into sun-transparent bags. Sandwiched plants were incubated for another month in a growth chamber to allow ERM colonised the Millipore membrane. At harvesting, ERM and root system was collected and frozen in liquid N and stored at -80°C until used. An aliquot of the roots was separated to estimate mycorrhizal colonization.

The *Saccharomyces cerevisiae* yeast strain used in this work was *ccc1*Δ, a mutant laking the vacuolar membrane transporter Ccc1 (Li et al., 2001) and *pmr1*Δ which is incapable of transferring manganese into Golgi vesicles and is unable to endure toxic concentrations of the metal (Lapinskas et al., 1995). Yeast cells were grown on YPD or minimal synthetic dextrose (SD) medium, supplemented with the appropriate amino acids.

RNA extraction and gene expression analyses

Total RNA extraction from fungal ERM developed in monoxenic and sandwich cultures was performed using the RNeasy Plant Mini Kit (Qiagen). Total RNA was extracted from chicory roots by using the phenol/SDS method, followed by LiCl precipitation (García-Rodríguez et al., 2007). RNAs were DNAse treated, using the RNA-free DNAse set (PROMEGA) according to manufacturer's instructions. DNAse-treated RNAs were quantified using the NanoDrop 1000 Spectrophotometer (Thermo Scientific) and 1 μg was used to synthetized cDNA using SuperScript IV Reverse Transcriptase (Invitrogen), in accordance with the instructions of the manufacturer.

RiCCC1s gene expression was analysed by real-time RT-PCR, using a QuantStudio 3 (Applied Biosystem) in the synthetized cDNAs. Each 12 µL reaction contained 1 µL of a 1:10 dilution of cDNA, 0.25 µL each primer and 6 µL iTaq (Bio-Rad). The real-time RT-PCR program consisted of an initial incubation at 95°C for 30 s, followed by 40 cycles of 95°C for 15 s, 60°C for 30 s and 72°C for 30 s, where the fluorescence signal was measured, and a final step with a heat-dissociation protocol to check the specificity of the PCR-amplification procedure. Specificity of the primer pairs (Supplementary Table 1) was determined by PCR amplification of *R. irregularis* and chicory cDNA, and efficiency was analysed through a real-time RT-PCR on several dilutions of cDNA. Gene expression was determined in at least three independent biological samples with the threshold cycle (Ct) determined in duplicate. Relative expression level was calculated using the $2^{-\Delta\Delta Ct}$ method and normalized to the *R. irregularis* elongation factor 1α expression. The standard error was computed from the average of the $2^{-\Delta\Delta Ct}$ values, for each biological sample.

RiCCC1s bioinformatic analyses

The putative sequences of the *RiCCC1*s were previously identified by Tamayo et al. (2014) (RiCCC1.1, JGI ID: 1590022; RiCCC1.2, JGI ID: 1538162; RiCCC1.3, JGI ID: 1456385). These sequences were used to run additional Blastps on the JGI (Joint Genome Institute) (https://genome.jgi.doe.gov/portal/) and NCBI (National Center for Biotechnology Information) (https://www.ncbi.nlm.nih.gov) databases to search for homologous sequences from other Glomeromycotina species. Homology and similarity studies were performed with SIAS (http://imed.med.ucm.es/Tools/sias.html). Potential transmembrane domains were predicted with TOPCONS (https://topcons.cbr.su.se/). Structural models were generated using Prosite's MyDomains (https://prosite.expasy.org/mydomains/). The 3D structure and were predicted with SWISS-Model (https://swissmodel.expasy.org/) based on the crystal structure of iron transporter VIT1 with zinc ions (ID: 6iu3.1.A). The putative ligands were analysed with 3D LigandSites (https://www.wass-michaelislab.org/3dlig) tools. /). The alignments of the putative amino acid sequences of the CCC1 of the different fungi were carried out using Clustal Omega (https://www.ebi.ac.uk/Tools/msa/clustalo/) and the phylogenetic relationships were calculated with the Neighbour-Joining method implemented in Mega-X.

RNA-sequencing (RNA-seq) data of the transcriptome of laser microdissected *Medicago truncatula* cells, containing arbuscules (ARB) or IRM and of ERM grown in monoxenic cultures were collected from the NCBI Gene Expression Omnibus database GSE99655. RNAseq data were analysed, as described by Zeng et al. (2018). DESeq2 tool implemented in Galaxy (https://usegalaxy.org/) was used to perform counts normalization.

Heterologous expression

R. irregularis CCC1s open reading frames (ORF) were amplified by PCR, with the corresponding primers (Supplementary Table 1), using ERM cDNA as template. Amplicons flanked with the sequences attB1 and attB2 were cloned in to the yeast-expression vector pDRf1-GW using the Gateway technology, according to the manufacturer instructions. PCR products were first cloned into pDONr221 before been cloned in the destination vector pDRf1-GW. All constructs were verified by sequencing. The yeast mutant strains *ccc1*Δ and *pmr1*Δ were transformed with the pDRf1-RiCCC1.1, pDRf1-RiCCC1.2, pDRf1-RiCCC1.3 constructs or with the empty vector (negative control). Transformed yeast cells were selected by uracil autotrophy in SD medium. Yeast liquid cultures grown to exponential phase were harvested by centrifugation, washed three times with milli-Q H_2O and adjusted to a final OD_{600}=1. For drop test, 5 µl of serial dilutions of the yeast liquid cultures were spotted on the selective plates. *ccc1*Δ transformants were spotted onto SD medium without uracil supplemented or not with 5 mM $FeSO_4$. *pmr1*Δ cells were spotted onto SD without uracil supplemented or not with 2 mM $MnCl_2$. Plates were incubated at 30 C for 72 h.

RiCCC1s subcellular localization

To assess subcellular localization of the *R. irregularis* CCC1 proteins, their open reading frames were fused to the enhanced green fluorescent protein (eGFP) in their carboxy-terminal ends and expressed in the *S. cerevisiae* mutant *ccc1*Δ. *RiCCC1.1*, *RiCCC1.2* and *RiCCC1.3* cDNAs were amplified without their stop codon, using the corresponding primers (Supplementary Table 1), and cloned into the yeast expression vector pGWFDR196, using the Gateway technology. Yeast transformed with pGWFDR196-RiCCC1.1, pGWFDR196-RiCCC1.2, pGWFDR196-RiCCC1.3 and the empty vector (negative control) were spotted onto SD without uracil supplemented or not with 5 mM $FeSO_4$ to check GFP-fusion proteins functionality. To determine RiCCC1s localization, yeast cells were grown in liquid SD without uracil until reaching the exponential phase. Then, cells were washed with distilled water and visualized with a Leica DMi8 microscope. GFP-tagged proteins were observed using a 483–501 nm excitation filter and a 512–548 nm emission filter.

Statistical analyses

Statgraphics Centurion XVI software was used for the statistical analysis of means and standard error determinations. For comparison of treatments, a one-way ANOVA followed by a Duncan test ($p < 0.05$) were performed.

Results

R. irregularis has three Ccc1 paralogs

A previous genome-wide analysis of *R. irregularis* revealed the presence in its genome of three genes, *RiCCC1.1*, *RiCCC1.2* and *RiCCC1.3*, putatively encoding vacuolar Fe transporters (Tamayo et al. 2014). Their full-length cDNAs contain open reading frames of 762-822 base pairs. The deduced amino acid sequences of *RiCCC1.1*, *RiCCC1.2* and *RiCCC1.3* comprise 257, 253 and 273 residues, respectively. Comparison of the full-length cDNAs with the genomic DNA sequences revealed the presence of eight introns in RiCCC1.1, six in RiCCC1.2 and three in RiCCC1.3 (Figure 1a). Sequence similarity among the deduced amino acids of the different RiCCC1s ranges from 12 to 17%. RiCCC1s amino acid sequence also show low sequence homology to the *S. cerevisiae* CCC1, ranging from 11.67% to 13.61%, with RiCCC1.1 showing the highest similarity (13.61%) (Figure 1b). However, they contain the typical features of the CCC1/VIT family. Secondary structure analysis revealed that they all have five transmembrane domain (TMD) and the amino terminus facing the cytosol (Figures 1 c,d). The 3D structure of RiCC1.1, RiCCC1.2 and RiCCC1.3 showed the presence of the characteristic Metal Binding Domain (MBD) composed by two α-helices (H1 and H3) facing the cytosol between transmembrane domains 2 and 3 and the C-terminal end of the second transmembrane domain (Figures 1d,e). Analysis of the RiCCC1s amino acid sequences revealed two clusters of amino acid residues located in the C-terminal end of the second transmembrane domain and the 3 α-helix able to bind Zn, Ni, Co and Fe (Figures 2a,b).

A phylogenetic analysis of the CCC1 sequences of different fungal taxonomic groups revealed that RiCCC1s were clustered with sequences from other Glomeromycotina. Glomerales possess three CCC1, whereas the Diversisporales have only one homologue. RiCCC1s were located in a branch with sequences belonging of other fungi of the order Glomerales, whereas the sequences of the order Diversisporales where clustered together in a different branch (Figure 3).

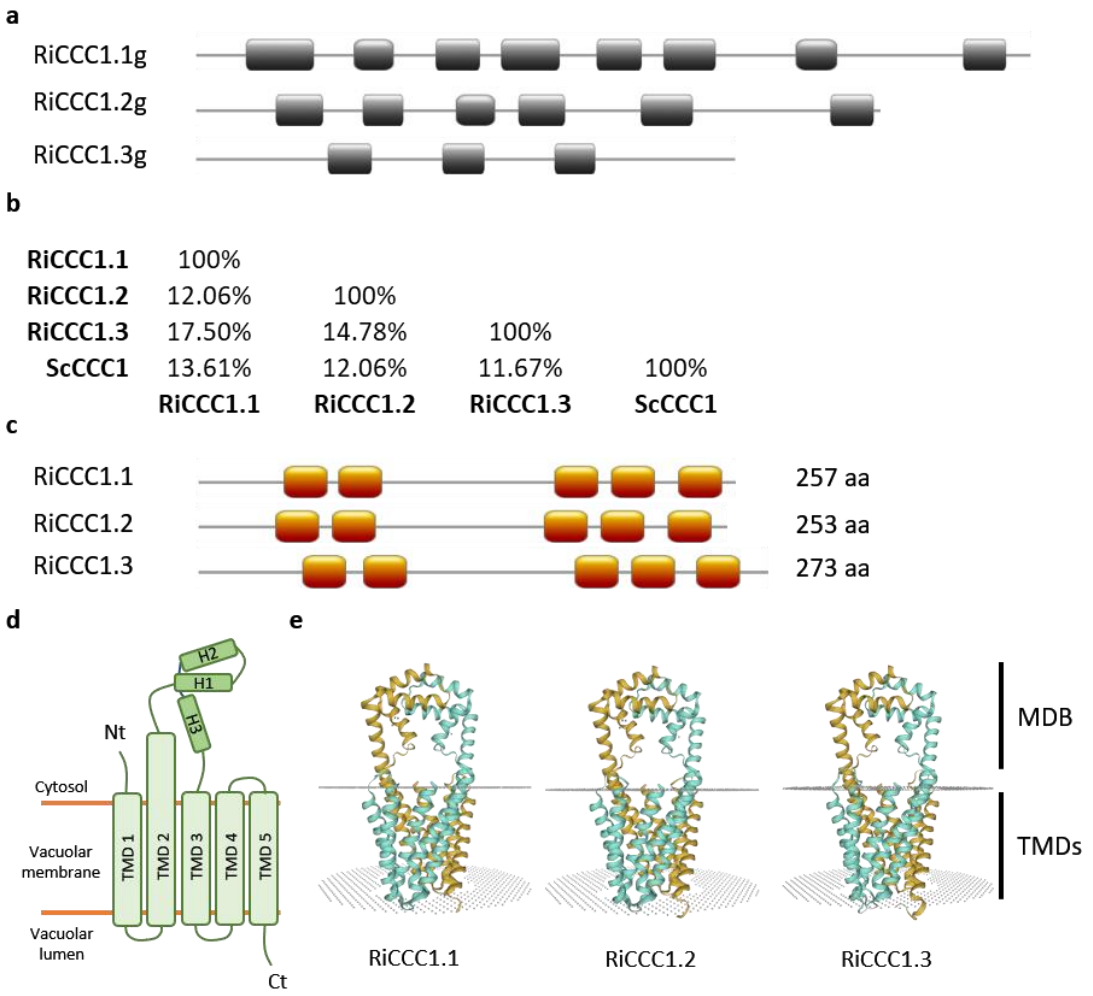

Figure 1. (**a**) Exon / Intron organization of *R. irregularis CCC1*s genes. (**b**) Percent similarity matrix of *R. irregularis* (Ri) and *Saccharomyces cerevisiae* (Sc) Ccc1/VIT proteins. (**c**) Secondary structure of RiCCC1s, orange boxes represent transmembrane domains. (**d**) Schematic representation of a Ccc1/VIT protein monomer. Transmembrane domains (TMD1-5) are represented in light green rectangles and the 3 helices (H1-3) that conforms the MDB are coloured in dark green. "Ct" and "Nt" represents the carboxy- and amino-terminus respectively. (**e**) Predicted 3D structure of RiCCC1 homo-dimers. Different colours represent the two monomers. Tertiary structures were predicted by SWISS-MODEL software, based on the crystal structure of the vacuolar iron transporter VIT1 of *Eucalyptus grandis* with zinc ions (ID: 6iu3.1.A). MBD indicates the Metal Binding Domain and TMDs the Transmembrane Domains.

a

		Residue	Amino Acid	Probability (0-1)	Ligands
RiCCC1.1	Cluster 1	107	GLU	1	Zn, Ni, Co, Fe
		110	GLU	0.66	
		118	GLU	0.99	
		121	GLU	0.99	
	Cluster 2	91	LEU	1	Zn, Ni
		93	ALA	0.37	
		94	LYS	0.07	
		95	SER	0.3	
		96	GLU	0.18	
RiCCC1.2	Cluster 1	101	ARG	0.58	Zn, Ni, Co, Fe
		102	GLU	1	
		105	GLU	0.66	
		113	GLU	0.99	
		116	GLU	0.99	
	Cluster 2	86	LEU	1	Zn, Ni
		88	ALA	0.37	
		89	LYS	0.05	
		90	SER	0.3	
		91	ASP	0.15	
RiCCC1.3	Cluster 1	118	GLU	1	Zn, Ni, Co, Fe
		121	ASP	0.86	
		129	GLU	0.98	
		132	GLU	0.31	
		165	ARG	1	
	Cluster 2	102	ALA	1	Zn
		103	THR	0.21	
		104	LEU	0.19	
		105	LYS	0.16	
		106	ALA	0.2	
		107	ALA	0.14	

b

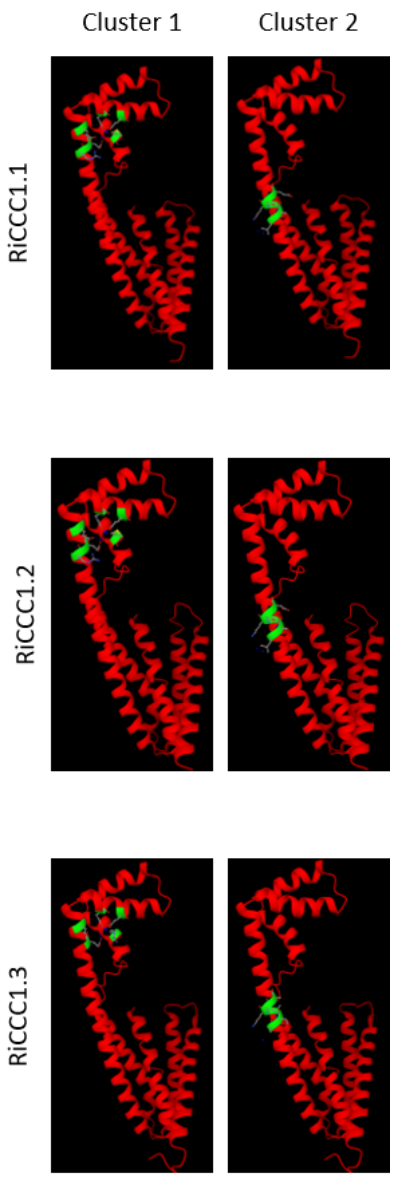

Figure 2. Clusters of amino acids residues putatively able to ligand metals. (**a**) "Residue" and "Amino Acid" indicates ubication and the amino acids that belong to each cluster respectively, "Probability" assess the probability of each amino acid to participate on ligand binding and "Ligands" shows the ligands that are capable of binding. (**b**) Localization of the ligand clusters (coloured in green) in the 3D structure.

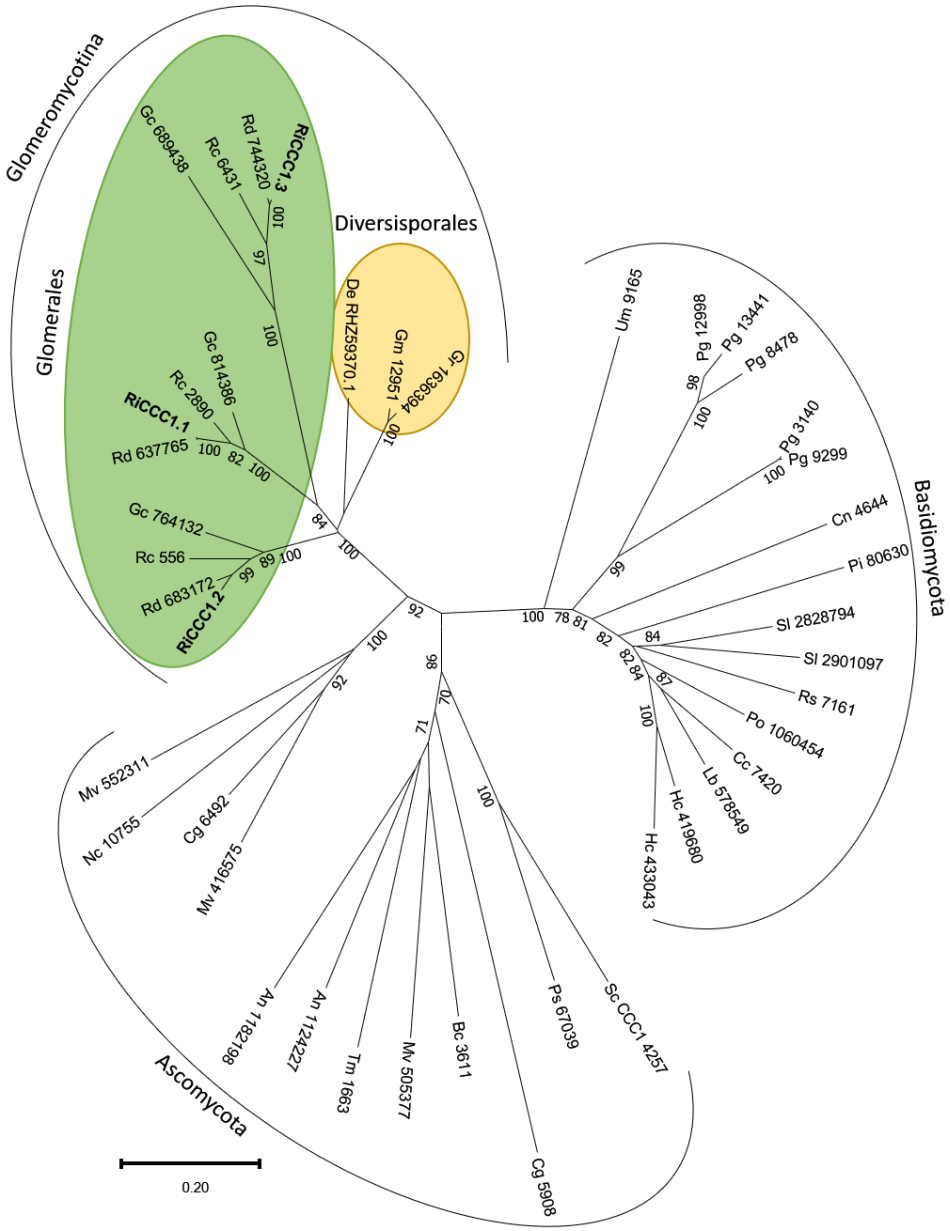

Figure 3. Phylogenetic relationships of the *R. irregularis* CCC1 proteins with homologous sequences selected from different fungal taxonomic groups. The yellow and green circles group the Diversisporales and Glomerales sequences, respectively. Protein JGI identification numbers are indicated. An, *Aspergillus niger*; Bc, *Botrytis cinerea*; Cc, *Coprinopsis cinerea*; Cn, *Cryptococcus neoformans*; De, *Diversispora epigaea*; Gc, *Glomus cerebriforme*; Gm, *Gigaspora margarita*; Gr, *Gigaspora rosea*; Lb, *Laccaria bicolor*; Nc, *Neurospora crassa*; Pi, *Piriformospora indica*; Pg, *Puccinia graminis*; Rc, *Rhizophagus clarus*; Rd, *Rhizophagus diaphanus*; Ri, *Rhizophagus irregularis*; Sc, *Saccharomyces cerevisiae*; Sl, *Suillus luteus*; Tm, *Tuber melanosporum*; Um, *Ustilago maydis*. The *R. irregularis* sequences are in bold.

Expression profiles of the R. irregularis CCC1 genes

The gene expression profiles of *RiCCC1.1*, *RiCCC1.2* and *RiCCC1.3* were investigated by using RNA-sequencing data retrieved from ERM, laser-microdissected *Medicago truncatula* cortical cells containing arbuscules and laser-microdissected *M. truncatula* root cells containing IRM (Zeng et al., 2018, 2020). All *RiCCC1s* genes were detected in all fungal structures although they were

differentially expressed (Figure 4). *RiCCC1.2* was the most highly expressed gene in the ERM, while. *RiCCC1.3* was the most highly expressed gene in the IRM. However, no significant differences were found between the expression levels of *RiCCC1.1* and *RiCCC1.3* in arbuscules. Differences in phylogeny and expression patterns suggest that RiCCC1.1, RiCCC1.2 and RiCCC1.3 may have distinct functions.

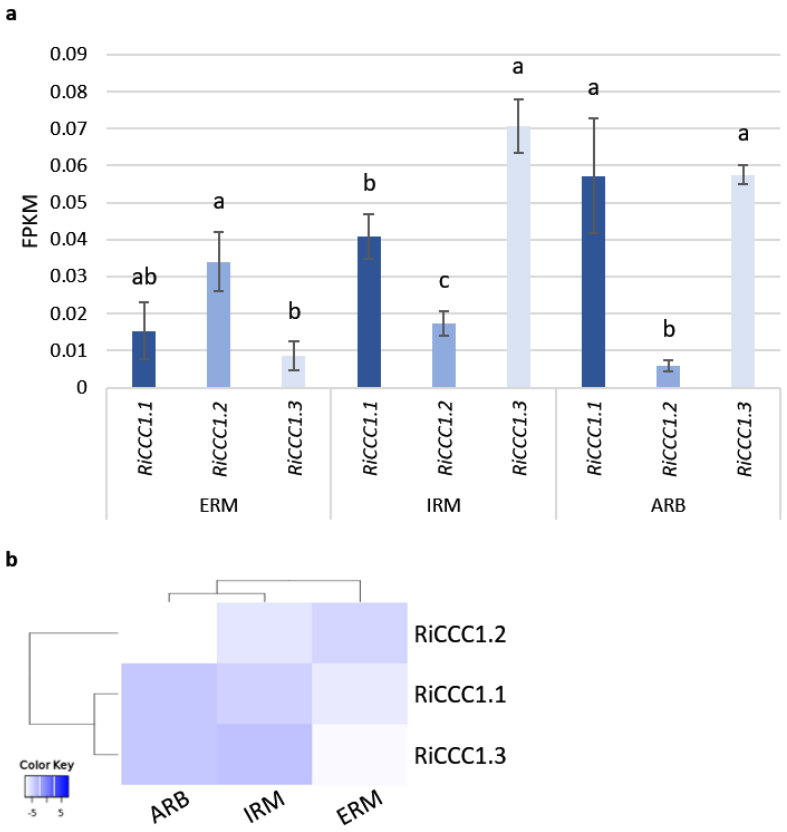

Figure 4. Expression patterns of *R. irregularis CCC1* genes. (**a**) RiCCC1s expression data obtained from RNAseq analysis of ERM from monoxenic cultures and IRM and arbuscules (ARB) collected by laser microdissection, from *M. truncatula* roots. Error bars represent standard error. Different letters indicate significant differences ($p < 0.05$, n = 3). (**b**) Heatmap showing the hierarchical clustering of *RiCCC1* genes, grouped according to the expression patterns in ERM, IRM and ARB. Gradient colour ranging from white to bright blue corresponds to expression values log2 transformed.

Functional characterization of RiCCC1.1, RiCCC1.2 and RiCCC1.3 in yeast

To test if the RiCCC1 proteins exhibit Fe transport activity, they were expressed in the mutant yeast strain *ccc1*Δ lacking the Fe vacuolar transporter Ccc1, which is sensitive to high levels of extracellular Fe (Li et al., 2001). To that end, *RiCCC1.1*, *RiCCC1.2* and *RiCCC1.3* full-length cDNAs were expressed under the control of the yeast PMA1 promoter in the mutant cells and plated on SD medium supplemented with high Fe concentrations. Transformed yeast cells expressing *RiCCC1.1* and *RiCCC1.2* complemented the phenotype of the *ccc1*Δ cells, although RiCCC1.1 restored more efficiently the mutant phenotype than RiCCC1.2 (Figure 5a). However, the *ccc1*Δ

mutant strain transformed with the empty control vector pDRf1-GW or with pDRf1:RiCCC1.3 failed to grow on SD media supplemented with 5 mM $FeSO_4$. This data indicates that RiCCC1.1 and RiCCC1.2 are able to complement the function of CCC1 as a vacuolar Fe transporter in yeast.

Subsequently, given that ScCcc1 protein may also transport Mn to the vacuole or to Golgi vesicles (Cockrell et al., 2014; Lapinskas et al., 1996; Li et al., 2008), the ability of the RiCCC1 proteins to complement the mutant yeast *pmr1*Δ was tested. *pmr1*Δ is unable to grow under high concentrations of Mn, therefore, transformed cells were spotted onto SD media supplemented or not (positive control) with 2 mM $MnCl_2$ (Figure 5b). As observed for the *ccc1*Δ mutants, RiCCC1.1 and RiCCC1.2 transformed cells restored the ability of the mutant to grow in the Mn-supplemented media. Therefore, a likely function of RiCCC1.1. and RiCCC1.2 is to transport cytosolic ferrous ions to the vacuoles and Mn from cytosol to the vacuole and/or Golgi vesicles.

We next investigated subcellular localization of RiCCC1.1 and RiCCC1.2 in the heterologous system using green fluorescent protein GFP-tagged versions of the proteins. Functionality of the RiCCC1.1 and RiCCC1.2 fusion proteins was assessed before their visualization by fluorescence microscopy. The RiCCC1.1 fusion protein reverted the mutant phenotype. However, the transformed cells expressing the GFP RiCCC1.2 protein were unable to grow in SD media supplemented with high Fe concentrations, indicating that GFP tagging either disrupts its biochemical function or subcellular location (Figure 5c). In yeast, the RiCCC1.1-GFP fusion protein localizes to the vacuolar membrane. Cells expressing the empty vector, used as negative control, showed a general cytosolic fluorescence (Figure 5d).

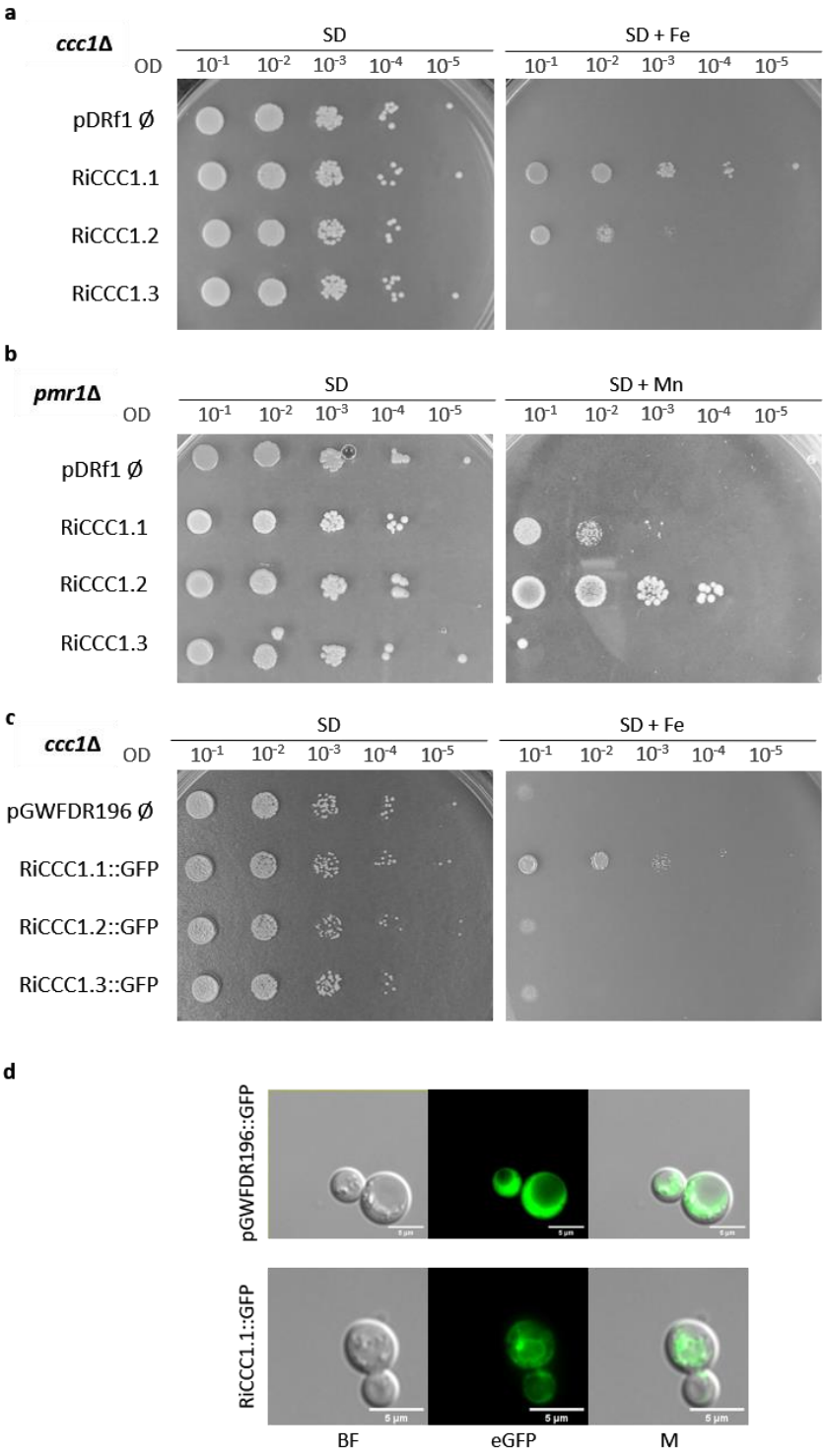

Figure 5. Analysis of RiCCC1s function in yeast. (a) *ccc1*Δ cells transformed with the empty vector pDRf1-GW or expressing *RiCCC1.1*, *RiCCC1.2* or *RiCCC1.3* were spotted on SD without uracil supplemented or not with 5 mM $FeSO_4$. (**b**) *pmr1*Δ yeast cells transformed with the empty vector pDRf1-GW or expressing *RiCCC1.1*, *RiCCC1.2* or *RiCCC1.3* were spotted on SD without uracil supplemented or not with 2 mM $MnCl_2$. (**c**) *ccc1*Δ cells expressing GFP (empty vector pGWFDR196) or *RiCCC1.1*, *RiCCC1.2* or *RiCCC1.3* tagged with GFP in C-terminal were spotted on SD without uracil supplemented or not with 5 mM $FeSO_4$. (**d**) *ccc1*Δ cells expressing GFP (empty vector pGWFDR196) or C-terminal GFP-tagged version of RiCCC1.1, RiCCC1.2 or RiCCC1.3 were visualized in a fluorescence microscope. BF, bright field; eGFP, enhanced GFP fluorescence; M, merged images.

Environmental Fe concentration regulates RiCCC1.2 expression

To further understand the role of RiCCC1s isoforms on Fe homeostasis in *R. irregularis*, their expression levels were analysed by real-time RT-PCR in ERM and IRM grown in association with chicory plants in the *in vivo* sandwich system and in ERM grown *in vitro* in monoxenic cultures, under Fe-sufficient and -limiting. Compared to Fe-sufficient controls (50 µM Fe in the sandwhich system and 45 µM in monoxenic cultures), transcript abundance of *RiCCC1.2* decreased under Fe deficiency in the ERM, but increased in the IRM (Figure 6a). Expression of *RiCCC1.1* and *RiCCC1.3* was not significantly different from that of control ERM and IRM grown on standard media. To determine if RiCCC1s could play a role on ERM Fe tolerance, their expression was analysed in ERM from monoxenic cultures and exposed for 16h to 45 mM Fe and in ERM grown for 20 days in a medium supplemented with 45 mM Fe. Expression of *RiCCC1.3* was transiently up-regulated by Fe toxicity.

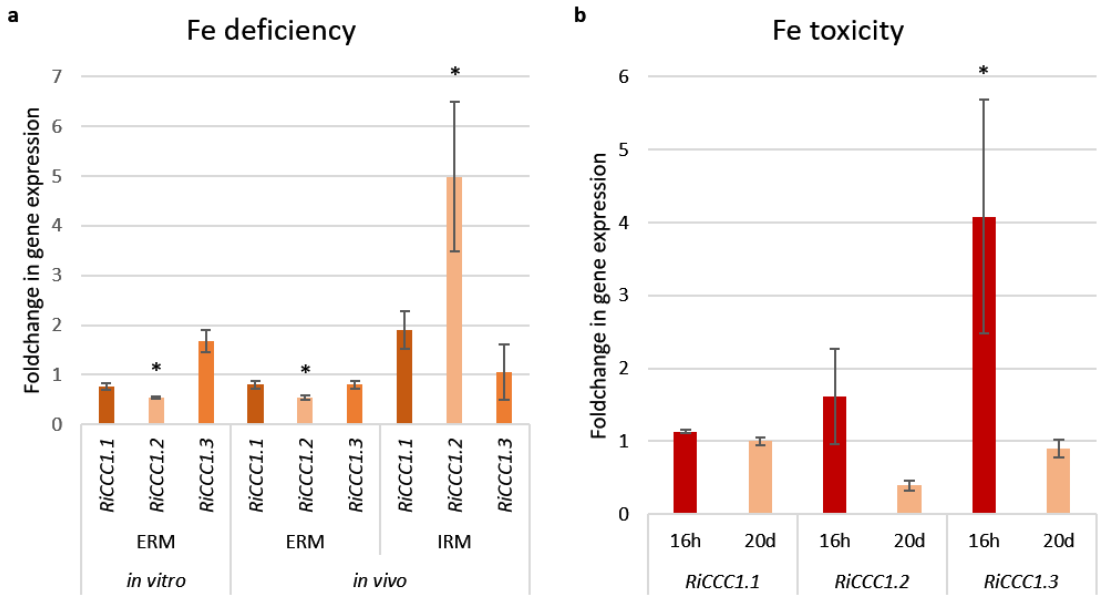

Figure 6. Effect of Fe availability on *RiCCC1s* expression. (**a**) Gene expression was analysed in RNAs isolated from mycorrhizal chicory roots (IRM), ERM collected from the whole plant bidimensional culture system (*in vivo*) and ERM developed in monoxenic cultures (*in vitro*). In the *in vivo* system, plants were watered half-strength Hoagland solution (control, 50 µM Fe) or a modified nutrient solution without Fe (-Fe). In the *in vitro* system, ERM was grown in liquid M medium without Fe and exposed 3 days to 0.5 mM ferrozine (-Fe) or in liquid M medium control (45 µM Fe). (**b**) Gene expression was analysed in RNA isolated from ERM grown in monoxenic cultures. Fe toxicity condition was established by exposing ERM control for 16 h to 45 mM Fe (16 h) or growing ERM for 20 d in media supplemented with 45 mM Fe (20 d). Relative expression levels were calculatedby the $2^{-\Delta\Delta CT}$ method using as reference samples the ERM or IRM grown in starndard conditions. Bars represent standard error. Asterisks indicate significant differences ($p < 0.05$; n = 3), in comparison to the corresponding control value.

Mn availability regulates RiCCC1.2 expression

Since it has been described that transporters of the CCC1/VIT family could play a role in Mn homeostasis, the effect of Mn availability on *RiCCC1*s expression was also assessed. Firstly, the effect of Mn deficiency was analysed in ERM and IRM grown in the in vivo sandwich system and in ERM obtained *in vitro* in monoxenic cultures. Transcript levels of *RiCCC1.1*, *RiCCC1.2* and *RiCCC1.3* were not significantly affected by Mn deficiency neither in the ERM nor in the IRM (Figure 7a). To assess the role of RiCCC1s in Mn tolerance, their expression was determined in ERM exposed to 1 mM Mn for 16h. Mn toxicity only decreased *RiCCC1.2* transcript levels in the ERM (Figure 7b).

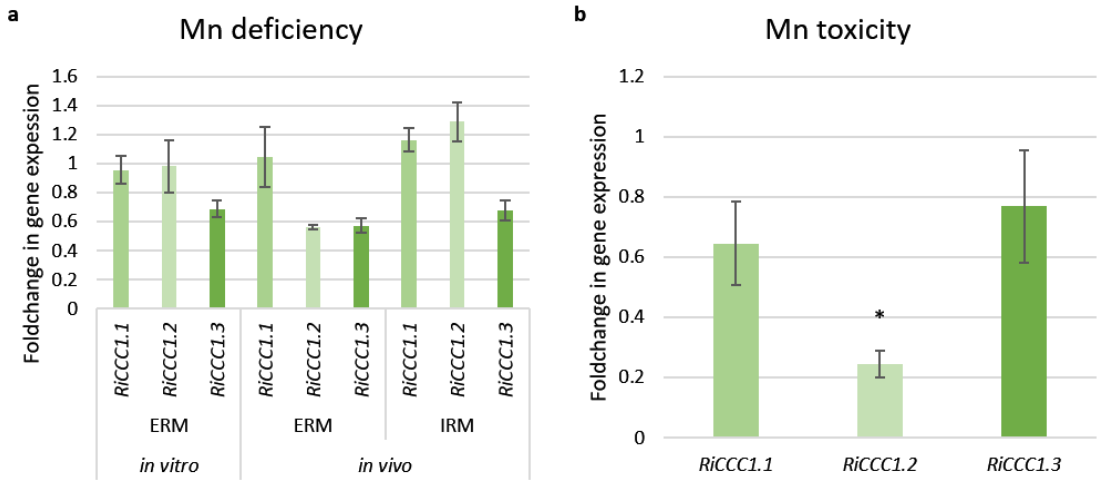

Figure 7. Effect of Mn availability on *RiCCC1s* expression. (**a**) Gene expression was analysed in RNAs isolated from mycorrhizal chicory roots (IRM), ERM collected in the whole plant bidimensional culture system (*in vivo*) and ERM developed in monoxenic cultures (*in vitro*). In the *in vivo* system, plants were watered with half-strength Hoagland solution (control, 4.5 µM Mn) or a modified nutrient solution without Mn (-Mn). In the *in vitro* system, ERM was grown in liquid M medium without Mn (-Mn) or in liquid M medium control (2 µM Mn). (**b**) Gene expression was analysed in RNA isolated from ERM grown in monoxenic cultures. Mn toxicity condition was established by exposing ERM control for 16 h to 1 mM Mn (16 h). Relative expression levels were calculated by the $2^{-\Delta\Delta CT}$ method using as reference sample the control IRM or ERM samples grown in complete M medium. Bars represent standard error. Asterisks indicate significant differences ($p < 0.05$; n = 3), in comparison to the corresponding control value.

Discussion

Various studies have shown the potential of AM fungi to increase plant tolerance under Fe toxic conditions. One of the mechanisms used by AM fungi to increase plant metal tolerance is by reducing metal availability through its accumulation both in the ERM and IRM. In this work, we show that the *R. irregularis RiCCC1.1* and *RiCCC1.2* genes encode proteins involved in Fe detoxification and in Mn homeostasis.

Despite the deduced amino acid sequences of the *RiCCC1* genes display low homology to the CCC1/VIT transporters of other species, our complementation assays revealed that RiCCC1.1 and

RiCCC1.2 are the orthologues of the yeast vacuolar Fe transporter CCC1 (Li et al., 2001). Low similarity between sequences of the Ccc1/VIT proteins of different species has been previously reported (Sorribes-Dauden et al., 2020). However, all the Ccc1/VIT proteins described so far contain the essential domains and residues required for Fe transport (Kato et al., 2019) . The RiCCC1 sequences also present the structural features characteristics of the Ccc1/VIT proteins. They contain five transmembrane domains with the amino terminus facing the cytosol and the MBD formed by H1 and H3 helices and the C-terminal end of the second transmembrane domain (Kato et al., 2019). It is hypothesized that MBD facilitates the incorporation of Fe from siderophores and other molecules (Kato et al., 2019). Although only RiCCC1.1 and RiCCC1.2 were able to transport Fe and Mn in yeast, RiCCC1.3 also presents the essential domains required for metal transport. In addition, bioinformatic analyses showed clusters of amino acids residues located in the MBD that are probably able to bind Zn, Ni, Co and Fe. Cluster 1 of RiCCC1 and RiCCC1.2, but not that of RiCCC1.3, were rich in glutamic acid residues, which seems to be necessary for the correct functioning of the MDB (Kato et al., 2019). RiCCC1.3 cluster 1 also present glutamic acid residues but to a lesser extent, this could be the reason why RiCCC1.3 did not show Fe transporter activity. Mutation analysis of glutamic acid residues of the *Eucalyptus grandis* VIT1 significantly reduce the ability to restore *ccc1Δ* mutant phenotype (Kato et al., 2019), so *RiCCC*1.3 could be a pseudogene. In the pathogen fungus *Aspergillus fumigatus* only the homologue cccA transport Fe into the vacuole and increase Fe resistance (Gsaller et al., 2012). Secondly, RiCCC1.3 could transport other nutrients as indicated by the bioinformatic analysis of the amino acid's residue clusters, *Triticum aestivum* VIT2 is involve in Zn transport in addition to Fe and Mn (Connorton et al., 2017).

Most fungal species harbour one or two genes encoding CCC1 proteins in their genomes (Gsaller et al., 2012). However, three putative paralogs have been discovered in the Glomerales species. The phylogenetic analysis revealed that Glomeromycotina Ccc1/VIT sequences are separated from other fungal division and divided in two clusters, a group belonging to Glomerales and another for Diversisporales. The three paralogues of Glomerales were divided in three branches with one homologous sequence of each species on each branch. All Glomerales species have Ccc1/VIT sequences in the three branches, suggesting that the three homologues may be necessary for proper Fe homeostasis for them. According to data extracted from the RNA-seq, *RiCCC1*s are differentially expressed in fungal tissues. Taken together, phylogeny and expression data suggest that RiCCC1.1, RiCCC1.2 and RiCCC1.3 may have distinct functions.

RiCCC1.1 and RiCCC1.2 were able to revert de mutant phenotype of the *ccc1*Δ strain, lacking the vacuolar Fe transporter ScCCC1, and *pmr1*Δ, unable to transport cytosolic Mn to Golgi

vesicles, which indicates that both encodes a Ccc1 transporter that mediates Fe and Mn transport. However, RiCCC1.1 restored more efficiently the *ccc1*Δ phenotype whereas RiCCC1.2 restored better the *pmr1*Δ, which indicates a specialization of functions between the homologues. Ccc1/VIT1 proteins seems to present differences in transport substrates, although *AtVIT1* encoded a Fe and Mn transporter its knockdown only modified Fe distribution (Kim et al., 2006). Also, TaVIT2 transport Zn unlike its homologue TaVIT1 (Connorton et al., 2017). RiCCC1.1 was localized in the vacuolar membrane by yeast localization assays whereas RiCCC1.2 localization could no be demonstrated in yeast. Unlike RiCCC1.1, RiCCC1.2 GFP-tagged version did not reverse the mutant phenotype, most likely as a consequence of protein folding error due to fusion to eGFP that prevented its correct activity (Frommer & Ninnemann, 1995).

Although both RiCCC1.1 and RiCCC1.2 are Fe transporters, only RiCCC1.2 was regulated by Fe availability. As expected for a vacuolar importer, *RiCCC1.2* expression decrease in ERM grown under Fe deficiency conditions collected in both the *in vivo* and *in vitro* systems. Under Fe-deficiency, ScCCC1 and *Candida glabrata* CCC1 are regulated post-transcriptionally, ScCth2 homologues promote the degradation of *CCC1* mRNA to limit vacuolar Fe storage (Gerwien et al., 2016; Li et al., 2008; Puig et al., 2005). Interestingly, the opposite occurs in IRM where the gene expression increased in Fe-limited conditions, perhaps, to limit Fe transfer to host. *Lotus japonicus* SEN protein, homologue of ScCCC1 and AtVIT1, has an important role in rhizobial symbiosis, *Ljsen1* mutation prevents nitrogen fixation (Hakoyama et al., 2012) so RiCCC1.2 could be important for mycorrhizal symbiosis. *RiCCC1.2* could be silenced using the Host-induced gene silencing (HIGS) technique to further understand the role of RiCCC1.2 in IRM (Helber et al., 2011; Voß et al., 2018).

In ERM exposed to Fe toxic condition for 16 h, *RiCCC1.2* transcripts showed an upward trend, but the differences were not statistically significant. In yeast, ScCCC1 expression is activated in response to Fe excess (Li et al., 2008) as well as the expression of the *Ccc1* genes of *C. glabrata* (Gerwien et al., 2016) and *A. fumigatus* (Gsaller et al., 2012). Expression of *RiCCC1.3* was transiently up-regulated by Fe toxicity which indicates that despite not having demonstrated transporter activity, it is regulated as a vacuolar Fe transporter, which supports the hypothesis that it could be a pseudogene. Despite RiCCC1.2 is a Mn transporter involve in Mn resistance its expression was downregulated in ERM exposed for 16h to 1 mM Mn. It could be hypothesised that RiCCC1.2 could also act as sensor involve in metal tolerance, further studies are necessary to unravel the role of RiCCC1.2 in Mn tolerance.

In this study, the characterization of vacuolar Fe transporters in the arbuscular mycorrhizal fungus *R. irregularis* was described for the first time. The expression of the *R. irregularis CCC1*

genes was found to vary in different fungal structures. RiCCC1.1 and RiCCC1.2 encode functional Fe transporters, with RiCCC1.1 localized in the vacuolar membrane and RiCCC1.2 regulated by Fe availability and Mn toxicity. Further research is necessary to understand the role of RiCCC1.2 in metal tolerance.

References

Arosio, P., Ingrassia, R., & Cavadini, P. (2009). Ferritins: A family of molecules for iron storage, antioxidation and more. *Biochimica et Biophysica Acta (BBA) - General Subjects*, *1790*(7), 589–599. https://doi.org/10.1016/j.bbagen.2008.09.004

Camenzind, T., Homeier, J., Dietrich, K., Hempel, S., Hertel, D., Krohn, A., Leuschner, C., Oelmann, Y., Olsson, P. A., Suárez, J. P., & Rillig, M. C. (2016). Opposing effects of nitrogen versus phosphorus additions on mycorrhizal fungal abundance along an elevational gradient in tropical montane forests. *Soil Biology and Biochemistry*, *94*, 37–47. https://doi.org/10.1016/j.soilbio.2015.11.011

Chabot, S., Bécard, G., & Piché, Y. (1992). Life Cycle of *Glomus Intraradix* in Root Organ Culture. *Mycologia*, *84*(3), 315–321. https://doi.org/10.1080/00275514.1992.12026144

Cockrell, A., McCormick, S. P., Moore, M. J., Chakrabarti, M., & Lindahl, P. A. (2014). Mössbauer, EPR, and Modeling Study of Iron Trafficking and Regulation in *Δccc1* and *CCC1-up Saccharomyces cerevisiae*. *Biochemistry*, *53*(18), 2926–2940. https://doi.org/10.1021/bi500002n

Comas, L. H., Callahan, H. S., & Midford, P. E. (2014). Patterns in root traits of woody species hosting arbuscular and ectomycorrhizas: implications for the evolution of belowground strategies. *Ecology and Evolution*, *4*(15), 2979–2990. https://doi.org/10.1002/ece3.1147

Connorton, J. M., Jones, E. R., Rodríguez-Ramiro, I., Fairweather-Tait, S., Uauy, C., & Balk, J. (2017). Wheat Vacuolar Iron Transporter TaVIT2 Transports Fe and Mn and Is Effective for Biofortification. *Plant Physiology*, *174*(4), 2434–2444. https://doi.org/10.1104/pp.17.00672

Cornejo, P., Meier, S., Borie, G., Rillig, M. C., & Borie, F. (2008). Glomalin-related soil protein in a Mediterranean ecosystem affected by a copper smelter and its contribution to Cu and Zn sequestration. *Science of The Total Environment*, *406*(1–2), 154–160. https://doi.org/10.1016/j.scitotenv.2008.07.045

Devi, T. S., Gupta, S., & Kapoor, R. (2019). Arbuscular Mycorrhizal Fungi in Alleviation of Cold Stress in Plants. In *Advancing Frontiers in Mycology & Mycotechnology* (pp. 435–455). Springer Singapore. https://doi.org/10.1007/978-981-13-9349-5_17

Ferreira Vilela, L. A., & Barbosa, M. V. (2019). Contribution of Arbuscular Mycorrhizal Fungi in Promoting Cadmium Tolerance in Plants. In *Cadmium Tolerance in Plants* (pp. 553–586). Elsevier. https://doi.org/10.1016/B978-0-12-815794-7.00021-7

Ferrol, N., Tamayo, E., & Vargas, P. (2016). The heavy metal paradox in arbuscular mycorrhizas: from mechanisms to biotechnological applications. *Journal of Experimental Botany*, *67*(22), 6253–6265. https://doi.org/10.1093/jxb/erw403

Frommer, W. B., & Ninnemann, O. (1995). Heterologous Expression of Genes in Bacterial, Fungal, Animal, and Plant Cells. *Annual Review of Plant Physiology and Plant Molecular Biology*, *46*(1), 419–444. https://doi.org/10.1146/annurev.pp.46.060195.002223

García-Rodríguez, S., Azcón-Aguilar, C., & Ferrol, N. (2007). Transcriptional regulation of host enzymes involved in the cleavage of sucrose during arbuscular mycorrhizal symbiosis. *Physiologia Plantarum*, *129*(4), 737–746. https://doi.org/10.1111/j.1399-3054.2007.00873.x

Gerwien, F., Safyan, A., Wisgott, S., Hille, F., Kaemmer, P., Linde, J., Brunke, S., Kasper, L., & Hube, B. (2016). A Novel Hybrid Iron Regulation Network Combines Features from Pathogenic and Nonpathogenic Yeasts. *MBio*, *7*(5). https://doi.org/10.1128/mBio.01782-16

Ghasemi Siani, N., Fallah, S., Pokhrel, L. R., & Rostamnejadi, A. (2017). Natural amelioration of Zinc oxide nanoparticle toxicity in fenugreek (Trigonella foenum-gracum) by arbuscular mycorrhizal (Glomus intraradices) secretion of glomalin. *Plant Physiology and Biochemistry*, *112*, 227–238. https://doi.org/10.1016/j.plaphy.2017.01.001

Gsaller, F., Eisendle, M., Lechner, B. E., Schrettl, M., Lindner, H., Müller, D., Geley, S., & Haas, H. (2012). The interplay between vacuolar and siderophore-mediated iron storage in Aspergillus fumigatus. *Metallomics*, *4*(12), 1262. https://doi.org/10.1039/c2mt20179h

Hakoyama, T., Niimi, K., Yamamoto, T., Isobe, S., Sato, S., Nakamura, Y., Tabata, S., Kumagai, H., Umehara, Y., Brossuleit, K., Petersen, T. R., Sandal, N., Stougaard, J., Udvardi, M. K., Tamaoki, M., Kawaguchi, M., Kouchi, H., & Suganuma, N. (2012). The Integral Membrane Protein SEN1 is Required for Symbiotic Nitrogen Fixation in Lotus japonicus Nodules. *Plant and Cell Physiology*, *53*(1), 225–236. https://doi.org/10.1093/pcp/pcr167

Helber, N., Wippel, K., Sauer, N., Schaarschmidt, S., Hause, B., & Requena, N. (2011). A Versatile Monosaccharide Transporter That Operates in the Arbuscular Mycorrhizal Fungus *Glomus* sp Is Crucial for the Symbiotic Relationship with Plants . *The Plant Cell*, *23*(10), 3812–3823. https://doi.org/10.1105/tpc.111.089813

Kato, T., Kumazaki, K., Wada, M., Taniguchi, R., Nakane, T., Yamashita, K., Hirata, K., Ishitani, R., Ito, K., Nishizawa, T., & Nureki, O. (2019). Crystal structure of plant vacuolar iron transporter VIT1. *Nature Plants*, *5*(3), 308–315. https://doi.org/10.1038/s41477-019-0367-2

Kim, S. A., Punshon, T., Lanzirotti, A., Li, L., Alonso, J. M., Ecker, J. R., Kaplan, J., & Guerinot, M. lou. (2006). Localization of Iron in *Arabidopsis* Seed Requires the Vacuolar Membrane Transporter VIT1. *Science*, *314*(5803), 1295–1298. https://doi.org/10.1126/science.1132563

Lanquar, V., Lelièvre, F., Bolte, S., Hamès, C., Alcon, C., Neumann, D., Vansuyt, G., Curie, C., Schröder, A., Krämer, U., Barbier-Brygoo, H., & Thomine, S. (2005). Mobilization of vacuolar iron by AtNRAMP3 and AtNRAMP4 is essential for seed germination on low iron. *The EMBO Journal*, *24*(23), 4041–4051. https://doi.org/10.1038/sj.emboj.7600864

Lapinskas, P. J., Cunningham, K. W., Liu, X. F., Fink, G. R., & Culotta, V. C. (1995). Mutations in PMR1 suppress oxidative damage in yeast cells lacking superoxide dismutase. *Molecular and Cellular Biology*, *15*(3), 1382–1388. https://doi.org/10.1128/MCB.15.3.1382

Lapinskas, P. J., Lin, S.-J., & Culotta, V. C. (1996). The role of the Saccharomyces cerevisiae CCC1 gene in the homeostasis of manganese ions. *Molecular Microbiology*, *21*(3), 519–528. https://doi.org/10.1111/j.1365-2958.1996.tb02561.x

Lehmann, A., & Rillig, M. C. (2015). Arbuscular mycorrhizal contribution to copper, manganese and iron nutrient concentrations in crops – A meta-analysis. *Soil Biology and Biochemistry*, *81*, 147–158. https://doi.org/10.1016/j.soilbio.2014.11.013

Li, L., Bagley, D., Ward, D. M., & Kaplan, J. (2008). Yap5 Is an Iron-Responsive Transcriptional Activator That Regulates Vacuolar Iron Storage in Yeast. *Molecular and Cellular Biology*, *28*(4), 1326–1337. https://doi.org/10.1128/MCB.01219-07

Li, L., Chen, O. S., Ward, D. M., & Kaplan, J. (2001). CCC1 Is a Transporter That Mediates Vacuolar Iron Storage in Yeast. *Journal of Biological Chemistry*, *276*(31), 29515–29519. https://doi.org/10.1074/jbc.M103944200

Li, L., & Ward, D. M. (2018). Iron toxicity in yeast: transcriptional regulation of the vacuolar iron importer Ccc1. *Current Genetics*, *64*(2), 413–416. https://doi.org/10.1007/s00294-017-0767-7

López-Lorca, V. M., Molina-Luzón, M. J., & Ferrol, N. (2022). Characterization of the NRAMP Gene Family in the Arbuscular Mycorrhizal Fungus Rhizophagus irregularis. *Journal of Fungi*, *8*(6), 592. https://doi.org/10.3390/JOF8060592

Nguyen, T. Q., Dziuba, N., & Lindahl, P. A. (2019). Isolated *Saccharomyces cerevisiae* vacuoles contain low-molecular-mass transition-metal polyphosphate complexes. *Metallomics*, *11*(7), 1298–1309. https://doi.org/10.1039/c9mt00104b

Pepe, A., Sbrana, C., Ferrol, N., & Giovannetti, M. (2017). An in vivo whole-plant experimental system for the analysis of gene expression in extraradical mycorrhizal mycelium. *Mycorrhiza*, *27*(7), 659–668. https://doi.org/10.1007/s00572-017-0779-7

Puig, S., Askeland, E., & Thiele, D. J. (2005). Coordinated remodeling of cellular metabolism during iron deficiency through targeted mRNA degradation. *Cell*, *120*(1), 99–110. https://doi.org/10.1016/j.cell.2004.11.032

Ramos-Alonso, L., Romero, A. M., Martínez-Pastor, M. T., & Puig, S. (2020). Iron Regulatory Mechanisms in Saccharomyces cerevisiae. *Frontiers in Microbiology*, *11*, 2222. https://doi.org/10.3389/fmicb.2020.582830

Riaz, M., Kamran, M., Fang, Y., Wang, Q., Cao, H., Yang, G., Deng, L., Wang, Y., Zhou, Y., Anastopoulos, I., & Wang, X. (2021). Arbuscular mycorrhizal fungi-induced mitigation of heavy metal phytotoxicity in metal contaminated soils: A critical review. *Journal of Hazardous Materials*, *402*, 123919. https://doi.org/10.1016/j.jhazmat.2020.123919

Ruth, B., Khalvati, M., & Schmidhalter, U. (2011). Quantification of mycorrhizal water uptake via high-resolution on-line water content sensors. *Plant and Soil*, *342*(1–2), 459–468. https://doi.org/10.1007/s11104-010-0709-3

Sharma, S., Anand, G., Singh, N., & Kapoor, R. (2017). Arbuscular Mycorrhiza Augments Arsenic Tolerance in Wheat (Triticum aestivum L.) by Strengthening Antioxidant Defense System and Thiol Metabolism. *Frontiers in Plant Science*, *8*, 906. https://doi.org/10.3389/fpls.2017.00906

Singh, R. P., Prasad, H. K., Sinha, I., Agarwal, N., & Natarajan, K. (2011). Cap2-HAP Complex Is a Critical Transcriptional Regulator That Has Dual but Contrasting Roles in Regulation of Iron Homeostasis in Candida albicans. *Journal of Biological Chemistry*, *286*(28), 25154–25170. https://doi.org/10.1074/jbc.M111.233569

Sorribes-Dauden, R., Peris, D., Martínez-Pastor, M. T., & Puig, S. (2020). Structure and function of the vacuolar Ccc1/VIT1 family of iron transporters and its regulation in fungi. *Computational and Structural Biotechnology Journal*, *18*, 3712–3722. https://doi.org/10.1016/j.csbj.2020.10.044

Spatafora, J. W., Chang, Y., Benny, G. L., Lazarus, K., Smith, M. E., Berbee, M. L., Bonito, G., Corradi, N., Grigoriev, I., Gryganskyi, A., James, T. Y., O'Donnell, K., Roberson, R. W., Taylor, T. N., Uehling, J., Vilgalys, R., White, M. M., & Stajich, J. E. (2016). A phylum-level phylogenetic classification of zygomycete fungi based on genome-scale data. *Mycologia*, *108*(5), 1028–1046. https://doi.org/10.3852/16-042

Tamayo, E., Gómez-Gallego, T., Azcón-Aguilar, C., & Ferrol, N. (2014). Genome-wide analysis of copper, iron and zinc transporters in the arbuscular mycorrhizal fungus *Rhizophagus irregularis*. *Frontiers in Plant Science*, *5*, 547. https://doi.org/10.3389/fpls.2014.00547

Tamayo, E., Knight, S. A. B., Valderas, A., Dancis, A., & Ferrol, N. (2018). The arbuscular mycorrhizal fungus *Rhizophagus irregularis* uses a reductive iron assimilation pathway for high-affinity iron uptake. *Environmental Microbiology*, *20*(5), 1857–1872. https://doi.org/10.1111/1462-2920.14121

Voß, S., Betz, R., Heidt, S., Corradi, N., & Requena, N. (2018). RiCRN1, a Crinkler Effector From the Arbuscular Mycorrhizal Fungus Rhizophagus irregularis, Functions in Arbuscule Development. *Frontiers in Microbiology*, *9*(SEP), 2068. https://doi.org/10.3389/fmicb.2018.02068

Wipf, D., Krajinski, F., Tuinen, D., Recorbet, G., & Courty, P. (2019). Trading on the arbuscular mycorrhiza market: from arbuscules to common mycorrhizal networks. *New Phytologist*, *223*(3), 1127–1142. https://doi.org/10.1111/nph.15775

Wu, S., Zhang, X., Chen, B., Wu, Z., Li, T., Hu, Y., Sun, Y., & Wang, Y. (2016). Chromium immobilization by extraradical mycelium of arbuscular mycorrhiza contributes to plant chromium tolerance. *Environmental and Experimental Botany*, *122*, 10–18. https://doi.org/10.1016/j.envexpbot.2015.08.006

Wu, S., Zhang, X., Huang, L., & Chen, B. (2019). Arbuscular mycorrhiza and plant chromium tolerance. *Soil Ecology Letters*, *1*(3–4), 94–104. https://doi.org/10.1007/s42832-019-0015-9

Zeng, T., Holmer, R., Hontelez, J., Lintel-Hekkert, B., Marufu, L., Zeeuw, T., Wu, F., Schijlen, E., Bisseling, T., & Limpens, E. (2018). Host- and stage-dependent secretome of the arbuscular mycorrhizal fungus *Rhizophagus irregularis*. *The Plant Journal*, *94*(3), 411–425. https://doi.org/10.1111/tpj.13908

Zeng, T., Rodriguez-Moreno, L., Mansurkhodzaev, A., Wang, P., Berg, W., Gasciolli, V., Cottaz, S., Fort, S., Thomma, B. P. H. J., Bono, J., Bisseling, T., & Limpens, E. (2020). A lysin motif effector subverts chitin-triggered immunity to facilitate arbuscular mycorrhizal symbiosis. *New Phytologist*, *225*(1), 448–460. https://doi.org/10.1111/nph.16245

Supplementary Table 1. Oligonucleotides used in this study. Overhangs are underlined.

Primer	Sequence (5'-3')	Application
qRiCCC1.1.F	ACAACGCTGAGAGAAGGAGAGA	Real Time PCR
qRiCCC1.1.R	GGGTTTGGCTTTTCAAGGTTTAGC	Real Time PCR
qRiCCC1.2.F	CAAGCGCAATACAAACAGCA	Real Time PCR
qRiCCC1.2.R	TTTCCATACTTCGACTAATCTTACACC	Real Time PCR
qRiCCC1.3.F	TCATCCCTAGGAAATCGTCATC	Real Time PCR
qRiCCC1.3.R	GCCCATCCACCTACTGCTTT	Real Time PCR
qRiEF1αF	GCTATTTTGATCATTGCCGCC	Real Time PCR
qRiEF1αR	TCATTAAAACGTTCTTCCGACC	Real Time PCR
qCiEF1αF	CATGCGTCAGACGGTTGCTGT	Real Time PCR
qCiEF1αR	CTTCACTCCCTTCTTGGCTGC	Real Time PCR
RiCCC1.1.TOPO5	CACCATGATGGCCCTTCGTCAAAT	Cloning RiCCC1.1
RiCCC1.1.TOPO3	CTAATCCTCACGTCCAATTAAC	Cloning RiCCC1.1
RiCCC1.1.TOPO3gfp	TTCATCCTCACGTCCAATTAAC	Cloning RiCCC1.1 with STOP codon modified
RiCCC1.2.GW5	AAAGCAGGCTTCATGAGTCAACCATTACTTTC	Cloning RiCCC1.2
RiCCC1.2.GW3	GAAAGCTGGGTCTTATTTTTTCCATACTTCGA	Cloning RiCCC1.2
RiCCC1.2.TOPO5	CACCATGAGTCAACCATTACTTTC	Cloning RiCCC1.2 with STOP codon modified
RiCCC1.2.TOPO3gfp	TTCTTTTTTCCATACTTCGACTAA	Cloning RiCCC1.2 with STOP codon modified
RiCCC1.3.GW5	AAAGCAGGCTTCATGTCATCAATAGTGGAAGT	Cloning RiCCC1.3
RiCCC1.3.GW3	GAAAGCTGGGTCTCAAATAAATTCAAATAAAT	Cloning RiCCC1.3
RiCCC1.3.GW3gfp	GAAAGCTGGGTCTTCAATAAATTCAAATAAAT	Cloning RiCCC1.3 with STOP codon modified

CHAPTER 3:

Impact of arbuscular mycorrhiza on the iron deficiency response of *Solanum lycopersicum*

Adapted from López-Lorca, V. M., Molina-Luzón, M. J., Ferrol, N

Impact of arbuscular mycorrhiza on the iron deficiency response of *Solanum lycopersicum*.

Submitted to "Plant Physiology and Biochemistry"

Abstract

Plants have evolved highly efficient strategies to maintain iron (Fe) homeostasis. In this study, we report the impact of the arbuscular mycorrhizal (AM) symbiosis on the Fe-deficiency response of tomato plants and on its ionome. Characterization of the tomato VIT/VTL family members of the vacuolar Fe transporters is also described Shoot Fe concentration s decreased by Fe deficiency and AM colonization, whereasroot Fe concentration increased in AM plants both under Fe-limiting and –sufficient conditions. Fe deficiency decreased AM colonization s. Gene expression analyses revealed that *SlNRAMP1* expression increased in mycorrhizal roots under Fe-sufficient conditions, while *SlNRAMP3*, *SlCHLN*, *SlVIT1* and *SlVIT2* expression was down-regulated. Under Fe-deficient conditions, AM up-regulates expression the *SlFRO1*, *SlIRT1* and *SlNRAMP3* genes, encoding proteins involved in transport Fe into the cytosol. Functional characterization in yeast of the four members of the *SlVIT/VTL* gene family revealed that while *SlVIT1*, *SlVTL1* and *SlVTL2* encode proteins mediating Fe and Mn transport, *SlVTL2* only transports Mn. Expression of SLVTL2 was up-regulated by AM under Fe-deficient and –sufficient conditions. ¡ All these data show that expression of the tomato Fe-deficiency response genes is differentially regulated by AM under Fe-sufficient and -deficient conditions and suggest that AM colonization is regulated by Fe.

Introduction

Iron (Fe) is an essential micronutrient necessary for the correct development and survival of almost every organism, having structural roles in proteins and as enzymes cofactor. In plants, Fe is key in important processes, such as photosynthesis, mitochondrial respiration and nitrogen nutrition. Although abundant in nature, Fe is generally poorly accessible to plants, especially in alkaline soils, because it is mostly found in its oxidized state Fe (III). Fe deficiency leads to chlorosis and poor growth and development in plants (Kabir et al., 2013; Wang et al., 2007). Hence plants have evolved highly efficient strategies to acquire Fe from the rhizosphere (Grotz & Guerinot, 2006). All plant species but grasses use a mechanism known as Strategy I, involving a plasma membrane H^+-ATPase that acidifies the rhizosphere and solubilizes the Fe chelates, a ferric reductase (FRO1) that reduces Fe (III) to Fe (II) and Fe (II)-specific transporters (IRT and NRAMP1) for uptake across the plasma membrane. Grasses use a Strategy II consisting in the synthesis and release to the rhizosphere of phytosiderophores (PS) that chelate Fe (III); then the PS-Fe (III) complexes are transported into root cells through plasma membrane oligopeptide transporters YS1 or YS1-like. However, this distinction between both Fe uptake strategies is too simplistic. Under Fe deficiency, the model plant *Arabidopsis thaliana* secretes phenolic

compounds, particularly, coumarins to improve Fe mobilization and reduction (Fourcroy et al., 2014; Schmid et al., 2014). Coumarins mobilize Fe by chelation and the chelated Fe (III) can be reduced by FRO2 to release Fe (II), which is then taken up by IRT1 (Fourcroy et al., 2016). More recently, it has been shown that *A. thaliana* can take the Fe (III)-coumarin complex under high-pH conditions (Robe et al., 2021), which is very similar to the Strategy II used by grasses. Therefore, non-grasses seem to have to Fe uptake strategies, with the Strategy I working best under acidic conditions and the Strategy II-like strategy activated under alkaline or neutral conditions (Tsai & Schmidt, 2017). Similarly, rice, a Strategy II plant, can directly take up Fe (II) most likely through an IRT1 transporter like under low-oxygen conditions (Cheng et al., 2007; Ishimaru et al., 2006). After uptake into the root epidermis from the rhizosphere, small molecules facilitate solubility and transport of Fe (Clemens, 2019). In the symplast, Fe is transported to the endodermis in the form of Fe (II)-nicotianamine (NA) complexes. NA is a non-protein amino acid produced by S-adenosyl methionine by nicotianamine synthase (NAS). At the cellular level, Fe is either incorporated into proteins or compartmentalized into the vacuoles through transporters of the vacuolar iron transporter (VIT) family (Ram et al., 2021). VITs transporters are also involve in manganese homeostasis (Lapinskas et al., 1996).

Besides these intrinsic Fe uptake strategies, another strategy evolved by plants to cope with Fe deficiency is the establishment of associations with beneficial soil microorganisms. Fe absorption mediated by siderophores produced by rhizosphere microorganisms has long been shown to contribute to plant nutrition (Lurthy et al., 2020). However, the contribution of arbuscular mycorrhizal (AM) fungi, one of the most prominent groups of soil microorganisms that play a key role in plant nutrition, remains largely unexplored.

AM fungi belong to the subphylum Glomeromycotina and establish a mutualistic symbiosis, the so-called arbuscular mycorrhiza, with most terrestrial plant species (Azcón-Aguilar & Barea, 2015). The fungus colonizes the root cortex and develops an extensive network of extraradical hyphae in the soil. This external mycelium can absorb nutrients beyond the nutrient depletion zones, which are then delivered to the roots in the colonized-cortical cells, where the fungus develops highly-branched structures called arbuscules. In return, the plant provides carbon compounds to the fungus (Smith & Read, 2008). The main benefit of AM is an improved plant P status. However, root colonization by AM fungi often increases uptake of micronutrients when plants grow in deficient soils (Ferrol et al., 2016). The role of AM fungi in plant Zn and Cu nutrition has long been recognized. By contrast, data on the effect of mycorrhizal colonization on plant Fe nutrition are variable and inconsistent (Clark & Zeto, 1996). Some studies using ^{59}Fe as an isotopic marker has been shown that the fungus is able to absorb and transfer this metal to

sorghum (Caris et al., 1998), marigold (Suzuki et al., 2000) and maize (Kobae et al., 2014) but not to peanut plants (Caris et al., 1998). Recently, it has been suggested that increased Fe uptake under Fe-limiting conditions by mycorrhizal plants could be related to an increased Fe bioavailability at their rhizosphere, as an increased biosynthesis of phytosiderophores has been found in a Strategy II plant (Prity et al., 2020) and an increased ferric chelate reductase activity in various Strategy I plants (Kabir et al., 2020; Rahimi et al., 2021; Rahman et al., 2020).

This work was aimed at getting further insights into the mechanisms of Fe homeostasis in AM through the analysis of the impact of the symbiosis on the Fe-deficiency response of tomato plants. Tomato was chosen as a host plant because is an economically important crop that has been used as a model plant for studying iron homeostasis in Strategy I plants (Zamboni et al., 2012) and AM formation and function (Ho-Plágaro et al., 2018, 2019, 2020; Molinero-Rosales et al., 2019). A few genes involved in Fe homeostasis have been identified in tomato. *SlFRO1* and *SlIRT1* are involved in Fe uptake from the rhizosphere and are up-regulated by Fe-deficiency. SlNRAMP1 and SlNRAMP3 are two Fe transporters of the resistance-associated macrophage protein (NRAMP) family, whose transport function has been demonstrated in yeast (Bereczky et al., 2003). *SlCHLN* playing a role in Fe distribution has been characterized in the *chloroverva* mutant of Fe unable to synthesize NA (Higuchi et al., 1996). However, transporters of the VIT family remain uncharacterized in tomato. In this study, we report characterization of the tomato family and the expression patters of the tomato Fe-responsive genes in roots of non-mycorrhizal and mycorrhizal plants grown under Fe-sufficient and deficient conditions. The impact of Fe deficiency on the tomato ionome of mycorrhizal and non-mycorrhizal plants is also presented.

Materials and Methods

Biological materials and growth conditions

Tomato seeds (*Solanum lycopersicum* cv. Moneymaker) were surface sterilized with 5% commercial bleach for 3 min, washed with sterile water and maintained in sterile water for 2 hours. Afterwards seeds were germinated under sterile conditions on wet filter paper in Petri plates in darkness at 25 °C for 4 days. Germinated seeds were transferred pots containing 1.6 L of sterilized sand previously washed with 0.03 M HCl to eliminate metal traces and then rinsed with distilled water until pH 7. The AM fungal inoculum used was *Rhizophagus irregularis* DAOM 197189 (E. C. H. Chen et al., 2018) grown in monoxenic cultures. The inoculum was prepared blending the medium with sterile 2.5 mM citrate buffer (pH 6.0). Seedlings were inoculated by adding to the growth substrate 3 mL of the AM fungal inoculum containing 1650 spores (mycorrhizal treatment). Non-mycorrhizal plants were prepared by adding 3 mL of an inoculum

filtrate. Plants were developed in a growth chamber under 16 h light (24 °C)/8h dark (20 °C). They were watered twice a week with a modified half-strength Hoagland solution at pH 7.0 containing 62.5 μM KH_2PO_4 and 50 μM EDTA-Fe(III) (control treatment) or without EDTA-Fe(III) (Fe deficiency treatment). Each treatment consisted of seven replicates.

Finally, plants were harvested 12 weeks after inoculation. At harvesting, plant biomass was determined by measuring root and shoot fresh weights. An aliquot of each root system was separated to estimate mycorrhizal colonization. Roots and shoots were frozen in liquid nitrogen and stored at -80 °C until used.

The *ccc1*Δ and *pmr1*Δ mutants of the *Saccharomyces cerevisiae* yeast strain was used in this work. *ccc1*Δ lacks the vacuolar membrane transporter Ccc1 (Li et al., 2001) and *pmr1*Δ is unable to transport Mn into Golgi vesicles and cannot withstand toxic levels of the metal (Lapinskas et al., 1995). Yeast cells were grown on YPD or minimal synthetic dextrose (SD) medium, supplemented with the appropriate amino acids.

RNA extraction and cDNA synthesis

Total RNA was extracted from tomato roots using the phenol/SDS method followed by LiCl precipitation (García-Rodríguez et al., 2007). RNAs were treated with DNase using the RNA-free DNase set (PROMEGA) using the manufacturer's protocol. cDNAs were synthetized from 1 μg of total DNase-treated RNA in a 20 μl reaction using Super-Script IV Reverse Transcriptase (Invitrogen), according to the manufacturer´s instructions.

Gene expression analyses

Gene expression was studied by real-time RT-PCR using a QuantStudio 3 (Applied Biosystem) in the synthetized cDNAs. Each 12 μl reaction contained 1 μl of a 1:10 dilution of cDNA, 0.5 μl 10 mM each primer and 6 μl iTaq (Bio-Rad). The primer pairs used for qRT-PCR are presented in Supplementary Table 1. The specificity of the primer sets was analyzed by PCR amplification of the *R. irregularis* cDNA. The real-time RT-PCR program consisted of an initial incubation at 95ªC for 30 s, followed by 40 cycles of 95 °C for 15 s, 60 °C for 30 s and 72 °C for 30 s, where the fluorescence signal was measured, and a final step with a heat-dissociation protocol to check the specificity of PCR amplification procedure. Efficiency of the different primer pairs was determined through a real-time RT-PCR on several dilutions of cDNA. The results obtained for the different treatments were standardized to the expression levels of *SlEF1α*. Real-time RT-PCR determinations were carried out on at least three independent biological samples. Real time RT-PCR reactions were performed at least two times for each biological sample, with the threshold cycle (Ct) determined in duplicate. Relative expression levels were calculated using the $2^{\Delta CT}$

method (Schmittgen & Livak, 2008) and the standard error was computed from the average of the ΔCt values for each biological sample.

Mycorrhizal colonization

The presence of the fungal structures was observed in an aliquot of the root system of each tomato plant stained with trypan blue (Phillips & Hayman, 1970). Mycorrhizal colonization was estimated according to the Trouvelot method (Trouvelot et al., 1986) using the Mycocalc program (https://www2.dijon.inrae.fr/mychintec/Mycocalc-prg/download.html). The abundance of the fungus in the roots was also estimated by measuring the expression levels of the *R. irregularis* elongation factor 1α (*RiEF1α*; GenBank Accession No. DQ282611), using as internal control the expression levels of the tomato elongation factor 1a (GenBank Accession No. NM_001247106).

SlVIT sequence identification and analyses

The four *SlVIT* paralog sequences (Supplementary Table 2) were selected through a Blastp search in NCBI (National Center for Biotechnology Information; https://www.ncbi.nlm.nih.gov/) database using the SlVIT1 sequence deposited in the plant membrane protein database Aramemnon (http://aramemnon.uni-koeln.de/) as template. *Arabidopsis thaliana* VIT/VTL protein sequences were retrieved from The Arabidopsis Information Resource (TAIR, https://www.arabidopsis.org/). Conserved Domain Database at NCBI was used to identify conserved domains of proteins. Primer3 (https://primer3.ut.ee/) was used to design the gene-specific primers. Potential transmembrane domains were predicted using DeepTMHMM (https://dtu.biolib.com/DeepTMHMM). Structural models of the proteins were generated using MyDomains tool of Prosite (https://prosite.expasy.org/mydomains/). 3D models were predicted using the Phyre2 software (http://www.sbg.bio.ic.ac.uk/~phyre2/html/page.cgi?id=index) based on the crystal structure of iron transporter VIT1 with cobalt ion (ID: c6iu3A). The alignment of the putative amino acid sequences of the SlVIT/VTL were carried out using Mega-X. Homology and similarity percentages were performed with SIAS (http://imed.med.ucm.es/Tools/sias.html). Mega-X were used to calculate phylogenetic relationships with the Neighbour-Joining method.

Heterologous expression

ORFs of the *S. lycopersicum* VIT genes were amplified from cDNA extracted from tomato roots by PCR using the corresponding primers pairs (Supplementary Table 1) and cloned into the expression vector pDRF1-GW using Gateway technology (Invitrogen). To be recognized by de BP enzyme, full-length cDNA sequences were flanked with the sequences attB1 and attB2. PCR products were cloned following the manufacturer´s instruction. All constructs were verified by

sequencing. *S. cerevisiae* mutant strains *ccc1*Δ and *pmr1*Δ were transformed with the different pDRf1-VIT constructs or with the empty vector as negative control using a lithium acetate-based method (Schiestl & Gietz, 1989). Yeast transformants were selected in SD medium by uracil autotrophy. For drop tests, yeast transformants were harvested by centrifugation from a liquid culture grown to exponential phase in SD medium without uracil, washed three times with milli-Q H_2O and adjusted to a final OD_{600} of 1. Then, 5 μL of serial 1:10 dilutions were spotted on the corresponding selective medium. *ccc1*Δ transformants were spotted onto SD-URA supplemented or not with 5 mM $FeSO_4$. *pmr1*Δ transformed mutants were spotted onto SD without uracil supplemented or not with 2 mM MnCl2.

Elemental analyses

An aliquot of the shoot and root samples of each plant were oven-dried at 65 °C for two days, ground to a fine powder, ashed at 550 °C and digested in H_2O/HNO_3. Tissue nutrients concentrations were analyses by Inductively Coupled Plasma Optical Emission Spectroscopy (ICP-OES; ICP 6500 Duo Thermo) analysis in the Instrumentation Facility of the Estación Experimental del Zaidín, EEZ-CSIC, Granada, Spain.

Statistical analyses

Statgraphics Centurion XVI software was used for the statistical analysis of means and standard error determinations. For the comparison of the treatments, ANOVA two-ways followed by a Duncan test ($p<0.05$) were performed. Nutrients data were logarithm transformed and subjected to a sparse partial least-squares discriminant analysis (sPLSDA) by using METABOANALIST (https://www.metaboanalyst.ca/) web-based metabolomic package.

Results

Plant growth responses and Fe content

Shoot fresh weight was not affected by Fe deficiency or mycorrhizal colonization. However, root fresh weight increased under Fe deficiency both in non-mycorrhizal and mycorrhizal plants (Figure 1a). Shoot Fe concentration decreased in plants fertilized with a Fe-free nutrient solution. No significant differences were found between root Fe concentration of plants grown under Fe-sufficient and –deficient conditions. Relative to the non-inoculated plants, shoot Fe concentration decreased under Fe-sufficient conditions in mycorrhizal plants (Figure 1b). Fe concentration strongly increased in roots of mycorrhizal plants. Therefore, Fe translocation factor decreased both by Fe deficiency and mycorrhizal colonization (Figure 1c).

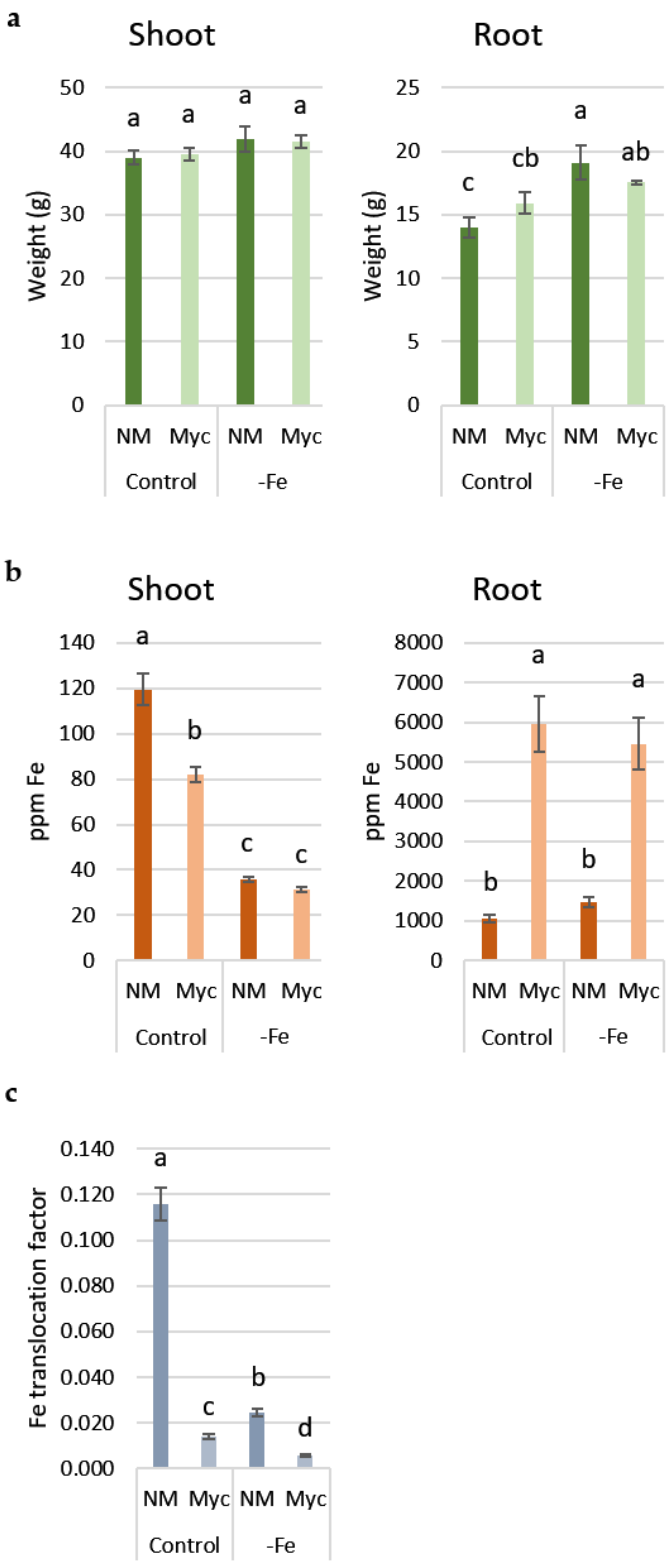

Figure 1. (a) Shoot and root fresh weight of mycorrhizal (Myc) and non-mycorrhizal (NM) plants developed under Fe-sufficient (Control) or Fe-deficient (-Fe) conditions. (b) Shoot and root Fe concentration of mycorrhizal (Myc) and non-mycorrhizal (NM) plants developed under Fe-sufficient (Control) or Fe-deficient (-Fe) conditions (**b**). (**c**) Fe tanslocation factor in mycorrhizal (Myc) and non-mycorrhizal (NM) plants developed under Fe-sufficient (Control) or Fe-deficient (-Fe) conditions. Values are means ± standard error. Different letters indicate significant differences ($p < 0.05$, n = 7) among treatments based on Duncan´s test.

Fe deficiency down-regulates AM-related genes

Microscopic observations of the trypan blue-stained roots revealed the presence of all fungal structures in roots of mycorrhizal plants but not in those of non-inoculated plants (Figure 1a). Mycorrhizal colonization was estimated by measuring the expression levels of the constitutively expressed gene *RiEF1α*. A 3-fold reduction of *RiEF1α* expression was detected in mycorrhizal roots of plants fertilized with a Fe-free nutrient solution (Figure 2b). To further explore the effect of Fe deficiency on AM development and function, we decided to determine expression of a panel of AM-marker genes, including *SlRAM1* (SolDB accession Solyc02g094340.1), *SlEXO84* (SolDB accession Solyc09g072720.2), *SlAMT2.2* (SolDB accession Solyc08g067080.1) and *SlPT4* (SolDB accession Solyc06g051850.1) (Ho-Plágaro et al., 2021). SlRAM1 is a GRAS transcription factor that regulates the expression of genes involved in arbuscule development, such as SlEXO1 playing a role in periarbuscular membrane formation, and nutrient transfer to the plant, such as SlPT4 and SlAMT2.2. involved in phosphate and ammonium transfer. An overall down-regulation of all the AM-related genes analyzed was detected under Fe deficient conditions (Figure 2b).

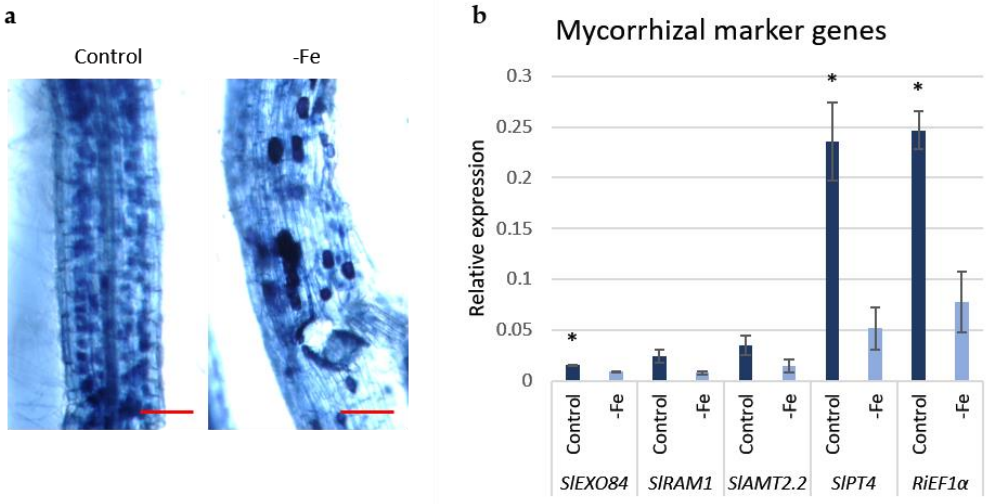

Figure 2. Effect of Fe defficiency in mycorrhizal colonization. (**a**) Detection of *R. irregularis* structures in *S. lycorpersicum* roots stained with trypan blue grown under control and Fe deficient (-Fe) conditions. Scale bar: 100 μm. (**b**) Mycorrhizal marker genes expression analyzed in RNAs isolated from colonized *S. lycopersicum* roots watered with 50μM Fe (Control) or a modified nutrient solution without Fe (-Fe). Relative expression levels were calculated using the $2^{-\Delta CT}$ method with *SlEF1α* as normalizer. Values are means ± standard error. Asterisks indicate significant differences ($p < 0.05$; n = 3).

Expression patterns of Fe deficiency-responsive genes

To assess the impact of AM on the Fe-deficiency response of tomato, expression patterns of the previously reported tomato genes playing a role in Fe uptake and distribution was assessed by RT-qPCR in roots of non-mycorrhizal and mycorrhizal plants grown under Fe-sufficient and -deficient conditions.

Transcripts of *SlFRO1*, the first component of the Strategy I Fe acquisition system, were not detected in roots of plants grown under Fe-sufficient conditions, probably because their levels were below the detection limit. Fe-deficiency significantly up-regulated *SlFRO1* expression, being this up-regulation higher in roots of mycorrhizal plants. Transcript levels of the second component of the Strategy I, the Fe permease *SlIRT1*, were not significantly affected by Fe-deficiency in non-mycorrhizal roots. However, *SlIRT1* expression was up-regulated by Fe-deficiency in mycorrhizal roots. Under Fe-sufficient conditions, *SlIRT1* expression was lower in mycorrhizal roots (Figure 3).

SlNRAMP1 expression levels increased in roots of mycorrhizal plants grown under Fe-optimal conditions. However, expression of the Fe transporter SlNRAMP3 was down-regulated by Fe-deficiency in non-mycorrhizal roots and by AM under Fe-sufficient conditions. Under Fe-limiting conditions *SlNRAMP3* expression increased in AM roots (Figure 3).

Expression of *SlCHLN*, encoding a protein required for the synthesis of the non-proteic amino acid that is essential for Fe distribution was down-regulated by Fe-deficiency and by AM (Figure 3).

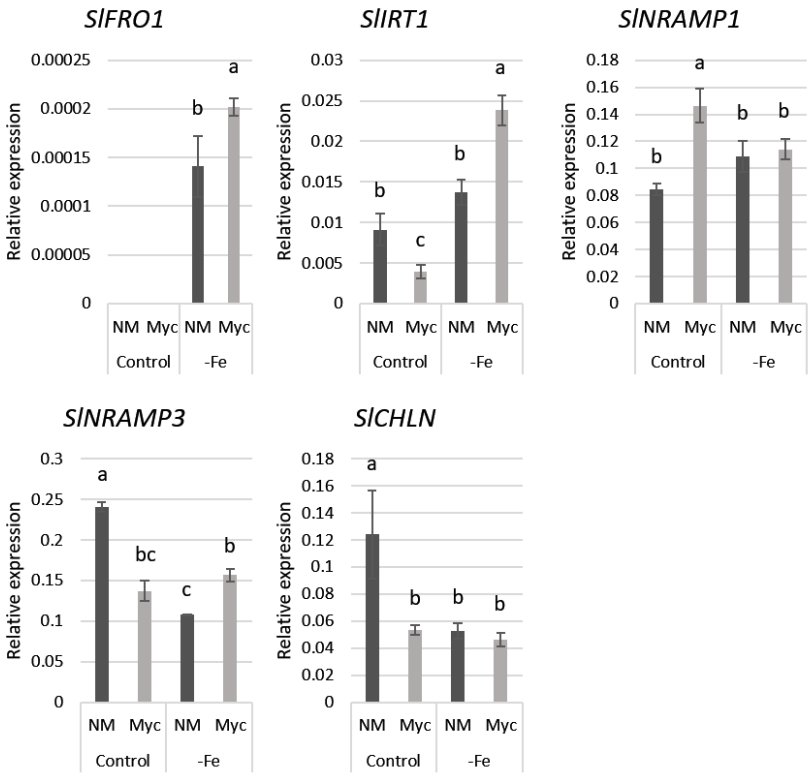

Figure 3. Effect of Fe-deficiency and mycorrhizal colonization on the expression of the Fe deficiency responsive genes of tomato. Gene expression was analysed in RNAs isolated from *S. lycopersicum* roots. Plants were watered with half-strength Hoagland solution (Control, 50 μM Fe) or a modified nutrient solution without Fe (-Fe). Relative expression levels were calculated, using the $2^{-\Delta CT}$ method with *SlEF1α* as normalizer. Values are means ± standard error. Different letters indicate significant differences ($p < 0.05$, n = 3).

The Solanum lycopersicum VIT/VTL family

The high accumulation of Fe observed in mycorrhizal roots prompted us to assess expression patterns of genes involved in vacuolar Fe compartmentalization. To that end, the tomato genome databases were searched for VIT transporters. Four genes putatively encoding vacuolar iron transporters were identified in the genome of *S. lycopersium* that were named *SlVIT1*, *SlVIT2*, *SlVTL1* and *SlVITL2* based on the secondary structure of their deduced amino acid sequences. Vacuolar iron Transporters Like (VTLs) are functional homologs of VITs that lack a cytosolic loop thought to mediate $Fe(II)/H^+$ antiport in VITs (Sorribes-Dauden et al., 2020). Selected SlVIT/VTL protein sequences contained the conserved domains of Ccc1/VIT1 family.

SlVIT1, *SlVIT2*, *SlVTL1* and *SlVTL2* full-length cDNAs contain open reading frames of 720, 846, 648 and 654 nucleotides, respectively. Their deduced amino acid sequences have 281-215 amino acid residues. The amino terminus of all of them faces the cytosol and all their proteins are predicted to have five transmembrane domains, with the amino terminus facing the cytosol. SlVIT1 and SlVIT2 possess the 3 three α-helix helices facing the cytosol between transmembrane domains 2 and 3, which, together with the C-terminal end of the second transmembrane domain, make up the Metal Binding Domain (MBD) (Kato et al., 2019) (Figure 4a-b). However, both SlVTL1 and SlVTL2 lack these cytoplasmic helices. Sequence similarity among the deduced amino acids ranges from 61.61%, between SlVTL1 and SlVTL2, to 24.94%, between SlVIT1 and SlVTL2 (Figure 4c). Phylogenetic relationship between VIT/VTL protein family of *S. lycopersicum* and *A. thaliana* clustered VIT proteins separately from VTL proteins (Figure 4d).

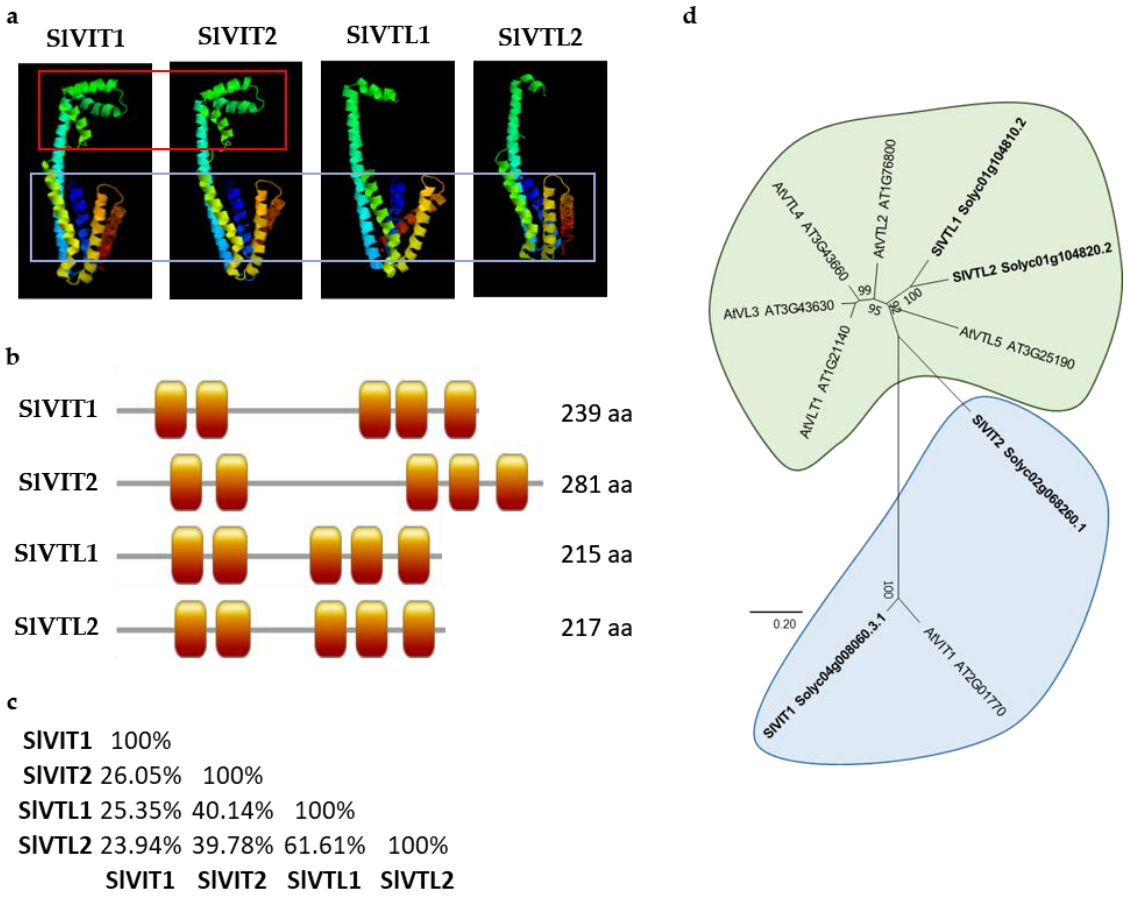

Figure 4. (**a**) Predicted 3D structure of *S. lycopersicum* VIT/VTL protein monomers. Red square indicate the Metal Binding Domains characteristic of VIT proteins and the blue square indicates the five transmembrane domains. Tertiary structures were predicted by Phyre2 software, based on the crystal structure of the iron transporter VIT1 of *Eucalyptus grandis* with cobalt ion (ID: c6iu3A). (**b**) Representation of the secondary structure of SlVIT/VTLs, orange boxes represent transmembrane domains. (**c**) Percent similarity matrix of SlVIT/VTLs proteins. (**d**) Phylogenetic relationships of the *S. lycopersicum* VIT/VTLs proteins (Sl) with homologous sequences from *A. thaliana* (At). Protein SolDB and TAIR accessions are indicated. The blue circle indicates VIT proteins while the green circle indicates VTL proteins. The *S. lycopersicum* sequences are in bold.

To assess if the SlVIT/VTL proteins transport Fe, their ability to restore the phenotype of a yeast strain disrupted in the *ccc1* gene (*ccc1*Δ) was tested. Yeast *ccc1* encodes a vacuolar transporter able to transport Fe to the vacuole. *ccc1*Δ cells fail to grow in SD-medium supplemented with high Fe concentrations due to its inability to store Fe in the vacuole. Expression of *SlVIT1*, *SlVTL1* and *SVTL2*, under the control of PMA1 promoter, complemented the phenotype of *ccc1*Δ cells. Nevertheless, the strain expressing *SlVIT2* or the empty vector pDRf1-GW could not grow on SD media supplemented with 5mM $FeSO_4$. These data demonstrate that *SlVIT1*, *SlVTL1* and *SlVTL2* cDNAs encode functional proteins that Fe transport (Figure 5a).

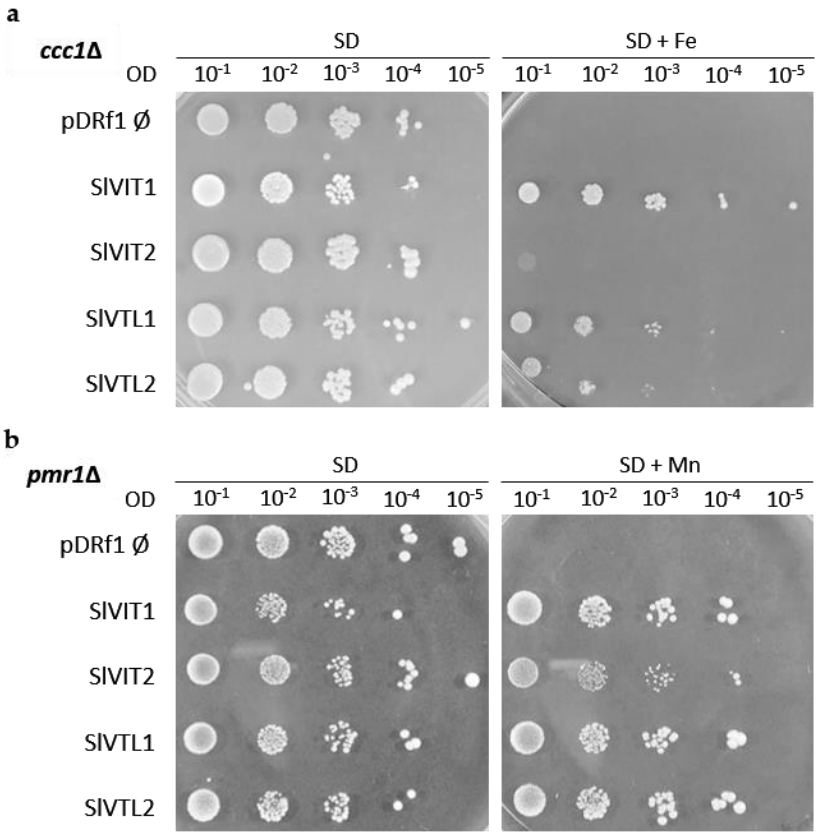

Figure 5. Analysis of *S. lycopersicum* VIT/VTLs function in yeast. *ccc1Δ* cells transformed with the empty vector pDRf1-GW or expressing *SlVIT1*, *SlVIT2*, *SlVTL1* or *SlVTL2* were spotted on SD without uracil supplemented or not with 5 mM FeSO4.

Then, the ability of SlVIT/VTL proteins to transport Mn was tested in the *pmr1*Δ mutant yeast strain. This mutant is defective in Mn transport to the Golgi vesicles and is unable to grow under Mn toxic concentration (Lapinskas et al., 1995). All mutant yeast expressing *SlVIT/VTL* genes restored theability of the mutant cells to grow in the Mn-supplemented media. These data all together, indicate that SlVIT1, SlVTL1 and SlVTL2 are functional Fe and Mn transporters, whereas SlVIT2 is specialized in Mn transport.

*SlVIT/VTL*s are differentially regulated by AM

Expression of three gene displaying an Fe detoxification activity in yeast, that is *SlVIT1*, *SlVTL1* and *SlVTL2*, was down-regulated by Fe-deficiency. Under Fe-sufficient conditions, transcript accumulation of *SlVIT1* and *SlVTL1* significantly decreased in mycorrhizal roots, while *SlVTL2* expression was not affected. SlVIT1 and SlVTL2 expression increased in colonized roots under Fe-deficient conditions (Figure 6).

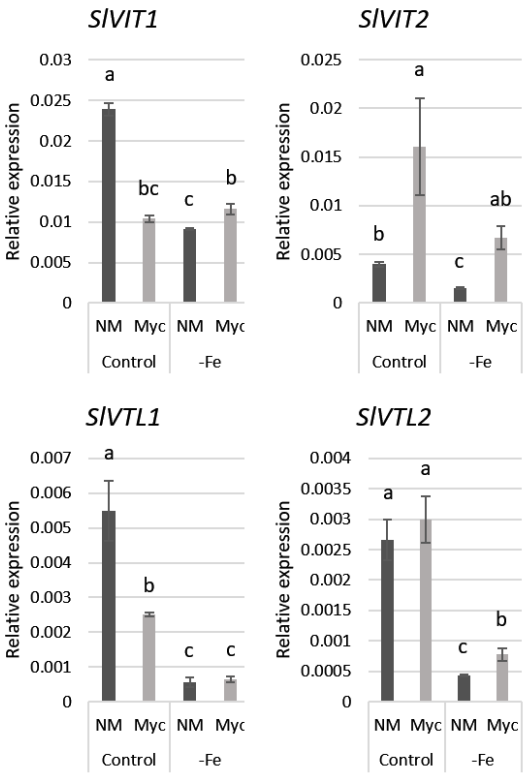

Figure 6. Effect of Fe deficiency and mycorrhizal colonization on *SlVIT/VTLs* expression. Gene expression was analysed in RNA isolated from *S. lycopersicum* roots. Plants were watered half-strength Hoagland solution (Control, 50 μM Fe) or a modified nutrient solution without Fe (-Fe). Relative expression levels were calculated, using the $2^{-\Delta CT}$ method with *SlEF1α* as normalizer. Values are means ± standard error. Different letters indicate significant differences ($p < 0.05$, n = 3).

Effects of Fe deficiency and mycorrhiza on the tomato ionome

Taking into account the reported interconnections between Fe and various macro- and micronutrients and the role of AM on plant mineral nutrition, the elemental composition of plants from the different treatments was determined. A supervised analysis (sPLSDA) of the data showed that both AM and Fe deficiency had a significant effect on the shoot and root nutrient profiles (Figure 7). Fe deficiency had a stronger impact on shoot nutrient accumulation while AM had a stronger impact on root nutrient content patterns. Fe deficiency significantly increased shoot Ca, P and S contents but decreased shoot Fe, Cu, K, Na and Zn contents both in non-mycorrhizal and mycorrhizal plants (Figure 8). In roots, Fe deficiency only affected Mo content of mycorrhizal plants, being higher under Fe-limited conditions (Figure 9). Under Fe-sufficient conditions, development of the symbiosis only affected shoot S, K and Fe contents. Shoot S content was significantly higher in mycorrhizal than in non-mycorrhizal plants, while the opposite trend was observed for K and Fe contents. Root P content of mycorrhizal plants was higher under Fe-deficiency than under Fe-sufficient conditions. However, the highest shoot P content was detected in shoots of non-mycorrhizal plants grown under Fe-deficient conditions.

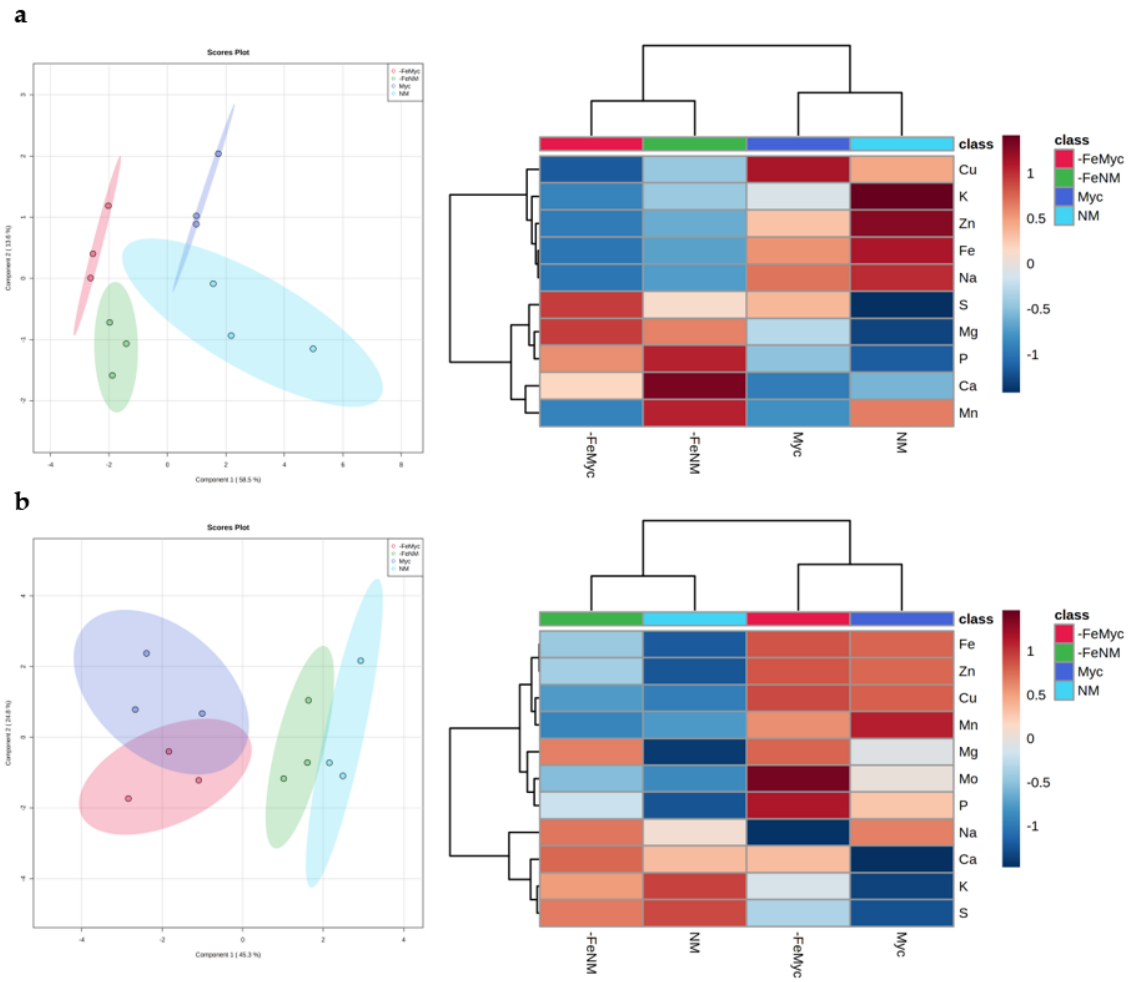

Figure 7. Effect of Fe deficiency and mycorrhizal colonization on the *S. lycopersicum* ionome. Shoot (**a**) and root (**b**) nutrient patterns of mycorrhizal (Myc) and non-mycorrhizal (NM) plants grown under Fe-sufficient (50 μM Fe) or Fe-deficient (-Fe) conditions were analysed by. Left: Principal Component Analyses (PCA); right: Heat maps and clustering of the nutrient content of tomato plants subjected to the different treatments.

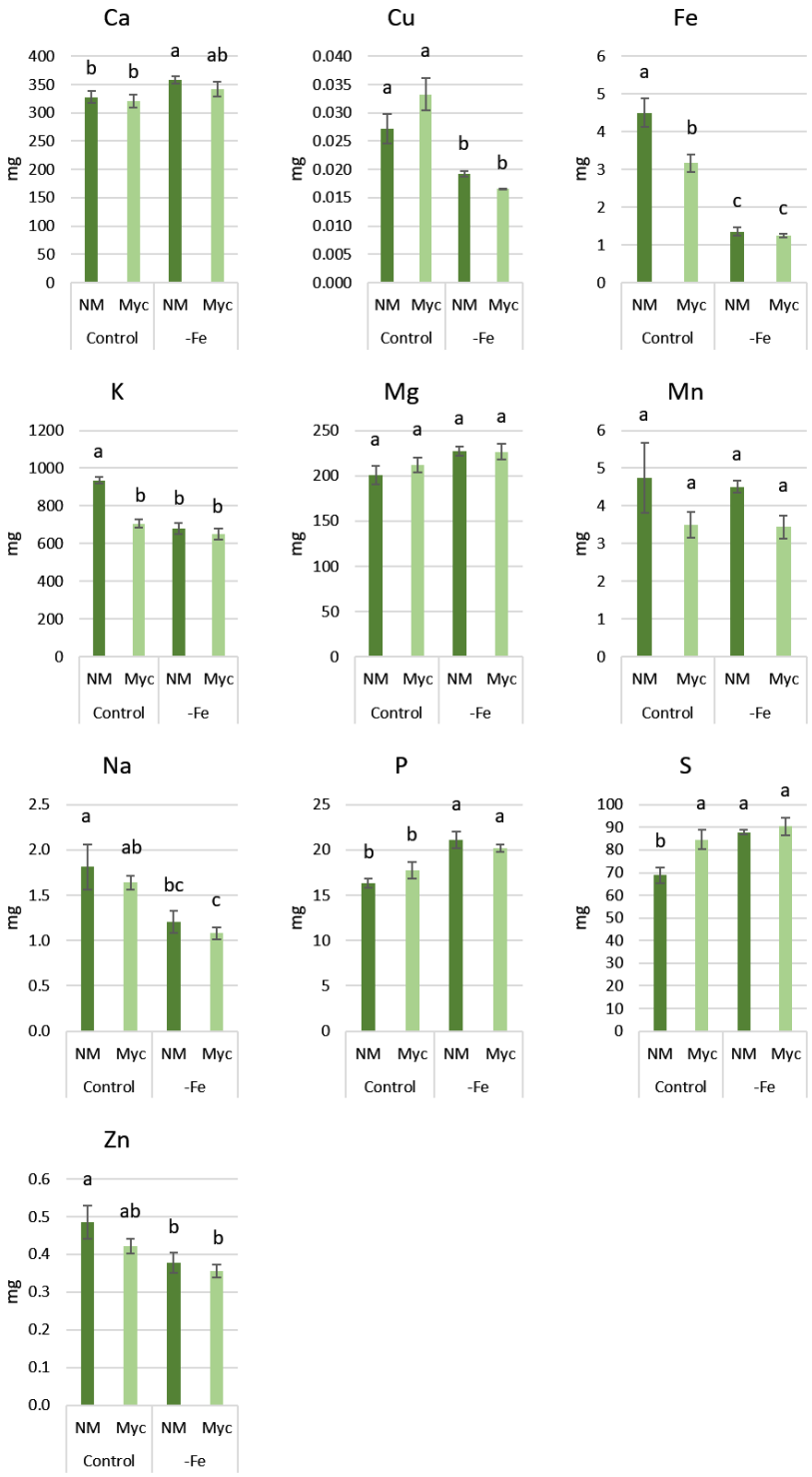

Figure 8. Shoot nutrient content of tomato plants subjected to the different treatments. Nutrient content (mg plant^{-1}) in non-mycorrhizal (NM) and mycorrhizal (Myc) plants grown under Fe-sufficient (control) and deficient Fe conditions (-Fe). Values are means ± standard error. Different letters show statistically significant differences ($P < 0.05$) among treatments based on Duncan's test.

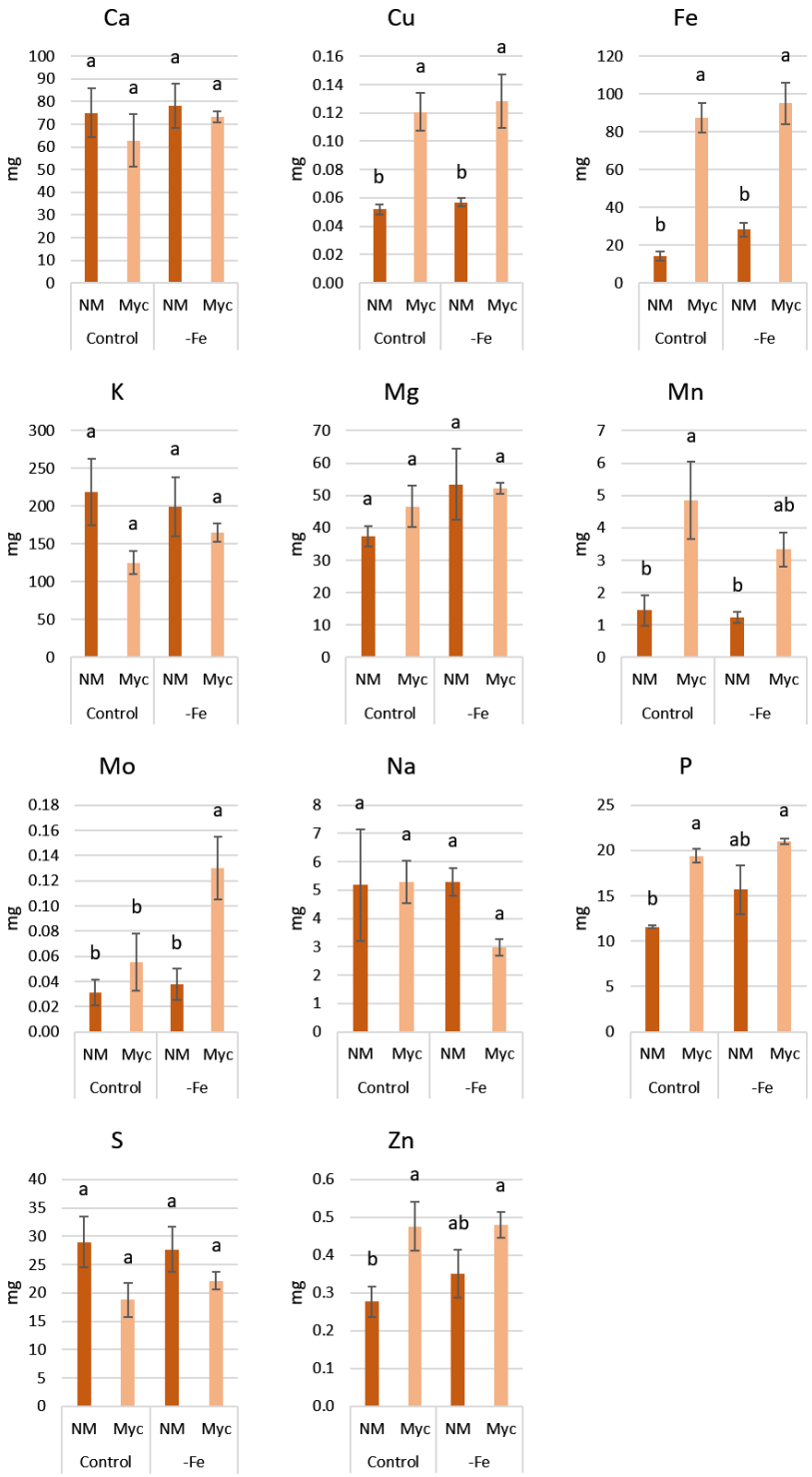

Figure 9. Root nutrient content of tomato plants subjected to the different treatments. Nutrient content (mg plant^{-1}) in non-mycorrhizal (NM) and mycorrhizal (MYC) plants grown under Fe-sufficient (control) and deficient Fe conditions (-Fe). Values are means ± standard error. Different letters show statistically significant differences ($P < 0.05$) among treatments based on Duncan's test.

Discussion

Despite the relevance of AM for plant mineral nutrition, the role of the AM symbiosis on plant Fe homeostasis has not been extensively studied. In this manuscript we have shown that

under Fe-sufficient and –deficient conditions the AM fungus *R. irregularis* increases tomato Fe content but decreased root to shoot Fe translocation. Furthermore, some clues about the molecular mechanisms underlying these effects are provided.

No significant differences were found between shoot biomass of non-mycorrhizal plants grown under Fe-sufficient and -deficient conditions; however, Fe-deficiency increased root biomass. This increase can be interpreted as a strategy of the plant to increase its foraging capacity. Although most reports show that Fe deficiency decrease plant biomass (C. W. Jin et al., 2009; C.-W. Jin et al., 2013; Ravet et al., 2009, 2012; Takahashi et al., 2001), under mild Fe-deficient conditions no effects on plant biomass have been found (Gruber et al., 2013). Since plants require between 50 to 150 ppm Fe for growth (Marschner, 2012), our Fe-deficiency treatment most likely reflects mild Fe deficiency since shoot Fe concentration of plants fertilized with a Fe-free nutrient solution was 35.67 ppm. These moderate Fe deficient conditions might be due to the low P content of the nutrient solution used to fertilized our plants, which was reduced to 62.5 μM P to avoid the negative impact of high P on AM development. The antagonistic interaction between P and Fe deficiencies have been reported in several plant species (Hirsch et al., 2006; Misson et al., 2005; Müller et al., 2007; Thibaud et al., 2010). Our results show that Fe content increased in mycorrhizal roots. These data agree with the conclusion of a previous meta-analysis of studies on the contribution of AM to crop micronutrient nutrition (Lehmann & Rillig, 2015). These authors showed that the positive effect of the AM symbiosis on Fe nutrition was only significant for roots and that depended on the environmental conditions and the host plant species.

Down-regulation of the tomato AM-related genes *SlEXO84*, *RiEF1α* and *SlPT4* and the downward trend of *SlRAM1* and *SlAMT2.2* expression in mycorrhizal roots fertilized with a Fe-free nutrient solution indicate that in tomato Fe deficiency decreases AM colonization and functionality. Since Fe is essential for plant and fungal metabolism, inhibition of mycorrhizal colonization by Fe deficiency could be because this micronutrient might be essential for AM establishment and function. In this respect, Fe deficiency in a plant has been shown to limit infection by pathogens with different lifestyles, ranging from necrotrophs to biotrophs (Trapet et al., 2021). Alternatively, since Fe deficiency increased Pi accumulation in mycorrhizal roots and since AM development is inhibited by high Pi concentrations (Shi et al., 2021), inhibition of AM colonization by Fe-deficiency might be due to the increased P accumulation under these conditions. Although the reason for the increased P content under Fe-deficient plants remains unknown, Fe deficiency alters the transcription of Pi-related genes (Moran Lauter et al., 2014). It has been suggested that the transcription factors PHR1 (Phosphate Starvation Response 1) and PHL1 (PHR1-Like) may integrate Fe and Pi signals (Briat et al., 2015). Since the major

transcriptional regulator of phosphate starvation responses in rice PHR2 is required for AM fungal root colonization and phosphate uptake (Das et al., 2022), it is tempting to hypothesize that PHR might act as a potential integrator of P and Fe signals in AM roots. However, further studies are required to understand the mechanisms regulating the link between Pi and Fe in AM. Other metals like Mn, Zn and Cu stablish a crosstalk with Fe. Zn and Mn share entry routes with Fe trough IRT and NRAMP transporters (Grotz & Guerinot, 2006). The interaction between Fe and Cu influences the uptake of each element by the other. In *A. thaliana*, low Fe increase the expression of *FRO4* and *FRO5* genes involved in Cu uptake, which leads to its accumulation under iron deficiency (Cai et al., 2021).

Up-regulation of ferric reductase *SlFRO1* gene under Fe-limiting conditions in mycorrhizal roots agrees with previous observations in other plant species and supports the view that Fe bioavailability increases in the rhizosphere of mycorrhizal plants (Kabir et al., 2020; Rahimi et al., 2021). *SlFRO1* encodes a plasma membrane ferric reductase, the enzyme responsible for increasing Fe availability at the epidermal roots in Strategy I plants (Robinson et al., 1999). As expected, under these conditions the expression *SlIRT1* expression also increased, which could explain the increased Fe content of the mycorrhizal roots. However, these expression patterns were different under Fe-sufficient conditions, as *SlFRO1* transcripts were not detected and *SlIRT1* transcript levels decreased in mycorrhizal roots. This trend concords with what has been reported in alfalfa roots (Rahman et al., 2020). Increased levels of *SlFRO1* transcripts in mycorrhizal roots under Fe-deficient but not under Fe-sufficient conditions have been also reported in quince and sunflower roots (Kabir et al., 2020; Rahimi et al., 2021). These data indicate that AM increase Fe bioavailability under Fe deficiency but not under Fe-sufficient conditions. Down-regulation of *SlIRT1* under optimal conditions suggests that Fe uptake through the root epidermal cells is inhibited in mycorrhizal roots. Down-regulation of the direct uptake pathway in a mycorrhizal root has been shown for P, N and Zn (Coccina et al., 2019; Liu et al., 1998; Pérez-Tienda et al., 2014). Increased transcript levels of *SlNRAMP1* in mycorrhizal roots grown under optimal Fe conditions suggests that its encoded protein mediates Fe uptake through the mycorrhizal pathway and could explain the increased Fe content of the mycorrhizal roots under optimal conditions. Functional characterization of *SlNRAMP1* is required for confirm this hypothesis. Down-regulation of *SlCHLN* in roots of mycorrhizal plants grown under Fe sufficient conditions and by Fe deficiency indicates a lower NA content in these roots. Due to its toxicity and low solubility, Fe has to be chelated in order to be translocated without causing damaging redox reactions. In the symplast, Fe is thought to be transported in the form of Fe-NA complexes. Fe can be also transported through the apoplastic space formed by the cell walls of the epidermis

and cortex cells to reach the endodermis, where the Casparian strip forces all Fe to pass into the symplast for its transport to the shoot (Connorton et al., 2017). In *Arabidopsis*, NA over-accumulation enhances translocation of Fe to shoot and decrease Fe levels in roots (L. Chen et al., 2018; Haydon et al., 2012). Therefore, the lower NA content of the mycorrhizal and Fe-deficient roots suggests a lower symplastic Fe concentration, which could explain the lower root to shoot translocation observed in these plants. Down-regulation of *SlCHLN* expression by Fe deficiency agrees with previous observations in tomato that NA concentrations increase in response to Fe overload (Pich et al., 2001). These authors suggested that besides its role in Fe allocation, NA plays a role in Fe detoxification since NA was detected in the vacuole of the Fe overloaded plants.

Fe (II) can be also stored in the vacuole through Vacuolar Iron Transporters (VIT) or Vacuolar iron transporters-like (VTL). VTLs are functionally homologous to VITs, the main difference being that VTLs lack the Metal Binding Domain (MBD) formed by 3 α-helices facing the cytosol between transmembrane domains 2 and 3 (Sorribes-Dauden et al., 2020). Out of the four *VIT/VTL* genes identified in the *S. lycopersium* genome, *SlVIT1* and *SlVIT2* present 3 α-helices facing the cytosol; however, *SlVTL1* and *SlVTL2* lack this metal binding domain. While *SlVIT2* encoded a Mn transporter involve in Mn detoxification, our functional analyses in yeast indicate that *SlVIT1*, *SlVTL1* and *SlVTL2* are functional homologues of the yeast Ccc1 vacuolar transporter that mediates Fe transport from the cytosol to the vacuole playing a role in Fe excess detoxification (Lapinskas et al., 1996; Li et al., 2001). As expected, *SlVIT1*, *SlVTL1* and *SlVTL2* expression decreased by Fe deficiency. The finding that under Fe sufficiency *SlVIT1* and *SlVTL1* were down-regulated in mycorrhizal roots suggests that AM decreases vacuolar Fe accumulation. These data together with the high Fe content of AM roots suggests a high requirement of Fe for AM development. This hypothesis is supported by the high expression levels of the *R. irregularis* high-affinity Fe transporter RiFTR1 in the intraradical fungal structures (Tamayo et al., 2018). The role of Fe in plant-microbe interactions has been recognized for a long time (Verbon et al., 2017). It can be a bargain chip, with microbes needing it for infections and growth, while plants will try to actively withhold it (Trapet et al., 2021). Plants have been known to employ strategies to extract iron from pathogens (Eichhorn et al., 2006); however, they must also provide it to beneficial microbes with which they form symbiotic or endophytic associations (Brear et al., 2020; Johnson et al., 2013).

In conclusion, data presented in this manuscript show that Fe deficiency inhibits AM colonization of tomato roots and that AM differentially regulates the tomato Fe deficiency responses under Fe-deficient and –sufficient conditions.

References

Azcón-Aguilar, C., & Barea, J. M. (2015). Nutrient cycling in the mycorrhizosphere. *Journal of Soil Science and Plant Nutrition*, *15*. https://doi.org/10.4067/S0718-95162015005000035

Bereczky, Z., Wang, H.-Y., Schubert, V., Ganal, M., & Bauer, P. (2003). Differential Regulation of nramp and irt Metal Transporter Genes in Wild Type and Iron Uptake Mutants of Tomato. *Journal of Biological Chemistry*, *278*(27), 24697–24704. https://doi.org/10.1074/jbc.M301365200

Brear, E. M., Bedon, F., Gavrin, A., Kryvoruchko, I. S., Torres-Jerez, I., Udvardi, M. K., Day, D. A., & Smith, P. M. C. (2020). GmVTL1a is an iron transporter on the symbiosome membrane of soybean with an important role in nitrogen fixation. *New Phytologist*, *228*(2), 667–681. https://doi.org/10.1111/nph.16734

Briat, J.-F., Dubos, C., & Gaymard, F. (2015). Iron nutrition, biomass production, and plant product quality. *Trends in Plant Science*, *20*(1), 33–40. https://doi.org/10.1016/j.tplants.2014.07.005

Cai, Y., Li, Y., & Liang, G. (2021). <scp>FIT</scp> and <scp>bHLH</scp> Ib transcription factors modulate iron and copper crosstalk in Arabidopsis. *Plant, Cell & Environment*, *44*(5), 1679–1691. https://doi.org/10.1111/pce.14000

Caris, C., Hördt, W., Hawkins, H.-J., Römheld, V., & George, E. (1998). Studies of iron transport by arbuscular mycorrhizal hyphae from soil to peanut and sorghum plants. *Mycorrhiza*, *8*(1), 35–39. https://doi.org/10.1007/s005720050208

Chen, E. C. H., Morin, E., Beaudet, D., Noel, J., Yildirir, G., Ndikumana, S., Charron, P., St-Onge, C., Giorgi, J., Krüger, M., Marton, T., Ropars, J., Grigoriev, I. v., Hainaut, M., Henrissat, B., Roux, C., Martin, F., & Corradi, N. (2018). High intraspecific genome diversity in the model arbuscular mycorrhizal symbiont *Rhizophagus irregularis*. *New Phytologist*, *220*(4), 1161–1171. https://doi.org/10.1111/nph.14989

Cheng, L., Wang, F., Shou, H., Huang, F., Zheng, L., He, F., Li, J., Zhao, F.-J., Ueno, D., Ma, J. F., & Wu, P. (2007). Mutation in Nicotianamine Aminotransferase Stimulated the Fe(II) Acquisition System and Led to Iron Accumulation in Rice. *Plant Physiology*, *145*(4), 1647–1657. https://doi.org/10.1104/pp.107.107912

Chen, L., Wang, G., Chen, P., Zhu, H., Wang, S., & Ding, Y. (2018). Shoot-Root Communication Plays a Key Role in Physiological Alterations of Rice (Oryza sativa) Under Iron Deficiency. *Frontiers in Plant Science*, *9*. https://doi.org/10.3389/fpls.2018.00757

Clark, R. B., & Zeto, S. K. (1996). Mineral acquisition by mycorrhizal maize grown on acid and alkaline soil. *Soil Biology and Biochemistry*, *28*(10–11), 1495–1503. https://doi.org/10.1016/S0038-0717(96)00163-0

Clemens, S. (2019). Metal ligands in micronutrient acquisition and homeostasis. *Plant, Cell & Environment*, *42*(10), 2902–2912. https://doi.org/10.1111/pce.13627

Coccina, A., Cavagnaro, T. R., Pellegrino, E., Ercoli, L., McLaughlin, M. J., & Watts-Williams, S. J. (2019). The mycorrhizal pathway of zinc uptake contributes to zinc accumulation in barley and wheat grain. *BMC Plant Biology*, *19*(1), 133. https://doi.org/10.1186/s12870-019-1741-y

Connorton, J. M., Jones, E. R., Rodríguez-Ramiro, I., Fairweather-Tait, S., Uauy, C., & Balk, J. (2017). Wheat Vacuolar Iron Transporter TaVIT2 Transports Fe and Mn and Is Effective for Biofortification. *Plant Physiology*, *174*(4), 2434–2444. https://doi.org/10.1104/pp.17.00672

Das, D., Paries, M., Hobecker, K., Gigl, M., Dawid, C., Lam, H.-M., Zhang, J., Chen, M., & Gutjahr, C. (2022). PHOSPHATE STARVATION RESPONSE transcription factors enable arbuscular mycorrhiza symbiosis. *Nature Communications*, *13*(1), 477. https://doi.org/10.1038/s41467-022-27976-8

Eichhorn, H., Lessing, F., Winterberg, B., Schirawski, J., Kämper, J., Müller, P., & Kahmann, R. (2006). A Ferroxidation/Permeation Iron Uptake System Is Required for Virulence in *Ustilago maydis*. *The Plant Cell*, *18*(11), 3332–3345. https://doi.org/10.1105/tpc.106.043588

Ferrol, N., Tamayo, E., & Vargas, P. (2016). The heavy metal paradox in arbuscular mycorrhizas: from mechanisms to biotechnological applications. *Journal of Experimental Botany*, *67*(22), 6253–6265. https://doi.org/10.1093/jxb/erw403

Fourcroy, P., Sisó-Terraza, P., Sudre, D., Savirón, M., Reyt, G., Gaymard, F., Abadía, A., Abadia, J., Álvarez-Fernández, A., & Briat, J. (2014). Involvement of the <scp>ABCG</scp> 37 transporter in secretion of scopoletin and derivatives by *Arabidopsis* roots in response to iron deficiency. *New Phytologist*, *201*(1), 155–167. https://doi.org/10.1111/nph.12471

Fourcroy, P., Tissot, N., Gaymard, F., Briat, J.-F., & Dubos, C. (2016). Facilitated Fe Nutrition by Phenolic Compounds Excreted by the Arabidopsis ABCG37/PDR9 Transporter Requires the IRT1/FRO2 High-Affinity Root Fe 2+ Transport System. *Molecular Plant*, *9*(3), 485–488. https://doi.org/10.1016/j.molp.2015.09.010

García-Rodríguez, S., Azcón-Aguilar, C., & Ferrol, N. (2007). Transcriptional regulation of host enzymes involved in the cleavage of sucrose during arbuscular mycorrhizal symbiosis. *Physiologia Plantarum*, *129*(4), 737–746. https://doi.org/10.1111/j.1399-3054.2007.00873.x

Grotz, N., & Guerinot, M. lou. (2006). Molecular aspects of Cu, Fe and Zn homeostasis in plants. *Biochimica et Biophysica Acta (BBA) - Molecular Cell Research*, *1763*(7), 595–608. https://doi.org/10.1016/j.bbamcr.2006.05.014

Gruber, B. D., Giehl, R. F. H., Friedel, S., & von Wirén, N. (2013). Plasticity of the Arabidopsis Root System under Nutrient Deficiencies. *Plant Physiology*, *163*(1), 161–179. https://doi.org/10.1104/pp.113.218453

Haydon, M. J., Kawachi, M., Wirtz, M., Hillmer, S., Hell, R., & Krämer, U. (2012). Vacuolar Nicotianamine Has Critical and Distinct Roles under Iron Deficiency and for Zinc Sequestration in *Arabidopsis*. *The Plant Cell*, *24*(2), 724–737. https://doi.org/10.1105/tpc.111.095042

Higuchi, K., Nishizawa, N., Römheld, V., Marschner, H., & Mori, S. (1996). Absence of nicotianamine synthase activity in the tomato mutant 'chloronerva.' *Journal of Plant Nutrition*, *19*(8–9), 1235–1239. https://doi.org/10.1080/01904169609365194

Hirsch, J., Marin, E., Floriani, M., Chiarenza, S., Richaud, P., Nussaume, L., & Thibaud, M. C. (2006). Phosphate deficiency promotes modification of iron distribution in Arabidopsis plants. *Biochimie*, *88*(11), 1767–1771. https://doi.org/10.1016/j.biochi.2006.05.007

Ho-Plágaro, T., Huertas, R., Tamayo-Navarrete, M. I., Ocampo, J. A., & García-Garrido, J. M. (2018). An improved method for Agrobacterium rhizogenes-mediated transformation of tomato suitable for the study of arbuscular mycorrhizal symbiosis. *Plant Methods*, *14*(1), 34. https://doi.org/10.1186/s13007-018-0304-9

Ho-Plágaro, T., Molinero-Rosales, N., Fariña Flores, D., Villena Díaz, M., & García-Garrido, J. M. (2019). Identification and Expression Analysis of GRAS Transcription Factor Genes Involved in the Control of Arbuscular Mycorrhizal Development in Tomato. *Frontiers in Plant Science*, *10*, 268. https://doi.org/10.3389/fpls.2019.00268

Ho-Plágaro, T., Morcillo, R. J. L., Tamayo-Navarrete, M. I., Huertas, R., Molinero-Rosales, N., López-Ráez, J. A., Macho, A. P., & García-Garrido, J. M. (2021). DLK2 regulates arbuscule hyphal branching during arbuscular mycorrhizal symbiosis. *New Phytologist*, *229*(1), 548–562. https://doi.org/10.1111/nph.16938

Ho-Plágaro, T., Tamayo-Navarrete, M. I., & García-Garrido, J. M. (2020). *Functional Analysis of Plant Genes Related to Arbuscular Mycorrhiza Symbiosis Using Agrobacterium rhizogenes-Mediated Root Transformation*

and Hairy Root Production (pp. 191–215). Springer, Singapore. https://doi.org/10.1007/978-981-15-4055-4_13

Ishimaru, Y., Suzuki, M., Tsukamoto, T., Suzuki, K., Nakazono, M., Kobayashi, T., Wada, Y., Watanabe, S., Matsuhashi, S., Takahashi, M., Nakanishi, H., Mori, S., & Nishizawa, N. K. (2006). Rice plants take up iron as an Fe^{3+} -phytosiderophore and as Fe^{2+}. *The Plant Journal*, *45*(3), 335–346. https://doi.org/10.1111/j.1365-313X.2005.02624.x

Jin, C. W., Du, S. T., Chen, W. W., Li, G. X., Zhang, Y. S., & Zheng, S. J. (2009). Elevated Carbon Dioxide Improves Plant Iron Nutrition through Enhancing the Iron-Deficiency-Induced Responses under Iron-Limited Conditions in Tomato. *Plant Physiology*, *150*(1), 272–280. https://doi.org/10.1104/pp.109.136721

Jin, C.-W., Liu, Y., Mao, Q.-Q., Wang, Q., & Du, S.-T. (2013). Mild Fe-deficiency improves biomass production and quality of hydroponic-cultivated spinach plants (Spinacia oleracea L.). *Food Chemistry*, *138*(4), 2188–2194. https://doi.org/10.1016/j.foodchem.2012.12.025

Johnson, L. J., Koulman, A., Christensen, M., Lane, G. A., Fraser, K., Forester, N., Johnson, R. D., Bryan, G. T., & Rasmussen, S. (2013). An Extracellular Siderophore Is Required to Maintain the Mutualistic Interaction of Epichloë festucae with Lolium perenne. *PLoS Pathogens*, *9*(5), e1003332. https://doi.org/10.1371/journal.ppat.1003332

Kabir, A. H., Debnath, T., Das, U., Prity, S. A., Haque, A., Rahman, M. M., & Parvez, M. S. (2020). Arbuscular mycorrhizal fungi alleviate Fe-deficiency symptoms in sunflower by increasing iron uptake and its availability along with antioxidant defense. *Plant Physiology and Biochemistry*, *150*, 254–262. https://doi.org/10.1016/j.plaphy.2020.03.010

Kabir, A. H., Paltridge, N. G., Roessner, U., & Stangoulis, J. C. R. (2013). Mechanisms associated with Fe-deficiency tolerance and signaling in shoots of *Pisum sativum*. *Physiologia Plantarum*, *147*(3), 381–395. https://doi.org/10.1111/j.1399-3054.2012.01682.x

Kato, T., Kumazaki, K., Wada, M., Taniguchi, R., Nakane, T., Yamashita, K., Hirata, K., Ishitani, R., Ito, K., Nishizawa, T., & Nureki, O. (2019). Crystal structure of plant vacuolar iron transporter VIT1. *Nature Plants*, *5*(3), 308–315. https://doi.org/10.1038/s41477-019-0367-2

Kobae, Y., Tomioka, R., Tanoi, K., Kobayashi, N. I., Ohmori, Y., Nishida, S., & Fujiwara, T. (2014). Selective induction of putative iron transporters, *OPT8a* and *OPT8b* , in maize by mycorrhizal colonization. *Soil Science and Plant Nutrition*, *60*(6), 843–847. https://doi.org/10.1080/00380768.2014.949854

Lapinskas, P. J., Cunningham, K. W., Liu, X. F., Fink, G. R., & Culotta, V. C. (1995). Mutations in PMR1 suppress oxidative damage in yeast cells lacking superoxide dismutase. *Molecular and Cellular Biology*, *15*(3), 1382–1388. https://doi.org/10.1128/MCB.15.3.1382

Lapinskas, P. J., Lin, S.-J., & Culotta, V. C. (1996). The role of the Saccharomyces cerevisiae CCC1 gene in the homeostasis of manganese ions. *Molecular Microbiology*, *21*(3), 519–528. https://doi.org/10.1111/j.1365-2958.1996.tb02561.x

Lehmann, A., & Rillig, M. C. (2015). Arbuscular mycorrhizal contribution to copper, manganese and iron nutrient concentrations in crops – A meta-analysis. *Soil Biology and Biochemistry*, *81*, 147–158. https://doi.org/10.1016/j.soilbio.2014.11.013

Li, L., Chen, O. S., Ward, D. M., & Kaplan, J. (2001). CCC1 Is a Transporter That Mediates Vacuolar Iron Storage in Yeast. *Journal of Biological Chemistry*, *276*(31), 29515–29519. https://doi.org/10.1074/jbc.M103944200

Liu, H., Trieu, A. T., Blaylock, L. A., & Harrison, M. J. (1998). Cloning and Characterization of Two Phosphate Transporters from *Medicago truncatula* Roots: Regulation in Response to Phosphate and to Colonization by Arbuscular Mycorrhizal (AM) Fungi. *Molecular Plant-Microbe Interactions®*, *11*(1), 14–22. https://doi.org/10.1094/MPMI.1998.11.1.14

Lurthy, T., Cantat, C., Jeudy, C., Declerck, P., Gallardo, K., Barraud, C., Leroy, F., Ourry, A., Lemanceau, P., Salon, C., & Mazurier, S. (2020). Impact of Bacterial Siderophores on Iron Status and Ionome in Pea. *Frontiers in Plant Science*, *11*, 730. https://doi.org/10.3389/fpls.2020.00730

Marschner, P. (2012). *Marschner's Mineral Nutrition of Higher Plants* (Third). Academic Press. https://books.google.es/books?hl=es&lr=&id=yqKV3USG41cC&oi=fnd&pg=PP1&dq=Marschner%E2%80%99s+mineral+nutrition+of+higher+plants+london&ots=Vc8MZ4wWAk&sig=eVwM-4aIEnOoRacsF3VgnabENk4#v=onepage&q=Marschner%E2%80%99s%20mineral%20nutrition%20of%20higher%20plants%20london&f=false

Martínez-Medina, A., van Wees, S. C. M., & Pieterse, C. M. J. (2017). Airborne signals from *Trichoderma* fungi stimulate iron uptake responses in roots resulting in priming of jasmonic acid-dependent defences in shoots of *Arabidopsis thaliana* and *Solanum lycopersicum*. *Plant, Cell & Environment*, *40*(11), 2691–2705. https://doi.org/10.1111/pce.13016

Misson, J., Raghothama, K. G., Jain, A., Jouhet, J., Block, M. A., Bligny, R., Ortet, P., Creff, A., Somerville, S., Rolland, N., Doumas, P., Nacry, P., Herrerra-Estrella, L., Nussaume, L., & Thibaud, M.-C. (2005). A genome-wide transcriptional analysis using *Arabidopsis thaliana* Affymetrix gene chips determined plant responses to phosphate deprivation. *Proceedings of the National Academy of Sciences*, *102*(33), 11934–11939. https://doi.org/10.1073/pnas.0505266102

Molinero-Rosales, N., Martín-Rodríguez, J. Á., Ho-Plágaro, T., & García-Garrido, J. M. (2019). Identification and expression analysis of the arbuscular mycorrhiza-inducible Rieske non-heme oxygenase Ptc52 gene from tomato. *Journal of Plant Physiology*, *237*, 95–103. https://doi.org/10.1016/j.jplph.2019.04.009

Moran Lauter, A. N., Peiffer, G. A., Yin, T., Whitham, S. A., Cook, D., Shoemaker, R. C., & Graham, M. A. (2014). Identification of candidate genes involved in early iron deficiency chlorosis signaling in soybean (Glycine max) roots and leaves. *BMC Genomics*, *15*(1), 702. https://doi.org/10.1186/1471-2164-15-702

Müller, R., Morant, M., Jarmer, H., Nilsson, L., & Nielsen, T. H. (2007). Genome-Wide Analysis of the Arabidopsis Leaf Transcriptome Reveals Interaction of Phosphate and Sugar Metabolism. *Plant Physiology*, *143*(1), 156–171. https://doi.org/10.1104/pp.106.090167

Nagy, R., Karandashov, V., Chague, V., Kalinkevich, K., Tamasloukht, M., Xu, G., Jakobsen, I., Levy, A. A., Amrhein, N., & Bucher, M. (2005). The characterization of novel mycorrhiza-specific phosphate transporters from Lycopersicon esculentum and Solanum tuberosum uncovers functional redundancy in symbiotic phosphate transport in solanaceous species. *The Plant Journal*, *42*(2), 236–250. https://doi.org/10.1111/j.1365-313X.2005.02364.x

Pérez-Tienda, J., Corrêa, A., Azcón-Aguilar, C., & Ferrol, N. (2014). Transcriptional regulation of host transporters and GS/GOGAT pathway in arbuscular mycorrhizal rice roots. *Plant Physiology and Biochemistry*, *75*, 1–8. https://doi.org/10.1016/j.plaphy.2013.11.029

Phillips, J. M., & Hayman, D. S. (1970). Improved procedures for clearing roots and staining parasitic and vesicular-arbuscular mycorrhizal fungi for rapid assessment of infection. *Transactions of the British Mycological Society*, *55*(1), 158-IN18. https://doi.org/10.1016/S0007-1536(70)80110-3

Pich, A., Manteuffel, R., Hillmer, S., Scholz, G., & Schmidt, W. (2001). Fe homeostasis in plant cells: Does nicotianamine play multiple roles in the regulation of cytoplasmic Fe concentration? *Planta*, *213*(6), 967–976. https://doi.org/10.1007/s004250100573

Prity, S. A., Sajib, S. A., Das, U., Rahman, M. M., Haider, S. A., & Kabir, A. H. (2020). Arbuscular mycorrhizal fungi mitigate Fe deficiency symptoms in sorghum through phytosiderophore-mediated Fe mobilization and restoration of redox status. *Protoplasma*, *257*(5), 1373–1385. https://doi.org/10.1007/s00709-020-01517-w

Rahimi, S., Baninasab, B., Talebi, M., Gholami, M., & Zarei, M. (2021). Arbuscular mycorrhizal fungi inoculation improves iron deficiency in quince via alterations in host root phenolic compounds and expression of genes. *Scientia Horticulturae*, *285*, 110165. https://doi.org/10.1016/j.scienta.2021.110165

Rahman, Md. A., Parvin, M., Das, U., Ela, E. J., Lee, S.-H., Lee, K.-W., & Kabir, A. H. (2020). Arbuscular Mycorrhizal Symbiosis Mitigates Iron (Fe)-Deficiency Retardation in Alfalfa (Medicago sativa L.) Through the Enhancement of Fe Accumulation and Sulfur-Assisted Antioxidant Defense. *International Journal of Molecular Sciences*, *21*(6), 2219. https://doi.org/10.3390/ijms21062219

Ram, H., Sardar, S., & Gandass, N. (2021). Vacuolar Iron Transporter (Like) proteins: Regulators of cellular iron accumulation in plants. *Physiologia Plantarum*, *171*(4), 823–832. https://doi.org/10.1111/ppl.13363

Ravet, K., Reyt, G., Arnaud, N., Krouk, G., Djouani, E.-B., Boucherez, J., Briat, J.-F., & Gaymard, F. (2012). Iron and ROS control of the DownSTream mRNA decay pathway is essential for plant fitness. *The EMBO Journal*, *31*(1), 175–186. https://doi.org/10.1038/emboj.2011.341

Ravet, K., Touraine, B., Boucherez, J., Briat, J.-F., Gaymard, F., & Cellier, F. (2009). Ferritins control interaction between iron homeostasis and oxidative stress in Arabidopsis. *The Plant Journal*, *57*(3), 400–412. https://doi.org/10.1111/j.1365-313X.2008.03698.x

Robe, K., Conejero, G., Gao, F., Lefebvre-Legendre, L., Sylvestre-Gonon, E., Rofidal, V., Hem, S., Rouhier, N., Barberon, M., Hecker, A., Gaymard, F., Izquierdo, E., & Dubos, C. (2021). Coumarin accumulation and trafficking in *Arabidopsis thaliana* : a complex and dynamic process. *New Phytologist*, *229*(4), 2062–2079. https://doi.org/10.1111/nph.17090

Robinson, N. J., Procter, C. M., Connolly, E. L., & Guerinot, M. lou. (1999). A ferric-chelate reductase for iron uptake from soils. *Nature*, *397*(6721), 694–697. https://doi.org/10.1038/17800

Schiestl, R. H., & Gietz, R. D. (1989). High efficiency transformation of intact yeast cells using single stranded nucleic acids as a carrier. *Current Genetics*, *16*(5–6), 339–346. https://doi.org/10.1007/BF00340712

Schmid, N. B., Giehl, R. F. H., Doll, S., Mock, H.-P., Strehmel, N., Scheel, D., Kong, X., Hider, R. C., & von Wiren, N. (2014). Feruloyl-CoA 6′-Hydroxylase1-Dependent Coumarins Mediate Iron Acquisition from Alkaline Substrates in Arabidopsis. *PLANT PHYSIOLOGY*, *164*(1), 160–172. https://doi.org/10.1104/pp.113.228544

Schmittgen, T. D., & Livak, K. J. (2008). Analyzing real-time PCR data by the comparative CT method. *Nature Protocols*, *3*(6), 1101–1108. https://doi.org/10.1038/nprot.2008.73

Shi, J., Zhao, B., Zheng, S., Zhang, X., Wang, X., Dong, W., Xie, Q., Wang, G., Xiao, Y., Chen, F., Yu, N., & Wang, E. (2021). A phosphate starvation response-centered network regulates mycorrhizal symbiosis. *Cell*, *184*(22), 5527-5540.e18. https://doi.org/10.1016/j.cell.2021.09.030

Smith, S. E., & Read, D. (2008). *Mycorrhizal Symbiosis*.

Sorribes-Dauden, R., Peris, D., Martínez-Pastor, M. T., & Puig, S. (2020). Structure and function of the vacuolar Ccc1/VIT1 family of iron transporters and its regulation in fungi. *Computational and Structural Biotechnology Journal*, *18*, 3712–3722. https://doi.org/10.1016/j.csbj.2020.10.044

Suzuki, H., Kumagai, H., Oohashi, K., Sakamoto, K., Inubushi, K., Enomoto, S., & Ambe, F. (2000). Uptake of 15 trace elements in arbuscular mycorrhizal marigold Measured by the multitracer technique. *Soil Science and Plant Nutrition*, *46*(2), 283–289. https://doi.org/10.1080/00380768.2000.10408784

Takahashi, M., Nakanishi, H., Kawasaki, S., Nishizawa, N. K., & Mori, S. (2001). Enhanced tolerance of rice to low iron availability in alkaline soils using barley nicotianamine aminotransferase genes. *Nature Biotechnology*, *19*(5), 466–469. https://doi.org/10.1038/88143

Tamayo, E., Knight, S. A. B., Valderas, A., Dancis, A., & Ferrol, N. (2018). The arbuscular mycorrhizal fungus *Rhizophagus irregularis* uses a reductive iron assimilation pathway for high-affinity iron uptake. *Environmental Microbiology*, *20*(5), 1857–1872. https://doi.org/10.1111/1462-2920.14121

Thibaud, M.-C., Arrighi, J.-F., Bayle, V., Chiarenza, S., Creff, A., Bustos, R., Paz-Ares, J., Poirier, Y., & Nussaume, L. (2010). Dissection of local and systemic transcriptional responses to phosphate starvation in Arabidopsis. *The Plant Journal*, *64*(5), 775–789. https://doi.org/10.1111/j.1365-313X.2010.04375.x

Trapet, P. L., Verbon, E. H., Bosma, R. R., Voordendag, K., van Pelt, J. A., & Pieterse, C. M. J. (2021). Mechanisms underlying iron deficiency-induced resistance against pathogens with different lifestyles. *Journal of Experimental Botany*, *72*(6), 2231–2241. https://doi.org/10.1093/jxb/eraa535

Trouvelot, A., Kough, J. L., & Gianinazzi-Pearson, V. (1986). Estimation of vesicular arbuscular mycorrhizal infection levels. Research for methods having a functional significance. *Physiological and Genetical Aspects of Mycorrhizae = Aspects Physiologiques et Genetiques Des Mycorhizes: Proceedings of the 1st European Symposium on Mycorrhizae, Dijon, 1-5 July 1985*. https://agris.fao.org/agris-search/search.do?recordID=US201301430989

Tsai, H. H., & Schmidt, W. (2017). Mobilization of Iron by Plant-Borne Coumarins. *Trends in Plant Science*, *22*(6), 538–548. https://doi.org/10.1016/j.tplants.2017.03.008

Verbon, E. H., Trapet, P. L., Stringlis, I. A., Kruijs, S., Bakker, P. A. H. M., & Pieterse, C. M. J. (2017). Iron and Immunity. *Annual Review of Phytopathology*, *55*(1), 355–375. https://doi.org/10.1146/annurev-phyto-080516-035537

Wang, M.-Y., Xia, R.-X., Hu, L.-M., Dong, T., & Wu, Q.-S. (2007). Arbuscular mycorrhizal fungi alleviate iron deficient chlorosis in *Poncirus trifoliata* L. Raf under calcium bicarbonate stress. *The Journal of Horticultural Science and Biotechnology*, *82*(5), 776–780. https://doi.org/10.1080/14620316.2007.11512304

Zamboni, A., Zanin, L., Tomasi, N., Pezzotti, M., Pinton, R., Varanini, Z., & Cesco, S. (2012). Genome-wide microarray analysis of tomato roots showed defined responses to iron deficiency. *BMC Genomics*, *13*(1), 101. https://doi.org/10.1186/1471-2164-13-101

Supplementary Table 1. Oligonucleotides used in this study. Overhangs are underlined.

Primer	Sequence (5'-3')	Application
SlRAM1.q1	CATCAAACTGCTTCCAGAGGACT	Real Time PCR (Ho-Plágaro et al., 2021)
SlRAM1.q2	GGATTTCAACATCATCATCGTCG	Real Time PCR (Ho-Plágaro et al., 2021)
SlEXO84.q1	CGGCTAAGATCTCAATTCTG	Real Time PCR (Ho-Plágaro et al., 2021)
SlEXO84.q2	ATAAGAGTGTCATCAGCATG	Real Time PCR (Ho-Plágaro et al., 2021)
SlAMT22.q1	CTCAGAATGTCAGAGGAAGAT	Real Time PCR (Ho-Plágaro et al., 2021)
SlAMT22.q2	CCAGCAGCAGTATCAGAA	Real Time PCR (Ho-Plágaro et al., 2021)
SlPT4.q1	GAAGGGGAGCCATTTAATGTGG	Real Time PCR (Nagy et al., 2005)
SlPT4.q2	CCATCTTGTGTGTATTGTTGTATC	Real Time PCR (Nagy et al., 2005)
qRiEF1αF	GCTATTTTGATCATTGCCGCC	Real Time PCR
qRiEF1αR	TCATTAAAACGTTCTTCCGACC	Real Time PCR
qSlFRO1.f.2	TTCTGGATTGGTGTTGTGGA	Real Time PCR (Martínez-Medina et al., 2017)
qSlFRO1.r.2	GCATGATGCAAGCGTAAGAA	Real Time PCR (Martínez-Medina et al., 2017)
qSlIRT1.f.2	CCACGGGCGTTAATAACTGT	Real Time PCR (Zamboni et al., 2012)
qSlIRT1.r.2	CACCCATAAAATCAGCAGCA	Real Time PCR (Zamboni et al., 2012)
qSlNRAMP1.F	TGGGACCACACAAGAACTCA	Real Time PCR
qSlNRAMP1.R	TATCAGCCAACCCACGAAAG	Real Time PCR
qSlNRAMP3.F	TGCTGTCAGTGGGATGTTGT	Real Time PCR
qSlNRAMP3.R	AATTCCCCGTGAAATGAGGT	Real Time PCR
qSiCHLN.F	GCGTTAGTTGGTATGGACAAAGA	Real Time PCR
qSiCHLN.R	TCCCGAGGATCTAGGACAGG	Real Time PCR
qSlVIT1.F	GCTTTGAGGAAGAACCGACA	Real Time PCR
qSlVIT1.R	GAGGAACAAATCCTCCCAAGA	Real Time PCR
qSlVIT2F	AGCAAGGTGAAGTCCCTCAT	Real Time PCR
qSlVIT2R	AGGTGTGAAAGAGTTGGACTGTA	Real Time PCR
qSlVTL1F	GGCAGAAGTCCAATGGTGAAA	Real Time PCR
qSlVTL1R	CCATGCCAGTACTAGAGCCAATT	Real Time PCR
qSlVTL2F	ACGTTGATGCCATGATCCTAATC	Real Time PCR
qSlVTL2R	GTCCCTCCTTGTCTTCTTCTTCT	Real Time PCR
SlEF-1F	GATTGGTGGTATTGGAACTGTC	Real Time PCR
SlEF-1R	AGCTTCGTGGTGCATCTC	Real Time PCR
SlVIT1GW5	AAAGCAGGCTTC ATGGCTGGTGAATCGGAGCA	Cloning SlVIT1
SlVIT1GW3	GAAAGCTGGGTC CTAGCCTTGAACAGCCTTGG	Cloning SlVIT1
SlVIT2TF	CACCATGGATTCTCCCAAATCAAC	Cloning SlVIT2
SlVIT2TR	CTAATCATCATAATCTCTCTTTGAA	Cloning SlVIT2
SlVTL1TF	CACCATGGCTGCTCAAAACCAAGTC	Cloning SlVTL1
SlVTL1TR	TCACAACTCCATGCCAGTAC	Cloning SlVTL1
SlVTL2TF	CACCATGGCTGCTGAAAACCATGTTC	Cloning SlVTL2
SlVTL2TR	TCACATCTCCATTCCAGCAG	Cloning SlVTL2

Supplementary Table 2. SlVIT/VTL protein accession numbers founds in the genome *S. lycopersicum*.

Protein	**ID**
SlVIT1	Solyc04g008060.3.1
SlVIT2	Solyc02g068260.1
SlVTL1	Solyc01g104810.2
SlVTL2	Solyc01g104820.2

CHAPTER 4:

Physiological and transcriptomic responses of the tomato mutant *chloronerva* affected in the regulation of iron metabolism to arbuscular mycorrhiza

Adapted from López-Lorca V.M., Ferrol N.

Physiological and transcriptomic responses of the tomato mutant *chloronerva* affected in the regulation of iron metabolism to arbuscular mycorrhiza.

To be submitted to "Frontiers in Plant Science"

Abstract

Arbuscular mycorrhiza (AM) is a widespread symbiosis in nature whose establishment and function is influenced by environmental factors. Mineral nutrients are known to influence AM. In this work, we investigated the importance of Fe homeostasis in the *Rhizophagus irregularis-Solanum lycopersicum* interaction by using the iron inefficient mutant *chloronerva* (*chln*) of tomato. AM development is impaired in a the *chln* mutant, but partially reverts its growth defect. RNA sequencing revealed a low number of differentially expressed genes in the "*chln* vs wild-type" comparison in mycorrhizal than in non-inoculated roots. Gene Ontology and Kyoto Encyclopedia of Genes and Genomes pathways enrichment analysis revealed differential metabolic responses to AM colonization between roots of wild-type and *chln* mutant plants. Expression of a subset of genes that have been previously shown to be required for AM was lower in mycorrhizal roots of *chln* mutants compared to the wild-type. The lower expression levels of the Pi starvation-induced genes in non-mycorrhizal *chln* roots compared to wild-type and the higher P concentration of the *chln* plants suggests that reduced AM colonization of *chln* may involve Pi signalling pathways. Over-expression of Fe-deficiency response genes in *chln* roots was mitigated by AM colonization, which suggests that root AM colonization contributes to increase Fe availability and distribution in the *chln* mutants. All these data together indicate that there exists a connection between AM and Fe homeostasis.

Introduction

Arbuscular mycorrhiza (AM) is one of the most ancient and widespread symbioses in nature (Lanfranco et al., 2016). The main advantage of the AM symbiosis is the exchange of nutrients: the plant provides up to 20% of the photosynthetically fixed organic carbon to the AM fungus (Roth & Paszkowski, 2017), whereas the AM fungus transfers mineral nutrients to the plant thanks to its efficiency in exploring and acquiring these resources from the soil (Smith et al., 2011). The predominant nutrient acquired through AM is phosphorus. However, AM fungi can also transfer to their host plants other central macronutrients, such as nitrogen and sulphur, and several micronutrients, such as zinc, copper and iron. In addition, plants colonized by AMF often show higher tolerance to biotic and abiotic stresses (Ferrol et al., 2016; Quiroga et al., 2017; Rivero et al., 2021).

This mutualistic interaction is established in successive steps. Host derived signal molecules, strigolactones (SLs), are exudated into the rhizosphere to attract AM fungi (Akiyama et al., 2005; Besserer et al., 2008). SLs positively regulate formation of hyphopodia on the host root epidermis (Kobae et al., 2018). Afterwards, AM fungal hyphae enter the root and grow into the root cortex, where the fungus penetrates single cells and develops highly branched hyphal structures, the

arbuscules (Lanfranco et al., 2018). Arbuscules are surrounded by a plant derived periarbuscular membrane, which, together with the arbuscule membrane, forms an extensive interface for nutrient exchange (Luginbuehl & Oldroyd, 2017). Establishment and functioning of the symbiosis require fundamental genetic reprogramming of root cells. Many of the players required for accommodation of AM fungi inside roots and for long-term symbiotic compatibility and nutrient exchange have been identified (Genre et al., 2005; Genre & Bonfante, 1998; Guether et al., 2009; Güimil et al., 2005; Pumplin & Harrison, 2009; Rich et al., 2017; Siciliano et al., 2007). Besides these endogenous factors, environmental factors affect AM formation and functioning. In particular, mineral nutrients are known to impact AM. In general, low nutrient levels promote symbiosis, whereas high nutrient levels are inhibitory (Smith & Read, 2008). Accumulating evidence indicates that the exchanged nutrients not only function as nourishment, but also act as signals that can drastically influence AM development. Therefore, AM development is strongly linked to symbiotic function (Lanfranco et al., 2018).

Phosphate has long been known to negatively impact AM (Balzergue et al., 2011; Branscheid et al., 2010; Essahibi et al., 2019; Shi et al., 2021). Inhibition of AM development by Pi is a systemic effect that depends on the nutritional status of the shoot. The major transcriptional regulator of phosphate starvation response PHR2 regulates AM by targeting genes required for pre-contact signalling, root colonization and AM function (Das et al., 2022). However, repression of AM colonization by high Pi is relieved when nitrogen becomes limiting probably to enable symbiotic nitrogen uptake (Nouri et al., 2014). When a fungal or plant Pi transporter gene essential for symbiosis are silenced arbuscule development is affected (Javot et al., 2007; Xie et al., 2016). However, this accelerated arbuscule degradation is suppressed when the plant is grown under nitrogen starvation conditions (Javot et al., 2011). These observations led to the hypothesis that fungus-delivered nutrients can act as cell-autonomous signals in the regulation of arbuscule maintenance. Therefore, nutrient-dependent regulation of AM colonization provides an important feedback mechanism for plants to promote or limit fungal colonization according to their needs.

In Chapter 3 we have shown that iron (Fe) deficiency inhibits *R. irregularis* colonization of tomato roots suggesting that this micronutrient regulates AM. Fe is an essential micronutrient for all living organisms, including plants and their associated microbes. As an indispensable co-factor of many enzymes, Fe is involved in various crucial metabolic processes that are required for the survival of plants and their associated microbes. Conversely, excessive Fe produces highly active reactive oxygen species, which are toxic to the cells of plants and microbes (Verbon et al., 2017). Therefore, plants and microorganisms have evolved sophisticated mechanisms to

modulate iron status at a moderate level for maintaining their fitness. In Arabidopsis, Fe starvation limits infection by necrotrophic, hemi-biotrophic and biotrophic pathogens (Liu et al., 2021). Fe deficiency-induced resistance is not simply caused by making Fe scarce to the pathogen, but is a plant-mediated defence response that requires the activity of ethylene and salicylic acid signalling (Trapet et al., 2021). On the other hand, Fe, due to its ability to generate reactive oxygen species, may also be used to kill the invader or execute cell death to prevent pathogen progression.

While plants have developed strategies to withdraw Fe from pathogens, they must provide it to symbionts and endophytes. For example, rhizobia in root nodules of legumes is a major sink for Fe as a cofactor of nitrogenase and many other enzymes required for nitrogen fixation (Brear et al., 2020). Fe uptake by the endophyte *Epichloe festucae* is also necessary to maintain its mutualistic interaction with *Lolium perenne* (Johnson et al., 2013). This chapter was aimed at elucidating the importance of Fe homeostasis in the *Rhizophagus irregularis-Solanum lycopersicum* interaction by using the iron inefficient mutant *chloronerva* (*chln*) of tomato. The *chln* mutant has a mutation in the *SlCHLN* gene encoding nicotinamine (NA) synthase, which is required to make the non-protein amino acid NA in the plant (Bienfait, 1988; Scholz et al., 1992). NA is required to complex ferrous iron in a soluble and available form within the cells and for its distribution in plants (Takahashi et al., 2003). In the *chln* mutant, the iron-deficiency response and uptake are constitutively stimulated and seedlings exhibit typical symptoms of iron deficiency with severe interveinal chlorosis (Ling et al., 1996).

Materials and Methods

Biological materials and growth conditions

Seeds of the tomato *chln* mutant and its wild type (*S. lycopersicum* cv. Bonnerbest) were provided by Dr. Petra Bauer. Surface-sterilized seeds were germinated on wet filter papers in petri plates under sterile conditions in darkness for 4 days at 25°C. Germinated seeds were placed in pots containing 1.6 L of a soil/sand mixture (1/10, v/v). Soil and sand were tindalized and autoclaved, respectively, before use. Half of the seedlings were inoculated with 1650 spores of *Rhizophagus irregularis* DAOM 197189 grown in monoxenic cultures. Tomato plants were grown at 24°C/20°C day/night and 16 h light photoperiod for 8 weeks in a grow chamber. Plants were fertilized twice a week with a modified half-strength (0.5X) Hoagland nutrient solution with 0.0625 mM KH_2PO_4 to promote mycorrhizal colonization. At harvesting, the root system of each plant was rinsed with distilled water and shoots and roots were cut and kept separated. An

aliquot of each root system was kept to estimate mycorrhizal colonization, the rest and the shoots were frozen in liquid N and stored at -80°C until used.

Mycorrhizal colonization

Mycorrhizal colonization was estimated in root samples stained with trypan blue (0.05 %) (Phillips & Hayman, 1970), using the Trouvelot method. The abundance of the fungus in the roots was also estimated molecularly by determining the expression of the *R. irregularis* elongation factor 1α (*RiEF1α*). Expression of the tomato phosphate transporter *SlPT4* mediating symbiotic Pi uptake was analysed as an indicator of AM functionality together with the periarbuscular membrane-localized transporter *SlAMT2.2* involved in phosphate and ammonium transfer and the regulatory genes *SlRAM1* and *SlEXO84* were estimated by real-time RT-qPCR.

RNA extraction and sequencing

Total RNA was extracted from tomato roots of all treatments (WTNM, WTMyc, *chln*NM and *chln*Myc) using RNeasy Plant Mini Kit (Qiagen), following the instructions of the manufacturer. RNAs were extracted from three independent pools of two plants of each treatment. DNAse digestion was perform during RNA purification using RNase-Free DNAse Set (Qiagen) following manufacturer protocol. RNA quantity and quality were determined with a Nanodrop spectrophotometer and sent to Novogene´s Transcriptome Sequencing services. To prepare cDNA libraries, messenger RNA was purified from total RNA by using poly-T oligo-attached magnetic beads. After the RNA had been fragmented, the first strand cDNA was synthesized. This was done by using random hexamer primers. Once the first strand had been completed, the second strand cDNA was synthesized. The library was checked with Qubit and quantified by real-time PCR. The Illumina Novaseq platform was used for sequencing, which employs a paired-end 150 bp sequencing strategy (short-reads).

The first step in processing the data was to remove adapter sequences, reads containing ploy-N, and low-quality reads from the raw data (raw reads) through in-house perl scripts. Resulting clean reads were used for all the downstream analyses. High quality reads were aligned to the reference genome of *S. lycopersicum* SL3.0.gca.000188115.3 assembly using HISAT2 v2.0.5. AM fungal genes expressed in colonized roots were detected by mapping the clean reads from WTMyc and *chln*Myc data to the *R. irregularis* genome rir_gca_000597685_1.

Counts v1.5.0-p3 was used to calculate the reads numbers mapped to each gene. Then, based on the length of the gene and reads count mapped to this gene, FPKM (Fragments Per Kilobase of transcript sequence per Millions) of each gene was calculated. A gene was only included in the downstream analysis if its FPKM value was greater than 0. A preliminary batch comparison of

replicates was performed using a multiple correlation test (Pearson's correlation) on FPKM values. Differentially expressed gene (DEG) between two treatments were identified with the DESeq2 R package (1.20.0). The p-values that resulted were adjusted using the Benjamini & Hochberg (1995) approach for controlling the false discovery rate. Genes with an adjusted p-value ≤ 0.05 and a log2foldchange ≥ 1 were considered to be differentially expressed. The groups compared were *chln*NM vs. WTtNM, WTMyc vs. WTNM, *chln*Myc vs. *chln*NM and *chln*Myc vs. WTMyc. To detect functional categories of biological processes (BP), molecular function (MF) and cellular component overrepresented, the set of DEG were analysed for Gene Ontology (GO) enrichment using the clusterProfiler R package. GO terms with an adjusted p-value ≤ 0.05 were considered to be significantly enriched with DEG. Enrichment analysis of Kyoto Encyclopedia of Genes and Genomes (KEGG) was also performed to annotates genes to pathway level.

cDNA synthesis and RT-qPCR

1µg of total DNAse-treated RNA was used to synthetize cDNA in a 20 µL reaction using Super-Script IV Reverse Transcriptase (Invitrogen). Gene expression data was analysed by real-time RT-PCR, using a QuantStudio 3 (Thermofisher) in the synthetized cDNAs. Each 12 µL reaction contained 1 µL of a 1:10 dilution of cDNA, 0.25 µL each primer and 6 µL iTaq (Bio-Rad). The real time RT-PCR program consisted of an initial incubation at 95°C for 30 s, followed by 40 cycles of 95°C for 15 s, 60°C for 30 s and 72°C for 30 s, where the fluorescence signal was measured, and a final step with a heat-dissociation protocol to check the specificity of the PCR-amplification procedure. The specificity and efficiency of the different primer pairs (Supplementary Table 1) were asses by PCR amplification of tomato cDNA and through a real-time RT-PCR on several dilutions of cDNA respectively. Expression of *SlEF1α* was used to standardized the results obtained. Real-time RT-PCR determinations were carried out on at least three independent biological samples. Real-time RT-PCR reactions were performed at least two times for each biological sample, with the threshold cycle (Ct) determined in duplicate. Relative expression level was calculated using the $2^{-\Delta CT}$ method (Schmittgen & Livak, 2008) and the standard error was computed from the average of the ΔCt values for each biological sample.

Determination of Fe and P concentrations

Aliquots of shoot and root samples from each plant were dried at 65ºC for two days and ground to fine powder. The resulting powder was analysed for nutrient concentration using Inductively Coupled Plasma Optical Emission Spectroscopy (ICP-OES; ICP 6500 Duo Thermo) using the technical service of the Estación Experimental del Zaidín, EEZ-CSIC from Granada, Spain.

Statistical analyses

The statistical analyses were performed using Statgraphics Centurion XVI software. Data were subjected to a two-way ANOVA, considering mycorrhization and genotype as factors. Post-hoc comparisons were evaluated using the Duncan's test to find out differences among groups of means ($P < 0.05$), when necessary. All analyses are based on at least three biological replicates per each treatment ($n \geq 3$).

Results

Mycorrhizal colonization is impaired in the chln mutant

To assess the impact of Fe on AM colonization, plants of the Fe deficient tomato *chln* mutant and its wild-type cv. Bonner Beste were inoculated with the AM fungus *R. irregularis*. Assessment of mycorrhizal colonization 8 weeks after inoculation revealed significant changes in the AM colonization patterns between wild-type and the *chln* mutants. Intensity of colonization (M) and arbuscules abundance (A) were significantly reduced in *chln* plants (Figure 1a,b). These data agree with the lower expression of the *R. irregularis* elongation factor 1α gene in roots of the *chln* plants (Figure 1c). The impact of the *chln* mutation on AM functionality was also assessed by determining transcript levels of the *SlPT4* gene encoding a Pi transporter mediating symbiotic Pi uptake in tomato roots. Down-regulation of *SlPT4* and the AM marker genes *SlEXO84*, *SlRAM1* and *SlAMT2.2* was detected in roots of the mutant plants (Figure 1c).

The growth defect of the *chln* mutant plants was partially recovered by AM fungal colonization (Figure 2).

Sequencing data and transcriptome mapping

To understand the underlying molecular bases of the lower AM colonization levels of the Fe-inefficient *chln* mutant, transcriptome root profiles of wild-type and *chln* mutant plants inoculated and non-inoculated with *R. irregularis* were analysed by RNAseq. Illumina RNA-sequencing yielded a total of 1.36 billion high-quality reads for all treatments, representing > 98 % of the total reads obtained. Good-quality reads where mapped onto the reference genome with HISAT2. About 83-93% of good reads where mapped onto the *S. lycopersicum* genome (SL3.0.gca.000188115.3 assembly ITAG3.2) across all samples. Out of the 35,092 predicted genes in the reference genome, from 22,990 (WTMyc3) up to 24,176 (WTNM2) genes were mapped, using a cut off value of FPKM > 0 to consider a gene expressed (Table 1). The Pearson's correlation coefficient (r) between FPKM values of each sample replicates sequenced set was > 0.95 in all cases (Table 2).

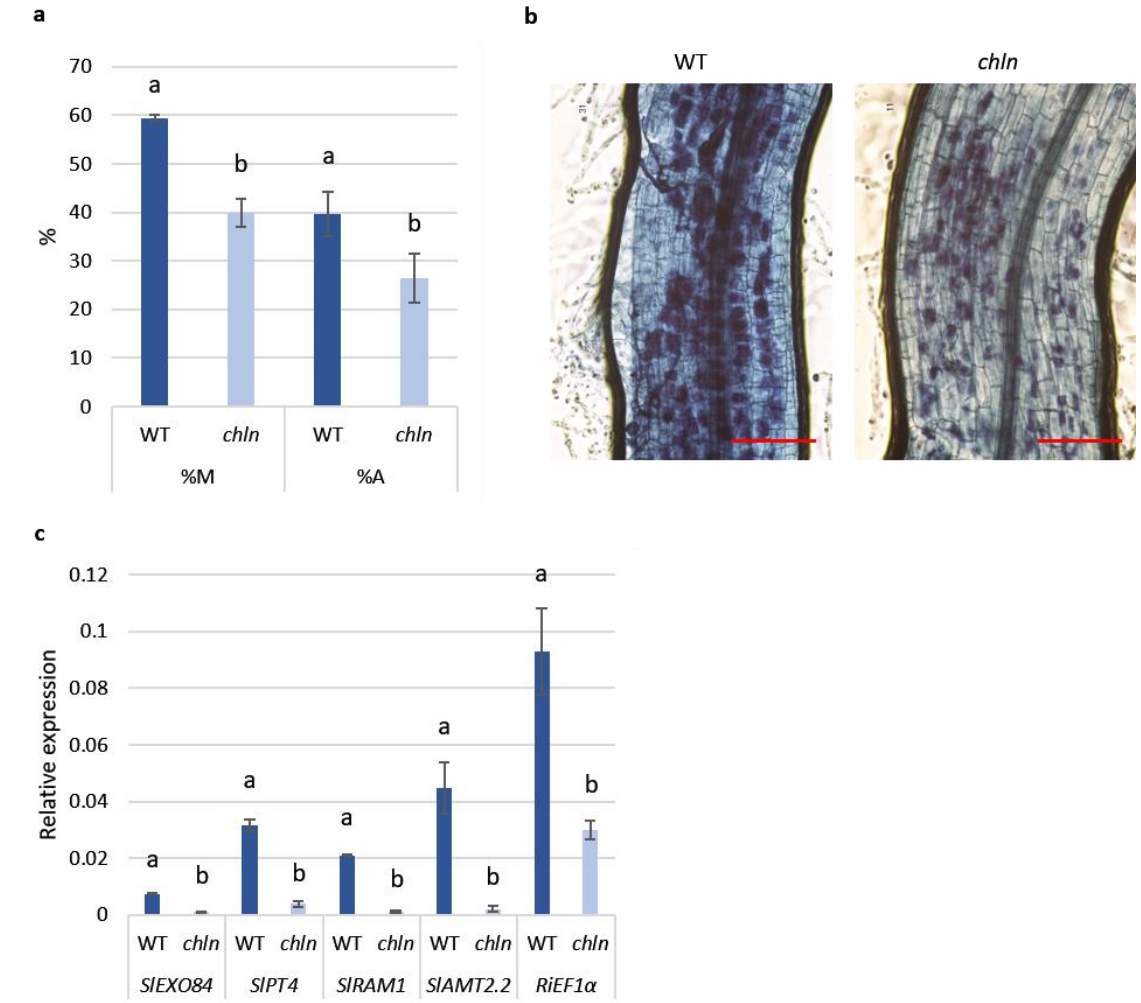

Figure 1. Efect of the *chln* mutation on AM colonization. (**a**,**b**) Mycorrhizal colonization of wild-type and chln mutant plants was estimated in root samples stained with trypan blue using the Trouvelot method. M%, intensity of the mycorrhizal colonization in the root system; A%, arbuscule abundance in the root system. Scale bar: 100 μm(**c**) Expression of the AM marker genes *SlEXO84*, *SlRAM1*, *SlAMT2.2*, *SlPT4* and *RiEF1α* in wild-type and *chln* tomato roots colonized with *R. irregularis*. Relative expression levels were calculated, using the $2^{-\Delta CT}$ method with *SlEF1α* as normalizer. Bars represent standard error. Different letters indicate significant differences ($p < 0.05$, n = 10).

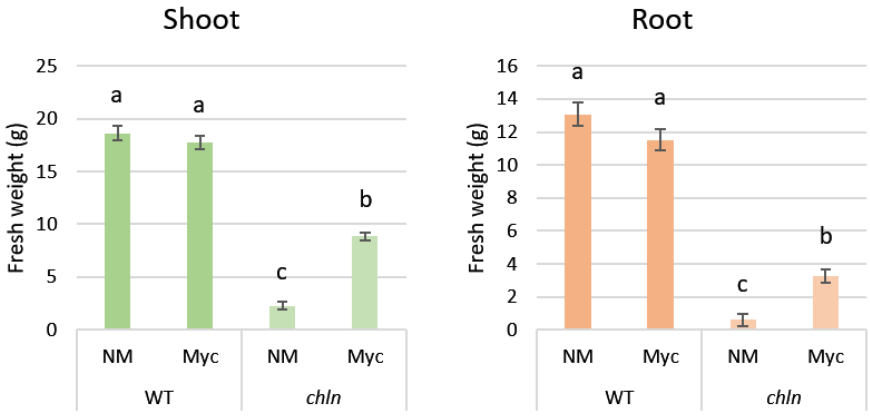

Figure 2. Shoot and root fresh weight of wild-type and chln mutant plants inoculated (Myc) and non-inoculated (NM) with the AM fungis *R. irregularis*. Different letters indicate significant differences ($p < 0.05$, n = 10).

Table 1. Statistic of reads obtained and reads mapped onto the tomato reference genome.

Sample	Total reads	Cleaned reads	Total clean bp (G)	Total mapped reads	Percentage of reads mapped	Expressed transcripts (FPKM > 0)
WTNM1	110.794 M	109.374 M	16.41G	102.087 M	93.34%	24,124
WTNM2	142.967 M	141.102 M	21.17G	132.446 M	93.87%	24,176
WTNM3	106.859 M	105.375 M	15.81G	94.877 M	90.04%	23,830
WTMyc1	111.000 M	109.640 M	16.45G	93.590 M	85.36%	23,827
WTMyc2	112.714 M	111.360 M	16.7G	97.246 M	87.33%	23,966
WTMyc3	103.977 M	102.486 M	15.37G	91.365 M	89.15%	22,990
***chln*NM1**	118.331 M	116.747 M	17.51G	106.682M	91.38%	23,258
***chln*NM2**	128.047 M	126.369 M	18.96G	114.814 M	90.86%	23,710
***chln*NM3**	108.626 M	107.401 M	16.11G	92.972 M	86.57%	23,019
***chln*Myc1**	126.094 M	124.666 M	18.7G	106.113 M	85.12%	23,538
***chln*Myc2**	106.212 M	104.810 M	15.72G	87.530 M	83.51%	23,417
***chln*Myc3**	105.302 M	103.998 M	15.6G	88.662 M	85.25%	23,508

Table 2. Pearson's correlation coefficient (r) between FPKM values of each sample replicates sequenced.

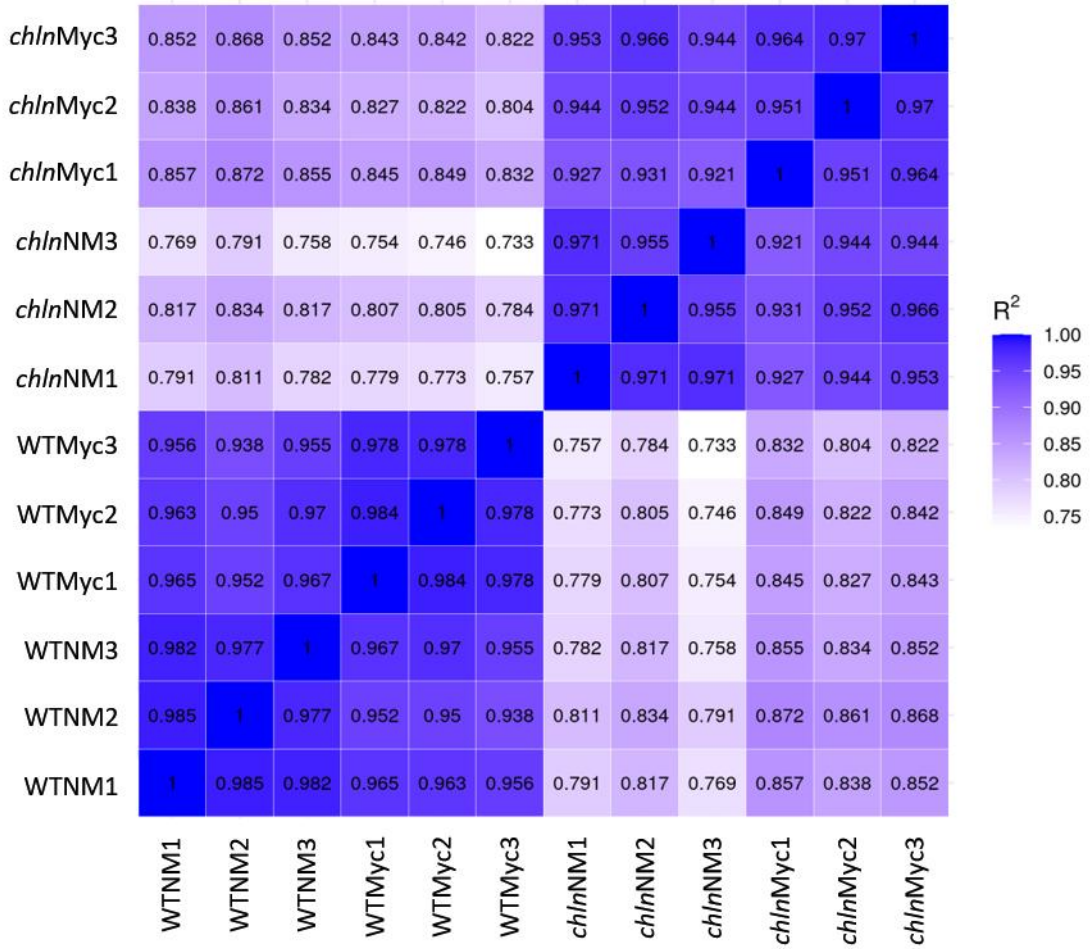

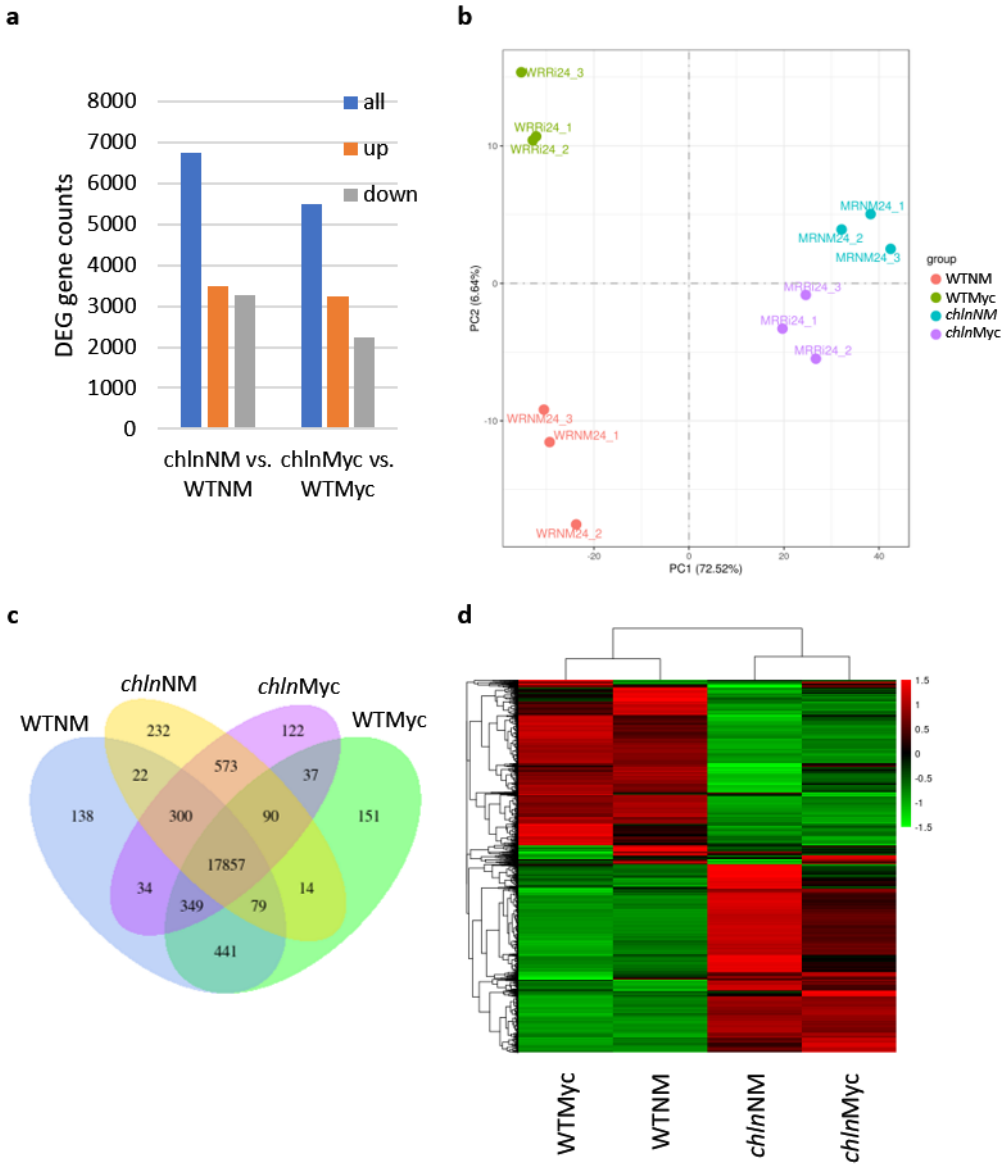

Figure 3. (**a**) Number of total up- and down-regulated differentially expresses genes (DEGs) in *chln* vs WT for non-inoculated (NM) and *R. irregularis*-inoculated (Myc) plants. (**b**) PCA plot for the transcriptome of the indicated samples. (**c**) Venn diagram showing the intersection of DEGs in the chln *vs* WT comparison for non-inoculated (NM) and *R. irregularis*-inoculated (Myc) samples of total DEGs comparing every treatment. (**d**) Heriarchical clustering of combined DEGs from non-inoculated (NM) and *R. irregularis*-inoculated (Myc) roots using normalized counts. Grading colour ranging from red to green correspond with the FPKM values.

Differential gene expression and enrichment analysis in tomato roots

To analyse differences in gene expression under our experimental conditions, the following treatments were compared "WTMyc vs WTNM", "*chln*Myc vs *chln*NM", "*chln*NM vs WTNM" and "*chln*Myc vs WTMyc". The differentially expressed genes (DEGs) (log2foldchange ≥ 1, padj ≤ 0.05) arose from 2.2% in the mycorrhizal plants WTMyc and *chln*Myc respect to their non-colonized controls (WTNM and *chln*NM, respectively) to 19.2% in the "*chln*NM vs. WTNM"

comparison of the total protein coding genes predicted in the SL3.0.gca.000188115.3 genome. A lower number of genes differed in expression in "*chln* vs WT" in AM compared to non-inoculated roots (Figure 3a). The drastic transcriptome modulation upon AM indicated by principal component analysis in the wild-type was clearly reduced for *chln* (Figure 3b). Significant changes in gene expression profiles of mycorrhizal wild-type and Fe-inefficient *chln* mutants were detected (Figure 3b,c,d).

The DEGs of the different comparisons were subjected to GO analysis to assign functional terms to the identified DEGs (Figure 4). The GO analysis of DEGs derived from the "WTMyc vs WTNM" comparison indicated that within "biological process" the terms "anion transport", "response to drug", "response to reactive oxygen species" and "response to hydrogen peroxide" were enriched. However, in the "*chln*Myc *vs chln*NM" comparison, the terms "defence response", "drug catabolic processes", "response to oxidative stress" and "response to inorganic substance" were most significantly enriched. In the cellular component category, the GO terms "extracellular region", "cell wall" and "external encapsulating structure" were highly enriched in response to AM in both the wild-type and *chln* mutant plants. In the molecular function category, the highly enriched genes in wild-type roots are implicated in "inorganic molecular entity transmembrane transporter", protein self-association" and "enzyme inhibitor activity". However, the terms "tetrapyrrole binding", "heme binding", "iron ion binding" and "oxidoreductase activity" were enriched in roots of *chln* plants. GO analysis of DEGs induced by the *chln* mutation in non-colonized roots showed that the terms related to "ribosome" were enriched in all the categories. In the molecular function category, the terms "inorganic molecular entity activity" and "tetrapyrrole binding" were also highly enriched. In the "*chln*Myc vs WTMyc" comparison, the GO terms "ion transmembrane" and "cell cycle" were enriched in the biological process category, the terms "extracellular region" and "ribosome" were more significantly enriched in the cell compartment category and the GO terms "tetrapyrrole binding", "heme binding" and "structural molecule activity" were more significantly enriched in the "molecular function" category (Figure 4).

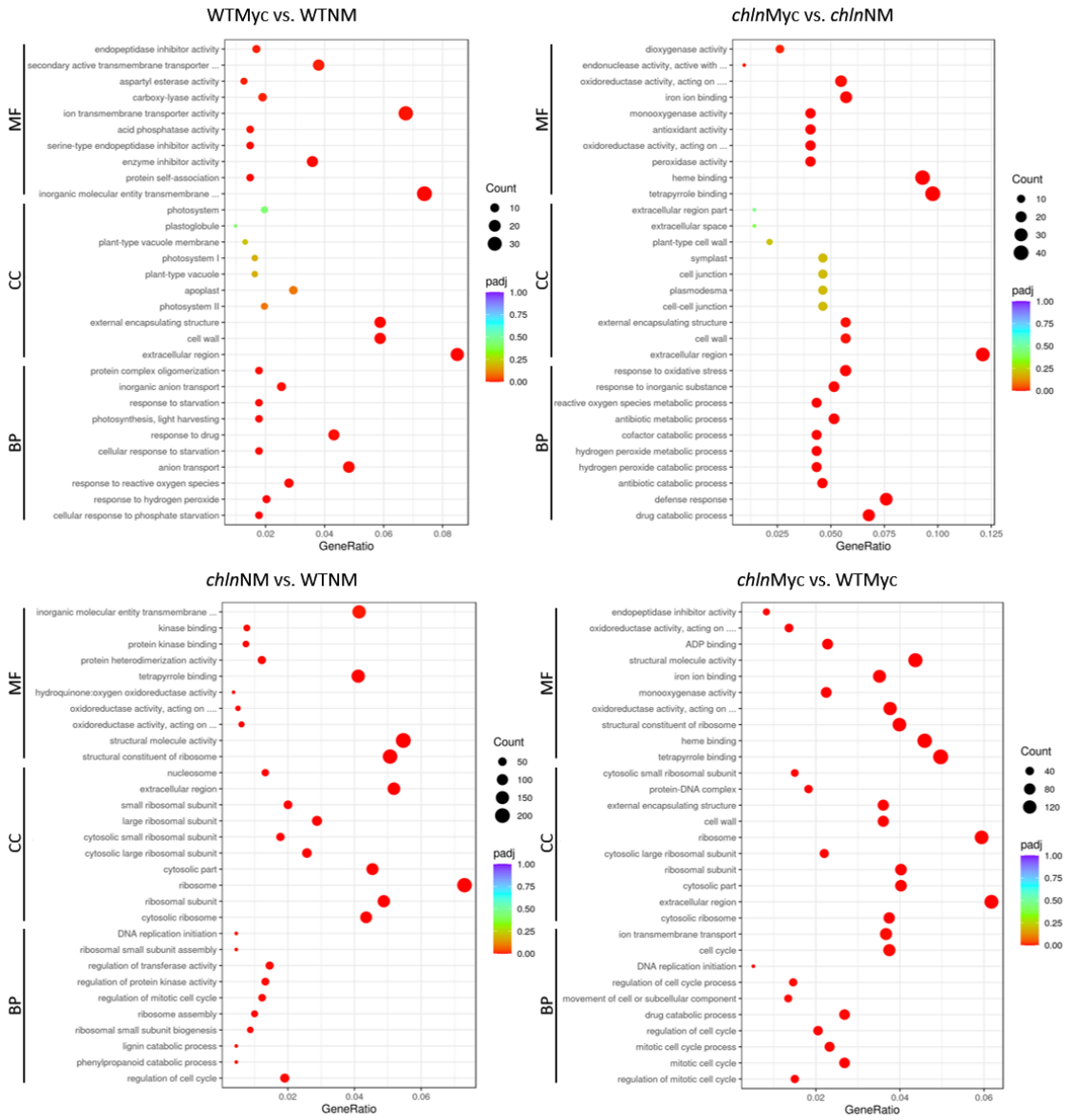

Figure 4. GO enrichment analysis of DEGs derived from the WTMyc *vs* WTNM, *chln*Myc vs *chln*NM, *chln* vs WTNM and *chln*Myc vs WTMyc comparisons. Circle size is proportional to the number of genes regulated in each GO term and circle colour, ranging from blue to red, the adjusted p-value. BP, Biological Processes; CC, Cellular Component; MF, Molecular Function.

Enrichment analysis of KEGG pathways showed that genes involved in carbon metabolism and protein processing in endoplasmic reticulum were most significantly represented in WT roots in response to AM colonization. However, genes involved in phenylpropanoid biosynthesis, MAPK signalling pathway and plant hormone signal transduction were the most highly enriched in roots of the *chln* mutant plants. Analysis of KEGG pathways in the "*chln* vs WT "comparison indicated that genes involved in "ribosome", carotenoid biosynthesis" and "phenylpropanoid biosynthesis" were the most significantly represented in roots of the *chln* mutant. Genes involved in "ribosome" and "phenylpropanoid biosynthesis" were also enriched

in the mycorrhizal roots of the *chln* mutants compared with the mycorrhizal roots of the wild-type (Figure 5).

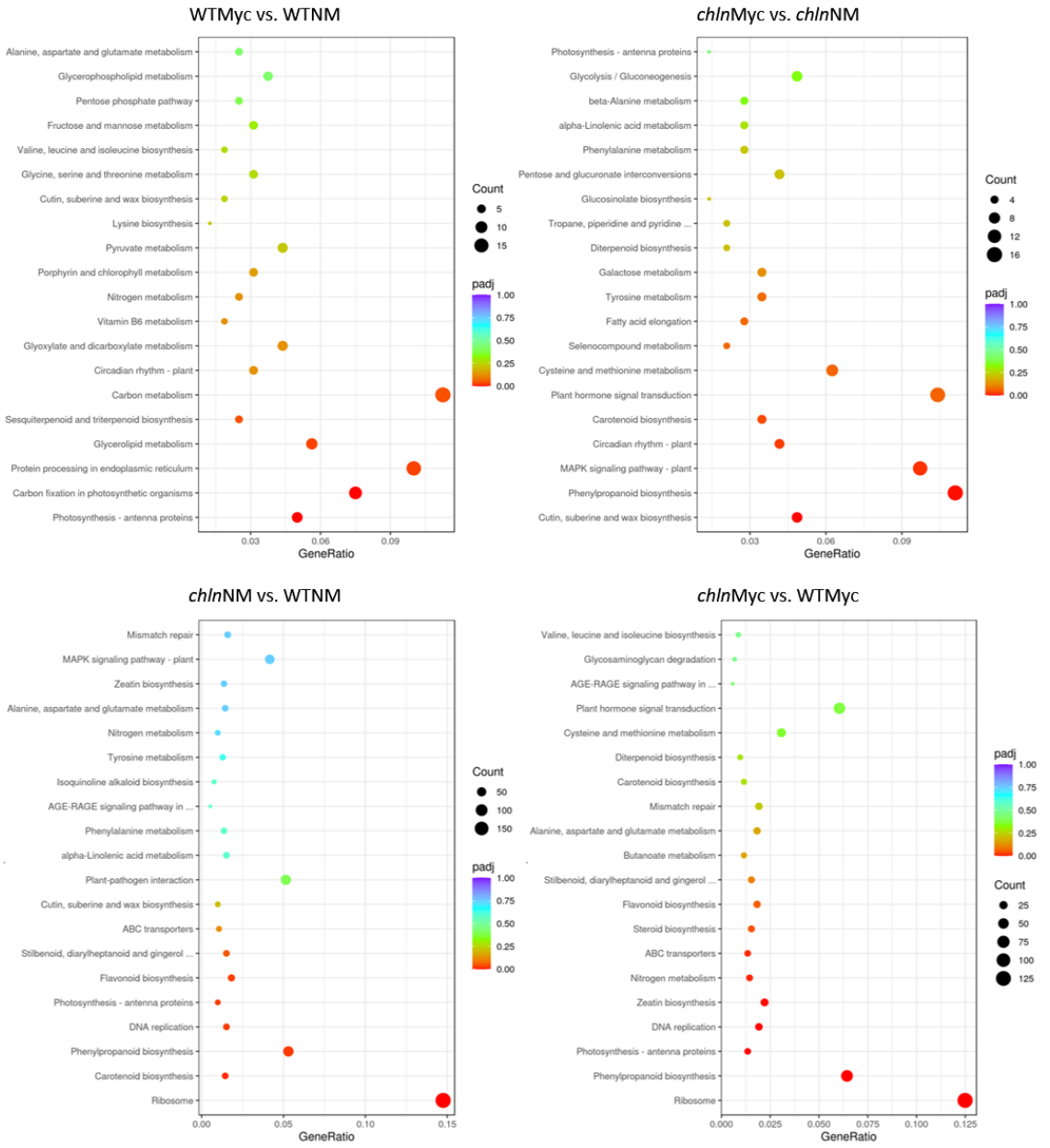

Figure 5. KEGG pathway enrichment analysis of DEGs derived from the WTMyc vs WTNM, *chln*Myc vs *chln*NM, *chln* vs WTNM and *chln*Myc vs WTMyc comparisons. Circle size is proportional to the number of genes regulated in each pathway and circle colour, ranging from blue to red, the adjusted p-value.

Identification of AM-related genes

To deeper explore this novel dataset, the expression profiles of genes described in the literature as specifically involved in AM symbiosis have been searched. These include genes involved in the biosynthesis of strigolactones for activation of the fungus prior to contact (*SlCCD8*), common symbiosis genes involved in signal transduction and regulation of

colonization (*SlSYMRK*, *SlCCaMK* (DMI3), *SlCYCLOPS* (IPD3)), AM-specific signalling and regulatory genes (*SlRAM1*, *SlRAM2*, *SlEXO84*, *SlEXO70i*) and genes encoding periarbuscular membrane-localized transporters involved in nutrient exchange between symbionts (*SlSTR*, *SlPT4* and *SlAMT2.2*). In agreement with the observed lower colonization levels of the *chln* roots, expression of all AM-related genes was lower in mycorrhizal roots of *chln* mutants compared to the wild-type (Figure 6).

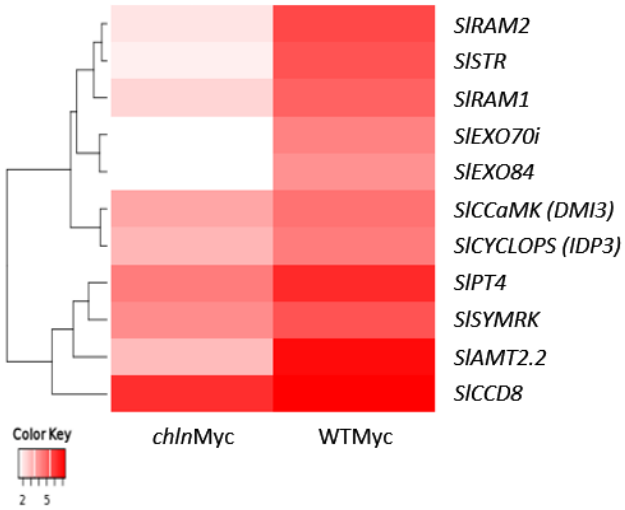

Figure 6. Expression profile of a subset of AM-related genes in chln and wild-type roots colonized by *R. irregularis*. Gradient color, ranging from red to bright red, corresponds to expression values in FPKM based on transcript accumulation in RNAseq of mycorrhizal *chln* and WT roots.

Identification of gene homologs associated with the Fe-deficiency response in tomato

To assess the impact of *chln* mutation and AM on Fe homeostasis, the expression levels of a panel of genes homologues to Fe-deficiency responsive genes in *Arabidopsis* was analysed (Chen et al., 2022). These homologues include genes encoding transcription factors, transporters, coumarin biosynthesis, Fe storage and other Fe-related genes, such as *SlFRO1* and *SlCHLN* (Figure 7). The transcription factors *SlbHLH067*, *SlbHLH068* and *SlFER*, which regulate the Fe-deficiency response and are required for up-regulation of Fe uptake genes, are highly expressed in roots of non-mycorrhizal *chln* mutant plants compared to WT. Accordingly, expression of the Fe uptake genes *SlFRO1*, *SlIRT1*, *SlIRT2* and *SlNRAMP1* was highly increased in these roots. The transcription factor *SlMYB10* regulating coumarin biosynthesis and secretion, the genes *SlCYP82C4-2* and *SlBGLU42* involved in the biosynthesis of coumarins and the ABC transporter *SlABCG37* mediating coumarin secretion were up-regulated in non-mycorrhizal *chln* roots compared to wild-type. Expression of the genes encoding the *SlNRAMP3* and *SlNRAMP4* transporters involved in Fe mobilization and was also up-regulated in the roots of the mutants. However, *SlFER1* and *SlFER3* encoding the Fe storage protein ferritin were detected to be down-

regulated. These data agree with previous reports that, despite displaying typical symptoms of Fe deficiency, the iron-deficiency response and uptake are constitutively stimulated in the *chln* mutant plants. However, expression of members of the vacuolar Fe transporter family were differentially expressed in roots of the *chln* mutants.

Transcription factors

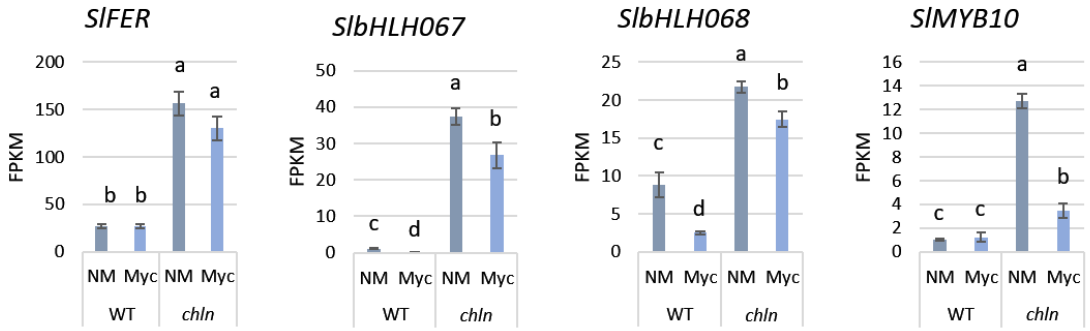

Transporters: Uptake

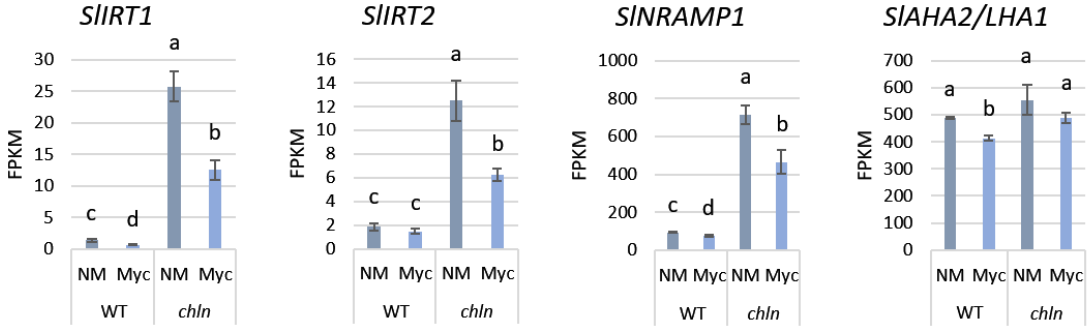

Transporters: Mobilization

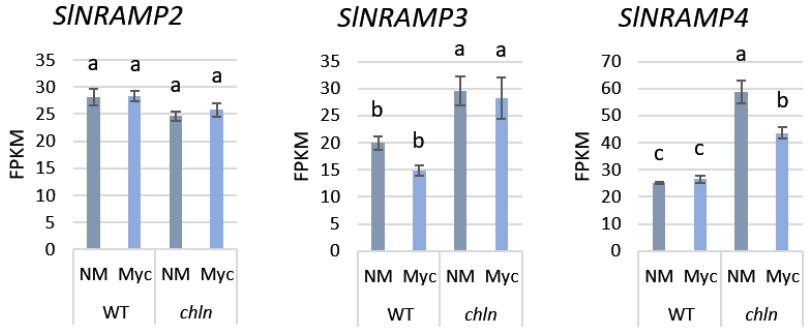

Transporters: Compartmentalization

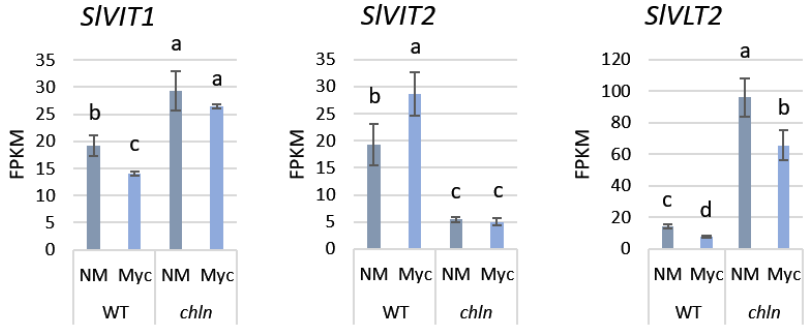

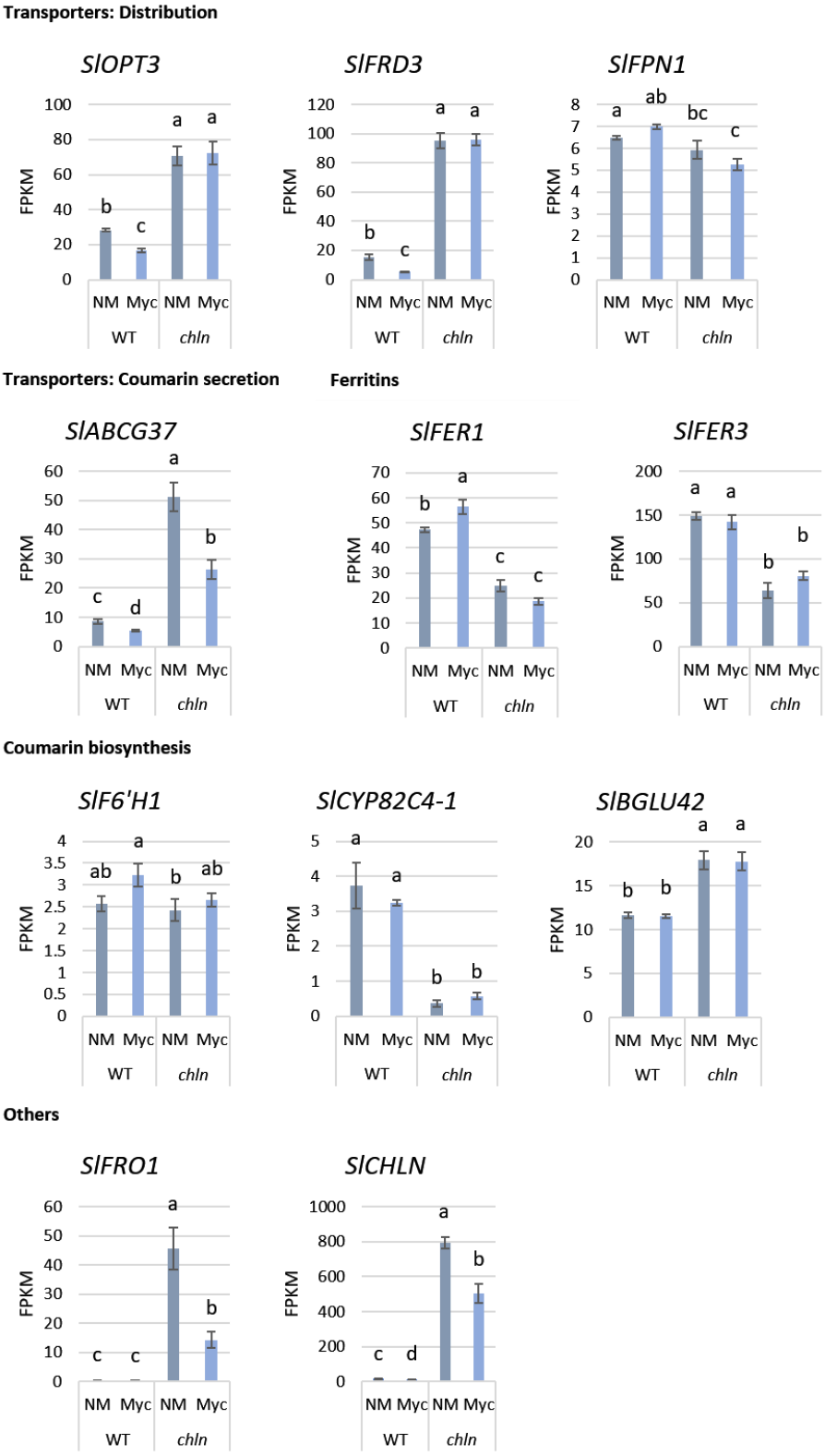

Figure 7. Effect of the *chln* mutation and AM colonization on Fe-deficiency responsive genes expression. RNAseq-based transcript accumulation in non-mycorrhizal (NM) and mycorrhizal (Myc) roots of chln and WT plants. Bars represent standard error. Different letters indicate significant differences ($p < 0.05$, n = 3).

SlCHLN, encoding the NA synthase, was the most highly expressed gene in roots of the mutant plants. However, these plants lack the ability to synthesise NA because a point mutation in its coding sequence renders a non-functional NA synthase (Ling et al., 1999). Transcript levels of the gene encoding the oligopeptide transporter *SlOPT3* involved in Fe distribution was also up-regulated in non-colonized roots of *chln* plants compared to wild-type.

In roots of wild-type plants, development of the symbiosis significantly up-regulates *SlIRT1*, *SlNRAMP1*, and *SlVIT2* expression, but down-regulates *SlAHA2*, *SlABCG37*, *SlOPT3*, *SlFRD3*, *SlVIT1*, *SlVLT2*, *SlCYP82C4-2* and *SlCHLN*. This expression pattern is similar to the one described in Chapter 3 in the tomato cv. Moneymaker, but different to the detected in the mutant. In the *chln* roots AM colonization significantly down-regulates the transcription factors *SlbHLH67*, *SlbHLH068*, the Fe uptake-related genes *SlFRO1*, *SlIRT1*, *SlIRT2* and *SlNRAMP1*, genes involved in biosynthesis and secretion of coumarins (*SlMYB10*, *SlCYP82C4-2* and *SlABCG37*), the NRAMP transporter *SlNRAMP4*, the vacuolar transporter *SlVLT2* and *SlCHLN*. However, no significant differences were observed between the expression patterns of genes encoding ferritins, the vacuolar iron transporters *SlVIT1* and *SlVIT2* and the ferroportin Fe efflux protein *SlFPN1* in non-mycorrhizal and mycorrhizal roots of the *chln* plants. These data suggest that development of the symbiosis reduces the Fe-deficiency response of the mutants.

The finding that AM colonization of the *chln* mutants partially reverted its retarded growth and Fe-deficiency response led us to assess if colonization affected Fe accumulation in the *chln* mutant plants. In agreement with previous observations that the *chln* mutant over-accumulates Fe, although in a non-soluble and unavailable form, shoot and root Fe concentration of the *chln* plants was significantly higher than in the wild-type plants. However, the effect of AM was different on Fe accumulation patterns. While root to shoot translocation decreases in WT plants, a higher root to shoot translocation was observed in the *chln* mutants. Total Fe uptake was lower in mycorrhizal than in non-mycorrhizal *chln* mutant plants (Figure 8).

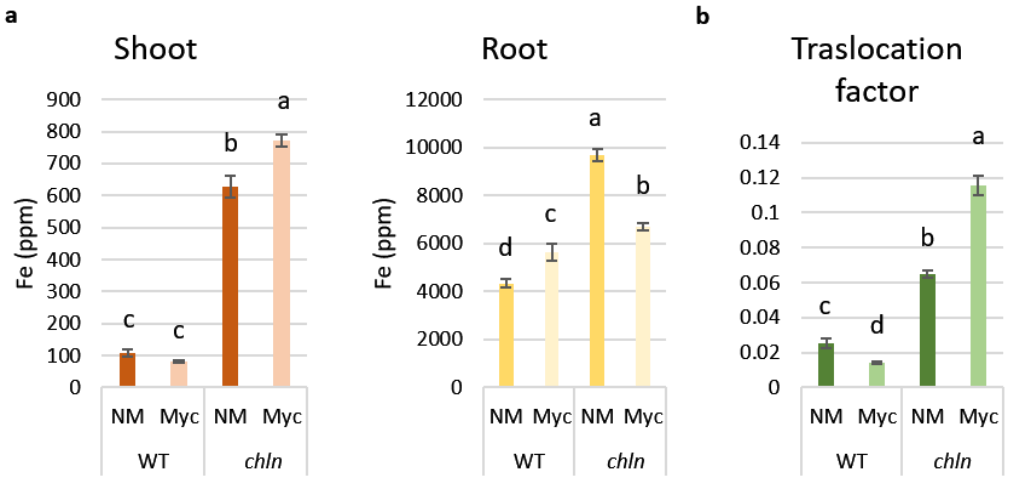

Figure 8. Shoot Fe concentration (a), root Fe concentration (b) and Fe translocation factor (c) of non-mycorrhizal (NM) and *R. irregularis*-colonized (Myc) chln and wild-type (WT) plants. Bars represent standard error. Different letters indicate significant differences ($p < 0.05$, n = 3).

Phosphate starvation response genes are down-regulated in chln roots

Taking into account that Fe availability affects P homeostasis and that P availability is one of the major factors regulating AM, expression of a subset of genes involved in the phosphate starvation response and P content of *chln* and wild-type plants were determined to further understand the reduced AM colonization of the *chln* roots. In non-mycorrhizal plants, shoot and root P concentrations were higher in *chln* mutants than in wild-type (Figure 9). Expression of genes encoding SPX domain containing proteins, Pi transporters and the tomato phosphate starvation response transcription factor SlPHL1 were analysed. *SlPHL1* expression was similar in roots of all treatments. In non-colonized roots, the six SPX domain containing proteins identified were down-regulated in *chln* mutant plants respect to wild-type. Expression of the SPX domain-containing proteins SlSPX3, SlPHT5-like and SlSPX2 was up-regulated in mycorrhizal roots of *chln* mutant plants. The four P uptake transporters identified were down-regulated in non-mycorrhizal roots of *chln* mutant plants compared to wild-type. Expression of the *SlPT4* transporter (Solyc06g051860) was up-regulated in mycorrhizal roots of *chln* mutants. In wild-type roots, expression of the phosphate starvation response was in general down-regulated in AM roots (Figure 10).

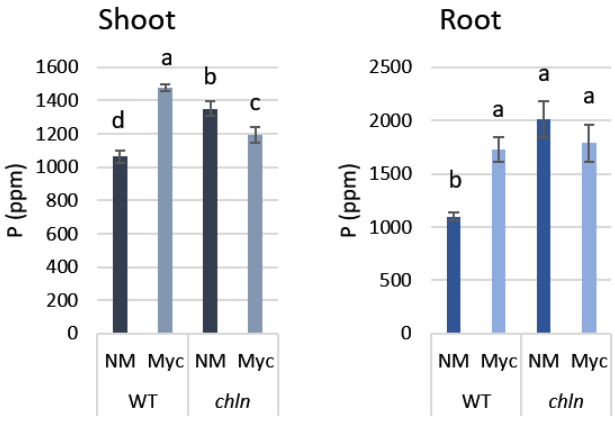

Figure 9. Shoot and root P concentration of non-mycorrhizal (NM) and *R. irregularis*-colonized (Myc) chln and wild-type (WT) plants. Bars represent standard error. Different letters indicate significant differences ($p < 0.05$, n = 3).

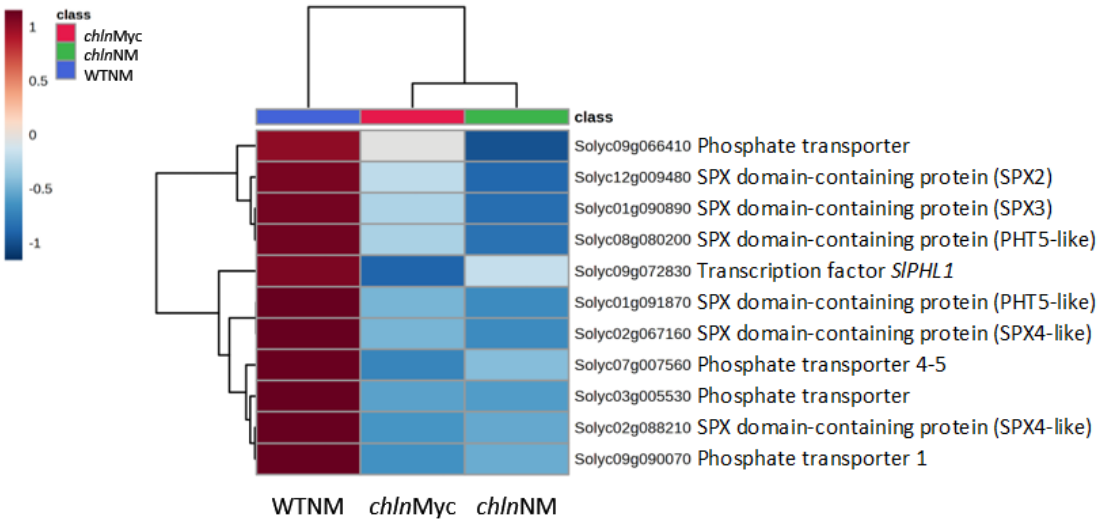

Figure 10. Effect of *chln* mutation and AM colonization on expression of a subset of tomato phosphate starvation responsive genes. Heatmap showing expression patterns of phosphate starvation response genes based on their transcript accumulation in the RNAseqs of non-mycorrhizal wild-type roots andnon-mycorhizal and mycorrhizal roots of chln mutant plants. Grading colour, ranging from red to blue, corresponds to FPKM values.

Discussion

The evolutionary and ecological success of the AM symbiosis relies on an efficient and multifactorial communication system for partner recognition and on a fine tuned and reciprocal metabolic regulation of each symbiont to reach an optimal integration. During the last years, tremendous progress has been made in understanding how the AM is established and regulated (Choi et al., 2018; Feng et al., 2019; Ho-Plágaro & García-Garrido, 2022; Kaur & Suseela, 2020; Liao et al., 2018). Exogenous nutrients have been shown to influence the interaction of the root systems with AM fungi (Carbonnel & Gutjahr, 2014). It is widely recognized that AM symbiosis is

particularly sensitive to Pi, the central nutrient provided by AM fungi (Nouri et al., 2014). Here, we show that AM development is impaired in a tomato Fe-inefficient mutant and that the AM fungus *R. irregularis* partially reverts the growth defect of the mutant.

Our comparative transcriptomics revealed significant changes in gene expression profiles of mycorrhizal wild-type and Fe-inefficient *chln* mutants. A set of known AM symbiosis-related genes, *SlCCD8*, *SlSYMRK*, *SlCaMK* (DMI3), *SlCYCLOPS* (IPD3), *SlRAM1*, *SlRAM2*, *SlEXO84*, *SlEXO70i*, *SlSTR*, *SlPT4* and *SlAMT2.2*, were transcriptionally promoted upon AM fungal colonization both in wild-type and *chln* roots, although to a lower extent in the mutant. These data are consistent with the lower colonization level of these roots and demonstrate that Fe is an important regulator of AM. Moreover, most AM-related genes showed reduced expression in *chln* even in the absence of the fungus (data not shown). This suggests that Fe conditions the root for AM symbiosis and that the lower cumulative expression of AM-relevant genes impairs AM in *chln* mutants. This expression pattern is similar to the described for the *phr2* mutant of rice lacking the major transcriptional regulator of phosphate starvation responses PHR2 (Das et al., 2022). PHR2 was shown to support AM development at low phosphate because it promotes the expression of a number of genes required for AM development and function already in the absence of AM fungi.

The lower expression levels of the Pi starvation-induced genes in non-mycorrhizal *chln* roots compared to wild-type together with the higher P concentration of the *chln* plants prompted us to hypothesize that the reduced AM colonization of *chln* and, therefore, the inhibitory effect of Fe deficiency on AM colonization may involve Pi signalling pathways. Despite expression of the Pi-starvation genes analysed varied between treatments, expression of *SlPHL1*, the tomato orthologue of rice OsPHR2 (Zhang et al., 2021), was similar in all samples. This is consistent with previous observations that PHR gene expression is not particularly Pi responsive and its transcript levels do not change in different Pi regimes (Rubio et al., 2001).

The antagonistic relationship between Pi and Fe has been described in various plant species (Bouain et al., 2019; Briat et al., 2015; Müller et al., 2007; Thibaud et al., 2010). For example, Fe-deficiency produces an over accumulation of Pi in apple plants (Valentinuzzi et al., 2019) and higher concentrations of Fe have been observed in Pi-deficient plants (Zheng et al., 2009). The transcription factors PHR1 and PHL1 have been shown to act as integrators of Pi and Fe homeostasis interactions in plants (Briat et al., 2015). Together all these data suggest that the PHR/PHL transcription factors may act as a regulator of the Pi-Fe-AM interaction. Further experiments are needed to confirm this hypothesis.

Our comparative transcriptomic analysis also revealed that the Fe-deficiency related genes are more highly expressed in roots of non-colonized *chln* plants. This is consistent with previous observations that the iron-deficiency response and uptake are constitutively stimulated the *chln* mutant (Ling et al., 1996). Increased transcript levels of transcription factor MYB10 regulating coumarin biosynthesis and secretion and of its target genes *CYP82C4-2, BGLU42* and *ABCG37* indicates that under Fe limitation, tomato secretes coumarins to improve Fe mobilization and solubilisation. This non-canonical Fe uptake pathway has been described so far in the model plant *Arabidopsis* (Fourcroy et al., 2014; Schmid et al., 2014). Coumarins mobilize Fe by chelation and the chelated Fe (III) can be reduced by FRO2 to release Fe(II), which is then taken up by IRT1 (Fourcroy et al., 2016). Therefore, tomato roots use both the Strategy I and coumarin secretion pathways for Fe uptake under Fe-limiting conditions. Up-regulation of the Fe uptake gene in non-mycorrhizal *chln* roots is consistent with their higher total Fe content relative to the wild-type. However, the *chln* plants display symptoms of Fe deficiency since, as detected by X ray microanalysis, this Fe is accumulated in an insoluble form preventing the mobility of Fe in the phloem transport stream, leading to an insufficient Fe delivery to growing apical meristems (Becker et al., 1989, 1995).

Reduced transcript levels of *SlFRO1*, *SlITR1*, *SlIRT2*, *SlNRAMP1*, *SlMYB10, SlCYP82C4-2* and *SlABCG37* upon AM colonization of *chln* plants indicates that the fungus contributes to mitigate the Fe-deficiency response of *chln* and concords with the lower Fe uptake of the mycorrhizal *chln* mutants compared to the non-mycorrhizal plants. Down-regulation of *SlCHLN* in *chln* roots suggests that the fungus contributes to increase Fe availability and distribution of the host plant. Given that the plant hormones ethylene and auxin (indolacetic acid) activate the Fe acquisition genes under Fe limitation (Bacaicoa et al., 2011; Lucena et al., 2006), that AM symbiosis alters plant hormonal homeostasis (Ludwig-Müller, 2010) and that ethylene and auxins regulate AM establishment and functionality (Etemadi et al., 2014; Foo, 2013; Foo et al., 2016; Hanlon & Coenen, 2011; Torres de Los Santos et al., 2011; Torres de los Santos et al., 2016), regulation of Fe deficiency responses in the *chln* mutant relative to wild-type and upon AM colonization might be dependent on hormonal balance modifications resulting from signal perception and transduction. This is supported by the enrichment of the "plant hormone signal transduction" pathway in mycorrhizal roots of the *chln* plants compared both to the mycorrhizal roots of the wild-type and to the non-inoculated *chln* roots. A deeper exploration of the RNAseq dataset obtained in this study is required to assess the regulatory role of phytohormones and their interaction with other regulatory processes in the phenotypic responses of the *chln* mutant.

In conclusion, this study highlights the connection of AM and Fe homeostasis, showing a reduced mycorrhizal colonization of an Fe-inefficient mutant and delicate gene regulation for plant growth optimization during AM symbiosis of the *chln* mutant.

References

Akiyama, K., Matsuzaki, K., & Hayashi, H. (2005). Plant sesquiterpenes induce hyphal branching in arbuscular mycorrhizal fungi. *Nature*, *435*(7043), 824–827. https://doi.org/10.1038/nature03608

Bacaicoa, E., Mora, V., Zamarreño, Á. M., Fuentes, M., Casanova, E., & García-Mina, J. M. (2011). Auxin: A major player in the shoot-to-root regulation of root Fe-stress physiological responses to Fe deficiency in cucumber plants. *Plant Physiology and Biochemistry*, *49*(5), 545–556. https://doi.org/10.1016/j.plaphy.2011.02.018

Balzergue, C., Puech-Pagès, V., Bécard, G., & Rochange, S. F. (2011). The regulation of arbuscular mycorrhizal symbiosis by phosphate in pea involves early and systemic signalling events. *Journal of Experimental Botany*, *62*(3), 1049–1060. https://doi.org/10.1093/jxb/erq335

Becker, R., Fritz, E., & Manteuffel, R. (1995). Subcellular Localization and Characterization of Excessive Iron in the Nicotianamine-less Tomato Mutant chloronerva. *Plant Physiology*, *108*(1), 269–275. https://doi.org/10.1104/pp.108.1.269

Becker, R., Pich, A., Scholz, G., & Seifert, K. (1989). Influence of nicotianamine and iron supply on formation and elongation of adventitious roots in hypocotyl cuttings of the tomato mutant "chloronerva" (Lycopersicon esculentum). *Physiologia Plantarum*, *76*(1), 47–52. https://doi.org/10.1111/j.1399-3054.1989.tb05451.x

Benjamini, Y., & Hochberg, Y. (1995). Controlling the False Discovery Rate: A Practical and Powerful Approach to Multiple Testing. *Journal of the Royal Statistical Society: Series B (Methodological)*, *57*(1), 289–300. https://doi.org/10.1111/j.2517-6161.1995.tb02031.x

Besserer, A., Bécard, G., Jauneau, A., Roux, C., & Séjalon-Delmas, N. (2008). GR24, a Synthetic Analog of Strigolactones, Stimulates the Mitosis and Growth of the Arbuscular Mycorrhizal Fungus *Gigaspora rosea* by Boosting Its Energy Metabolism . *Plant Physiology*, *148*(1), 402–413. https://doi.org/10.1104/pp.108.121400

Bienfait, H. F. (1988). Mechanisms in Fe-efficiency reactions of higher plants. *Journal of Plant Nutrition*, *11*(6–11), 605–629. https://doi.org/10.1080/01904168809363828

Bouain, N., Krouk, G., Lacombe, B., & Rouached, H. (2019). Getting to the Root of Plant Mineral Nutrition: Combinatorial Nutrient Stresses Reveal Emergent Properties. *Trends in Plant Science*, *24*(6), 542–552. https://doi.org/10.1016/j.tplants.2019.03.008

Branscheid, A., Sieh, D., Pant, B. D., May, P., Devers, E. A., Elkrog, A., Schauser, L., Scheible, W.-R., & Krajinski, F. (2010). Expression Pattern Suggests a Role of MiR399 in the Regulation of the Cellular Response to Local Pi Increase During Arbuscular Mycorrhizal Symbiosis. *Molecular Plant-Microbe Interactions®*, *23*(7), 915–926. https://doi.org/10.1094/MPMI-23-7-0915

Brear, E. M., Bedon, F., Gavrin, A., Kryvoruchko, I. S., Torres-Jerez, I., Udvardi, M. K., Day, D. A., & Smith, P. M. C. (2020). GmVTL1a is an iron transporter on the symbiosome membrane of soybean with an important role in nitrogen fixation. *New Phytologist*, *228*(2), 667–681. https://doi.org/10.1111/nph.16734

Briat, J.-F., Rouached, H., Tissot, N., Gaymard, F., & Dubos, C. (2015). Integration of P, S, Fe, and Zn nutrition signals in Arabidopsis thaliana: potential involvement of PHOSPHATE STARVATION RESPONSE 1 (PHR1). *Frontiers in Plant Science*, *06*(APR), 290. https://doi.org/10.3389/fpls.2015.00290

Carbonnel, S., & Gutjahr, C. (2014). Control of arbuscular mycorrhiza development by nutrient signals. *Frontiers in Plant Science*, *5*(SEP). https://doi.org/10.3389/fpls.2014.00462

Chen, W. W., Zhu, H. H., Wang, J. Y., Han, G. H., Huang, R. N., Hong, Y. G., & Yang, J. L. (2022). Comparative Physiological and Transcriptomic Analyses Reveal Altered Fe-Deficiency Responses in Tomato Epimutant Colorless Non-ripening. *Frontiers in Plant Science*, *12*. https://doi.org/10.3389/fpls.2021.796893

Choi, J., Summers, W., & Paszkowski, U. (2018). Mechanisms Underlying Establishment of Arbuscular Mycorrhizal Symbioses. *Annual Review of Phytopathology*, *56*(1), 135–160. https://doi.org/10.1146/annurev-phyto-080516-035521

Das, D., Paries, M., Hobecker, K., Gigl, M., Dawid, C., Lam, H.-M., Zhang, J., Chen, M., & Gutjahr, C. (2022). PHOSPHATE STARVATION RESPONSE transcription factors enable arbuscular mycorrhiza symbiosis. *Nature Communications*, *13*(1), 477. https://doi.org/10.1038/s41467-022-27976-8

Essahibi, A., Benhiba, L., Fouad, M. O., Babram, M. A., Ghoulam, C., & Qaddoury, A. (2019). Responsiveness of Carob (Ceratonia siliqua L.) Plants to Arbuscular Mycorrhizal Symbiosis Under Different Phosphate Fertilization Levels. *Journal of Plant Growth Regulation*, *38*(4), 1243–1254. https://doi.org/10.1007/s00344-019-09929-6

Etemadi, M., Gutjahr, C., Couzigou, J.-M., Zouine, M., Lauressergues, D., Timmers, A., Audran, C., Bouzayen, M., Bécard, G., & Combier, J.-P. (2014). Auxin Perception Is Required for Arbuscule Development in Arbuscular Mycorrhizal Symbiosis . *Plant Physiology*, *166*(1), 281–292. https://doi.org/10.1104/pp.114.246595

Feng, F., Sun, J., Radhakrishnan, G. v., Lee, T., Bozsóki, Z., Fort, S., Gavrin, A., Gysel, K., Thygesen, M. B., Andersen, K. R., Radutoiu, S., Stougaard, J., & Oldroyd, G. E. D. (2019). A combination of chitooligosaccharide and lipochitooligosaccharide recognition promotes arbuscular mycorrhizal associations in Medicago truncatula. *Nature Communications*, *10*(1), 5047. https://doi.org/10.1038/s41467-019-12999-5

Ferrol, N., Tamayo, E., & Vargas, P. (2016). The heavy metal paradox in arbuscular mycorrhizas: from mechanisms to biotechnological applications. *Journal of Experimental Botany*, *67*(22), 6253–6265. https://doi.org/10.1093/jxb/erw403

Foo, E. (2013). Auxin influences strigolactones in pea mycorrhizal symbiosis. *Journal of Plant Physiology*, *170*(5), 523–528. https://doi.org/10.1016/j.jplph.2012.11.002

Foo, E., McAdam, E. L., Weller, J. L., & Reid, J. B. (2016). Interactions between ethylene, gibberellins, and brassinosteroids in the development of rhizobial and mycorrhizal symbioses of pea. *Journal of Experimental Botany*, *67*(8), 2413–2424. https://doi.org/10.1093/jxb/erw047

Fourcroy, P., Sisó-Terraza, P., Sudre, D., Savirón, M., Reyt, G., Gaymard, F., Abadía, A., Abadia, J., Álvarez-Fernández, A., & Briat, J. (2014). Involvement of the <scp>ABCG</scp> 37 transporter in secretion of scopoletin and derivatives by *Arabidopsis* roots in response to iron deficiency. *New Phytologist*, *201*(1), 155–167. https://doi.org/10.1111/nph.12471

Fourcroy, P., Tissot, N., Gaymard, F., Briat, J.-F., & Dubos, C. (2016). Facilitated Fe Nutrition by Phenolic Compounds Excreted by the Arabidopsis ABCG37/PDR9 Transporter Requires the IRT1/FRO2 High-Affinity Root Fe 2+ Transport System. *Molecular Plant*, *9*(3), 485–488. https://doi.org/10.1016/j.molp.2015.09.010

Genre, A., & Bonfante, P. (1998). Actin versus tubulin configuration in arbuscule-containing cells from mycorrhizal tobacco roots. *New Phytologist*, *140*(4), 745–752. https://doi.org/10.1046/j.1469-8137.1998.00314.x

Genre, A., Chabaud, M., Timmers, T., Bonfante, P., & Barker, D. G. (2005). Arbuscular Mycorrhizal Fungi Elicit a Novel Intracellular Apparatus in *Medicago truncatula* Root Epidermal Cells before Infection[W]. *The Plant Cell*, *17*(12), 3489–3499. https://doi.org/10.1105/tpc.105.035410

Guether, M., Balestrini, R., Hannah, M., He, J., Udvardi, M. K., & Bonfante, P. (2009). Genome-wide reprogramming of regulatory networks, transport, cell wall and membrane biogenesis during arbuscular mycorrhizal symbiosis in *Lotus japonicus*. *New Phytologist*, *182*(1), 200–212. https://doi.org/10.1111/j.1469-8137.2008.02725.x

Güimil, S., Chang, H.-S., Zhu, T., Sesma, A., Osbourn, A., Roux, C., Ioannidis, V., Oakeley, E. J., Docquier, M., Descombes, P., Briggs, S. P., & Paszkowski, U. (2005). Comparative transcriptomics of rice reveals an ancient pattern of response to microbial colonization. *Proceedings of the National Academy of Sciences*, *102*(22), 8066–8070. https://doi.org/10.1073/pnas.0502999102

Hanlon, M. T., & Coenen, C. (2011). Genetic evidence for auxin involvement in arbuscular mycorrhiza initiation. *New Phytologist*, *189*(3), 701–709. https://doi.org/10.1111/j.1469-8137.2010.03567.x

Ho-Plágaro, T., & García-Garrido, J. M. (2022). Molecular Regulation of Arbuscular Mycorrhizal Symbiosis. *International Journal of Molecular Sciences*, *23*(11), 5960. https://doi.org/10.3390/ijms23115960

Ho-Plágaro, T., Morcillo, R. J. L., Tamayo-Navarrete, M. I., Huertas, R., Molinero-Rosales, N., López-Ráez, J. A., Macho, A. P., & García-Garrido, J. M. (2021). DLK2 regulates arbuscule hyphal branching during arbuscular mycorrhizal symbiosis. *New Phytologist*, *229*(1), 548–562. https://doi.org/10.1111/nph.16938

Javot, H., Penmetsa, R. V., Breuillin, F., Bhattarai, K. K., Noar, R. D., Gomez, S. K., Zhang, Q., Cook, D. R., & Harrison, M. J. (2011). Medicago truncatula mtpt4 mutants reveal a role for nitrogen in the regulation of arbuscule degeneration in arbuscular mycorrhizal symbiosis. *The Plant Journal*, *68*(6), 954–965. https://doi.org/10.1111/j.1365-313X.2011.04746.x

Javot, H., Penmetsa, R. V., Terzaghi, N., Cook, D. R., & Harrison, M. J. (2007). A *Medicago truncatula* phosphate transporter indispensable for the arbuscular mycorrhizal symbiosis. *Proceedings of the National Academy of Sciences*, *104*(5), 1720–1725. https://doi.org/10.1073/pnas.0608136104

Johnson, L. J., Koulman, A., Christensen, M., Lane, G. A., Fraser, K., Forester, N., Johnson, R. D., Bryan, G. T., & Rasmussen, S. (2013). An Extracellular Siderophore Is Required to Maintain the Mutualistic Interaction of Epichloë festucae with Lolium perenne. *PLoS Pathogens*, *9*(5), e1003332. https://doi.org/10.1371/journal.ppat.1003332

Kaur, S., & Suseela, V. (2020). Unraveling Arbuscular Mycorrhiza-Induced Changes in Plant Primary and Secondary Metabolome. *Metabolites*, *10*(8), 335. https://doi.org/10.3390/metabo10080335

Kobae, Y., Kameoka, H., Sugimura, Y., Saito, K., Ohtomo, R., Fujiwara, T., & Kyozuka, J. (2018). Strigolactone Biosynthesis Genes of Rice are Required for the Punctual Entry of Arbuscular Mycorrhizal Fungi into the Roots. *Plant and Cell Physiology*, *59*(3), 544–553. https://doi.org/10.1093/pcp/pcy001

Lanfranco, L., Bonfante, P., & Genre, A. (2016). The Mutualistic Interaction between Plants and Arbuscular Mycorrhizal Fungi. *Microbiology Spectrum*, *4*(6). https://doi.org/10.1128/microbiolspec.FUNK-0012-2016

Lanfranco, L., Fiorilli, V., & Gutjahr, C. (2018). Partner communication and role of nutrients in the arbuscular mycorrhizal symbiosis. *New Phytologist*, *220*(4), 1031–1046. https://doi.org/10.1111/nph.15230

Liao, D., Wang, S., Cui, M., Liu, J., Chen, A., & Xu, G. (2018). Phytohormones regulate the development of arbuscular mycorrhizal symbiosis. In *International Journal of Molecular Sciences* (Vol. 19, Issue 10). MDPI AG. https://doi.org/10.3390/ijms19103146

Ling, H.-Q., Koch, G., Bäumlein, H., & Ganal, M. W. (1999). Map-based cloning of *chloronerva*, a gene involved in iron uptake of higher plants encoding nicotianamine synthase. *Proceedings of the National Academy of Sciences*, *96*(12), 7098–7103. https://doi.org/10.1073/pnas.96.12.7098

Ling, H.-Q., Pich, A., Scholz, G., & Ganal, M. W. (1996). Genetic analysis of two tomato mutants affected in the regulation of iron metabolism. *Molecular and General Genetics MGG*, *252*(1–2), 87–92. https://doi.org/10.1007/BF02173208

Liu, Y., Kong, D., Wu, H.-L., & Ling, H.-Q. (2021). Iron in plant–pathogen interactions. *Journal of Experimental Botany*, *72*(6), 2114–2124. https://doi.org/10.1093/jxb/eraa516

Lucena, C., Waters, B. M., Romera, F. J., Garcia, M. J., Morales, M., Alcantara, E., & Perez-Vicente, R. (2006). Ethylene could influence ferric reductase, iron transporter, and H+-ATPase gene expression by affecting FER (or FER-like) gene activity. *Journal of Experimental Botany*, *57*(15), 4145–4154. https://doi.org/10.1093/jxb/erl189

Ludwig-Müller, J. (2010). Hormonal Responses in Host Plants Triggered by Arbuscular Mycorrhizal Fungi. In *Arbuscular Mycorrhizas: Physiology and Function* (pp. 169–190). Springer Netherlands. https://doi.org/10.1007/978-90-481-9489-6_8

Luginbuehl, L. H., & Oldroyd, G. E. D. (2017). Understanding the Arbuscule at the Heart of Endomycorrhizal Symbioses in Plants. *Current Biology*, *27*(17), R952–R963. https://doi.org/10.1016/j.cub.2017.06.042

Müller, R., Morant, M., Jarmer, H., Nilsson, L., & Nielsen, T. H. (2007). Genome-Wide Analysis of the Arabidopsis Leaf Transcriptome Reveals Interaction of Phosphate and Sugar Metabolism. *Plant Physiology*, *143*(1), 156–171. https://doi.org/10.1104/pp.106.090167

Nagy, R., Karandashov, V., Chague, V., Kalinkevich, K., Tamasloukht, M., Xu, G., Jakobsen, I., Levy, A. A., Amrhein, N., & Bucher, M. (2005). The characterization of novel mycorrhiza-specific phosphate transporters from Lycopersicon esculentum and Solanum tuberosum uncovers functional redundancy in symbiotic phosphate transport in solanaceous species. *The Plant Journal*, *42*(2), 236–250. https://doi.org/10.1111/j.1365-313X.2005.02364.x

Nouri, E., Breuillin-Sessoms, F., Feller, U., & Reinhardt, D. (2014). Phosphorus and Nitrogen Regulate Arbuscular Mycorrhizal Symbiosis in Petunia hybrida. *PLoS ONE*, *9*(3), e90841. https://doi.org/10.1371/journal.pone.0090841

Phillips, J. M., & Hayman, D. S. (1970). Improved procedures for clearing roots and staining parasitic and vesicular-arbuscular mycorrhizal fungi for rapid assessment of infection. *Transactions of the British Mycological Society*, *55*(1), 158-IN18. https://doi.org/10.1016/S0007-1536(70)80110-3

Pumplin, N., & Harrison, M. J. (2009). Live-Cell Imaging Reveals Periarbuscular Membrane Domains and Organelle Location in *Medicago truncatula* Roots during Arbuscular Mycorrhizal Symbiosis . *Plant Physiology*, *151*(2), 809–819. https://doi.org/10.1104/pp.109.141879

Quiroga, G., Erice, G., Aroca, R., Chaumont, F., & Ruiz-Lozano, J. M. (2017). Enhanced Drought Stress Tolerance by the Arbuscular Mycorrhizal Symbiosis in a Drought-Sensitive Maize Cultivar Is Related to a Broader and Differential Regulation of Host Plant Aquaporins than in a Drought-Tolerant Cultivar. *Frontiers in Plant Science*, *8*. https://doi.org/10.3389/fpls.2017.01056

Rich, M. K., Courty, P.-E., Roux, C., & Reinhardt, D. (2017). Role of the GRAS transcription factor ATA/RAM1 in the transcriptional reprogramming of arbuscular mycorrhiza in Petunia hybrida. *BMC Genomics*, *18*(1), 589. https://doi.org/10.1186/s12864-017-3988-8

Rivero, J., Lidoy, J., Llopis-Giménez, Á., Herrero, S., Flors, V., & Pozo, M. J. (2021). Mycorrhizal symbiosis primes the accumulation of antiherbivore compounds and enhances herbivore mortality in tomato. *Journal of Experimental Botany*, *72*(13), 5038–5050. https://doi.org/10.1093/jxb/erab171

Roth, R., & Paszkowski, U. (2017). Plant carbon nourishment of arbuscular mycorrhizal fungi. *Current Opinion in Plant Biology*, *39*, 50–56. https://doi.org/10.1016/j.pbi.2017.05.008

Rubio, V., Linhares, F., Solano, R., Martín, A. C., Iglesias, J., Leyva, A., & Paz-Ares, J. (2001). A conserved MYB transcription factor involved in phosphate starvation signaling both in vascular plants and in unicellular algae. *Genes & Development*, *15*(16), 2122–2133. https://doi.org/10.1101/gad.204401

Schmid, N. B., Giehl, R. F. H., Doll, S., Mock, H.-P., Strehmel, N., Scheel, D., Kong, X., Hider, R. C., & von Wiren, N. (2014). Feruloyl-CoA 6′-Hydroxylase1-Dependent Coumarins Mediate Iron Acquisition from Alkaline Substrates in Arabidopsis. *PLANT PHYSIOLOGY*, *164*(1), 160–172. https://doi.org/10.1104/pp.113.228544

Schmittgen, T. D., & Livak, K. J. (2008). Analyzing real-time PCR data by the comparative CT method. *Nature Protocols*, *3*(6), 1101–1108. https://doi.org/10.1038/nprot.2008.73

Scholz, G., Becker, R., Pich, A., & Stephan, U. W. (1992). Nicotianamine - a common constituent of strategies I and II of iron acquisition by plants: A review. *Journal of Plant Nutrition*, *15*(10), 1647–1665. https://doi.org/10.1080/01904169209364428

Shi, J., Zhao, B., Zheng, S., Zhang, X., Wang, X., Dong, W., Xie, Q., Wang, G., Xiao, Y., Chen, F., Yu, N., & Wang, E. (2021). A phosphate starvation response-centered network regulates mycorrhizal symbiosis. *Cell*, *184*(22), 5527-5540.e18. https://doi.org/10.1016/j.cell.2021.09.030

Siciliano, V., Genre, A., Balestrini, R., Cappellazzo, G., deWit, P. J. G. M., & Bonfante, P. (2007). Transcriptome Analysis of Arbuscular Mycorrhizal Roots during Development of the Prepenetration Apparatus. *Plant Physiology*, *144*(3), 1455–1466. https://doi.org/10.1104/pp.107.097980

Smith, S. E., Jakobsen, I., Grønlund, M., & Smith, F. A. (2011). Roles of Arbuscular Mycorrhizas in Plant Phosphorus Nutrition: Interactions between Pathways of Phosphorus Uptake in Arbuscular Mycorrhizal Roots Have Important Implications for Understanding and Manipulating Plant Phosphorus Acquisition. *Plant Physiology*, *156*(3), 1050–1057. https://doi.org/10.1104/pp.111.174581

Smith, S. E., & Read, D. (2008). *Mycorrhizal Symbiosis*.

Takahashi, M., Terada, Y., Nakai, I., Nakanishi, H., Yoshimura, E., Mori, S., & Nishizawa, N. K. (2003). Role of Nicotianamine in the Intracellular Delivery of Metals and Plant Reproductive Development. *The Plant Cell*, *15*(6), 1263–1280. https://doi.org/10.1105/tpc.010256

Thibaud, M.-C., Arrighi, J.-F., Bayle, V., Chiarenza, S., Creff, A., Bustos, R., Paz-Ares, J., Poirier, Y., & Nussaume, L. (2010). Dissection of local and systemic transcriptional responses to phosphate starvation in Arabidopsis. *The Plant Journal*, *64*(5), 775–789. https://doi.org/10.1111/j.1365-313X.2010.04375.x

Torres de los Santos, R., Molinero Rosales, N., Ocampo, J. A., & García-Garrido, J. M. (2016). Ethylene Alleviates the Suppressive Effect of Phosphate on Arbuscular Mycorrhiza Formation. *Journal of Plant Growth Regulation*, *35*(3), 611–617. https://doi.org/10.1007/s00344-015-9570-1

Torres de Los Santos, R., Vierheilig, H., Ocampo, J. A., & García Garrido, J. M. (2011). Altered pattern of arbuscular mycorrhizal formation in tomato ethylene mutants. *Plant Signaling & Behavior*, *6*(5), 755–758. https://doi.org/10.4161/psb.6.5.15415

Trapet, P. L., Verbon, E. H., Bosma, R. R., Voordendag, K., van Pelt, J. A., & Pieterse, C. M. J. (2021). Mechanisms underlying iron deficiency-induced resistance against pathogens with different lifestyles. *Journal of Experimental Botany*, *72*(6), 2231–2241. https://doi.org/10.1093/jxb/eraa535

Valentinuzzi, F., Venuti, S., Pii, Y., Marroni, F., Cesco, S., Hartmann, F., Mimmo, T., Morgante, M., Pinton, R., Tomasi, N., & Zanin, L. (2019). Common and specific responses to iron and phosphorus deficiencies

in roots of apple tree (Malus × domestica). *Plant Molecular Biology*, *101*(1–2), 129–148. https://doi.org/10.1007/s11103-019-00896-w

Verbon, E. H., Trapet, P. L., Stringlis, I. A., Kruijs, S., Bakker, P. A. H. M., & Pieterse, C. M. J. (2017). Iron and Immunity. *Annual Review of Phytopathology*, *55*(1), 355–375. https://doi.org/10.1146/annurev-phyto-080516-035537

Xie, X., Lin, H., Peng, X., Xu, C., Sun, Z., Jiang, K., Huang, A., Wu, X., Tang, N., Salvioli, A., Bonfante, P., & Zhao, B. (2016). Arbuscular Mycorrhizal Symbiosis Requires a Phosphate Transceptor in the Gigaspora margarita Fungal Symbiont. *Molecular Plant*, *9*(12), 1583–1608. https://doi.org/10.1016/j.molp.2016.08.011

Zhang, Y., Wang, Y., Wang, E., Wu, X., Zheng, Q., Han, Y., Lin, W., Liu, Z., & Lin, W. (2021). <scp>SlPHL1</scp> , a <scp>MYB-CC</scp> transcription factor identified from tomato, positively regulates the phosphate starvation response. *Physiologia Plantarum*, *173*(3), 1063–1077. https://doi.org/10.1111/ppl.13503

Zheng, L., Huang, F., Narsai, R., Wu, J., Giraud, E., He, F., Cheng, L., Wang, F., Wu, P., Whelan, J., & Shou, H. (2009). Physiological and Transcriptome Analysis of Iron and Phosphorus Interaction in Rice Seedlings . *Plant Physiology*, *151*(1), 262–274. https://doi.org/10.1104/pp.109.141051

Supplementary Table 1. Oligonucleotides used in this study.

Primer	Sequence (5'-3')	Application
SlRAM1.q1	CATCAAACTGCTTCCAGAGGACT	Real Time PCR (Ho-Plágaro et al., 2021)
SlRAM1.q2	GGATTTCAACATCATCATCGTCG	Real Time PCR (Ho-Plágaro et al., 2021)
SlEXO84.q1	CGGCTAAGATCTCAATTCTG	Real Time PCR (Ho-Plágaro et al., 2021)
SlEXO84.q2	ATAAGAGTGTCATCAGCATG	Real Time PCR (Ho-Plágaro et al., 2021)
SlAMT22.q1	CTCAGAATGTCAGAGGAAGAT	Real Time PCR (Ho-Plágaro et al., 2021)
SlAMT22.q2	CCAGCAGCAGTATCAGAA	Real Time PCR (Ho-Plágaro et al., 2021)
SlPT4.q1	GAAGGGGAGCCATTTAATGTGG	Real Time PCR (Nagy et al., 2005)
SlPT4.q2	CCATCTTGTGTGTATTGTTGTATC	Real Time PCR (Nagy et al., 2005)
qRiEF1αF	GCTATTTTGATCATTGCCGCC	Real Time PCR
qRiEF1αR	TCATTAAAACGTTCTTCCGACC	Real Time PCR
SlEF-1F	GATTGGTGGTATTGGAACTGTC	Real Time PCR
SlEF-1R	AGCTTCGTGGTGCATCTC	Real Time PCR

CHAPTER 5:

Overexpression of the *Rhizophagus irregularis* high-affinity iron transporter *RiFTR1* promotes arbuscular mycorrhizal colonization

Abstract

Iron (Fe) is an essential micronutrient for growth and development of all organisms, including plants and their associated microbes. In this study we report silencing and overexpression of the *RiFTR1* gene of the arbuscular mycorrhizal (AM) fungus *Rhizophagus irregularis,* which encodes a high-affinity plasma membrane Fe transporter highly expressed in the intraradical mycelium. Mining of the *R. irregularis* RNAseq databases revealed a higher accumulation of *RiFTR1* transcripts in arbuscules than in intraradical hyphae. RiFTR1 was partially silenced in the RNAi1 lines; however, moderate down-regulation of *RiFTR1* did not significantly influence mycorrhizal colonization by *R. irregularis*. *RiFTR1* overexpression increased mycorrhizal intensity, the number of arbuscules and expression of the AM symbiotic marker *MtPT4.* These data, indicate that RiFTR1 plays a positive role in AM colonization.

Introduction

Iron (Fe) plays a central role in all living organisms, including plants and their associated microbes. Although necessary for a wide range of metabolic activities, too much Fe can be toxic to plant cells s and microbes due to the generation of reactive oxygen species (Verbon et al., 2017). Plants and their associated microorganisms have developed sophisticated mechanisms to regulate Fe levels in order to sustain their fitness. For example, *Arabidopsis* plants are known to limit infection from necrotrophic, hemi-biotrophic and biotrophic pathogens when Fe levels are low (Liu et al., 2021). Moreover, this Fe starvation-induced resistance is not simply caused by limiting Fe availability to the pathogen, but is a plant-mediated defence response that requires the activity of ethylene and salicylic acid signalling (Trapet et al., 2021). Additionally, Fe can be used to kill the invader or trigger cell death to restrict pathogen development.

Plants have evolved strategies to withdraw Fe away from pathogens, while they must provide it to their symbionts and endophytes in order to thrive. For instance, rhizobia found in root nodules of legumes are major sinks of Fe, as it is required as a cofactor in nitrogenase and many other enzymes involved in nitrogen fixation (Brear et al., 2020). Moreover, the endophyte *Epichloe festucae* needs Fe to maintain its mutualistic relationship with *Lolium perenne* (Johnson et al., 2013).

A prominent group of microorganisms that establish a mutualistic symbiotic interaction with plants are arbuscular mycorrhizal (AM) fungi. These fungi colonize the root and forms highly branched structures, called arbuscules, inside the cortical cells. The arbuscules are surrounded by the plasma membrane of the cell that host them, the periarbuscular membrane, without crossing it. The periarbuscular membrane and the plasma membrane of the fungus have transporter

proteins that allow the exchange of nutrients between the plant and the fungus, and are separated by a new apoplastic compartment, the periarbuscular space. In the soil, AM fungi develop a network of extraradical mycelium. In Chapters 3 and 4, we have shown that Fe impacts AM fungal colonization of tomato roots. With the aim of getting further insights into the relevance of Fe on AM development and function, this chapter was aimed at studying by reverse genetics the impact of the *Rhizophagus irregularis* high-affinity Fe transporter RiFTR1 that is highly expressed in arbuscules (Tamayo et al., 2018) in AM development. To that end, *RiFTR1* was both silenced and overexpressed in *Medicago truncatula* roots through Host-Induced Gene Silencing (HIGS) and Host-Induced Gene Overexpressing (HIGO), respectively.

Materials and Methods

Plasmid construction

RNAi and overexpression target sequences were isolated by PCR using *R. irregularis* cDNA as template and the corresponding primer sets (Supplementary Table 1). Amplicons were flanked at their 5'ends with the CACC sequence to be cloned in the plant expression vectors using the Gateway technology. PCR products were first cloned into pENTR/D-TOPO before been cloned into the corresponding destination vector, according to the manufacturer instructions. Two target sequences were selected for HIGS, RiFTR1 RNAi-1 and RiFTR1 RNAi-2, with a length of 300 pb targeting the regions from -107 to 193 and 684 to 984, respectively, with respect to the start codon ATG (Supplementary Figure 1). Both target sequences did not contain intronic sequences and were checked to avoid off-targets effects due to sequence similarities in *Medicago truncatula* and *Rhizophagus irregularis*. The RNAi sequences were cloned into pK7GWIWG2II-RedRoot vector (https://www.psb.ugent.be/cores/gateway_vectors) using LR clonase II to produce the final silencing constructs. For constitutive *RiFTR1* overexpression (RiFTR1-OE), its open reading frame was cloned into the plant expression vector pUBIcGFP-DR (Kryvoruchko et al., 2016). All constructs were verified by sequencing. *Agrobacterium rhizogenes* MSU440 was transformed with the resulting RNAi and overexpression constructs or the empty vectors (negative control) to generate transgenic *M. truncatula* hairy roots.

Medicago truncatula transformation and mycorrhization

Composite *M. truncatula* plants were generated using the methodology of Boisson-Dernier et al. (2001). Seeds of *M truncatula* Jemalong A7 were surface-sterilised with undiluted H_2SO_4. Seeds were incubated for cold stratification at 4 °C in darkness for two days under sterile conditions in water-agar plates and germinated at 28 °C until the root reached 1-1.5 cm in length. Under sterile

conditions, 1 mm was cut from the root tip and the section surface was coated with the corresponding *A. rhizogenes* strains carrying the different constructs or the empty vectors by carefully scrapping over the bacterial lawn of a 2 days solid LB culture. Seedlings were then transferred to Fåhraeus medium (Fåhraeus, 1957) plates. Root area was covered with aluminium foil to prevent roots from receiving light. Plates were first incubated at 21 °C for one week (16h light/8h darkness) to promote *A. rhizogenes* infection and then incubated at 25 °C for 4 weeks. Successfully transformed roots were visually selected via constitutive expression of DsRED using a Fluorescent Stereo Microscope Leica M165 FC. Untransformed roots were removed and composite plants were transferred to new Fåhraeus medium plates supplemented with 200 μg/ml amoxicillin and cultivated at 25 °C for an additional week. Plants were then transferred into 50 mL Falcon tubes containing sterile sand inoculated with *R. irregularis* DAOM197198-colonized carrot roots previously propagated in monoxenic cultures (roots of 1 plates inoculum for 100 mL substrate). To prevent desiccation, plants were covered with sun-transparent bags (Sigma-Aldrich). Plants were incubated at 25 °C for five weeks (16h light/8h darkness) and were watered twice a week with 5ml mL of a half-strength low Pi (20 μM) (Hewitt, 1966). At harvesting, roots were washed with distilled water to eliminate the substrate, and shoots and roots were separated. Shoots were frozen in liquid N and stored at -80 °C until used. An aliquot of each root system was kept to estimate mycorrhizal colonization and the rest was frozen in liquid N.

Root colonization measurements

Trypan blue staining was used to estimate AM fungal colonization in the root systems of each plant. The Trouvelot method was used to quantify mycorrhizal colonization (Trouvelot et al., 1986).

RNA extraction and cDNA synthesis

Total RNA was extracted from *M. truncatula* roots using the innuPREP Plant RNA Kit (Analitik Jena), following the manufacturer's instructions. DNAse treatment was performed in column during RNA extraction using RNase-Free DNAse Set (Qiagen), following the manufacturer´s protocol. DNAse-treated RNAs quantification was carried out with a NanoDrop 1000 Spectrophotometer (Thermo Scientific). Then, Super-Script IV Reverse Transcriptase (Invitrogen) was used to synthetize cDNA in a 20 μL from 500 ng of total DNAse-treated RNA.

Gene expression analyses

Gene expression was assessed by real-time RT-PCR using a QuantStudio 3 (Applied Biosystem) in the synthetized cDNAs. Each 12 μl reaction contained 1 μl of a 2:10 dilution of

cDNA, 0.5 µl 10 mM each primer (Supplementary Table 1) and 6 µl iTaq (Bio-Rad), using a 96-well plate. The specificity of the primer sets was analyzed by PCR amplification of the *R. irregularis* cDNA. The real-time PCR program consisted of a 30 s incubation at 95 °C, followed by 40 cycles of 15 s at 95 °C, 30 s at 60 °C and 30 s at 72 °C, where the fluorescence signal was measured. A melting curve was used to check the specificity of the PCR amplification procedure after the final PCR cycle. Efficiency of the different primer pairs was determined through a real-time PCR on several dilutions of cDNA. Gene expressions were carried out on at least three independent biological samples. Real time PCR reactions were performed at least two times for each biological sample, with the threshold cycle (Ct) determined in duplicate. The relative transcription levels were calculated by using the $2^{-\Delta CT}$ method (Schmittgen & Livak, 2008) and the standard error was computed from the average of the ΔCt values for each biological sample. Plant transcript levels and transcript levels of the translation elongation factor 1-alpha of *R. irregularis* (*RiTEF1α*) were normalized to the translation elongation factor 1-alpha of *M. truncatula* (*MtTEF1α*) while fungal transcripts were normalized to *RiTEF1α*.

Transcriptomic data analysis

RNAseq data from laser microdissected *Medicago truncatula* cells containing arbuscules or intraradical hyphae and from extraradical mycelium grown in monoxenic cultures wer collected from NCBI's Gene Expression Omnibus (GEO) GSE99655 database. Data were processed by following the protocol of Zeng et al. (2018), and normalized using the DESeq2 tool on Galaxy (https://usegalaxy.org).

Statistical analyses

The statistical analysis of means and standard error determinations was conducted with Statgraphics Centurion XVI software. An ANOVA one-way test followed by a Duncan test ($p<0.05$) was then used to compare the treatments.

Results

RiFTR1 is mainly expressed in the arbuscules

Previous studies have shown that RiFTR1 is more highly expressed in mycorrhizal roots than in the ERM (Tamayo et al., 2018). As a first step to functionally characterize *RiFTR1*, the expression pattern of RiFTR1 in the different structures the fungus develops within the roots was investigated in the RNA-sequencing data from *R. irregularis* transcriptome databases (Zeng et al., 2018, 2020). *RiFTR1* transcripts were detected in the RNAseq data obtained from extraradical

mycelium grown in monoxenic cultures (ERM), laser micro-dissected *M. truncatula* root cells containing intraradical hyphae (IRM) and laser micro-dissected *M. truncatula* cortical cells containing arbuscules (ARB). However, *RiFTR1* was mainly expressed in the arbuscules. A 43-fold increase in *RiFTR1* expression was observed in the arbuscules respect to the expression in the IRM and the ERM (Figure 3).

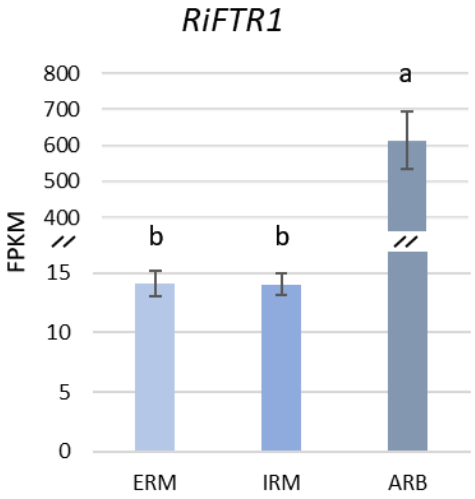

Figure 1. Expression pattern of *R. irregularis* FTR1 based on RNA-seq analyses of *M. truncatula* root cells containing arbuscules (ARB) or IRM, collected by laser microdissection, and ERM grown in monoxenic cultures. The reads from the RNAseq of *RiFTR1* obtained on each treatment were normalized for sequencing depth and length of the gene to obtain FPKM values. Error bars represent standard error from three biological replicates. Different letters indicate significant differences ($p < 0.05$).

RiFTR1 silencing by HIGS

In order to link the function of RiFTR1 to the colonization of the fungus and the development of the AM symbiosis and, since there are no known stable transformation protocols for AM fungi, we attempted its inactivation using HIGS (Nowara et al., 2010) This methodology has been used to successfully silence AM fungal genes that are highly expressed in the *in planta* phase of the fungus (Helber et al., 2011; Tsuzuki et al., 2016; Voß et al., 2018).

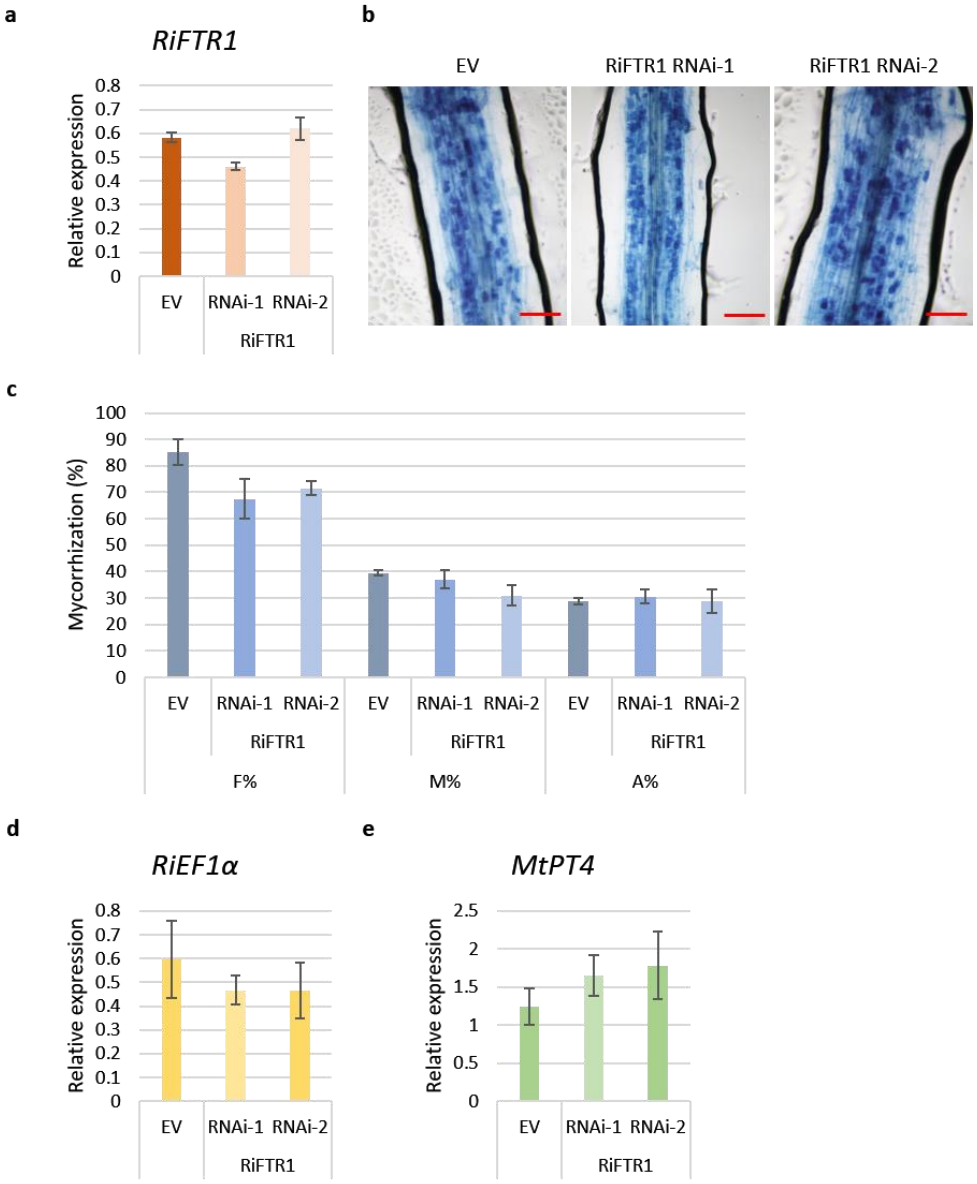

Figure 2. Host-induced gene silencing of *RiFTR1* in mycorrhizal *M. truncatula* plants. (**a**) Transcript abundance of *RiFTR1* in roots of *M. truncatula* composite plants transformed with the EV or with the silencing constructs RiFTR1 RNAi-1 or RiFTR1 RNAi-2. (**b**) Mycorrhizal colonization was observed in trypan blue stained roots. Scale bar: 100µm (**c**) Mycorrhization level of transformed roots was quantified by the Trouvelot method. F%, frequency of acolonization; M% intensity of mycorrhiza; A% arbuscule abundance. (**d**) Transcript levels of *RiEF1α* in control (EV) and RiFTR1 RNAi-1 and RiFTR1 RNAi-2 lines were determined using *MtEF1α* as endogenous control. (**e**) Expression levels of the *M. truncatula* symbiotic marker *MtPT4* in control (EV) and RiFTR1 RNAi-1 and RiFTR1 RNAi-2 lines were determined using *MtEF1α* as endogenous control. Asterisks indicate statistically significant differences from respective control lines. Error bars indicate the means of four biological replicates with SE values.

To silence *RiFTR1*, two RNAi-silencing constructs were used that targeted different 300 pb fragments of the gene at its 5′ region. The transformed *M. truncatula* plants with hairy roots were screened by red fluorescence and inoculated with *R. irregularis*. Silencing of *RiFTR1* expression was assessed by RT-qPCR in mycorrhizal transformed roots (Figure 1). The results show that the RiFTR1 RNAi-1 construct reduced expression of *RiFTR1* in planta, only by 20 %, as compared to

control plants transformed with the empty vector, although the difference is not statistically significative. *RiFTR1* expression was not affected in roots transformed with RiFTR1 RNAi-2 (Figure 1a). Similar silencing levels, 30%, we found for the *R. irregularis* RiCNR1 effector (Voß et al., 2018) and expression of nuclear targeted effector *RiNLE1* could not be successfully knocked down (Wang et al., 2021). This is not surprising considering the mechanism of function of HIGS and the difficulties of obtaining fully down-regulated fungal transcripts with this methodology. The moderate down-regulation of *RiFTR1* in the RNAi-1 lines did not significantly influence the intraradical structures of *R. irregularis* within the roots, when compared with the control roots transformed with the empty vector (Figure 1b,c). This correlated with the similar transcript levels of the *R. irregularis* constitutively expressed elongation factor *RiEF1α* and the symbiotic plant phosphate transporter *MtPT4* in roots transformed with the empty vector and in roots transformed with the silencing constructs (Figure 1d,e). The lack of effect of *RiFTR1* silencing in the mycorrhizal phenotype might be either because *RiFTR1* does not play a role in mycorrhizal colonization or because the expression levels of *RiFTR1* in the RNAi-1 lines is enough to sustain the symbiosis.

Overexpression of RiFTR1 increases AM colonization

As an alternative approach to study the role of RiFTR1 in AM symbiosis, we investigated the effect of *RiFTR1* overexpression on mycorrhizal colonization. Therefore, the open reading frame of *RiFTR1* was expressed in *M. truncatula* under the control of the constitutive Ubiquitin1 promoter. The transformed *M. truncatula* plants with hairy roots were screened by red fluorescence and inoculated with *R. irregularis*. Overexpression of *RiFTR1* was confirmed by RT-qPCR in mycorrhizal roots of composite plants transformed with the RiFTR1-OE construct (Figure 2a). A 2.9-fold increase in RiFTR1 expression was detected in the RiFTR1-OE lines compared to empty vector controls. RiFTR1 overexpression did not led to a significant increase in mycorrhizal frequency (F%), but increased mycorrhizal intensity (M%) and in the number of arbuscules (A%) (Figure 2b,c). This agrees with the upward trend expression of the *R. irregularis* *RiEF1α* reference gene and the increase of the AM marker *MtPT4* in the RiFTR1-OE roots compared with controls roots (Figure 2d,e). These results indicate that RiFTR1 plays a positive role in AM colonization.

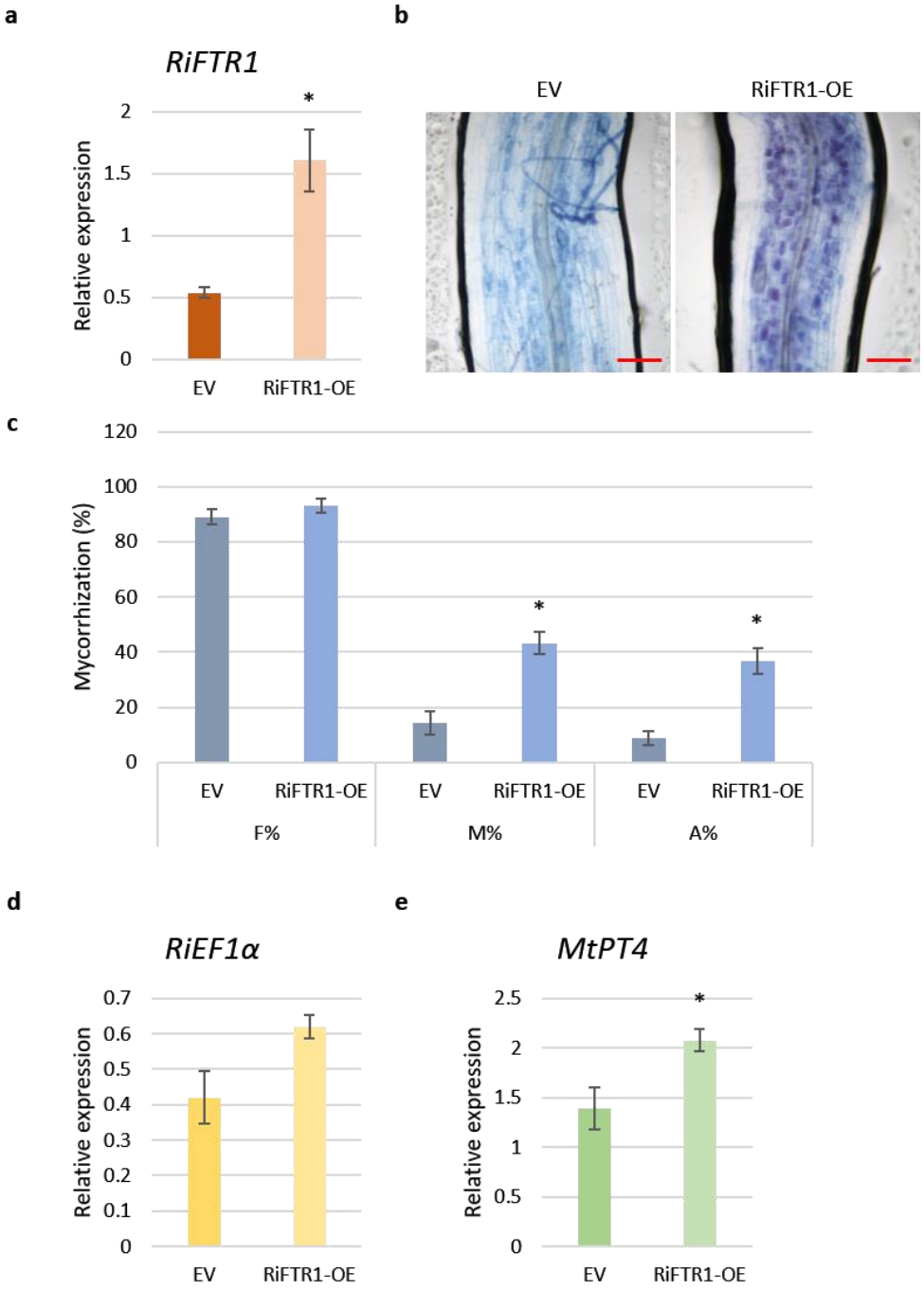

Figure 3. Host-induced gene silencing of *RiFTR1* in mycorrhizal *M. truncatula* plants. (**a**) Mycorrhizal colonization was observed in trypan blue stained roots. (**b**) Transcript abundance of *RiFTR1* in roots of *M. truncatula* composite plants transformed with the EV or with the silencing constructs RiFTR1 RNAi-1 or RiFTR1 RNAi-2. Scale bar: 100µm. (**c**) Mycorrhization level of transformed roots was quantified by the Trouvelot method. F%, frequency of acolonization; M% intensity of mycorrhiza; A% arbuscule abundance. (**d**) Transcript levels of *RiEF1α* in control (EV) and RiFTR1 RNAi-1 and RiFTR1 RNAi-2 lines were determined using *MtEF1α* as endogenous control. (**e**) Expression levels of the *M. truncatula* symbiotic marker *MtPT4* in control (EV) and RiFTR1 RNAi-1 and RiFTR1 RNAi-2 lines were determined using *MtEF1α* as endogenous control. Asterisks indicate statistically significant differences from respective control lines. Error bars indicate the means of four biological replicates with SE values.

Discussion

Data presented in this chapter show that overexpression of the high-affinity Fe transporter *RiFTR1* leads to an increase in mycorrhizal colonization and arbuscule abundance. These data reveal the significance of RiFTR1 for AM symbiosis. In this respect, various studies have shown that high-affinity Fe transporters are required for maintenance of several mutualistic plant-microbe interactions (Brear et al., 2020; Johnson et al., 2013; Walton et al., 2020) and for the colonization and virulence of pathopatogenic fungi (Albarouki et al., 2014; Eichhorn et al., 2006; Oide et al., 2006).

Previous functional analyses in yeast revealed that *RiFTR1* encodes a functional Fe transporter that is expressed in the plasma membrane and that it is involved in Fe uptake by the ERM and IRM (Tamayo et al., 2018). These authors hypothesized that the fungus might exert some control over the amount of Fe that is transferred to the plant. Since *RiFTR1* is mainly expressed in the arbuscules, the major place for nutrient exchange between symbionts, RiFTR1 may play a major role in Fe reuptake from the apoplast of the arbuscular interface that is formed in arbuscule-colonized cortical cells, probably, to meet the fungal Fe demands for its growth and activity. This agrees with previous observations in Chapters 3 and 4 that mycorrhizal colonization is inhibited when the symbiosis is developed under Fe deficient conditions (Chapter 3) and in an iron-inefficient tomato mutant (Chapter 4). The requirement of iron for AM fungal colonization is not surprising given that this transition metal is an essential micronutrient that participates in many cellular electron transfer reactions involved in a wide array of biochemical processes essential for growth (Marschner, 1995). Since Fe is also required for the metabolism and activity of host plant cells, a competition for Fe acquisition between the two partners may occur in cells harbouring arbuscules. Therefore, tight control of RiFTR1 in arbuscules might be required for this complex mechanism.

Our data suggest that RiFTR1 could be involved in fine-tuning Fe homeostasis at the arbuscular interface dependent on the iron status of the two symbionts. The iron retrieved by RiFTR1 could act as a signal to stimulate the activity of arbuscules during symbiosis. This is supported by the higher transcript levels of the *M. truncatula* phosphate transporter PT4 mediating symbiotic Pi uptake in the *RiFTR1* overexpressing roots. On the other hand, the higher mycorrhizal colonization of the *RiFTR1* overexpressing roots suggests that iron could be an important signal in the regulation of arbuscule development and *R. irregularis* hyphal growth in roots. Therefore, it is tempting to hypothesize that RiFTR1 as an iron sensor may participate in iron sensing and signalling pathways in *R. irregularis*. Since RiFTR1 possess iron transport capacity (Tamayo et al., 2018) and also regulates the activity of *R. irregularis* in the root, it might

be a transceptor, a membrane protein that functions as a transporter and a receptor (Holsbeeks et al., 2004). In this respect, the yeast orthologue of RiFTR1 has been shown to function as a transceptor capable of transporting iron (Eide et al., 1996) and triggering the protein kinase A (PKA) signalling pathway in response to Fe availability (Schothorst et al., 2017). In addition, the iron transporter IRT1 of *Arabidopsis thaliana* also functions as a metal transceptor that not only takes up iron from the environment but also mediates metal sensing and signalling (Cointry & Vert, 2019). Since the initial discovery of transceptors in yeast, the concept of transceptors has spread to other organisms (Kriel et al., 2011). In the AM fungus *Gigaspora margarita*, the phosphate transporter GigmPT is a transceptor that is involved in phosphate uptake a sensing through the activation of the PKA signalling cascade (Xie et al., 2016). The mycorrhiza-specific phosphate transporters MtPT4 of *M. truncatula* (Javot et al., 2007), OsPT11 of *Oryza sativa* (Yang et al., 2012) and AsPT4 of *Astragalus sinicus* (Xie et al., 2013) also act as Pi sensors in the periarbuscular membrane, as their mutation not only inhibits symbiotic Pi uptake but also leads to premature arbuscule degeneration and to symbiosis abortion. All these data together indicate that nutrient sensing in the symbiotic interfases regulates mycorrhizal development and that it is a potential mechanism by which the plant and the fungus are able to coordinate the AM symbiosis with their nutrient status.

In conclusion, RiFTR1 is proposed to be a main Fe sensor in *R. irregularis*, being involved in Fe acquisition from the rhizosphere or Fe reabsorption from the apoplast of the symbiotic interphase. Further studies are required to determine if RiFTR1 senses extracellular iron changes through the activation of the PKA pathways and to define the underlying iron sensing and signalling mechanisms.

References

Albarouki, E., Schafferer, L., Ye, F., Wirén, N., Haas, H., & Deising, H. B. (2014). Biotrophy-specific downregulation of siderophore biosynthesis in <scp> *C* </scp> *olletotrichum graminicola* is required for modulation of immune responses of maize. *Molecular Microbiology*, *92*(2), 338–355. https://doi.org/10.1111/mmi.12561

Boisson-Dernier, A., Chabaud, M., Garcia, F., Bécard, G., Rosenberg, C., & Barker, D. G. (2001). *Agrobacterium rhizogenes* -Transformed Roots of *Medicago truncatula* for the Study of Nitrogen-Fixing and Endomycorrhizal Symbiotic Associations. *Molecular Plant-Microbe Interactions®*, *14*(6), 695–700. https://doi.org/10.1094/MPMI.2001.14.6.695

Brear, E. M., Bedon, F., Gavrin, A., Kryvoruchko, I. S., Torres-Jerez, I., Udvardi, M. K., Day, D. A., & Smith, P. M. C. (2020). GmVTL1a is an iron transporter on the symbiosome membrane of soybean with an important role in nitrogen fixation. *New Phytologist*, *228*(2), 667–681. https://doi.org/10.1111/nph.16734

Cointry, V., & Vert, G. (2019). The bifunctional transporter-receptor <scp>IRT</scp> 1 at the heart of metal sensing and signalling. *New Phytologist*, *223*(3), 1173–1178. https://doi.org/10.1111/nph.15826

Eichhorn, H., Lessing, F., Winterberg, B., Schirawski, J., Kämper, J., Müller, P., & Kahmann, R. (2006). A Ferroxidation/Permeation Iron Uptake System Is Required for Virulence in *Ustilago maydis*. *The Plant Cell*, *18*(11), 3332–3345. https://doi.org/10.1105/tpc.106.043588

Eide, D., Broderius, M., Fett, J., & Guerinot, M. L. (1996). A novel iron-regulated metal transporter from plants identified by functional expression in yeast. *Proceedings of the National Academy of Sciences*, *93*(11), 5624–5628. https://doi.org/10.1073/pnas.93.11.5624

Fåhraeus, G. (1957). The Infection of Clover Root Hairs by Nodule Bacteria Studied by a Simple Glass Slide Technique. *Microbiology*, *16*(2), 374–381. https://doi.org/10.1099/00221287-16-2-374

Helber, N., Wippel, K., Sauer, N., Schaarschmidt, S., Hause, B., & Requena, N. (2011). A Versatile Monosaccharide Transporter That Operates in the Arbuscular Mycorrhizal Fungus *Glomus* sp Is Crucial for the Symbiotic Relationship with Plants. *The Plant Cell*, *23*(10), 3812–3823. https://doi.org/10.1105/tpc.111.089813

Hewitt, E. J. (1966). Sand and water culture methods used in the study of plant nutrition. In *Commonwealth Agricultural Bureaux*. Farnham Royal, UK.

Holsbeeks, I., Lagatie, O., van Vuland, A., van de Velde, S., & Thevelein, J. (2004). The eukaryotic plasma membrane as a nutrient-sensing device. *Trends in Biochemical Sciences*, *29*(10), 556–564. https://doi.org/10.1016/j.tibs.2004.08.010

Javot, H., Penmetsa, R. V., Terzaghi, N., Cook, D. R., & Harrison, M. J. (2007). A *Medicago truncatula* phosphate transporter indispensable for the arbuscular mycorrhizal symbiosis. *Proceedings of the National Academy of Sciences*, *104*(5), 1720–1725. https://doi.org/10.1073/pnas.0608136104

Johnson, L. J., Koulman, A., Christensen, M., Lane, G. A., Fraser, K., Forester, N., Johnson, R. D., Bryan, G. T., & Rasmussen, S. (2013). An Extracellular Siderophore Is Required to Maintain the Mutualistic Interaction of Epichloë festucae with Lolium perenne. *PLoS Pathogens*, *9*(5), e1003332. https://doi.org/10.1371/journal.ppat.1003332

Kriel, J., Haesendonckx, S., Rubio-Texeira, M., van Zeebroeck, G., & Thevelein, J. M. (2011). From transporter to transceptor: Signaling from transporters provokes re-evaluation of complex trafficking and regulatory controls. *BioEssays*, *33*(11), 870–879. https://doi.org/10.1002/bies.201100100

Kryvoruchko, I. S., Sinharoy, S., Torres-Jerez, I., Sosso, D., Pislariu, C. I., Guan, D., Murray, J., Benedito, V. A., Frommer, W. B., & Udvardi, M. K. (2016). MtSWEET11, a Nodule-Specific Sucrose Transporter of *Medicago truncatula*. *Plant Physiology*, *171*(1), 554–565. https://doi.org/10.1104/pp.15.01910

Liu, Y., Kong, D., Wu, H.-L., & Ling, H.-Q. (2021). Iron in plant–pathogen interactions. *Journal of Experimental Botany*, *72*(6), 2114–2124. https://doi.org/10.1093/jxb/eraa516

Marschner, H. (1995). Functions of Mineral Nutrients: Micronutrients. In *Marschner's Mineral Nutrition of Higher Plants* (pp. 313–404). Elsevier. https://doi.org/10.1016/B978-0-08-057187-4.50015-1

Nowara, D., Gay, A., Lacomme, C., Shaw, J., Ridout, C., Douchkov, D., Hensel, G., Kumlehn, J., & Schweizer, P. (2010). HIGS: Host-Induced Gene Silencing in the Obligate Biotrophic Fungal Pathogen *Blumeria graminis* . *The Plant Cell*, *22*(9), 3130–3141. https://doi.org/10.1105/tpc.110.077040

Oide, S., Moeder, W., Krasnoff, S., Gibson, D., Haas, H., Yoshioka, K., & Turgeon, B. G. (2006). *NPS6* , Encoding a Nonribosomal Peptide Synthetase Involved in Siderophore-Mediated Iron Metabolism, Is a Conserved Virulence Determinant of Plant Pathogenic Ascomycetes. *The Plant Cell*, *18*(10), 2836–2853. https://doi.org/10.1105/tpc.106.045633

Schmittgen, T. D., & Livak, K. J. (2008). Analyzing real-time PCR data by the comparative CT method. *Nature Protocols*, *3*(6), 1101–1108. https://doi.org/10.1038/nprot.2008.73

Schothorst, J., van Zeebroeck, G., & Thevelein, J. (2017). Identification of Ftr1 and Zrt1 as iron and zinc micronutrient transceptors for activation of the PKA pathway in Saccharomyces cerevisiae. *Microbial Cell*, *4*(3), 74–89. https://doi.org/10.15698/mic2017.03.561

Tamayo, E., Knight, S. A. B., Valderas, A., Dancis, A., & Ferrol, N. (2018). The arbuscular mycorrhizal fungus *Rhizophagus irregularis* uses a reductive iron assimilation pathway for high-affinity iron uptake. *Environmental Microbiology*, *20*(5), 1857–1872. https://doi.org/10.1111/1462-2920.14121

Trapet, P. L., Verbon, E. H., Bosma, R. R., Voordendag, K., van Pelt, J. A., & Pieterse, C. M. J. (2021). Mechanisms underlying iron deficiency-induced resistance against pathogens with different lifestyles. *Journal of Experimental Botany*, *72*(6), 2231–2241. https://doi.org/10.1093/jxb/eraa535

Trouvelot, A., Kough, J. L., & Gianinazzi-Pearson, V. (1986). Estimation of vesicular arbuscular mycorrhizal infection levels. Research for methods having a functional significance. *Physiological and Genetical Aspects of Mycorrhizae = Aspects Physiologiques et Genetiques Des Mycorhizes: Proceedings of the 1st European Symposium on Mycorrhizae, Dijon, 1-5 July 1985*. https://agris.fao.org/agris-search/search.do?recordID=US201301430989

Tsuzuki, S., Handa, Y., Takeda, N., & Kawaguchi, M. (2016). Strigolactone-Induced Putative Secreted Protein 1 Is Required for the Establishment of Symbiosis by the Arbuscular Mycorrhizal Fungus *Rhizophagus irregularis*. *Molecular Plant-Microbe Interactions®*, *29*(4), 277–286. https://doi.org/10.1094/MPMI-10-15-0234-R

Verbon, E. H., Trapet, P. L., Stringlis, I. A., Kruijs, S., Bakker, P. A. H. M., & Pieterse, C. M. J. (2017). Iron and Immunity. *Annual Review of Phytopathology*, *55*(1), 355–375. https://doi.org/10.1146/annurev-phyto-080516-035537

Voß, S., Betz, R., Heidt, S., Corradi, N., & Requena, N. (2018). RiCRN1, a Crinkler Effector From the Arbuscular Mycorrhizal Fungus Rhizophagus irregularis, Functions in Arbuscule Development. *Frontiers in Microbiology*, *9*(SEP), 2068. https://doi.org/10.3389/fmicb.2018.02068

Walton, J. H., Kontra-Kováts, G., Green, R. T., Domonkos, Á., Horváth, B., Brear, E. M., Franceschetti, M., Kaló, P., & Balk, J. (2020). The *Medicago truncatula* Vacuolar iron Transporter-Like proteins VTL4 and VTL8 deliver iron to symbiotic bacteria at different stages of the infection process. *New Phytologist*, *228*(2), 651–666. https://doi.org/10.1111/nph.16735

Wang, J., Wang, J., He, J., Zhu, Y., Qiao, N., & Ge, Y. (2021). Arbuscular mycorrhizal fungi and plant diversity drive restoration of nitrogen-cycling microbial communities. *Molecular Ecology*, *30*(16), 4133–4146. https://doi.org/10.1111/mec.16030

Xie, X., Huang, W., Liu, F., Tang, N., Liu, Y., Lin, H., & Zhao, B. (2013). Functional analysis of the novel mycorrhiza-specific phosphate transporter <scp>A</scp> s <scp>PT</scp> 1 and <scp>PHT</scp> 1 family from *<scp>A</scp> stragalus sinicus* during the arbuscular mycorrhizal symbiosis. *New Phytologist*, *198*(3), 836–852. https://doi.org/10.1111/nph.12188

Xie, X., Lin, H., Peng, X., Xu, C., Sun, Z., Jiang, K., Huang, A., Wu, X., Tang, N., Salvioli, A., Bonfante, P., & Zhao, B. (2016). Arbuscular Mycorrhizal Symbiosis Requires a Phosphate Transceptor in the Gigaspora margarita Fungal Symbiont. *Molecular Plant*, *9*(12), 1583–1608. https://doi.org/10.1016/j.molp.2016.08.011

Yang, S.-Y., Grønlund, M., Jakobsen, I., Grotemeyer, M. S., Rentsch, D., Miyao, A., Hirochika, H., Kumar, C. S., Sundaresan, V., Salamin, N., Catausan, S., Mattes, N., Heuer, S., & Paszkowski, U. (2012). Nonredundant Regulation of Rice Arbuscular Mycorrhizal Symbiosis by Two Members of the *PHOSPHATE TRANSPORTER1* Gene Family. *The Plant Cell*, *24*(10), 4236–4251. https://doi.org/10.1105/tpc.112.104901

Zeng, T., Holmer, R., Hontelez, J., Lintel-Hekkert, B., Marufu, L., Zeeuw, T., Wu, F., Schijlen, E., Bisseling, T., & Limpens, E. (2018). Host- and stage-dependent secretome of the arbuscular mycorrhizal fungus *Rhizophagus irregularis*. *The Plant Journal*, *94*(3), 411–425. https://doi.org/10.1111/tpj.13908

Zeng, T., Rodriguez-Moreno, L., Mansurkhodzaev, A., Wang, P., Berg, W., Gasciolli, V., Cottaz, S., Fort, S., Thomma, B. P. H. J., Bono, J., Bisseling, T., & Limpens, E. (2020). A lysin motif effector subverts chitin-triggered immunity to facilitate arbuscular mycorrhizal symbiosis. *New Phytologist*, *225*(1), 448–460. https://doi.org/10.1111/nph.16245

Supplementary Table 1. Oligonucleotides used in this study. Overhangs are underlined.

Primer	Sequence (5'-3')	Application
RiFTR1.RNAi1f	CACCAGGCATATCCCTCTCAAATAAATAAATAG	RiFTR1 RNAi-1 isolation
RiFTR1.RNAi1r	GATAGCACCAATTAATAAAGAAACTCC	RiFTR1 RNAi-1 isolation
RiFTR1.RNAi2f	CACCTATGAACAAGTTTTATGGCAATTAG	RiFTR1 RNAi-2 isolation
RiFTR1.RNAi2r	TCGTCATAATTTCATTTTTAAATAAATTAAG	RiFTR1 RNAi-2 isolation
RiFTR1.TOPO.F	CACCATGGTTTATTTATTCGATG	Cloning RiFTR1
RiFTR1.TOPO.R	TTAAGCTGCATTCACAATAGCAG	Cloning RiFTR1
qRiFTR1F	AGGATCGCATAGGATGTCAA	Real Time PCR
qRiFTR1R	AGAAAAGACCAGCGGCAAC	Real Time PCR
qRiEF1αF	GCTATTTTGATCATTGCCGCC	Real Time PCR
qRiEF1αR	TCATTAAAACGTTCTTCCGACC	Real Time PCR

Supplementary Figure 1. Target sequences (5′-3′) selected for HIGS, RiFTR1 RNAi-1 and RiFTR1 RNAi-2. UTR sequences are in blue.

RiFTR1 RNAi-1

aggcatatccctctcaaataaataaatagtgtcagttcttttgtcaatttttttttttaaaaaaaatatattttaacgacaaaattaacgacaa
aattcgtacataATGGTTTATTTATTCGATGTTCCCGCTTATTTCATTCTCTTAAGAGAAACT
CTTGAGGCTACAATTATTCTTGCAGTTCTCTTAGGGTTCATCGATAAATTGGTTCTTGA
CGATGAATCAGTACGAAAGAAACTTAAAAGACAAATTTGGTATGGAACTGCTGCTG
GTTTAGGAGTTTCTTTATTAATTGGTG

RiFTR1 RNAi-2

TATGAACAAGTTTTATGGCAATTAGATTGTTGTGATAACAAAAATCGTTTCTGGTCAC
TTATGTCGACAATATTCGGATGGAGAAATAAAGCTACCGTTGGAACAACAGTTGGTT
ATTTTATATATTGGATTTTCGTCGTACTTGTAGCCATGTTCATGTTGTATAGAGAAAA
GAGAAAACATAACGATCAATCTAATAATGTTGAAAAAAATGAAAGAGATGAAAGA
AATGAAAAGGATGATCAAGCTGCTATTGTGAATGCAGCTTAAtttatttatttaaaaatgaaattat
gacga

DISCUSIÓN GENERAL

Con el objetivo de obtener una visión integradora de los resultados obtenidos en los distintos capítulos de la presente Tesis Doctoral, se presentan y discuten los resultados mas relevantes para dar una visión global de nuestra contribución al estudio de los mecanismos de homeostasis de hierro (Fe) en la simbiosis micorrícica arbuscular (MA).

El Fe es un micronutriente esencial para el desarrollo y supervivencia de la mayoría de los organismos, ya que desempeñado un papel estructural clave en muchas proteínas y actúa como cofactor de múltiples enzimas. A pesar de que el Fe es uno de los elementos más abundantes en la naturaleza, a menudo no está disponible para las plantas debido a que se encuentra principalmente en su estado oxidado, Fe (III), lo que se agrava en los suelos alcalinos Por otro lado, los residuos procedentes de actividades antropogénicas pueden dan lugar a la acumulación de Fe en los ecosistemas. El Fe en altas concentraciones genera especies reactivas de oxígeno que son perjudiciales para el crecimiento y el desarrollo. De ahí, que los organismos hayan desarrollado una serie de estrategias altamente eficientes que les permitan controlar la homeostasis de Fe. Este control se consigue gracias a la actuación coordinada de una serie de procesos que regulan no solo la adquisición del metal del suelo, sino también su distribución a través de la planta, utilización y almacenamiento en los diferentes compartimentos subcelulares. Todos estos procesos requieren de la actuación de proteínas transportadoras de metales codificadas por familias multigénicas y que están localizadas en diferentes membranas celulares y subcelulares. Otra estrategia que utilizan las plantas para superar condiciones tanto de deficiencia como de toxicidad de Fe es establecer asociaciones con hongos MA, puesto que mejoran el estado nutricional de la planta hospedadora, en caso de deficiencias, y la protege de los daños provocados por concentraciones tóxicas. Sin embargo, poco se conoce acerca del efecto que el desarrollo de la simbiosis ejerce sobre la regulación de los sistemas homeostáticos de Fe de la planta ni de los sistemas de transporte de Fe en la simbiosis MA. En la Tesis Doctoral se han caracterizado algunas proteínas transportadoras del hongo MA *Rhizophagus irregularis* que podrían desempeñar un papel relevante en la homeostasis de Fe y se ha analizado el impacto de la simbiosis sobre la homeostasis de Fe de la planta hospedadora

En cuanto a los transportadores de Fe del hongo, el gen *RiSMF3.2* del hongo MA *Rhizophagus irregularis* codifica un transportador funcional de membrana plasmática de la familia de transportadores de metales NRAMP, que transporta Mn y Fe. Como cabría esperar para un transportador de membrana plasmática, la expresión de *RiSMF3.2* disminuyó cuando el micelio extrarradical (ERM) se desarrolló durante 20 días bajo toxicidad de Fe. El incremento de los niveles de expresión de RiSMF3.2 a las pocas horas de la exposición del ERM a altas concentraciones de Fe sugiere bien que se trata de un transportador de baja afinidad que opera

cuando las concentraciones del sustrato en el exterior son elevadas o que está implicado en la respuesta temprana del hongo a la toxicidad, por lo que podría tener una función sensora además de la de transporte. Los otros miembros de la familia NRAMP identificados en el genoma de *R. irregularis*, *RiSMF1*, *RiSMF2* y *RiSMF3.1*, no pudieron caracterizarse funcionalmente debido a que no complementaron el fenotipo mutante de las levaduras *smf1*Δ y *fet3fet4*Δ, que carecen de sistemas de captación de Mn y de Fe, respectivamente, probablemente debido a un artefacto del sistema heterólogo. Sin embargo, la observación de que *RiSMF1* se reguló transcripcionalmente por Fe y Mn sugiere que está implicado en la homeostasis de estos metales. Concretamente, en el caso del Fe, los mayores niveles de transcripción observados en condiciones de deficiencia de este micronutriente en el ERM indican su participación en la mitigación de la deficiencia de Fe, ya sea incrementando su captación de la solución de suelo o movilizando las reservas vacuolares. Un estudio previo identificó dos transportadores de Fe en *R. irregularis,* las permeasas RiFTR1 and RiFTR2 (Tamayo et al., 2018). RiFTR1 es un transportador de alta afinidad de Fe que se expresa en la membrana plasmática y que está implicado en la absorción de Fe mientras que RiFTR2 está implicada en el mantenimiento de la homeostasis de Fe en condiciones de deficiencia. Todos estos datos indican que *R. irregularis* dispone, al menos de dos sistemas para la adquisición de Fe, los transportadores RiFTR1 y RiNRAMP3.2. Se necesitan estudios adicionales para determinar si RiSMF1 está implicado en la captación del hierro externo o en la movilización de las reservas vacuolares de Fe, así como la contribución relativa de los diferentes transportadores a la absorción de Fe por el hongo.

Aunque la expresión de *RiSMF1* se regula por Mn, la inhibición observada en condiciones de deficiencia es inesperada para un transportador implicado en el transporte del metal hacia el citosol. Sin embargo, patrones de expresión similares de transportadores NRAMP se han observado en otros organismos. Por ejemplo, la expresión del gen *AoNramp1* de *Aspergillus oryzae* incrementa en condiciones tóxicas de Mn (Fan et al., 2021) y la de los genes *CsNRAMP1*, *CsNRAMP4* and *CsNRAMP5* de pepino disminuyó en condiciones de deficiencia (Zhang et al., 2021). Actualmente se desconoce cómo la disponibilidad de Mn regula la expresión de los genes NRAMP. Como se ha descrito para los transportadores smf1p and smf2p de levadura (Portnoy et al., 2000), los genes *SMF* de *R. irregularis* podrían regularse a nivel post-traduccional.

La inducción de la expresión de *RiSMF3.1* en el micelio intrarradical por deficiencia de Mn pone de manifiesto que el hongo necesita incrementar su Mn citosólico en estas condiciones, quizá para proveer a las enzimas dependientes de Mn como la Mn superóxido dismutasa mitocondrial y proteínas implicadas en la glicosilación de proteínas secretoras del aparato de Golgi (Crowley et al., 2000).

El genoma de *R. irregularis* contiene tres genes que potencialmente codifican transportadores de Fe y Mn vacuolares de la familia Ccc1/VIT1, *RiCCC1.1*, *RiCCC1.2* y *RiCCC1.3*. *RiCCC1.1* y *RiCCC1.2* fueron capaces de revertir el fenotipo mutante de la levadura *ccc1*Δ, que carece de transporte vacuolar de Fe, y de a levadura *pmr1*Δ, sensible al manganeso. Solo se pudo ubicar en vacuola a RiCCC1.1 mediante localización en levadura. A pesar de ello, solo la expresión de *RiCCC1.2* se reguló por disponibilidad de Fe y Mn. Como se espera de un transportador vacuolar, la expresión de *RiCCC1.2* disminuyó en ERM bajo condiciones de deficiencia de Fe. Under Fe-deficiency, *Saccharomyces cerevisiae* CCC1 and *Candida glabrata* CCC1 are regulated post-transcriptionally, ScCth2 homologues promote the degradation of *CCC1* mRNA to limit vacuolar Fe storage (Gerwien et al., 2016; Li et al., 2008; Puig et al., 2005). Por otro lado, en las mismas condiciones de deficiencia de Fe, en IRM la expresión incrementó, quizá para limitar el transporte de Fe al hospedador. En este sentido RiCCC1.2 podría tener un papel importante en la simbiosis MA, la proteína SEN de *Lotus japonicus* es un homólogo de ScCCC1 y *Arabidopsis thaliana* VIT1 cuya mutación *Ljsen1* interfiere en la fijación de nitrógeno en la simbiosis rizobial (Hakoyama et al., 2012). Se podría profundizar en el estudio de la función de RiCCC1.2 en el IRM mediante Silenciamiento Génico Inducido por el Hospedador (HIGS) (Helber et al., 2011; Voß et al., 2018). ERM expuesto 16 horas a condiciones tóxicas de Fe, la expresión de *RiCCC1.2* muestra una tendencia al alza, pero las diferencias no son significativas. No se pudo determinar la función de RiCCC1.3, pero el incremento en la expresión transitorio por toxicidad de Fe sugiere que está involucrado en la homeostasis de este metal.

El análisis de la regulación por la simbiosis de la expresión de los genes de *S. lycopersicum* implicados en la homeostasis de Fe también ha sido objeto de esta Tesis Doctoral. La inhibición de la colonización micorrícica en condiciones de deficiencia de Fe y la gran acumulación de Fe detectada en las raíces de las plantas micorrizadas indica que este micronutriente es esencial para el desarrollo de la simbiosis y que el hongo puede actúar como un sumidero de Fe. El aumento de los niveles de transcripción de la reductasa de hierro de membrana plasmática SlFRO1 y del transportador de hierro SlIRT1 en raíces micorrizadas de tomate en condiciones de deficiencia de hierro indican que el desarrollo de la simbiosis aumenta la disponibilidad de hierro en la rizosfera y su captación por las células epidérmicas. En cambio, cuando la concentración de Fe es suficiente la expresión de *SlFRO1* es indetectable y la de *SlIRT1* disminuye en plantas micorrizadas. Esto indica que la micorrización solo mejora la disponibilidad de Fe en condiciones de deficiencia y que en condiciones con suficiente Fe se inhibe la vía directa de captación de Fe por la raíz micorrizada. Una inhibición de la via directa de captación de nutrientes en las raíces micorrizadas se ha descrito también para el fósforo, el nitrógeno y zinc (Coccina et al., 2019; Liu et al., 1998;

Pérez-Tienda et al., 2014). La vía de captación micorrícica de hierro podría estar mediada por el transportador SlNRAMP1, cuya expresión incrementa en raíces micorrizadas, podría mediar la captación de Fe a través de la vía simbiótica o micorrícica a nivel de las células corticales colonizadas por arbúsculos. Sin embargo, se requieren más estudios para confirmar esta hipótesis.

La inhibición transcripcional de la nicotianamina sintasa SlCHLN en raíces de plantas micorrizadas cultivadas en condiciones óptimas de hierro y por deficiencia de Fe indica que estas raíces tienen menor un contenido de nicotianamina (NA), lo que podría explicar la menor translocación de hierro desde la raíz a la parte aérea en estas plantas. En este sentido, se ha comprobado en *Arabidopsis*, que la acumulación de NA incrementa la traslocación de Fe a la parte aérea (Chen et al., 2018; Haydon et al., 2012).

La alta acumulación de Fe observada en las raíces micorrizadas nos llevó a caracterizar genes que codifican proteínas de la familia de los transportadores vacuolares de Fe VIT/VTL de tomate. De los cuatro miembros de la familia VIT/VTL identificados en las bases de datos del genoma del tomate, los genes *SlVIT1*, *SlVIT2* y *SlVTL2* codifican transportadores de Fe que median el transporte del exceso de Fe desde el citosol a la vacuola cuya expresión se inhibe en condiciones de deficiencia. La inhibición de la expresión de los genes *SlVIT1* y *SlVTL1* en las raíces micorrizadas indica que el desarrollo de la simbiosis disminuye la acumulación de Fe en las vacuolas, lo que junto con los altos niveles de Fe detectados en las raíces micorrizadas sugiere que el desarrollo de la simbiosis requiere de altos niveles de este micronutriente. Esta hipótesis se ve avalada por los altos niveles de expresión del transportador RiFTR1 en el micelio intrarradical (Tamayo et al., 2018) y más específicamente en los arbúsculos, como se ha descrito en esta memoria.

Además de su papel en la homeostasis de Fe, los transportadores SlVIT1, SlVIT2 y SlVTL2 junto con SlVIT2 están implicados en la homeostasis de Mn, ya que fueron capaces de revertir la sensibilidad a concentraciones tóxicas de Mn del mutante de levadura *pmr1*Δ que carece de la ATPasa que transporta Mn al Golgi (Lapinskas et al., 1995). La inducción de la expresión de SlVIT2, que media el transporte al aparato de Golgi, pero no de Fe a las vacuolas, en las raíces micorrizadas sugiere que el Mn también es importante en la simbiosis.La observación de que la disponibilidad de Fe regula el desarrollo de las MAs nos llevó a analizar el desarrollo de la colonización micorrícica en el mutante natural de tomate *chloronerva*, defectivo en la síntesis de NA y que tiene la homeostasis de Fe alterada, así como el impacto de las MA sobre el mutante. Se observó que la colonización micorrícica disminuyó en las plantas mutantes y que la micorrización revertía parcialmente el defecto de crecimiento del mutante. Los análisis de

expresión global realizados revelaron que la expresión de los genes relacionados con la simbiosis MA *SlCCD8*, *SlSYMRK*, *SlCaMK* (DMI3), *SlCYCLOPS* (IPD3), *SlRAM1*, *SlRAM2*, *SlEXO84*, *SlEXO70i*, *SlSTR*, *SlPT4* and *SlAMT2.2* disminuyó en las raíces *chln*, lo que concuerda con lo observado histológicamente y mediante RT-qPCR. Teniendo en cuenta el antagonismo fósforo-hierro descrito en varias especies vegetales (Bouain et al., 2019; Briat et al., 2015; Thibaud et al., 2010) y que altas concentraciones de fósforo inhiben la simbiosis MA (Nouri et al., 2014), decidimos analizar los patrones de expresión de genes implicados la respuesta a deficiencia de fosfato. La menor acumulación de los transcritos de estos genes en las raíces no micorrizadas de las plantas mutantes con respecto a las de las plantas mutantes correlaciona con el mayor contenido de fósforo de las plantas mutantes. Todos estos resultados nos llevan a proponer que la menor colonización micorrícica observada en los mutantes *chln* y, por lo tanto, el efecto inhibitorio de la deficiencia de Fe sobre el desarrollo de la simbiosis podría involucrar vías de señalización de Pi.

Por otra parte, los análisis transcriptómicos mostraron que los genes de respuesta a deficiencia de Fe están sobreexpresados en las raíces no micorrizadas de las plantas mutantes *chln,* lo que coincide con observaciones previas de que la respuesta de deficiencia de Fe *chln* está estimulada constitutivamente en el mutante *chln* (Ling et al., 1996). Esto hace que los mutantes acumulen una elevada concentración de Fe en sus tejidos, aunque la carencia de NA en estas plantas hace que este Fe no esté disponible para las células vegetales (Becker et al., 1989, 1995). La expresión de los genes de respuesta de deficiencia a Fe disminuyó en las raíces micorrizadas de estas plantas, lo que concuerda con el hecho de que las plantas micorrizadas mutantes tengan un menor contenido de Fe que las no micorrizadas. Todos estos datos en su conjunto indican que las MAs contribuyen a aumentar la disponibilidad y distribución de Fe en la planta hospedadora.

Por último, teniendo en cuenta que en varias interacciones mutualistas planta-microorganismo se ha demostrado que los transportadores de Fe de alta afinidad del microorganismo son esenciales para el mantenimiento de la interacción (Brear et al., 2020; Johnson et al., 2013; Walton et al., 2020), decidimos analizar el impacto del de la actividad del transportador de alta afinidad RiFTR1 de *R. irregularis* en sobre el desarrollo de la simbiosis micorrícico arbuscular. La sobreexpresión de RiFTR1 incrementó la colonización micorrícica, el número de arbúsculos y la funcionalidad de la simbiosis. Estos resultados sugieren que el Fe captado por RiFTR1 a nivel de los arbúsculos podría actuar como señal para estimular su actividad y desarrollo, así como el crecimiento de las hifas dentro de la raíz. Al igual que se ha descrito para el transportador de fosfato de alta afinidad de *Gigaspora margarita*, proponemos que RiFTR1 podría como un sensor que participaría en las vías de detección y señalización de los

niveles de Fe en *R. irregularis*. Dado que RiFTR1 es un transportador de Fe (Tamayo et al., 2018) y que regula el desarrollo de *R. irregularis* en la raíz podría ser un transceptor. Se requieren más estudios para determinar si RiFTR1 detecta cambios extracelulares de Fe y las rutas de señalización.

El trabajo llevado a cabo en la presente Tesis Doctoral expone la importancia de la homeostasis de Fe, tanto en los hongos micorrícico arbusculares como en la simbiosis MA, y pone de manifiesto algunos de los componentes que la regulan. A pesar de los nuevos conocimientos generados, se requieren más estudios que nos permitan entender en mayor profundidad el papel del Fe en la simbiosis MA.

CONCLUSIONS

1. The *Rhizophagus irregularis* NRAMP family of metal transporters is composed of four members: RiSMF1, RiSMF2, RiSMF3.1 and RiSMF3.2. *RiSMF1* is the most highly expressed gene and it is up-regulated by iron deficiency in the extraradical mycelium. *RiSMF3.1* expression increases by manganese deficiency in the intraradical mycelium, and *RiSMF3.2* encodes a plasma membrane protein that mediates manganese and iron uptake. RiSMF1, RiSMF2, RiSMF3.1 function could not be determined, but their gene expression patterns suggest a role for RiSMF1 in iron homeostasis in the extraradical mycelium and for RiSMF3.1 in manganese homeostasis in the intraradical mycelium.
2. The *Rhizophagus irregularis* genome harbors three genes orthologous to the *Saccharomyces cerevisiae* vacuolar iron transporter ScCcc1: *RiCCC1.1*, *RiCCC1.2* and *RiCCC1.3*. *RiCCC1.1* and *RiCCC1.2* encode vacuolar iron transporters likely involved in mobilization of the vacuolar Fe reserves under iron deficiency and in Fe detoxification under iron toxicity. RiCCC1.1. and RiCCC1.2 rescue manganese sensitivity of the *pmr1*Δ mutant yeast, which indicates that they play a role in manganese tolerance in *Rhizophagus irregularis*. RiCCC1.3 function could not be determined, but its expression patterns suggest that it is involved in iron homeostasis.
3. *Rhizophagus irregularis* intraradical mycelium development and sporulation are inhibited by iron deficiency, which highlights the importance of iron as an essential micronutrient for the fungus and for development of the arbuscular mycorrhizal symbiosis.
4. Increased transcript levels of the tomato plasma membrane ferric reductase SlFRO1 and of the iron transporter SlIRT1 under iron deficiency in mycorrhizal roots indicates that development of the symbiosis increases iron bioavailability in the rhizosphere and uptake by the epidermal cells. Down-regulation of SlIRT1 expression in mycorrhizal roots under iron-sufficient conditions suggests an inhibition of the direct iron uptake pathway. The mycorrhizal iron uptake pathway could be mediated the plasma membrane SlNRAMP1 transporter that is up-regulated in mycorrhizal roots under optimal conditions.
5. Down-regulation of the nicotianamine synthase SlCHLN gene in roots of mycorrhizal plants grown under iron sufficient conditions and by iron deficiency indicates a lower nicotianamine content of these roots, which could explain the reduced root to shoot iron translocation in these plants.
6. Four members of the *Solanum lycopersicum* VIT/VTL family of vacuolar iron transporters have been characterized. *SlVIT1*, *SlVTL1* and *SlVTL2* encode functional iron and manganese transporters while *SlVIT2* encodes a manganese transporter. Down-

regulation of *SlVIT1*, *SlVTL1* and *SlVTL2* in non-mycorrhizal roots by iron deficiency indicates a lower vacuolar iron compartmentalization, an effect that was partially reverted for *SlVIT1* and *SlVTL2* in mycorrhizal roots. Under iron optimal conditions, *SlVIT1* and *SlVTL1* expression is down-regulated in mycorrhizal roots while expression of the manganese transporter *SlVIT2* is up-regulated.

7. Growth defect of the tomato mutant *chloronerva,* unable to synthesize nicotianamine and affected in the regulation of iron metabolism, is partially reverted in mycorrhizal plants. Development of the symbiosis reduced the number of differentially expressed genes in roots of the *chloronerva* mutant plants compared to the wild-type. Over-expression of iron deficiency response genes in *chloronerva* roots was mitigated by mycorrhization, which suggests that arbuscular mycorrhiza contributes to increase iron availability and distribution in *chloronerva* mutant plants.
8. Inhibition of mycorrhizal colonization of the iron-inefficient tomato mutant *chloronerva* reveals the significance of iron homeostasis for arbuscular mycorrhizal formation.
9. Host induced overexpression of the *Rhizophagus irregularis* plasma membrane iron transporter RiFTR1 increases mycorrhizal colonization of *Medicago truncatula* composite plants.

CONCLUSIONES

1. La familia de transportadores de metales NRAMP de *Rhizophagus irregularis* está compuesta por cuatro miembros: RiSMF1, RiSMF2, RiSMF3.1 y RiSMF3.2. *RiSMF1* es el gen que presenta mayores niveles de expresión y se activa transcripcionalmente en el micelio extrarradical en condiciones de deficiencia de hierro. La expresión de *RiSMF3.1* aumenta por la deficiencia de manganeso en el micelio intrarradical. *RiSMF3.2* codifica una proteína de membrana plasmática que media la captación de manganeso y hierro. Aunque no se pudo determinar la función de RiSMF1, RiSMF2, RiSMF3.1, sus patrones de expresión génica sugieren para RiSMF1 un papel en la homeostasis de hierro en el micelio extrarradical y para RiSMF3.1 en la homeostasis de manganeso en el micelio intrarradical.
2. El genoma de *Rhizophagus irregularis* contiene tres genes ortólogos del transportador de hierro vacuolar de *Saccharomyces cerevisiae* ScCcc1: *RiCCC1.1*, *RiCCC1.2* y *RiCCC1.3*. *RiCCC1.1* y *RiCCC1.2* codifican transportadores de hierro de vacuola, probablemente, involucrados en la movilización de las reservas vacuolares de Fe en situaciones de deficiencia de hierro y en detoxificación del exceso del metal condiciones de toxicidad. RiCCC1.1 y RiCCC1.2 revierten la sensibilidad a manganeso del mutante de levadura *pmr1*Δ, lo que indica que desempeñan un papel en la tolerancia *Rhizophagus irregularis* al manganeso. No se pudo determinar la función de RiCCC1.3, pero sus patrones de expresión sugieren que está involucrado en la homeostasis de hierro.
3. El desarrollo del micelio intrarradical y la esporulación de *Rhizophagus irregularis* se inhiben por la deficiencia de hierro, lo que refleja la importancia del hierro como micronutriente esencial en el hongo y en la simbiosis micorrícica arbuscular.
4. El aumento de los niveles de transcripción de la reductasa de hierro de membrana plasmática SlFRO1 y del transportador de hierro SlIRT1 en raíces micorrizadas de tomate en condiciones de deficiencia de hierro indican que el desarrollo de la simbiosis aumenta la disponibilidad de hierro en la rizosfera y su captación por las células epidérmicas. La inhibición de la expresión de *SlIRT1* en raíces micorrizadas en condiciones óptimas de hierro sugiere una inhibición de la vía directa de captación de este nutriente. La vía de captación micorrícica de hierro podría estar mediada por el transportador de membrana plasmática SlNRAMP1, cuya expresión incrementa en raíces micorrizadas.
5. La inhibición transcripcional de la nicotianamina sintasa SlCHLN en raíces de plantas micorrizadas cultivadas en condiciones óptimas de hierro y por deficiencia de Fe indica que estas raíces tienen menor un contenido de nicotianamina, lo que podría explicar la menor translocación de hierro desde la raíz a la parte aérea en estas plantas.

6. Se han caracterizado cuatro miembros de la familia de transportadores de hierro vacuolares *Solanum lycopersicum* VIT/VTL. *SlVIT1*, *SlVTL1* y *SlVTL2* codifican transportadores de hierro y manganeso, mientras que *SlVIT2* codifica un transportador de manganeso. La inhibición de la expresión de *SlVIT1*, *SlVTL1* y *SlVTL2* en raíces no micorrizadas por condiciones de deficiencia de hierro indica una menor compartimentación de hierro en las vacuolas de estas plantas, efecto que se revirtió parcialmente para *SlVIT1* y *SlVTL2* en las raíces micorrizadas. En condiciones óptimas de hierro, la expresión de *SlVIT1* y *SlVTL1* disminuyó en las raíces micorrizadas, mientras que la expresión del transportador de manganeso *SlVIT2* incrementó.
7. El defecto de crecimiento del mutante de tomate *chloronerva*, incapaz de sintetizar nicotianamina y afectado en la regulación del metabolismo de hierro, se revirtió parcialmente en las plantas micorrizadas. El desarrollo de la simbiosis redujo el número de genes expresados diferencialmente en las raíces de las plantas mutantes y con respecto al silvestre. La sobreexpresión de los genes de respuesta a deficiencia de hierro en raíces de las plantas *chloronerva* se mitigó en raíces micorrizadas, lo que sugiere que las micorrizas arbusculares contribuyen a aumentar la disponibilidad y distribución de Fe en los mutantes *chloronerva*.
8. La inhibición de la colonización micorrícica del mutante de tomate *chloronerva,* incapazaz de regular el metabolismo del hierro, revela la importancia de la homeostasis de este micronutriente para la formación de las micorrizas arbusculares.
9. La sobreexpresión inducida por el huésped del transportador de hierro de membrana plasmática RiFTR1 de *Rhizophagus irregularis* aumenta la colonización micorrícica de plantas compuestas de *Medicago truncatula*.

BIBLIOGRAFÍA GENERAL

Akiyama, K., Matsuzaki, K., & Hayashi, H. (2005). Plant sesquiterpenes induce hyphal branching in arbuscular mycorrhizal fungi. *Nature*, *435*(7043), 824-827. https://doi.org/10.1038/nature03608

Alexander, T., Toth, R., Meier, R., & Weber, H. C. (1989). Dynamics of arbuscule development and degeneration in onion, bean, and tomato with reference to vesicular–arbuscular mycorrhizae in grasses. *Canadian Journal of Botany*, *67*(8), 2505-2513. https://doi.org/10.1139/b89-320

Aroca, R., Porcel, R., & Ruiz-Lozano, J. M. (2007). How does arbuscular mycorrhizal symbiosis regulate root hydraulic properties and plasma membrane aquaporins in *Phaseolus vulgaris* under drought, cold or salinity stresses? *New Phytologist*, *173*(4), 808-816. https://doi.org/10.1111/j.1469-8137.2006.01961.x

Artursson, V., Finlay, R. D., & Jansson, J. K. (2006). Interactions between arbuscular mycorrhizal fungi and bacteria and their potential for stimulating plant growth. *Environmental Microbiology*, *8*(1), 1-10. https://doi.org/10.1111/j.1462-2920.2005.00942.x

Atkinson, A., & Guerinot, M. lou. (2011). Metal Transport. En *Plant Cell Monographs* (Vol. 19, pp. 303-330). Springer, Berlin, Heidelberg. https://doi.org/10.1007/978-3-642-13431-9_14

Azcón-Aguilar, C., Bago, B., & Barea, J. M. (1999). Saprophytic Growth of Arbuscular Mycorrhizal Fungi. En *Mycorrhiza* (pp. 391-408). Springer Berlin Heidelberg. https://doi.org/10.1007/978-3-662-03779-9_16

Bago, B. (2000). Putative sites for nutrient uptake in arbuscular mycorrhizal fungi. *Plant and Soil*, *226*, 263-274. https://doi.org/10.1023/A:1026456818903

Bago, B., Azcón-Aguilar, C., Goulet, A., & Piche, Y. (1998). Branched absorbing structures (BAS): a feature of the extraradical mycelium of symbiotic arbuscular mycorrhizal fungi. *New Phytologist*, *139*(2), 375-388. https://doi.org/10.1046/j.1469-8137.1998.00199.x

Bago, B., Azcón-Aguilar, C., & Piché, Y. (1998). Architecture and developmental dynamics of the external mycelium of the arbuscular mycorrhizal fungus *Glomus intraradices* grown under monoxenic conditions. *Mycologia*, *90*(1), 52-62. https://doi.org/10.1080/00275514.1998.12026878

Barea, J. M., & Azcón-Aguilar, C. (2013). Evolution, biology and ecological effects of arbuscular mycorrhizas. En *Symbiosis: Evolution, biology and ecological effects* (pp. 1-34). Nova Science Publishers, Inc.

Barea, J.-M., Ferrol, N., Azcón-Aguilar, C., & Azcón, R. (2008). *Mycorrhizal symbioses* (pp. 143-163). Springer, Dordrecht. https://doi.org/10.1007/978-1-4020-8435-5_7

Barea, J.-M., Pozo, M. J., Azcón, R., & Azcón-Aguilar, C. (2005). Microbial co-operation in the rhizosphere. *Journal of Experimental Botany*, *56*(417), 1761-1778. https://doi.org/10.1093/jxb/eri197

Bécard, G., & Pfeffer, P. E. (1993). Status of nuclear division in arbuscular mycorrhizal fungi during in vitro development. *Protoplasma*, *174*(1-2), 62-68. https://doi.org/10.1007/BF01404043

Becker, R., Fritz, E., & Manteuffel, R. (1995). Subcellular Localization and Characterization of Excessive Iron in the Nicotianamine-less Tomato Mutant chloronerva. *Plant Physiology*, *108*(1), 269–275. https://doi.org/10.1104/pp.108.1.269

Becker, R., Pich, A., Scholz, G., & Seifert, K. (1989). Influence of nicotianamine and iron supply on formation and elongation of adventitious roots in hypocotyl cuttings of the tomato mutant "chloronerva" (Lycopersicon esculentum). *Physiologia Plantarum*, *76*(1), 47–52. https://doi.org/10.1111/j.1399-3054.1989.tb05451.x

Bianciotto, V., Lumini, E., Bonfante, P., & Vandamme, P. (2003). 'Candidatus Glomeribacter gigasporarum' gen. nov., sp. nov., an endosymbiont of arbuscular mycorrhizal fungi. *International Journal of Systematic and Evolutionary Microbiology*, *53*(1), 121-124. https://doi.org/10.1099/ijs.0.02382-0

Bianciotto, V., Lumini, E., Lanfranco, L., Minerdi, D., Bonfante, P., & Perotto, S. (2000). Detection and Identification of Bacterial Endosymbionts in Arbuscular Mycorrhizal Fungi Belonging to the Family Gigasporaceae. *Applied and Environmental Microbiology*, *66*(10), 4503-4509. https://doi.org/10.1128/AEM.66.10.4503-4509.2000

Bonfante, P., & Venice, F. (2020). Mucoromycota: going to the roots of plant-interacting fungi. *Fungal Biology Reviews*, *34*(2), 100-113. https://doi.org/10.1016/j.fbr.2019.12.003

Bouain, N., Krouk, G., Lacombe, B., & Rouached, H. (2019). Getting to the Root of Plant Mineral Nutrition: Combinatorial Nutrient Stresses Reveal Emergent Properties. *Trends in Plant Science*, *24*(6), 542–552. https://doi.org/10.1016/j.tplants.2019.03.008

Bravo, A., Brands, M., Wewer, V., Dörmann, P., & Harrison, M. J. (2017). Arbuscular mycorrhiza-specific enzymes FatM and <scp>RAM</scp> 2 fine-tune lipid biosynthesis to promote development of arbuscular mycorrhiza. *New Phytologist*, *214*(4), 1631-1645. https://doi.org/10.1111/nph.14533

Brear, E. M., Bedon, F., Gavrin, A., Kryvoruchko, I. S., Torres-Jerez, I., Udvardi, M. K., Day, D. A., & Smith, P. M. C. (2020). GmVTL1a is an iron transporter on the symbiosome membrane of soybean with an important role in nitrogen fixation. *New Phytologist*, *228*(2), 667–681. https://doi.org/10.1111/nph.16734

Breuillin-Sessoms, F., Floss, D. S., Gomez, S. K., Pumplin, N., Ding, Y., Levesque-Tremblay, V., Noar, R. D., Daniels, D. A., Bravo, A., Eaglesham, J. B., Benedito, V. A., Udvardi, M. K., & Harrison, M. J. (2015). Suppression of Arbuscule Degeneration in *Medicago truncatula phosphate transporter4* Mutants Is Dependent on the Ammonium Transporter 2 Family Protein AMT2;3. *The Plant Cell*, *27*(4), 1352-1366. https://doi.org/10.1105/tpc.114.131144

Briat, J.-F., Dubos, C., & Gaymard, F. (2015). Iron nutrition, biomass production, and plant product quality. *Trends in Plant Science*, *20*(1), 33–40. https://doi.org/10.1016/j.tplants.2014.07.005

Brundrett, M. C., & Tedersoo, L. (2018). Evolutionary history of mycorrhizal symbioses and global host plant diversity. *New Phytologist*, *220*(4), 1108-1115. https://doi.org/10.1111/nph.14976

Calabrese, S., Pérez-Tienda, J., Ellerbeck, M., Arnould, C., Chatagnier, O., Boller, T., Schüßler, A., Brachmann, A., Wipf, D., Ferrol, N., & Courty, P.-E. (2016). GintAMT3 – a Low-Affinity Ammonium Transporter of the Arbuscular Mycorrhizal *Rhizophagus irregularis*. *Frontiers in Plant Science*, *7*, 679. https://doi.org/10.3389/fpls.2016.00679

Calvo-Polanco, M., Molina, S., Zamarreño, A. M., García-Mina, J. M., & Aroca, R. (2014). The Symbiosis with the Arbuscular Mycorrhizal Fungus Rhizophagus irregularis Drives Root Water Transport in Flooded Tomato Plants. *Plant and Cell Physiology*, *55*(5), 1017-1029. https://doi.org/10.1093/pcp/pcu035

Calvo-Polanco, M., Sánchez-Castro, I., Cantos, M., García, J. L., Azcón, R., Ruiz-Lozano, J. M., Beuzón, C. R., & Aroca, R. (2016). Effects of different arbuscular mycorrhizal fungal backgrounds and soils on olive plants growth and water relation properties under well-watered and drought conditions. *Plant, Cell & Environment*, *39*(11), 2498-2514. https://doi.org/10.1111/pce.12807

Cappellazzo, G., Lanfranco, L., Fitz, M., Wipf, D., & Bonfante, P. (2008). Characterization of an Amino Acid Permease from the Endomycorrhizal Fungus *Glomus mosseae*. *Plant Physiology*, *147*(1), 429-437. https://doi.org/10.1104/pp.108.117820

Caris, C., Hördt, W., Hawkins, H.-J., Römheld, V., & George, E. (1998). Studies of iron transport by arbuscular mycorrhizal hyphae from soil to peanut and sorghum plants. *Mycorrhiza*, *8*(1), 35-39. https://doi.org/10.1007/s005720050208

Cavagnaro, T. R. (2014). *Arbuscular Mycorrhizas and Their Role in Plant Zinc Nutrition* (pp. 189-200). Springer, Berlin, Heidelberg. https://doi.org/10.1007/978-3-662-45370-4_11

Cellier, M., & Gros, P. (2004). *The NRAMP Family*. Springer Science & Business Media.

Chen, E. C., Mathieu, S., Hoffrichter, A., Sedzielewska-Toro, K., Peart, M., Pelin, A., Ndikumana, S., Ropars, J., Dreissig, S., Fuchs, J., Brachmann, A., & Corradi, N. (2018). Single nucleus sequencing reveals evidence of inter-nucleus recombination in arbuscular mycorrhizal fungi. *ELife*, *7*. https://doi.org/10.7554/eLife.39813

Cheng, L., Wang, F., Shou, H., Huang, F., Zheng, L., He, F., Li, J., Zhao, F.-J., Ueno, D., Ma, J. F., & Wu, P. (2007). Mutation in Nicotianamine Aminotransferase Stimulated the Fe(II) Acquisition System and Led to Iron Accumulation in Rice. *Plant Physiology*, *145*(4), 1647-1657. https://doi.org/10.1104/pp.107.107912

Chen, L., Wang, G., Chen, P., Zhu, H., Wang, S., & Ding, Y. (2018). Shoot-Root Communication Plays a Key Role in Physiological Alterations of Rice (Oryza sativa) Under Iron Deficiency. *Frontiers in Plant Science*, *9*. https://doi.org/10.3389/fpls.2018.00757

Cipollini, D., Rigsby, C. M., & Barto, E. K. (2012). Microbes as Targets and Mediators of Allelopathy in Plants. *Journal of Chemical Ecology*, *38*(6), 714-727. https://doi.org/10.1007/s10886-012-0133-7

Coccina, A., Cavagnaro, T. R., Pellegrino, E., Ercoli, L., McLaughlin, M. J., & Watts-Williams, S. J. (2019). The mycorrhizal pathway of zinc uptake contributes to zinc accumulation in barley and wheat grain. *BMC Plant Biology*, *19*(1), 133. https://doi.org/10.1186/s12870-019-1741-y

Connorton, J. M., Jones, E. R., Rodríguez-Ramiro, I., Fairweather-Tait, S., Uauy, C., & Balk, J. (2017). Wheat Vacuolar Iron Transporter TaVIT2 Transports Fe and Mn and Is Effective for Biofortification. *Plant Physiology*, *174*(4), 2434-2444. https://doi.org/10.1104/pp.17.00672

Cooke, J. C., Gemma, J. N., & Koske, R. E. (1987). Observations of Nuclei in Vesicular-Arbuscular Mycorrhizal Fungi. *Mycologia*, *79*(2), 331-333. https://doi.org/10.1080/00275514.1987.12025715

Cooper, K. M., & Tinker, P. B. (1978). Translocation and transfer of nutrients in vesicular-arbuscular mycorrhizas. ii. uptake and translocation of phosphorus, zinc and sulphur. *New Phytologist*, *81*(1), 43-52. https://doi.org/10.1111/j.1469-8137.1978.tb01602.x

Corradi, N., & Brachmann, A. (2017). Fungal Mating in the Most Widespread Plant Symbionts? *Trends in Plant Science*, *22*(2), 175-183. https://doi.org/10.1016/j.tplants.2016.10.010

Corrêa, A., Cruz, C., Pérez-Tienda, J., & Ferrol, N. (2014). Shedding light onto nutrient responses of arbuscular mycorrhizal plants: Nutrient interactions may lead to unpredicted outcomes of the symbiosis. *Plant Science*, *221-222*, 29-41. https://doi.org/10.1016/j.plantsci.2014.01.009

Crowley, J. D., Traynor, D. A., & Weatherburn, D. C. (2000). Enzymes and Protein Containing Manganese: An Overview. In *Metal Ions in Biological Systems* (Vol. 37, pp. 209–278).

Cruz, C., Egsgaard, H., Trujillo, C., Ambus, P., Requena, N., Martins-Loução, M. A., & Jakobsen, I. (2007). Enzymatic Evidence for the Key Role of Arginine in Nitrogen Translocation by Arbuscular Mycorrhizal Fungi. *Plant Physiology*, *144*(2), 782-792. https://doi.org/10.1104/pp.106.090522

de Silva, D. M., Askwith, C. C., Eide, D., & Kaplan, J. (1995). The FET3 Gene Product Required for High Affinity Iron Transport in Yeast Is a Cell Surface Ferroxidase. *Journal of Biological Chemistry*, *270*(3), 1098-1101. https://doi.org/10.1074/jbc.270.3.1098

Desirò, A., Salvioli, A., Ngonkeu, E. L., Mondo, S. J., Epis, S., Faccio, A., Kaech, A., Pawlowska, T. E., & Bonfante, P. (2014). Detection of a novel intracellular microbiome hosted in arbuscular mycorrhizal fungi. *The ISME Journal*, *8*(2), 257-270. https://doi.org/10.1038/ismej.2013.151

DiDonato, R. J., Roberts, L. A., Sanderson, T., Eisley, R. B., & Walker, E. L. (2004). *Arabidopsis Yellow Stripe-Like2 (YSL2)*: a metal-regulated gene encoding a plasma membrane transporter of nicotianamine-metal complexes. *The Plant Journal*, *39*(3), 403-414. https://doi.org/10.1111/j.1365-313X.2004.02128.x

Eivazi, F., & Weir, C. C. (1989). Phosphorus and mycorrhizal interaction on uptake of P and trace elements by maize. *Fertilizer Research*, *21*(1), 19-22. https://doi.org/10.1007/BF01054731

Ezawa, T., Cavagnaro, T. R., Smith, S. E., Smith, F. A., & Ohtomo, R. (2004). Rapid accumulation of polyphosphate in extraradical hyphae of an arbuscular mycorrhizal fungus as revealed by histochemistry and a polyphosphate kinase/luciferase system. *New Phytologist*, *161*(2), 387-392. https://doi.org/10.1046/j.1469-8137.2003.00966.x

Fan, J., Zhang, H., Li, Y., Chen, Z., Chen, T., Zeng, B., & Zhang, Z. (2021). Identification and characterization of Nramp transporter AoNramp1 in *Aspergillus oryzae*. *Biotech*, *11*(10), 452. https://doi.org/10.1007/s13205-021-02998-z

Ferrol, N., Azcón-Aguilar, C., & Pérez-Tienda, J. (2019). Review: Arbuscular mycorrhizas as key players in sustainable plant phosphorus acquisition: An overview on the mechanisms involved. *Plant Science*, *280*, 441-447. https://doi.org/10.1016/j.plantsci.2018.11.011

Ferrol, N., Tamayo, E., & Vargas, P. (2016). The heavy metal paradox in arbuscular mycorrhizas: from mechanisms to biotechnological applications. *Journal of Experimental Botany*, *67*(22), 6253-6265. https://doi.org/10.1093/jxb/erw403

Flis, P., Ouerdane, L., Grillet, L., Curie, C., Mari, S., & Lobinski, R. (2016). Inventory of metal complexes circulating in plant fluids: a reliable method based on HPLC coupled with dual elemental and high-resolution molecular mass spectrometric detection. *New Phytologist*, *211*(3), 1129-1141. https://doi.org/10.1111/nph.13964

Forbes, P. J., Millam, S., Hooker, J. E., & Harrier, L. A. (1998). Transformation of the arbuscular mycorrhiza Gigaspora rosea by particle bombardment. *Mycological Research*, *102*(4), 497-501. https://doi.org/10.1017/S0953756297005273

Genre, A., Chabaud, M., Balzergue, C., Puech-Pagès, V., Novero, M., Rey, T., Fournier, J., Rochange, S., Bécard, G., Bonfante, P., & Barker, D. G. (2013). Short-chain chitin oligomers from arbuscular mycorrhizal fungi trigger nuclear <scp>C</scp> a $^{2+}$ spiking in <*scp*>*M*</*scp*> *edicago truncatula* roots and their production is enhanced by strigolactone. *New Phytologist*, *198*(1), 190-202. https://doi.org/10.1111/nph.12146

Genre, A., Chabaud, M., Faccio, A., Barker, D. G., & Bonfante, P. (2008). Prepenetration Apparatus Assembly Precedes and Predicts the Colonization Patterns of Arbuscular Mycorrhizal Fungi within the Root Cortex of Both *Medicago truncatula* and *Daucus carota* . *The Plant Cell*, *20*(5), 1407-1420. https://doi.org/10.1105/tpc.108.059014

Genre, A., & Russo, G. (2016). Does a Common Pathway Transduce Symbiotic Signals in Plant–Microbe Interactions? *Frontiers in Plant Science*, *7*, 96. https://doi.org/10.3389/fpls.2016.00096

Gerwien, F., Safyan, A., Wisgott, S., Hille, F., Kaemmer, P., Linde, J., Brunke, S., Kasper, L., & Hube, B. (2016). A Novel Hybrid Iron Regulation Network Combines Features from Pathogenic and Nonpathogenic Yeasts. *MBio*, *7*(5). https://doi.org/10.1128/mBio.01782-16

Giovannetti, M., Fortuna, P., Citernesi, A. S., Morini, S., & Nuti, M. P. (2001). The occurrence of anastomosis formation and nuclear exchange in intact arbuscular mycorrhizal networks. *New Phytologist*, *151*(3), 717-724. https://doi.org/10.1046/j.0028-646x.2001.00216.x

Gómez-Gallego, T., Benabdellah, K., Merlos, M. A., Jiménez-Jiménez, A. M., Alcon, C., Berthomieu, P., & Ferrol, N. (2019). The *Rhizophagus irregularis* Genome Encodes Two CTR Copper Transporters That Mediate Cu Import Into the Cytosol and a CTR-Like Protein Likely Involved in Copper Tolerance. *Frontiers in Plant Science*, *10*, 604. https://doi.org/10.3389/fpls.2019.00604

Gomez, S. K., Javot, H., Deewatthanawong, P., Torres-Jerez, I., Tang, Y., Blancaflor, E. B., Udvardi, M. K., & Harrison, M. J. (2009). Medicago truncatula and Glomus intraradices gene expression in cortical cells harboring arbuscules in the arbuscular mycorrhizal symbiosis. *BMC Plant Biology*, *9*(1), 10. https://doi.org/10.1186/1471-2229-9-10

Govindarajulu, M., Pfeffer, P. E., Jin, H., Abubaker, J., Douds, D. D., Allen, J. W., Bücking, H., Lammers, P. J., & Shachar-Hill, Y. (2005). Nitrogen transfer in the arbuscular mycorrhizal symbiosis. *Nature*, *435*(7043), 819-823. https://doi.org/10.1038/nature03610

Grotz, N., & Guerinot, M. lou. (2006). Molecular aspects of Cu, Fe and Zn homeostasis in plants. *Biochimica et Biophysica Acta (BBA) - Molecular Cell Research*, *1763*(7), 595-608. https://doi.org/10.1016/j.bbamcr.2006.05.014

Guether, M., Balestrini, R., Hannah, M., He, J., Udvardi, M. K., & Bonfante, P. (2009). Genome-wide reprogramming of regulatory networks, transport, cell wall and membrane biogenesis during arbuscular mycorrhizal symbiosis in *Lotus japonicus*. *New Phytologist*, *182*(1), 200-212. https://doi.org/10.1111/j.1469-8137.2008.02725.x

Haas, H., Eisendle, M., & Turgeon, B. G. (2008). Siderophores in Fungal Physiology and Virulence. *Annual Review of Phytopathology*, *46*(1), 149-187. https://doi.org/10.1146/annurev.phyto.45.062806.094338

Hakoyama, T., Niimi, K., Yamamoto, T., Isobe, S., Sato, S., Nakamura, Y., Tabata, S., Kumagai, H., Umehara, Y., Brossuleit, K., Petersen, T. R., Sandal, N., Stougaard, J., Udvardi, M. K., Tamaoki, M., Kawaguchi, M., Kouchi, H., & Suganuma, N. (2012). The Integral Membrane Protein SEN1 is Required for Symbiotic Nitrogen Fixation in Lotus japonicus Nodules. *Plant and Cell Physiology*, *53*(1), 225–236. https://doi.org/10.1093/pcp/pcr167

Halary, S., Malik, S.-B., Lildhar, L., Slamovits, C. H., Hijri, M., & Corradi, N. (2011). Conserved Meiotic Machinery in Glomus spp., a Putatively Ancient Asexual Fungal Lineage. *Genome Biology and Evolution*, *3*, 950-958. https://doi.org/10.1093/gbe/evr089

Harrison, M. J., Dewbre, G. R., & Liu, J. (2002). A Phosphate Transporter from *Medicago truncatula* Involved in the Acquisition of Phosphate Released by Arbuscular Mycorrhizal Fungi. *The Plant Cell*, *14*(10), 2413-2429. https://doi.org/10.1105/tpc.004861

Haselwandter, K., Haas, H., Häninger, G., & Winkelmann, G. (2020). Siderophores in plant root tissue: Tagetes patula nana colonized by the arbuscular mycorrhizal fungus Gigaspora margarita. *BioMetals*, *33*(2-3), 137-146. https://doi.org/10.1007/s10534-020-00238-0

Haydon, M. J., Kawachi, M., Wirtz, M., Hillmer, S., Hell, R., & Krämer, U. (2012). Vacuolar Nicotianamine Has Critical and Distinct Roles under Iron Deficiency and for Zinc Sequestration in *Arabidopsis*. *The Plant Cell*, *24*(2), 724–737. https://doi.org/10.1105/tpc.111.095042

Helber, N., & Requena, N. (2008). Expression of the fluorescence markers DsRed and GFP fused to a nuclear localization signal in the arbuscular mycorrhizal fungus *Glomus intraradices*. *New Phytologist*, *177*(2), 537-548. https://doi.org/10.1111/j.1469-8137.2007.02257.x

Helber, N., Wippel, K., Sauer, N., Schaarschmidt, S., Hause, B., & Requena, N. (2011). A Versatile Monosaccharide Transporter That Operates in the Arbuscular Mycorrhizal Fungus *Glomus* sp Is Crucial for the Symbiotic Relationship with Plants . *The Plant Cell*, *23*(10), 3812-3823. https://doi.org/10.1105/tpc.111.089813

Hijikata, N., Murase, M., Tani, C., Ohtomo, R., Osaki, M., & Ezawa, T. (2010). Polyphosphate has a central role in the rapid and massive accumulation of phosphorus in extraradical mycelium of an arbuscular mycorrhizal fungus. *The New Phytologist*, *186*(2), 285-289. https://www.jstor.org/stable/27797549

Hosny, M., Gianinazzi-Pearson, V., & Dulieu, H. (1998). Nuclear DNA content of 11 fungal species in Glomales. *Genome*, *41*(3), 422-428. https://doi.org/10.1139/g98-038

Hoysted, G. A., Kowal, J., Jacob, A., Rimington, W. R., Duckett, J. G., Pressel, S., Orchard, S., Ryan, M. H., Field, K. J., & Bidartondo, M. I. (2018). A mycorrhizal revolution. *Current Opinion in Plant Biology*, *44*, 1-6. https://doi.org/10.1016/j.pbi.2017.12.004

Ishimaru, Y., Suzuki, M., Tsukamoto, T., Suzuki, K., Nakazono, M., Kobayashi, T., Wada, Y., Watanabe, S., Matsuhashi, S., Takahashi, M., Nakanishi, H., Mori, S., & Nishizawa, N. K. (2006). Rice plants take up iron as an Fe^{3+} -phytosiderophore and as Fe^{2+}. *The Plant Journal*, *45*(3), 335-346. https://doi.org/10.1111/j.1365-313X.2005.02624.x

Jany, J., & Pawlowska, T. E. (2010). Multinucleate Spores Contribute to Evolutionary Longevity of Asexual Glomeromycota. *The American Naturalist*, *175*(4), 424-435. https://doi.org/10.1086/650725

Javot, H., Penmetsa, R. V., Terzaghi, N., Cook, D. R., & Harrison, M. J. (2007). A *Medicago truncatula* phosphate transporter indispensable for the arbuscular mycorrhizal symbiosis. *Proceedings of the National Academy of Sciences*, *104*(5), 1720-1725. https://doi.org/10.1073/pnas.0608136104

Jin, H., Pfeffer, P. E., Douds, D. D., Piotrowski, E., Lammers, P. J., & Shachar-Hill, Y. (2005). The uptake, metabolism, transport and transfer of nitrogen in an arbuscular mycorrhizal symbiosis. *New Phytologist*, *168*(3), 687-696. https://doi.org/10.1111/j.1469-8137.2005.01536.x

Johnson, L. J., Koulman, A., Christensen, M., Lane, G. A., Fraser, K., Forester, N., Johnson, R. D., Bryan, G. T., & Rasmussen, S. (2013). An Extracellular Siderophore Is Required to Maintain the Mutualistic Interaction of Epichloë festucae with Lolium perenne. *PLoS Pathogens*, *9*(5), e1003332. https://doi.org/10.1371/journal.ppat.1003332

Jung, S. C., Martinez-Medina, A., Lopez-Raez, J. A., & Pozo, M. J. (2012). Mycorrhiza-Induced Resistance and Priming of Plant Defenses. *Journal of Chemical Ecology*, *38*(6), 651-664. https://doi.org/10.1007/s10886-012-0134-6

Juwarkar, A. A., & Jambhulkar, H. P. (2008). Phytoremediation of coal mine spoil dump through integrated biotechnological approach. *Bioresource Technology*, *99*(11), 4732-4741. https://doi.org/10.1016/j.biortech.2007.09.060

Kabir, A. H., Debnath, T., Das, U., Prity, S. A., Haque, A., Rahman, M. M., & Parvez, M. S. (2020). Arbuscular mycorrhizal fungi alleviate Fe-deficiency symptoms in sunflower by increasing iron uptake and its availability along with antioxidant defense. *Plant Physiology and Biochemistry*, *150*, 254-262. https://doi.org/10.1016/j.plaphy.2020.03.010

Kamel, L., Keller-Pearson, M., Roux, C., & Ané, J. (2017). Biology and evolution of arbuscular mycorrhizal symbiosis in the light of genomics. *New Phytologist*, *213*(2), 531-536. https://doi.org/10.1111/nph.14263

Kameoka, H., Maeda, T., Okuma, N., & Kawaguchi, M. (2019). Structure-Specific Regulation of Nutrient Transport and Metabolism in Arbuscular Mycorrhizal Fungi. *Plant and Cell Physiology*, *60*(10), 2272-2281. https://doi.org/10.1093/pcp/pcz122

Keymer, A., & Gutjahr, C. (2018). Cross-kingdom lipid transfer in arbuscular mycorrhiza symbiosis and beyond. *Current Opinion in Plant Biology*, *44*, 137-144. https://doi.org/10.1016/j.pbi.2018.04.005

Kikuchi, Y., Hijikata, N., Ohtomo, R., Handa, Y., Kawaguchi, M., Saito, K., Masuta, C., & Ezawa, T. (2016). Aquaporin-mediated long-distance polyphosphate translocation directed towards the host in arbuscular mycorrhizal symbiosis: application of virus-induced gene silencing. *New Phytologist*, *211*(4), 1202-1208. https://doi.org/10.1111/nph.14016

Kim, S. A., & Guerinot, M. lou. (2007). Mining iron: Iron uptake and transport in plants. *FEBS Letters*, *581*(12), 2273-2280. https://doi.org/10.1016/j.febslet.2007.04.043

Kim, S. A., Punshon, T., Lanzirotti, A., Li, L., Alonso, J. M., Ecker, J. R., Kaplan, J., & Guerinot, M. lou. (2006). Localization of Iron in *Arabidopsis* Seed Requires the Vacuolar Membrane Transporter VIT1. *Science*, *314*(5803), 1295-1298. https://doi.org/10.1126/science.1132563

Klironomos, J. N., McCune, J., Hart, M., & Neville, J. (2000). The influence of arbuscular mycorrhizae on the relationship between plant diversity and productivity. *Ecology Letters*, *3*(2), 137-141. https://doi.org/10.1046/j.1461-0248.2000.00131.x

Kobae, Y., Tamura, Y., Takai, S., Banba, M., & Hata, S. (2010). Localized Expression of Arbuscular Mycorrhiza-Inducible Ammonium Transporters in Soybean. *Plant and Cell Physiology*, *51*(9), 1411-1415. https://doi.org/10.1093/pcp/pcq099

Kobae, Y., Tomioka, R., Tanoi, K., Kobayashi, N. I., Ohmori, Y., Nishida, S., & Fujiwara, T. (2014). Selective induction of putative iron transporters, *OPT8a* and *OPT8b* , in maize by mycorrhizal colonization. *Soil Science and Plant Nutrition*, *60*(6), 843-847. https://doi.org/10.1080/00380768.2014.949854

Kosman, D. J. (2010). Redox Cycling in Iron Uptake, Efflux, and Trafficking. *Journal of Biological Chemistry*, *285*(35), 26729-26735. https://doi.org/10.1074/jbc.R110.113217

Kosuta, S., Chabaud, M., Lougnon, G., Gough, C., Dénarié, J., Barker, D. G., & Bécard, G. (2003). A Diffusible Factor from Arbuscular Mycorrhizal Fungi Induces Symbiosis-Specific *MtENOD11* Expression in Roots of *Medicago truncatula* . *Plant Physiology*, *131*(3), 952-962. https://doi.org/10.1104/pp.011882

Kretzschmar, T., Kohlen, W., Sasse, J., Borghi, L., Schlegel, M., Bachelier, J. B., Reinhardt, D., Bours, R., Bouwmeester, H. J., & Martinoia, E. (2012). A petunia ABC protein controls strigolactone-dependent symbiotic signalling and branching. *Nature*, *483*(7389), 341-344. https://doi.org/10.1038/nature10873

Kriel, J., Haesendonckx, S., Rubio-Texeira, M., van Zeebroeck, G., & Thevelein, J. M. (2011). From transporter to transceptor: Signaling from transporters provokes re-evaluation of complex trafficking and regulatory controls. *BioEssays*, *33*(11), 870-879. https://doi.org/10.1002/bies.201100100

Lanfranco, L., Fiorilli, V., & Gutjahr, C. (2018). Partner communication and role of nutrients in the arbuscular mycorrhizal symbiosis. *New Phytologist*, *220*(4), 1031-1046. https://doi.org/10.1111/nph.15230

Lanquar, V., Lelièvre, F., Bolte, S., Hamès, C., Alcon, C., Neumann, D., Vansuyt, G., Curie, C., Schröder, A., Krämer, U., Barbier-Brygoo, H., & Thomine, S. (2005). Mobilization of vacuolar iron by AtNRAMP3 and AtNRAMP4 is essential for seed germination on low iron. *The EMBO Journal*, *24*(23), 4041-4051. https://doi.org/10.1038/sj.emboj.7600864

Lapinskas, P. J., Cunningham, K. W., Liu, X. F., Fink, G. R., & Culotta, V. C. (1995). Mutations in PMR1 suppress oxidative damage in yeast cells lacking superoxide dismutase. *Molecular and Cellular Biology*, *15*(3), 1382–1388. https://doi.org/10.1128/MCB.15.3.1382

Lee, Y.-J., & George, E. (2005). Contribution of Mycorrhizal Hyphae to the Uptake of Metal Cations by Cucumber Plants at Two Levels of Phosphorus Supply. *Plant and Soil*, *278*(1-2), 361-370. https://doi.org/10.1007/s11104-005-0373-1

Lehmann, A., & Rillig, M. C. (2015). Arbuscular mycorrhizal contribution to copper, manganese and iron nutrient concentrations in crops – A meta-analysis. *Soil Biology and Biochemistry*, *81*, 147-158. https://doi.org/10.1016/j.soilbio.2014.11.013

Li, L., Bagley, D., Ward, D. M., & Kaplan, J. (2008). Yap5 Is an Iron-Responsive Transcriptional Activator That Regulates Vacuolar Iron Storage in Yeast. *Molecular and Cellular Biology*, *28*(4), 1326–1337. https://doi.org/10.1128/MCB.01219-07

Li, L., Chen, O. S., Ward, D. M., & Kaplan, J. (2001). CCC1 Is a Transporter That Mediates Vacuolar Iron Storage in Yeast. *Journal of Biological Chemistry*, *276*(31), 29515-29519. https://doi.org/10.1074/jbc.M103944200

Lin, K., Limpens, E., Zhang, Z., Ivanov, S., Saunders, D. G. O., Mu, D., Pang, E., Cao, H., Cha, H., Lin, T., Zhou, Q., Shang, Y., Li, Y., Sharma, T., van Velzen, R., de Ruijter, N., Aanen, D. K., Win, J., Kamoun, S., … Huang, S. (2014). Single Nucleus Genome Sequencing Reveals High Similarity among Nuclei of an Endomycorrhizal Fungus. *PLoS Genetics*, *10*(1), e1004078. https://doi.org/10.1371/journal.pgen.1004078

Ling, H.-Q., Pich, A., Scholz, G., & Ganal, M. W. (1996). Genetic analysis of two tomato mutants affected in the regulation of iron metabolism. *Molecular and General Genetics MGG*, *252*(1–2), 87–92. https://doi.org/10.1007/BF02173208

Liu, A., Hamel, C., Hamilton, R. I., Ma, B. L., & Smith, D. L. (2000). Acquisition of Cu, Zn, Mn and Fe by mycorrhizal maize (*Zea mays L.*) grown in soil at different P and micronutrient levels. *Mycorrhiza*, *9*(6), 331-336. https://doi.org/10.1007/s005720050277

Liu, H., Trieu, A. T., Blaylock, L. A., & Harrison, M. J. (1998). Cloning and Characterization of Two Phosphate Transporters from *Medicago truncatula* Roots: Regulation in Response to Phosphate and to Colonization by Arbuscular Mycorrhizal (AM) Fungi. *Molecular Plant-Microbe Interactions®*, *11*(1), 14-22. https://doi.org/10.1094/MPMI.1998.11.1.14

Li, X.-L., Marschner, H., & George, E. (1991). Acquisition of phosphorus and copper by VA-mycorrhizal hyphae and root-to-shoot transport in white clover. *Plant and Soil*, *136*(1), 49-57. https://doi.org/10.1007/BF02465219

López-Pedrosa, A., González-Guerrero, M., Valderas, A., Azcón-Aguilar, C., & Ferrol, N. (2006). GintAMT1 encodes a functional high-affinity ammonium transporter that is expressed in the extraradical mycelium of Glomus intraradices. *Fungal Genetics and Biology*, *43*(2), 102-110. https://doi.org/10.1016/j.fgb.2005.10.005

Lumini, E., Bianciotto, V., Jargeat, P., Novero, M., Salvioli, A., Faccio, A., Bécard, G., & Bonfante, P. (2007). Presymbiotic growth and sporal morphology are affected in the arbuscular mycorrhizal fungus Gigaspora margarita cured of its endobacteria. *Cellular Microbiology*, *9*(7), 1716-1729. https://doi.org/10.1111/j.1462-5822.2007.00907.x

MacDonald, R. M., Chandler, M. R., & Mosse, B. (1982). The occurrence of bacterium-like organelles in vesicular arbuscular mycorrhizal fungi. *New Phytologist*, *90*(4), 659-663. https://doi.org/10.1111/j.1469-8137.1982.tb03275.x

Mäder, P., Vierheilig, H., Streitwolf-Engel, R., Boller, T., FREY, B., Christie, P., & Wiemken, A. (2000). Transport of 15N from a soil compartment separated by a polytetrafluoroethylene membrane to plant roots via the hyphae of arbuscular mycorrhizal fungi. *New Phytologist*, *146*(1), 155-161. https://doi.org/10.1046/j.1469-8137.2000.00615.x

Maillet, F., Poinsot, V., André, O., Puech-Pagès, V., Haouy, A., Gueunier, M., Cromer, L., Giraudet, D., Formey, D., Niebel, A., Martinez, E. A., Driguez, H., Bécard, G., & Dénarié, J. (2011). Fungal lipochitooligosaccharide symbiotic signals in arbuscular mycorrhiza. *Nature*, *469*(7328), 58-63. https://doi.org/10.1038/nature09622

Manck-Götzenberger, J., & Requena, N. (2016). Arbuscular mycorrhiza Symbiosis Induces a Major Transcriptional Reprogramming of the Potato SWEET Sugar Transporter Family. *Frontiers in Plant Science*, *7*(APR2016), 487. https://doi.org/10.3389/fpls.2016.00487

Mendoza-Cózatl, D. G., Xie, Q., Akmakjian, G. Z., Jobe, T. O., Patel, A., Stacey, M. G., Song, L., Demoin, D. W., Jurisson, S. S., Stacey, G., & Schroeder, J. I. (2014). OPT3 Is a Component of the Iron-Signaling Network between Leaves and Roots and Misregulation of OPT3 Leads to an Over-Accumulation of Cadmium in Seeds. *Molecular Plant*, *7*(9), 1455-1469. https://doi.org/10.1093/mp/ssu067

Morrissey, J., Baxter, I. R., Lee, J., Li, L., Lahner, B., Grotz, N., Kaplan, J., Salt, D. E., & Guerinot, M. lou. (2009). The Ferroportin Metal Efflux Proteins Function in Iron and Cobalt Homeostasis in *Arabidopsis* . *The Plant Cell*, *21*(10), 3326-3338. https://doi.org/10.1105/tpc.109.069401

Nadal, M., & Paszkowski, U. (2013). Polyphony in the rhizosphere: presymbiotic communication in arbuscular mycorrhizal symbiosis. *Current Opinion in Plant Biology*, *16*(4), 473-479. https://doi.org/10.1016/j.pbi.2013.06.005

Naumann, M., Schüßler, A., & Bonfante, P. (2010). The obligate endobacteria of arbuscular mycorrhizal fungi are ancient heritable components related to the Mollicutes. *The ISME Journal*, *4*(7), 862-871. https://doi.org/10.1038/ismej.2010.21

Nouri, E., Breuillin-Sessoms, F., Feller, U., & Reinhardt, D. (2014). Phosphorus and Nitrogen Regulate Arbuscular Mycorrhizal Symbiosis in Petunia hybrida. *PLoS ONE*, *9*(3), e90841. https://doi.org/10.1371/journal.pone.0090841

Oldroyd, G. E. D. (2013). Speak, friend, and enter: signalling systems that promote beneficial symbiotic associations in plants. *Nature Reviews Microbiology*, *11*(4), 252-263. https://doi.org/10.1038/nrmicro2990

Parniske, M. (2008). Arbuscular mycorrhiza: the mother of plant root endosymbioses. *Nature Reviews Microbiology*, *6*(10), 763-775. https://doi.org/10.1038/nrmicro1987

Pérez-Tienda, J., Corrêa, A., Azcón-Aguilar, C., & Ferrol, N. (2014). Transcriptional regulation of host transporters and GS/GOGAT pathway in arbuscular mycorrhizal rice roots. *Plant Physiology and Biochemistry*, *75*, 1-8. https://doi.org/10.1016/j.plaphy.2013.11.029

Pérez-Tienda, J., Testillano, P. S., Balestrini, R., Fiorilli, V., Azcón-Aguilar, C., & Ferrol, N. (2011). GintAMT2, a new member of the ammonium transporter family in the arbuscular mycorrhizal fungus *Glomus intraradices*. *Fungal Genetics and Biology*, *48*(11), 1044-1055. https://doi.org/10.1016/j.fgb.2011.08.003

Pimprikar, P., Carbonnel, S., Paries, M., Katzer, K., Klingl, V., Bohmer, M. J., Karl, L., Floss, D. S., Harrison, M. J., Parniske, M., & Gutjahr, C. (2016). A CCaMK-CYCLOPS-DELLA Complex Activates Transcription of RAM1 to Regulate Arbuscule Branching. *Current Biology*, *26*(8), 987-998. https://doi.org/10.1016/j.cub.2016.01.069

Pimprikar, P., & Gutjahr, C. (2018). Transcriptional Regulation of Arbuscular Mycorrhiza Development. *Plant and Cell Physiology*, *59*(4), 678-695. https://doi.org/10.1093/pcp/pcy024

Pirozynski, K. A., & Malloch, D. W. (1975). The origin of land plants: A matter of mycotrophism. *Biosystems*, *6*(3), 153-164. https://doi.org/10.1016/0303-2647(75)90023-4

Portnoy, M. E., Liu, X. F., & Culotta, V. C. (2000). *Saccharomyces cerevisiae* Expresses Three Functionally Distinct Homologues of the Nramp Family of Metal Transporters. *Molecular and Cellular Biology*, *20*(21), 7893–7902. https://doi.org/10.1128/MCB.20.21.7893-7902.2000

Pozo, M. J., Jung, S. C., López-Ráez, J. A., & Azcón-Aguilar, C. (2010). Impact of Arbuscular Mycorrhizal Symbiosis on Plant Response to Biotic Stress: The Role of Plant Defence Mechanisms. En *Arbuscular Mycorrhizas: Physiology and Function* (pp. 193-207). Springer Netherlands. https://doi.org/10.1007/978-90-481-9489-6_9

Prity, S. A., Sajib, S. A., Das, U., Rahman, M. M., Haider, S. A., & Kabir, A. H. (2020). Arbuscular mycorrhizal fungi mitigate Fe deficiency symptoms in sorghum through phytosiderophore-mediated Fe mobilization and restoration of redox status. *Protoplasma*, *257*(5), 1373-1385. https://doi.org/10.1007/s00709-020-01517-w

Puig, S., Askeland, E., & Thiele, D. J. (2005). Coordinated remodeling of cellular metabolism during iron deficiency through targeted mRNA degradation. *Cell*, *120*(1), 99–110. https://doi.org/10.1016/j.cell.2004.11.032

Quiroga, G., Erice, G., Aroca, R., Chaumont, F., & Ruiz-Lozano, J. M. (2017). Enhanced Drought Stress Tolerance by the Arbuscular Mycorrhizal Symbiosis in a Drought-Sensitive Maize Cultivar Is Related to a Broader and Differential Regulation of Host Plant Aquaporins than in a Drought-Tolerant Cultivar. *Frontiers in Plant Science*, *8*. https://doi.org/10.3389/fpls.2017.01056

Rahimi, S., Baninasab, B., Talebi, M., Gholami, M., & Zarei, M. (2021). Arbuscular mycorrhizal fungi inoculation improves iron deficiency in quince via alterations in host root phenolic compounds and expression of genes. *Scientia Horticulturae*, *285*, 110165. https://doi.org/10.1016/j.scienta.2021.110165

Rellán-Álvarez, R., Giner-Martínez-Sierra, J., Orduna, J., Orera, I., Rodríguez-Castrillón, J. Á., García-Alonso, J. I., Abadía, J., & Álvarez-Fernández, A. (2010). Identification of a Tri-Iron(III), Tri-Citrate Complex in the Xylem Sap of Iron-Deficient Tomato Resupplied with Iron: New Insights into Plant Iron Long-Distance Transport. *Plant and Cell Physiology*, *51*(1), 91-102. https://doi.org/10.1093/pcp/pcp170

Riaz, M., Kamran, M., Fang, Y., Wang, Q., Cao, H., Yang, G., Deng, L., Wang, Y., Zhou, Y., Anastopoulos, I., & Wang, X. (2021). Arbuscular mycorrhizal fungi-induced mitigation of heavy metal phytotoxicity in metal contaminated soils: A critical review. *Journal of Hazardous Materials*, *402*, 123919. https://doi.org/10.1016/j.jhazmat.2020.123919

Rillig, M. C., Aguilar-Trigueros, C. A., Bergmann, J., Verbruggen, E., Veresoglou, S. D., & Lehmann, A. (2015). Plant root and mycorrhizal fungal traits for understanding soil aggregation. *Source: The New Phytologist*, *205*(4), 1385-1388. https://www.jstor.org/stable/newphytologist.205.4.1385

Rivero, J., Lidoy, J., Llopis-Giménez, Á., Herrero, S., Flors, V., & Pozo, M. J. (2021). Mycorrhizal symbiosis primes the accumulation of antiherbivore compounds and enhances herbivore mortality in tomato. *Journal of Experimental Botany*, *72*(13), 5038-5050. https://doi.org/10.1093/jxb/erab171

Robe, K., Conejero, G., Gao, F., Lefebvre-Legendre, L., Sylvestre-Gonon, E., Rofidal, V., Hem, S., Rouhier, N., Barberon, M., Hecker, A., Gaymard, F., Izquierdo, E., & Dubos, C. (2021). Coumarin accumulation and trafficking in *Arabidopsis thaliana* : a complex and dynamic process. *New Phytologist*, *229*(4), 2062-2079. https://doi.org/10.1111/nph.17090

Ropars, J., Toro, K. S., Noel, J., Pelin, A., Charron, P., Farinelli, L., Marton, T., Krüger, M., Fuchs, J., Brachmann, A., & Corradi, N. (2016). Evidence for the sexual origin of heterokaryosis in arbuscular mycorrhizal fungi. *Nature Microbiology*, *1*(6), 16033. https://doi.org/10.1038/nmicrobiol.2016.33

Roth, R., & Paszkowski, U. (2017). Plant carbon nourishment of arbuscular mycorrhizal fungi. *Current Opinion in Plant Biology*, *39*, 50-56. https://doi.org/10.1016/j.pbi.2017.05.008

Ruíz-Lozano, J. M., del Carmen Perálvarez, M., Aroca, R., & Azcón, R. (2011). The application of a treated sugar beet waste residue to soil modifies the responses of mycorrhizal and non mycorrhizal lettuce plants to drought stress. *Plant and Soil*, *346*(1-2), 153-166. https://doi.org/10.1007/s11104-011-0805-z

Ruth, B., Khalvati, M., & Schmidhalter, U. (2011). Quantification of mycorrhizal water uptake via high-resolution on-line water content sensors. *Plant and Soil*, *342*(1-2), 459-468. https://doi.org/10.1007/s11104-010-0709-3

Ruyter-Spira, C., Al-Babili, S., van der Krol, S., & Bouwmeester, H. (2013). The biology of strigolactones. *Trends in Plant Science*, *18*(2), 72-83. https://doi.org/10.1016/j.tplants.2012.10.003

Ryan, M. H., & Angus, J. F. (2003). Arbuscular mycorrhizae in wheat and field pea crops on a low P soil: increased Zn-uptake but no increase in P-uptake or yield. En *Plant and Soil* (Vol. 250). https://doi.org/10.1023/A:1022839930134

Saha, R., Saha, N., Donofrio, R. S., & Bestervelt, L. L. (2013). Microbial siderophores: a mini review. *Journal of Basic Microbiology*, *53*(4), 303-317. https://doi.org/10.1002/jobm.201100552

Sanders, I. R. (1999). No sex please, we're fungi. *Nature*, *399*(6738), 737-738. https://doi.org/10.1038/21544

Schutzendubel, A., & Polle, A. (2002). Plant responses to abiotic stresses: heavy metal-induced oxidative stress and protection by mycorrhization. *Journal of Experimental Botany*, *53*(372), 1351-1365. https://doi.org/10.1093/jexbot/53.372.1351

Schüβler, A., Schwarzott, D., & Walker, C. (2001). A new fungal phylum, the Glomeromycota: phylogeny and evolution. *Mycological Research*, *105*(12), 1413-1421. https://doi.org/10.1017/S0953756201005196

Senovilla, M., Abreu, I., Escudero, V., Cano, C., Bago, A., Imperial, J., & González-Guerrero, M. (2020). MtCOPT2 is a Cu+ transporter specifically expressed in *Medicago truncatula* mycorrhizal roots. *Mycorrhiza*, *30*(6), 781-788. https://doi.org/10.1007/s00572-020-00987-3

Sheng, M., Tang, M., Zhang, F., & Huang, Y. (2011). Influence of arbuscular mycorrhiza on organic solutes in maize leaves under salt stress. *Mycorrhiza*, *21*(5), 423-430. https://doi.org/10.1007/s00572-010-0353-z

Simard, S. W. (2018). Mycorrhizal Networks Facilitate Tree Communication, Learning, and Memory. En *Memory and Learning in Plants* (pp. 191-213). Springer, Cham. https://doi.org/10.1007/978-3-319-75596-0_10

Sisó-Terraza, P., Luis-Villarroya, A., Fourcroy, P., Briat, J.-F., Abadía, A., Gaymard, F., Abadía, J., & Álvarez-Fernández, A. (2016). Accumulation and Secretion of Coumarinolignans and other Coumarins in Arabidopsis thaliana Roots in Response to Iron Deficiency at High pH. *Frontiers in Plant Science*, *7*, 1711. https://doi.org/10.3389/fpls.2016.01711

Smith, S. E., Jakobsen, I., Grønlund, M., & Smith, F. A. (2011). Roles of Arbuscular Mycorrhizas in Plant Phosphorus Nutrition: Interactions between Pathways of Phosphorus Uptake in Arbuscular Mycorrhizal

Roots Have Important Implications for Understanding and Manipulating Plant Phosphorus Acquisition. *Plant Physiology*, *156*(3), 1050-1057. https://doi.org/10.1104/pp.111.174581

Smith, S. E., & Read, D. (2008). *Mycorrhizal Symbiosis*.

Smith, S. E., & Smith, F. A. (2011). Roles of Arbuscular Mycorrhizas in Plant Nutrition and Growth: New Paradigms from Cellular to Ecosystem Scales. *Annual Review of Plant Biology*, *62*(1), 227-250. https://doi.org/10.1146/annurev-arplant-042110-103846

Spatafora, J. W., Chang, Y., Benny, G. L., Lazarus, K., Smith, M. E., Berbee, M. L., Bonito, G., Corradi, N., Grigoriev, I., Gryganskyi, A., James, T. Y., O'Donnell, K., Roberson, R. W., Taylor, T. N., Uehling, J., Vilgalys, R., White, M. M., & Stajich, J. E. (2016). A phylum-level phylogenetic classification of zygomycete fungi based on genome-scale data. *Mycologia*, *108*(5), 1028-1046. https://doi.org/10.3852/16-042

St-Arnaud, M., Hamel, C., Vimard, B., Caron, M., & Fortin, J. A. (1996). Enhanced hyphal growth and spore production of the arbuscular mycorrhizal fungus Glomus intraradices in an in vitro system in the absence of host roots. *Mycological Research*, *100*(3), 328-332. https://doi.org/10.1016/S0953-7562(96)80164-X

Stearman, R., Yuan, D. S., Yamaguchi-Iwai, Y., Klausner, R. D., & Dancis, A. (1996). A Permease-Oxidase Complex Involved in High-Affinity Iron Uptake in Yeast. *Science*, *271*(5255), 1552-1557. https://doi.org/10.1126/science.271.5255.1552

Sugiura, Y., Akiyama, R., Tanaka, S., Yano, K., Kameoka, H., Marui, S., Saito, M., Kawaguchi, M., Akiyama, K., & Saito, K. (2020). Myristate can be used as a carbon and energy source for the asymbiotic growth of arbuscular mycorrhizal fungi. *Proceedings of the National Academy of Sciences*, *117*(41), 25779-25788. https://doi.org/10.1073/pnas.2006948117

Tamayo, E., Figueira-Galán, D., Manck-Götzenberger, J., & Requena, N. (2022). Overexpression of the Potato Monosaccharide Transporter StSWEET7a Promotes Root Colonization by Symbiotic and Pathogenic Fungi by Increasing Root Sink Strength. *Frontiers in Plant Science*, *13*. https://doi.org/10.3389/fpls.2022.837231

Tamayo, E., Gómez-Gallego, T., Azcón-Aguilar, C., & Ferrol, N. (2014). Genome-wide analysis of copper, iron and zinc transporters in the arbuscular mycorrhizal fungus *Rhizophagus irregularis*. *Frontiers in Plant Science*, *5*, 547. https://doi.org/10.3389/fpls.2014.00547

Tamayo, E., Knight, S. A. B., Valderas, A., Dancis, A., & Ferrol, N. (2018). The arbuscular mycorrhizal fungus *Rhizophagus irregularis* uses a reductive iron assimilation pathway for high-affinity iron uptake. *Environmental Microbiology*, *20*(5), 1857-1872. https://doi.org/10.1111/1462-2920.14121

Tang, N., San Clemente, H., Roy, S., Bécard, G., Zhao, B., & Roux, C. (2016). A Survey of the Gene Repertoire of Gigaspora rosea Unravels Conserved Features among Glomeromycota for Obligate Biotrophy. *Frontiers in Microbiology*, *7*(MAR), 233. https://doi.org/10.3389/fmicb.2016.00233

Tedersoo, L., May, T. W., & Smith, M. E. (2010). Ectomycorrhizal lifestyle in fungi: global diversity, distribution, and evolution of phylogenetic lineages. *Mycorrhiza*, *20*(4), 217-263. https://doi.org/10.1007/s00572-009-0274-x

Tian, B., Pei, Y., Huang, W., Ding, J., & Siemann, E. (2021). Increasing flavonoid concentrations in root exudates enhance associations between arbuscular mycorrhizal fungi and an invasive plant. *The ISME Journal*, *15*(7), 1919-1930. https://doi.org/10.1038/s41396-021-00894-1

Tian, C., Kasiborski, B., Koul, R., Lammers, P. J., Bücking, H., & Shachar-Hill, Y. (2010). Regulation of the Nitrogen Transfer Pathway in the Arbuscular Mycorrhizal Symbiosis: Gene Characterization and the Coordination of Expression with Nitrogen Flux . *Plant Physiology*, *153*(3), 1175-1187. https://doi.org/10.1104/pp.110.156430

Tisserant, E., Kohler, A., Dozolme-Seddas, P., Balestrini, R., Benabdellah, K., Colard, A., Croll, D., da Silva, C., Gomez, S. K., Koul, R., Ferrol, N., Fiorilli, V., Formey, D., Franken, Ph., Helber, N., Hijri, M., Lanfranco, L., Lindquist, E., Liu, Y., … Martin, F. (2012). The transcriptome of the arbuscular mycorrhizal fungus *Glomus*

intraradices (DAOM 197198) reveals functional tradeoffs in an obligate symbiont. *New Phytologist*, *193*(3), 755-769. https://doi.org/10.1111/j.1469-8137.2011.03948.x

Thibaud, M.-C., Arrighi, J.-F., Bayle, V., Chiarenza, S., Creff, A., Bustos, R., Paz-Ares, J., Poirier, Y., & Nussaume, L. (2010). Dissection of local and systemic transcriptional responses to phosphate starvation in Arabidopsis. *The Plant Journal*, *64*(5), 775–789. https://doi.org/10.1111/j.1365-313X.2010.04375.x

Tisserant, E., Malbreil, M., Kuo, A., Kohler, A., Symeonidi, A., Balestrini, R., Charron, P., Duensing, N., Frei dit Frey, N., Gianinazzi-Pearson, V., Gilbert, L. B., Handa, Y., Herr, J. R., Hijri, M., Koul, R., Kawaguchi, M., Krajinski, F., Lammers, P. J., Masclaux, F. G., … Martin, F. (2013). Genome of an arbuscular mycorrhizal fungus provides insight into the oldest plant symbiosis. *Proceedings of the National Academy of Sciences*, *110*(50), 20117-20122. https://doi.org/10.1073/pnas.1313452110

Tsai, H. H., & Schmidt, W. (2017). Mobilization of Iron by Plant-Borne Coumarins. *Trends in Plant Science*, *22*(6), 538-548. https://doi.org/10.1016/j.tplants.2017.03.008

van der Heijden, M. G. A., Bardgett, R. D., & van Straalen, N. M. (2008). The unseen majority: soil microbes as drivers of plant diversity and productivity in terrestrial ecosystems. *Ecology Letters*, *11*(3), 296-310. https://doi.org/10.1111/j.1461-0248.2007.01139.x

Voß, S., Betz, R., Heidt, S., Corradi, N., & Requena, N. (2018). RiCRN1, a Crinkler Effector From the Arbuscular Mycorrhizal Fungus Rhizophagus irregularis, Functions in Arbuscule Development. *Frontiers in Microbiology*, *9*(SEP), 2068. https://doi.org/10.3389/fmicb.2018.02068

Wagg, C., Jansa, J., Stadler, M., Schmid, B., & van der Heijden, M. G. A. (2011). Mycorrhizal fungal identity and diversity relaxes plant–plant competition. *Ecology*, *92*(6), 1303-1313. https://doi.org/10.1890/10-1915.1

Wang, E., Schornack, S., Marsh, J. F., Gobbato, E., Schwessinger, B., Eastmond, P., Schultze, M., Kamoun, S., & Oldroyd, G. E. D. (2012). A Common Signaling Process that Promotes Mycorrhizal and Oomycete Colonization of Plants. *Current Biology*, *22*(23), 2242-2246. https://doi.org/10.1016/j.cub.2012.09.043

Wang, J., Wang, J., He, J., Zhu, Y., Qiao, N., & Ge, Y. (2021). Arbuscular mycorrhizal fungi and plant diversity drive restoration of nitrogen-cycling microbial communities. *Molecular Ecology*, *30*(16), 4133-4146. https://doi.org/10.1111/mec.16030

Wang, S., Chen, A., Xie, K., Yang, X., Luo, Z., Chen, J., Zeng, D., Ren, Y., Yang, C., Wang, L., Feng, H., López-Arredondo, D. L., Herrera-Estrella, L. R., & Xu, G. (2020). Functional analysis of the OsNPF4.5 nitrate transporter reveals a conserved mycorrhizal pathway of nitrogen acquisition in plants. *Proceedings of the National Academy of Sciences*, *117*(28), 16649-16659. https://doi.org/10.1073/pnas.2000926117

Walton, J. H., Kontra-Kováts, G., Green, R. T., Domonkos, Á., Horváth, B., Brear, E. M., Franceschetti, M., Kaló, P., & Balk, J. (2020). The *Medicago truncatula* Vacuolar iron Transporter-Like proteins VTL4 and VTL8 deliver iron to symbiotic bacteria at different stages of the infection process. *New Phytologist*, *228*(2), 651–666. https://doi.org/10.1111/nph.16735

Watts-Williams, S. J., & Cavagnaro, T. R. (2014). Nutrient interactions and arbuscular mycorrhizas: a meta-analysis of a mycorrhiza-defective mutant and wild-type tomato genotype pair. *Plant and Soil*, *384*(1-2), 79-92. https://doi.org/10.1007/s11104-014-2140-7

Watts-Williams, S. J., Smith, F. A., McLaughlin, M. J., Patti, A. F., & Cavagnaro, T. R. (2015). How important is the mycorrhizal pathway for plant Zn uptake? *Plant and Soil*, *390*(1-2), 157-166. https://doi.org/10.1007/s11104-014-2374-4

Watts-Williams, S. J., Wege, S., Ramesh, S. A., Berkowitz, O., Gilliham, M., Whelan, J., & Tyerman, S. D. (2020). Identification of a unique ZIP transporter involved in zinc uptake via the arbuscular mycorrhizal fungal pathway. *BioRxiv*. https://doi.org/10.1101/2020.09.28.317669

Wewer, V., Brands, M., & Dörmann, P. (2014a). Fatty acid synthesis and lipid metabolism in the obligate biotrophic fungus *Rhizophagus irregularis* during mycorrhization of *Lotus japonicus*. *The Plant Journal*, *79*(3), 398-412. https://doi.org/10.1111/tpj.12566

Wewer, V., Brands, M., & Dörmann, P. (2014b). Fatty acid synthesis and lipid metabolism in the obligate biotrophic fungus *Rhizophagus irregularis* during mycorrhization of *Lotus japonicus*. *The Plant Journal*, *79*(3), 398-412. https://doi.org/10.1111/tpj.12566

Wijayawardene, N. N., Pawłowska, J., Letcher, P. M., Kirk, P. M., Humber, R. A., Schüßler, A., Wrzosek, M., Muszewska, A., Okrasińska, A., Istel, Ł., Gęsiorska, A., Mungai, P., Lateef, A. A., Rajeshkumar, K. C., Singh, R. v., Radek, R., Walther, G., Wagner, L., Walker, C., … Hyde, K. D. (2018). Notes for genera: basal clades of Fungi (including Aphelidiomycota, Basidiobolomycota, Blastocladiomycota, Calcarisporiellomycota, Caulochytriomycota, Chytridiomycota, Entomophthoromycota, Glomeromycota, Kickxellomycota, Monoblepharomycota, Mortierellomycota, Mucoromycota, Neocallimastigomycota, Olpidiomycota, Rozellomycota and Zoopagomycota). *Fungal Diversity*, *92*(1), 43-129. https://doi.org/10.1007/s13225-018-0409-5

Wipf, D., Krajinski, F., Tuinen, D., Recorbet, G., & Courty, P. (2019). Trading on the arbuscular mycorrhiza market: from arbuscules to common mycorrhizal networks. *New Phytologist*, *223*(3), 1127-1142. https://doi.org/10.1111/nph.15775

Xie, X., Lai, W., Che, X., Wang, S., Ren, Y., Hu, W., Chen, H., & Tang, M. (2022). A SPX domain-containing phosphate transporter from *Rhizophagus irregularis* handles phosphate homeostasis at symbiotic interface of arbuscular mycorrhizas. *New Phytologist*, *234*(2), 650-671. https://doi.org/10.1111/nph.17973

Xie, X., Lin, H., Peng, X., Xu, C., Sun, Z., Jiang, K., Huang, A., Wu, X., Tang, N., Salvioli, A., Bonfante, P., & Zhao, B. (2016). Arbuscular Mycorrhizal Symbiosis Requires a Phosphate Transceptor in the Gigaspora margarita Fungal Symbiont. *Molecular Plant*, *9*(12), 1583-1608. https://doi.org/10.1016/j.molp.2016.08.011

Yang, S.-Y., Grønlund, M., Jakobsen, I., Grotemeyer, M. S., Rentsch, D., Miyao, A., Hirochika, H., Kumar, C. S., Sundaresan, V., Salamin, N., Catausan, S., Mattes, N., Heuer, S., & Paszkowski, U. (2012). Nonredundant Regulation of Rice Arbuscular Mycorrhizal Symbiosis by Two Members of the *PHOSPHATE TRANSPORTER1* Gene Family. *The Plant Cell*, *24*(10), 4236-4251. https://doi.org/10.1105/tpc.112.104901

Zhai, Z., Gayomba, S. R., Jung, H., Vimalakumari, N. K., Piñeros, M., Craft, E., Rutzke, M. A., Danku, J., Lahner, B., Punshon, T., Guerinot, M. lou, Salt, D. E., Kochian, L. v., & Vatamaniuk, O. K. (2014). OPT3 Is a Phloem-Specific Iron Transporter That Is Essential for Systemic Iron Signaling and Redistribution of Iron and Cadmium in *Arabidopsis*. *The Plant Cell*, *26*(5), 2249-2264. https://doi.org/10.1105/tpc.114.123737

Zhang, H., Li, G., Cao, N., Yang, H., & Zhu, F. (2021). Genome-wide identification and expression analysis of NRAMP transporter genes in *Cucumis sativus* and *Citrullus lanatus*. *Canadian Journal of Plant Science*, *101*(3), 377–392. https://doi.org/10.1139/cjps-2020-0062

Zielińska-Dawidziak, M. (2015). Plant Ferritin—A Source of Iron to Prevent Its Deficiency. *Nutrients*, *7*(2), 1184-1201. https://doi.org/10.3390/nu7021184

Zou, Y. -N., Wu, Q. -S., & Kuča, K. (2021). Unravelling the role of arbuscular mycorrhizal fungi in mitigating the oxidative burst of plants under drought stress. *Plant Biology*, *23*(S1), 50-57. https://doi.org/10.1111/plb.13161